Role of Biofuels and Biomass Feedstocks in Decarbonizing the U.S. Economy by 2050

Course No: C10-007
Credit: 10 PDH

Ahmad Hammouz, P.Eng., LEED AP

Continuing Education and Development, Inc.

P: (877) 322-5800
info@cedengineering.com

This course was adapted from the National Renewable Energy Laboratory, Publication No. NREL/TP-5100-87279, "The Role of Biofuels and Biomass Feedstocks for Decarbonizing the U.S. Economy by 2050", which is in the public domain.

Table of Contents

List of Figures

List of Tables

1 Introduction

Biomass resources offer significant potential for reducing U.S. greenhouse gas (GHG) emissions. Biomass such as woody crops, energy crops, and agricultural and forestry residues can be used to provide energy and products with low GHG emissions compared to conventional fossil-based alternatives, and the carbon intensity of biofuels and bioproducts can even be negative when coupled with carbon capture and sequestration (CCS). However, the scale and product composition of the future bioeconomy is not well understood. Much of the potential is yet untapped, and the wide range of possible biomass applications poses challenges for technology developers, investors, and policymakers given the uncertainty of technological progress and the anticipated evolution of the market in which they will compete.

This study sheds light on the potential magnitude of biomass availability and its conversion for various end uses in the context of scenarios of U.S. economywide decarbonization and explores the complementary relationship between an integrated assessment model (IAM) and detailed bottom-up process models. Integrated assessment modeling approaches offer analyses with broader economic competition across decarbonization pathways, whereas detailed bottom-up process modeling approaches offer more granularity in the resources and technologies needed to realize those pathways (Figure 1.1).

Relying on one family of models can result in gaps. For instance, the process parameterization of IAMs is relatively limited in its ability to capture various conversion pathways and could therefore result in oversimplification. Contrastingly, bottom-up models often rely on system expansion and/or consequential approaches to capture economywide changes, which may result in substantial ambiguities. As biomass is a limited resource with associated atmospheric carbon dioxide (CO_2) uptake, the choice of how it is used has implications for achieving net-zero GHG emissions economywide. Employing it in one set of applications precludes its use in others. Biomass deployment affects not only the sectors where it is used but also the technologies and rate of transition that will be required in other sectors where biomass is not available. For instance, using biofuels in transportation can ease a transition from fossil fuels by permitting internal combustion engine vehicles to remain on the road. Diverting biobased resources from fuels would require more drastic changes to transportation technologies such as greater adoption of battery electric or hydrogen fuel cell vehicles. On the other hand, bioelectricity with CCS could provide negative emissions that offset emissions from other hard-to-decarbonize sources (e.g., natural gas generators for stabilizing the electricity grid). Furthermore, certain biofuel pathways require significant hydrogen inputs and, as such, the economics and the CO_2 intensity of those fuels could be dependent on advances in hydrogen production technologies.

By bringing together integrated assessment modeling and bottom-up process modeling approaches, this study explores several potential biomass utilization projections across fuels, power, and products, i.e., various feedstock-to-X options, and evaluates those projections based on a set of environmental, economic, and energy metrics. This exploratory study is a first step toward improving the consistency between integrated assessment modeling and process modeling efforts related to the use of biomass resources to produce low-carbon fuels and products in the context of a decarbonized U.S. economy. It suggests a framework that could be used to understand which sectors and applications might be the best uses for limited sustainable

biomass feedstocks to support net-zero GHG emissions economywide by 2050. This framework is also capable of providing insights into the necessary capital investments for the build-out of biorefineries, fuel and/or chemical markets, and supply-chain infrastructure required to scale up the bioeconomy under various scenarios. This is accomplished through soft-linking across various models as discussed in subsequent chapters.

The specific objectives of this report are to:

- Demonstrate a wide range of bioeconomy scale-up projections consistent with economywide decarbonization (Chapters 2–3)
- Identify costs, environmental metrics, and risks from potential constraints on the production of fuels, power, and products from biomass, as well as other knowledge gaps that could prevent bioeconomy scale-up at the required rates (Chapters 4–6)
- Explore areas of consistency and divergence for the aforementioned findings
- Qualitatively explore possible implications for equity such as equitable access to research and development benefits and economic development opportunities for rural communities and those adversely affected by persistent poverty and disproportionate environmental burdens such as air and water pollution impacts (Chapter 7).

Given the wide breadth of the subject matter, this report focuses on a reduced set of biomass feedstock-to-X pathways at a higher readiness (see Table 1.1). The selected pathways have low or negative life-cycle GHG emissions, consistent with deep decarbonization scenarios, illustrate potential competition for limited biomass feedstocks, and have significant implications for GHG emissions and carbon dioxide removal (CDR). The selection of pathways also encompasses a broad array of potential end uses—such as producing sustainable aviation fuel (SAF) to meet aviation fuel demand and producing ethanol and methanol building-block chemicals for conversion to bioproducts (e.g., ethylene from ethanol via dehydration and propylene from methanol)—to represent competition for biomass use.

Table 1.1. Summary of Conversion Pathways Examined

Feedstock Category	Conversion Process	Intermediates	Products	Use Sector(s)
Herbaceous	Biochemical conversion	Ethanol[a]	Jet fuel, ethanol, and ethylene	Aviation Heavy-duty vehicles (HDVs) Chemical
Herbaceous and woody	Gasification[b] and Fischer-Tropsch (FT) synthesis	Syngas	Jet fuel, FT diesel, naphtha,[c] and ammonia	Aviation and HDVs Chemical
Herbaceous and woody	Gasification and synthesis	Methanol	Methanol	Marine or HDVs Chemical
Herbaceous and woody	Catalytic fast pyrolysis (CFP) and upgrading[b]	Pyrolysis oil	Jet fuel and CFP Diesel	Aviation and HDVs
Herbaceous and woody	Bioelectricity with CCS	N/A	Electricity	Electric grid
Wet waste	Hydrothermal liquefaction (HTL) and hydrotreating	Biocrude	Jet fuel and HTL diesel	Aviation and HDVs
Wet waste	Anaerobic digestion	Biogas	Renewable natural gas	Natural gas distr.
Wet waste	Arrested methanogenesis and volatile fatty acid upgrading	Volatile fatty acid	Jet fuel and naphtha Polylactic acid	Aviation and HDVs Plastic
Fats, oils, and greases	Hydroprocessed esters and fatty acids	N/A	Jet fuel Renewable diesel	Aviation HDVs
Fats, oils, and greases	Transesterification	N/A	Biodiesel	HDVs

[a] This pathway also serves as a proxy for similar pathways with butanol, 2,3-BDO, farnesene, or isoprene as intermediates.

[b] Gasification and CFP could also leverage existing refinery infrastructure and, as a transition strategy, syngas and pyrolysis oil could be coprocessed with conventional petroleum in a refinery. To manage scope, we represent this by adjusting the capital requirements for corresponding processes.

[c] We consider an option where the naphtha coproduct is sent to steam cracking to produce ethylene and propylene.

Given the short timeline of the study, the scenarios could not be completely harmonized, which led to some differences. The main difference is that the scenarios analyzed by the Global Change Analysis Model (GCAM) in Chapter 2 (henceforth referred to as GCAM-DECARB) were harmonized with assumptions from bottom-up models across a range of inputs, including second-generation bioenergy crop yields, bioenergy transportation and preprocessing costs, and bioenergy conversion pathway costs and efficiencies. The scenarios analyzed by the bottom-up models in Chapters 3–6 predated this harmonization and will be referred to as GCAMv6.

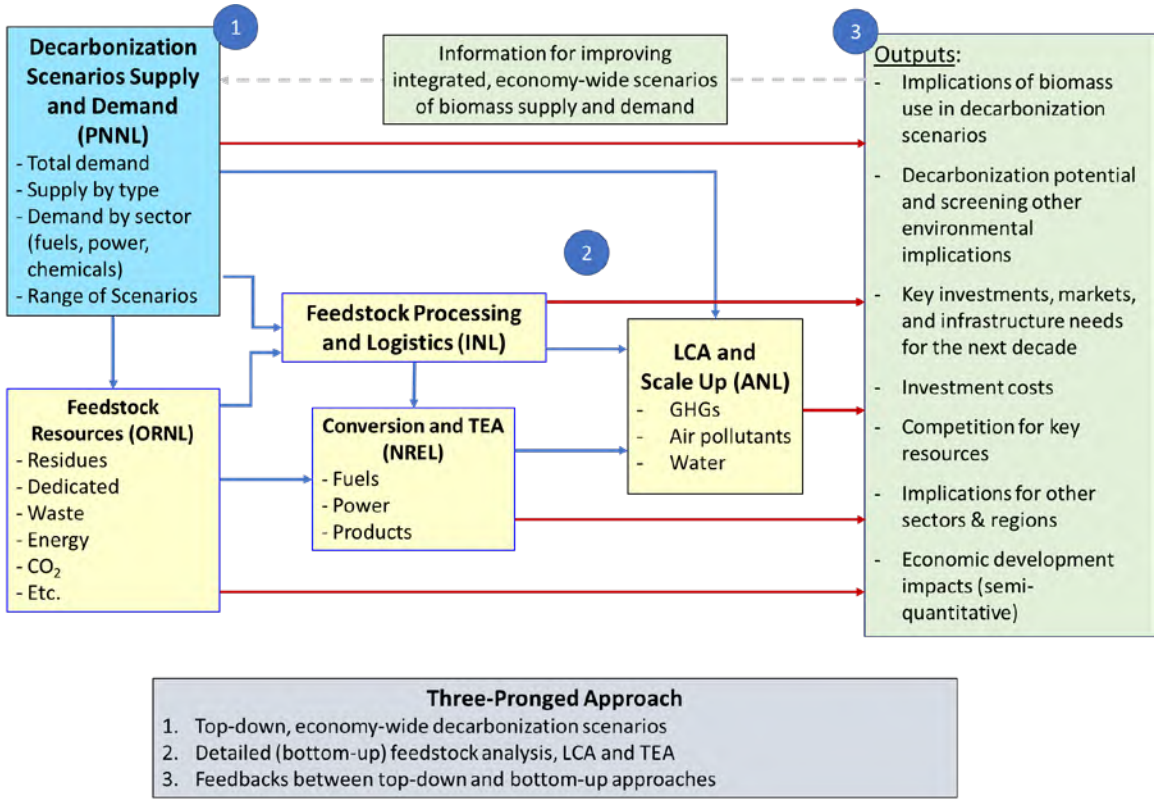

Figure 1.1. Project approach and specialization of the multilab team

Top-down integrated assessment modeling (GCAM) approaches are shown in blue, and bottom-up modeling approaches are shown in yellow. Green boxes denote outcomes that result from comparing and synthesizing these top-down and bottom-up assessment results. Blue lines depict interactions and results transfer between models, and red lines depict metrics and other analysis findings contributing to the project outcomes.

We developed an initial set of economywide scenarios that incorporate varying levels and types of biomass utilization using an IAM, which identified potential feedstock demand and the adoption of key biobased pathways. We then tested and reevaluated these initial top-down scenarios through a cascading set of bottom-up assessments of biomass resource, preprocessing, and conversion techno-economic assessments (TEAs). These detailed analyses give a closer look at the biobased supply chains, provide more accurate costs and emissions estimates, and identify pinch points that more aggregate top-down approaches may miss. Subsequently, a combination of IAM outputs and bottom-up assessments were used to develop economic metrics such as minimum sustainable fuel price; environmental metrics such as life cycle GHG emissions per unit of power, fuel, or product; and scalability metrics such as rates of land use changes.

For the economywide decarbonization scenarios, we used GCAM, which is an IAM used recently for the U.S. Department of State and the U.S. Executive Office of the President report *The Long-Term Strategy of the United States: Pathways to Net-Zero Greenhouse Gas Emissions by 2050* (U.S. DOS 2021). IAMs provide an essential top-down, coupled cross-sectoral perspective on the evolution of the different sectors of the global economy and their competition for the most economical use of limited resources such as arable land and biomass. However, IAMs have a broad and stylized long-term focus by nature, and they often cannot provide a

specific road map for near-term action. For instance, GCAM has limited geographic resolution and has a coarse differentiation of biomass feedstocks (Gregg and Smith 2010). Thus, there are opportunities to complement the *coarse biomass demand* projected by GCAM with detailed bottom-up assessment of potential supply of specific feedstocks and associated supply chain and biorefinery performance. GCAM is used to provide scenario results that specify carbon prices and key parameters such as the electricity generation grid mix, hydrogen production technology mix, fuel use by various end-use categories, natural gas use, and heat use. The GCAM scenarios developed for this analysis are discussed in detail in Chapter 2, and the inputs from GCAM to the various process models are described in Chapters 3–6.

This "sprint" study was conducted over the course of six months with the goal of demonstrating how top-down and bottom-up modeling approaches could be deployed in a consistent framework to address important questions about the role of bioenergy in a deeply decarbonized U.S. economy. Within this condensed timeline, we were able to generate an initial set of scenarios using the default GCAMv6 model for use by the bottom-up modeling teams (Chapters 3–6) and then update GCAM with data from those bottom-up assessments and rerun the scenarios within GCAM, demonstrating a first step toward an iterative harmonization of the top-down and bottom-up modeling paradigms. We refer to the resulting updated version of GCAM, detailed in Chapter 2, as GCAM-DECARB. Chapters 3–6 present bottom-up assessments aligned with the original set of "GCAMv6" scenarios based on default parameters prior to harmonization.

For both sets of scenarios, the Reference scenario assumes no explicit policy representation and limited advancements in liquid biofuel conversion technologies. The initial set of GCAMv6 decarbonization scenarios include: 1) one where novel biofuel conversion technologies become available but no SAF production targets are represented (DAC.Ref_noSAF) and 2) another that requires the production of 35 billion gallons of liquid biofuels in 2050, consistent with the SAF Grand Challenge volumetric target for meeting U.S. jet fuel demand, excluding coproducts (DAC.Ref_BF35bil.gal).

In addition to reflecting key model improvements including updated second-generation bioenergy crop yields and yield improvement, bioenergy transportation and preprocessing costs, bioenergy conversion pathway costs and efficiencies, and separate tracking of aviation fuels relative to other liquid fuel, the updated GCAM-DECARB scenarios presented in Chapter 2 consider sensitivity analysis around the cost and performance of direct air capture (DAC) technologies as well as an additional, more ambitious target for liquid biofuel production beyond the original 35-billion-gallon target. Across all GCAM scenarios there is no explicit constraint on the level of biomass supply; rather, supply is determined within the model based on competition between biomass and other land uses (e.g., agriculture, forestry) and bioenergy's competitiveness with other fuels in energy transformation and end-use sectors.

Chapter 3 discusses the biomass resource analysis. Bottom-up assessment tools can provide a much finer-resolution view of the supply, cost, and viability of specific feedstocks and conversion technologies underlying the key biobased pathways prioritized by GCAM. Biomass resource assessment is used to identify which agricultural residues and energy crops are most likely to supply biomass in different U.S. regions, considering environmental limitations and land competition. The quantities of feedstocks available and the locations from which they can be economically collected in sufficient quantities to support economies of scale at conversion

facilities are specified leveraging the extensive, regionalized biomass supply curves under different scenarios from the 2016 Billion-Ton Report (Langholtz 2016).

Chapter 4 provides details on the transport and logistic parameters for biomass. Based on the biomass resource analysis results and the pathways presented in Table 1.1, we modeled the energy, material inputs, and costs associated with biomass harvesting, transportation, logistics, preservation, storage, and preprocessing based on approaches developed in connection with previous DOE Office of Energy Efficiency and Renewable Energy (EERE) studies. Our analysis considered how biomass resources and preprocessing technologies result in feedstocks of different quality specifications appropriate for specific purposes. For example, biomass conversion to fuels and biomass combustion for bioelectricity have very different tolerances for feedstock lignin and ash content. This biomass logistics analysis provides the requirements to transport and supply biomass feedstocks with suitable properties to conversion reactors.

Conversion process modeling and TEA are carried out in Chapter 5. The requirements for conversion of biomass feedstocks to fuels and bulk chemicals at commercial-scale facilities are estimated using process models and then used to estimate the costs of the fuels and products from each pathway presented in Table 1.1. The conversion process modeling provides the energy and input requirements for producing the fuels, electricity, and chemicals required to meet demand and, together with feedstock logistics modeling, provides cost estimates. The TEA also estimates economic benefits of feedstock production and conversion activities.

The results of the biomass logistics analysis in Chapter 4 and the conversion process modeling in Chapter 5 are used as an input to the Greenhouse gases, Regulated Emissions, and Energy use in Technologies (GREET) model to estimate environmental metrics such as life cycle GHG emissions, energy consumption, and water consumption for each technology pathway (Table 1.1). The GREET supply-chain results are then further used as inputs to the Air emissions, Greenhouse gas emissions, and Energy use model for the Bioeconomy (Bioeconomy AGE), in which they are scaled up to estimate the U.S. economywide environmental effects of the decarbonization scenarios. These results complement the integrated assessment modeling by providing a bottom-up perspective on the total decarbonization potential for the technology deployment scenarios specified by GCAM. The GREET and Bioeconomy AGE modeling are described in Chapter 6.

At several points during this iterative analysis, the outputs from the biomass resource assessment and process modeling (Chapters 3–6) were compared with the projections from GCAM to determine their consistency and to identify sources of variation. The biomass resource assessment and Bioeconomy AGE analysis were also used to compare the supply of and end-use demand for fuels and chemicals based on the bottom-up, process-based approach and the levels projected at a more aggregate resolution by GCAM. The cause of gaps between the GCAM integrated assessment modeling and the detailed, bottom-up estimates is discussed in Chapter 7 and used to propose strategies to further harmonize across these ongoing modeling efforts. It is important to note that a key driver of this study was to provide results quickly to efficiently guide further EERE efforts to understand the implications of decarbonization goals and scenarios for EERE research and development.

References

Gregg, J. S., and S. J. Smith, 2010. "Global and regional potential for bioenergy from agricultural and forestry residue biomass." *Mitigation and Adaptation Strategies for Global Change* 15: 241-262.

Langholtz, M. H., B. J. Stokes, and L. M. Eaton. 2016. *2016 Billion-ton Report: Advancing Domestic Resources for a Thriving Bioeconomy, Volume 1: Economic Availability of Feedstock.* Oak Ridge, TN: Oak Ridge National Laboratory. ORNL/TM-2016/160. https://doi.org/10.2172/1271651.

U.S. DOS. 2021. *The Long-Term Strategy of the United States: Pathways to Net-Zero Greenhouse Gas Emissions by 2050*. Washington, DC: U.S. Department of State. https://www.whitehouse.gov/wp-content/uploads/2021/10/US-Long-Term-Strategy.pdf.

2 Decarbonization Scenario Analysis—Economywide Supply and Demand Modeling

2.1 Background

GCAM was used to develop economywide U.S. net-zero GHG emission scenarios, with a focus on the role of bioenergy supply and demand. Six main net-zero GHG emission scenarios were evaluated, which spanned different assumptions about biofuels policy and direct air capture technology. The bioenergy outcomes in these scenarios were compared to the broader integrated assessment literature (Clarke et al. 2022, Browning et al. 2023) and shared with the other modeling teams in this study to evaluate the scenarios using more spatially, temporally, and technologically detailed tools. These comparisons helped to identify key structural or data gaps in GCAM where information from bottom-up modeling tools can help enhance the model's representation of bioenergy pathways.

The primary results of these GCAM scenarios and comparisons were:

1. In scenarios that reach net-zero GHG emissions by mid-century, bioenergy supply increases steeply, from ~5 EJ in 2020 to between 14 EJ and 23 EJ in 2050. Biomass plays an important role because of its ability to generate negative emissions and provide a low-carbon replacement for fossil fuels in hard-to-electrify sectors for which few other low-carbon alternatives exist. Negative emissions are highly valued in net-zero scenarios because certain emissions sources, such as non-CO_2 emissions from agriculture (e.g., nitrous oxide [N_2O] emissions from fertilizer use, methane [CH_4] from livestock) and CO_2 emissions from heavy transport and industry applications, are very challenging to reduce to zero.
2. Sustainable fuel targets shift biomass demand into liquid fuel production. Without these targets, in both the GCAM scenarios and the broader IAM literature (Clarke et al. 2022, Browning et al. 2023), bioenergy tends to be primarily used for electricity and/or hydrogen production and paired with carbon capture and sequestration (CCS).
3. Bioenergy crop yields, transportation and preprocessing costs, and conversion pathway costs and efficiencies were harmonized with the bottom-up models. In addition, we set up separate tracking of aviation fuels within GCAM to better understand SAF targets. In the future, options to improve bioenergy pathways in GCAM include harmonizing bioenergy crop nonland production costs and fertilizer requirements, explicitly representing preprocessing and/or conversion pathways, and incorporating additional bioenergy conversion pathways and liquid fuel grades.

This chapter describes the progress of this work area and is structured as follows. First, we describe our methodology, including an overview of GCAM, a description of updates to GCAM informed by data from the other bottom-up models available in this project, and our scenario structure. Next, we describe GCAM results for a reference scenario and several decarbonization scenarios that reach net-zero GHG emissions by 2050. It may be noted that due to the short time frame of this six-month sprint study, the scenarios presented here differ somewhat from the GCAM scenarios used by the bottom-up models in subsequent chapters of this report. The two sets of scenarios are similar in design, but the scenarios presented in this chapter include updates

to GCAM informed by the bottom-up models, while the scenarios in Chapters 3–6 do not reflect these GCAM improvements. We also include a comparison of our scenarios with the broader integrated assessment scenario literature to explore a range of potential roles for biomass in U.S. deep decarbonization pathways (Byers et al. 2022). We conclude the chapter with a discussion of key observations and future research directions.

2.2 Methods

2.2.1 Global Change Analysis Model

GCAM is designed to assess long-term, multisector implications of policies and technology strategies across the globe (Calvin et al. 2019). For example, GCAM was used to develop a series of potential pathways for reducing U.S. GHG emissions to net-zero by 2050 for the recent White House report, *The Long-Term Strategy of the United States: Pathways to Net-Zero Greenhouse Gas Emissions by 2050* (U.S. DOS 2021). In the results presented here, we ran the model until 2050 to capture the United States' transition to net-zero GHG emissions by mid-century, in accordance with the White House's 2050 goals.

GCAM captures key economic competition at various stages of the bioenergy life cycle. On the production side, biomass competes for land allocation with other land uses, including food crops, animal agriculture, and forestry. The harvested biomass feedstock can then be traded in a global market, with biomass trade represented using an Armington trade approach (Armington 1969) that distinguishes between domestic consumption, exports, and imports for all 32 energy-economic regions.[10] On the consumption side, biomass competes with other energy resources (e.g., gas, oil, solar, wind) for the production of secondary energy carriers, namely electricity, liquid fuels, gas, and hydrogen. Finally, end use sectors, including buildings, industry, and transportation, demand these secondary energy carriers to provide end-use energy services (e.g., heating, cooling, transportation, and industrial power and feedstocks). Solid biomass is also demanded for certain end uses such as wood stoves for heat in buildings.

Throughout GCAM's representation of the bioenergy system, information is aggregated at several points (Figure 2.1). Biomass supply is tracked by water basin for first-generation energy crops (e.g., corn, soy, oil crops) and second-generation energy crops (e.g., herbaceous and woody crops). First-generation energy crops are food crops and make up most present-day liquid biofuels; second-generation energy crops, or purpose-grown energy crops, are trees or grasses (woody or herbaceous crops) that are grown solely for use as bioenergy. Additional biomass supply is provided by municipal solid waste (MSW) and crop residues, both tracked at the national scale. Second-generation crops, MSW, and crop residues are then combined into a single homogenous biomass commodity. First-generation crops from all water basins are tracked separately as national corn, sugar, and oil crop (e.g., soy) commodities (which can be consumed as food or converted to biofuels). Bioenergy-specific technologies (e.g., corn ethanol production, conventional power production with and without CCS) convert biomass feedstock commodities into generic secondary energy carriers. For example, biomass (excluding first-generation energy crops) is converted to liquid fuels by either cellulosic ethanol or Fischer-Tropsch (FT) technologies, but the resulting liquid fuel product that end users demand is not differentiated by

Second-generation bioenergy crops entail dedicated energy crops, i.e., where the primary functionality is not food. re the nation's domestic bioenergy supply meets 100% of its demand.

feedstock (including biogenic vs. fossil origin). By default, different grades of liquid fuels (e.g., gasoline vs. diesel vs. jet) are not explicitly tracked. This aggregation provides an opportunity for bottom-up models to add detail to GCAM's economywide results.

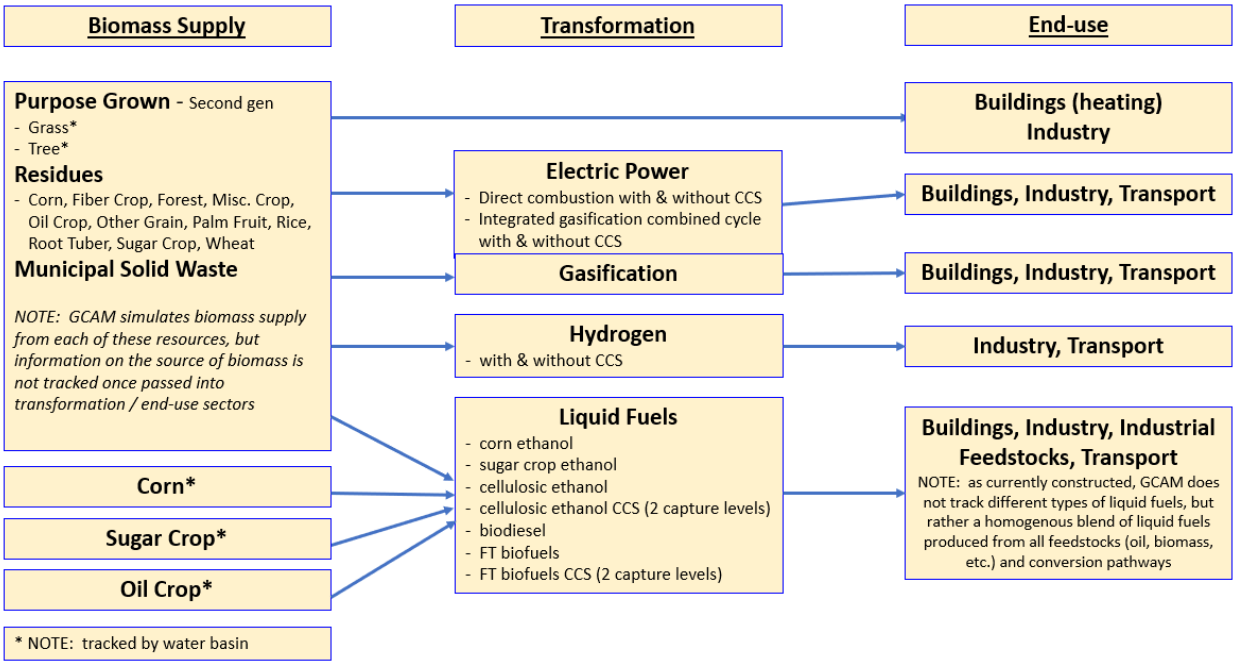

Figure 2.1. GCAM's modeling of the bioenergy supply chain, beginning with biomass supply from purpose-grown crops, agricultural residues, and municipal solid waste (left); then energy transformation to electricity, gas, hydrogen, or liquid fuel (center); and finally its end-use consumption in buildings, industry, and transportation (right)

2.2.2 Updates to Model Structure and Data

For this study, we use the most recent version of GCAM, GCAMv6 (JGCRI 2022). Compared with previous versions of GCAM, including the version used in the U.S. *Long-Term Strategy* analysis, this latest version includes a more detailed representation of the industrial sector, represents more crop commodities, and offers an updated representation of hydrogen supply, transport, and end-use technologies. Additionally, several model parameters were updated over the course of this study based on the analyses described in subsequent chapters. Specifically, second-generation bioenergy crop yields; bioenergy processing costs and efficiency; and refining costs, efficiency, and byproduct production for cellulosic ethanol and FT biofuel production technologies were all updated for this analysis. Finally, a separate representation of the aviation fuels sector was added to this analysis to better capture the competition between biomass and oil in aviation fuels since production of SAF has been deemed a priority use of bioenergy (The White House 2021), consistent with many deep decarbonization analyses. The priorities laid out in the SAF Grand Challenge are grounded in numerous analyses that support two key findings: 1) SAF is the only viable near-term solution capable of achieving net-zero emissions from the aviation sector (U.S. DOE et al. 2022, FAA 2021); and 2) the use of biomass to produce SAF is one of the highest-priority applications of biomass to meet economywide net-zero emissions targets (Uppink et al. [2023], IEA [2021]). This new sector has technology options (from oil and biomass feedstocks) consistent with GCAM's default liquid refining sector, but includes updates to several parameters for bioliquids technologies. To better represent SAF conversion pathways,

costs, efficiencies, production ratios (ratio between SAF and other liquid products like gasoline and diesel blendstocks), and carbon capture rates were all updated for this new aviation fuels sector. In the revised GCAM structure, aviation technologies consume the new aviation fuel commodity, while all other end-use technologies consume GCAM's original generic refined liquid fuel commodity. This structure allowed GCAM to track the production of SAF relative to other liquid fuel types and enforce policies that target specific levels of SAF production (see Section 2.2.3 on Scenario Design).

This "sprint" study was conducted over the course of six months with the goal of demonstrating how top-down and bottom-up modeling approaches could be deployed in a consistent framework to address important questions about the role of bioenergy in a deeply decarbonized U.S. economy. Within this condensed timeline, we were able to generate an initial set of scenarios using the default GCAMv6 model for use by the bottom-up modeling teams (Chapters 3–6), and then to update GCAM with data from those bottom-up assessments and re-run the scenarios within GCAM, demonstrating a first step toward an iterative harmonization of the top-down and bottom-up modeling paradigms. We refer to the resulting updated version of GCAM as GCAM-DECARB, and the remainder of this chapter details the results of the GCAM-DECARB scenarios reflecting initial harmonization with the bottom-up models. However, Chapters 3–6 reflect bottom-up assessments aligned with the original set of GCAM scenarios based on default "GCAMv6" parameters prior to harmonization.

Leveraging analysis performed by Oak Ridge National Laboratory (ORNL) (Chapter 3), we updated baseline bioenergy crop yields and future yield improvement rates for second-generation grass and tree bioenergy crops within U.S. water basins. For any agricultural commodity in GCAM, yields vary based on which of four represented management strategies (irrigated/rainfed combined with higher/lower management intensity (e.g., mechanization, other inputs)) are implemented. ORNL bioenergy crop yields by basin were used to update base yields for only one of GCAM's four agricultural management strategies: the rainfed with high-intensity management strategy (see Appendix Table A.2.1for a comparison). This GCAM management strategy was selected because 1) the ORNL yield assumptions consider only rainfed energy crop production, and 2) ORNL yields are generally more consistent with the high-intensity management strategy in GCAM. Nitrogen fertilizer application rates and other nonland production costs for bioenergy crops were not harmonized with ORNL data as part of this project.

GCAM's default yield improvement assumptions vary by water basin and management strategy based on projections from the Food and Agriculture Organization of the United Nations. Average yield improvements for second-generation biomass crops in the United States are 0.52% per year in 2020 in GCAM's default assumptions, decreasing to an average of 0.33% per year in 2040 (Table 2.1). The inclusion of updated assumptions from ORNL increases the 2020 yield improvement to 0.98% per year in 2020, decreasing to 0.82% per year in 2040 (see Table 2.1). ORNL's analysis extends only to 2040, so GCAM's default global, long-term bioenergy crop yield improvement rate of 0.2% per year was applied from 2040 to 2050.

Table 2.1. Updates to Second-Generation Biomass Yield Improvement Assumptions (% Improvement Per Year)

Year	GCAMv6 Defaults (average)	GCAM-DECARB Updates (average)
2020	0.51%	0.98%
2025	0.49%	0.93%
2030	0.48%	0.89%
2035	0.30%	0.85%
2040	0.33%	0.82%
2045	0.32%	0.20%
2050	0.31%	0.20%

The GCAMv6 defaults are a simple average across all U.S. water basins and agricultural management practices.

In addition, GCAM's bioenergy preprocessing costs and efficiency were altered based on analysis by Idaho National Laboratory (INL) (Chapter 4). INL's logistics and preprocessing analysis and the National Renewable Energy Laboratory's (NREL's) conversion facility TEA are both based on bio-refineries with a throughput capacity of 2,205 dry short tons per day. GCAM does not represent bioenergy preprocessing for individual feedstocks, but average preprocessing costs and efficiencies can be represented for its aggregated biomass commodity (combining second-generation crops, MSW, and crop residues). However, preprocessing costs and dry matter (biomass) losses can vary significantly by preprocessing system, which INL modeled for several combinations of feedstock type and conversion pathway. Specifically, INL provided cost and loss data for four biomass preprocessing systems: herbaceous biomass (ethanol pathway; baled/dry), herbaceous biomass (ethanol pathway; chopped/wet), woody biomass (gasification pathway), and woody biomass (pyrolysis pathway). INL also provided data on total biomass quantities processed via each pathway (i.e., preprocessing system), which were based on the detailed ORNL biomass supply modeling (Chapter 3). These quantity data were used to calculate weighted-average feedstock preprocessing costs and efficiencies for use in GCAM. With these adjustments, costs of preprocessing decreased from $2.92 per gigajoule (GJ; default GCAM value) to $2.66/GJ (weighted-average INL value), but preprocessing losses of 6.8% were included (dry matter losses in biomass processing were previously not reflected in GCAM). Additionally, energy inputs to biomass processing were added, with 0.0145 GJ of electricity and 0.0007 GJ of gas required to process 1 GJ of biomass.

Finally, NREL's TEA (Chapter 5) of different liquid biofuel pathways informed an update to cellulosic ethanol and FT biofuel refining efficiency, cost, CCS removal fraction, and by-product output (Table A.2.2). GCAM represents each biorefining pathway both without CCS and with two levels of CCS technologies, where an increasing percentage of carbon is removed for an increasing cost. By default, GCAM assumes some improvement in biomass conversion efficiency and nonenergy (e.g., capital, operations and maintenance) costs over time for each liquid biofuel technology. NREL's data were not time-varying, so the updated liquid biofuel conversion costs and efficiencies are constant over time. Relative to GCAM's default assumptions, the updated conversion technology representation from NREL resulted in decreased conversion efficiency and increased cost for all cellulosic ethanol technologies. However, for FT biofuel refining technologies, both efficiency and cost decreased as a result of

the data updates. Note that for cellulosic ethanol, separate pathways producing 1) 100% gasoline blendstock and 2) roughly 80% jet fuel blendstock and 20% gasoline blendstock were represented.

2.2.3 Scenario Design

To explore the role bioenergy could play in U.S. deep decarbonization pathways, we developed seven scenarios: a Reference scenario with no explicit policy representation, and six scenarios that achieve net-zero GHG emissions in the United States in 2050. Broadly, these emission reductions are reached through a combination of decreasing positive GHG emissions and increasing negative emissions (with the latter provided by both the land sink and CDR technologies). To reach the net-zero GHG emissions target, GCAM applies a uniform, economywide carbon price that adds costs to emitting technologies and incentivizes CDR. It is important to note that the scenarios presented in this report (Reference and net-zero GHG) do not include a representation of the recently passed Inflation Reduction Act. Furthermore, the uniform carbon price employed in these scenarios represents a simple, stylized policy for achieving long-term emissions targets in a cost-effective manner. In the real world, decarbonization may be pursued via a variety of policies, including a collection of sectoral policies. Thus, the allocation of biomass across economic sectors may unfold differently in alternate policy regimes than it does with the uniform carbon price simplification employed in this analysis.

To focus on the U.S. bioeconomy and simplify data transfers with the bottom-up models (which do not have global scope), these scenarios do not allow the United States to trade biomass internationally beyond 2020; domestic bioenergy demand is constrained to be provided by domestic supply in all scenarios. Additionally, there are no explicit constraints on the level of biomass supply in these GCAM scenarios, such as a billion-ton ceiling corresponding to the Billion-Ton Report (BT16; U.S. DOE 2016). Biomass becomes more expensive as demand increases, and GCAM endogenously captures interactions between increasing demand for bioenergy production and other land uses like agriculture or afforestation to increase terrestrial carbon sinks. Chapter 3 (Feedstock Resource Assessment) compares supply levels from GCAM scenarios to data from the 2016 Billion-Ton Report, which reflects more restrictive and spatially resolved sustainability constraints.

We explored two key sensitivities in the net-zero scenarios—DAC technology costs and SAF targets (Table 2.2). The DAC sensitivity was chosen because DAC competes with bioenergy in the production of negative emissions, which is provided by bioenergy with carbon capture and storage (BECCS)[11]. To reach net-zero GHG emissions, some combination of natural (e.g., land sink) and technological (e.g., DAC and BECCS) solutions would likely need to be deployed to balance out remaining residual emissions. For the DAC sensitivities, we explore cases with reference nonenergy costs (e.g., capital, operations and maintenance) and energy efficiency assumptions for DAC (DAC.Ref) as well as those with lower DAC costs and higher DAC efficiency (DAC.Adv). Our hypothesis was that less expensive DAC would reduce the demand for bioenergy due to a reduced need for negative emissions from BECCS since CDR from DAC is more prevalent.

[11] Here, this includes both biofuel production pathways with sequestration of emissions from the conversion stage and bioelectricity with capture and sequestration of the combustion emissions.

For the second sensitivity, a key policy that may impact bioenergy deployment is the SAF Grand Challenge (The White House 2021), in which multiple federal agencies have set goals to increase SAF deployment. The 2050 goal for this program is to meet 100% of aviation fuel demand with SAF; aviation fuel demand is projected to reach 35 billion gallons per year by mid-century according to the U.S. Energy Information Administration's (EIA's) Annual Energy Outlook 2021 (EIA 2021). Because most SAF production processes coproduce other biofuel grades, it is expected that reaching the 35-billion-gallon SAF goal would require a total of 50–60 billion gallons of biofuel production per year (i.e., 15–25 billion gallons of coproduced non-SAF biofuels).

For our scenarios, we explored three different levels of liquid biofuels targets. In each of the three cases, coproducts from SAF production are tracked within GCAM; the difference between the scenarios is the extent to which bioenergy is prioritized for SAF and other liquid biofuels production. In the noSAF scenario, SAF technologies are available and compete with fossil-based fuels to meet aviation fuel demand, but no specific target for SAF deployment (in terms of market share or production volume) is specified. In the SAF100pct scenario, SAF must meet 100% of GCAM's endogenous aviation fuel demand in 2050, but no specific volumetric biofuels target is imposed. However, aviation fuel demand in 2050 for GCAM's net-zero scenarios is lower (roughly 30% lower) than reflected in the SAF Grand Challenge (i.e., 35 billion gallons per year in 2050), meaning total biofuel production in the SAF100pct case is lower than expected by the SAF Grand Challenge. Thus, we included the BF50bil.gal scenario as an illustrative high-biofuel scenario that is consistent with total liquid biofuel volumes of the SAF Grand Challenge (i.e., 35 billion gallons plus coproducts). The BF50bil.gal scenario reflects 56 billion gallons of total liquid biofuel production, which is consistent with production of 35 billion gallons of SAF via a roughly even split between the cellulosic ethanol/ethanol to jet and FT synthetic paraffinic kerosene (FT-SPK) jet fuel conversion pathways (given their respective coproduct ratios). In the BF50bil.gal scenario, the excess biofuel remaining after fulfilling 100% of the aviation sector demand is used wherever liquid fuel demands remain in the energy system, primarily in shipping, heavy trucking, and industry.

Table 2.2. GCAM Scenarios (Reference Scenario Not Included)

Scenario Name	DAC Technology[a]	SAF Target
Reference	Reference DAC cost, but no emissions policy to drive deployment.	No SAF target
DAC.Ref_noSAF	Reference DAC cost ($2021/tCO_2$) $285.75 (gas tech) $343.93 (gas + elec tech)	No SAF target
DAC.Ref_SAF100pct		SAF meets 100% of endogenous aviation fuel demand in 2050
DAC.Ref_BF50bil.gal		SAF meets 100% of endogenous aviation fuel demand; 56 billion gallons of total liquid biofuels (including SAF) are produced in 2050
DAC.Adv_noSAF	Advanced DAC cost (2021$/tCO2) $156.80 (gas tech) $183.20 (gas + elec tech)	No SAF target
DAC.Adv_SAF100pct		SAF meets 100% of endogenous aviation fuel demand in 2050
DAC.Adv_BF50bil.gal		SAF meets 100% of endogenous aviation fuel demand; 56 billion gallons of total liquid biofuels (including SAF) are produced in 2050

[a] DAC technologies represent solvent-based DAC systems with self-generated electricity (natural gas combined cycle with CCS; "gas tech") or with externally purchased electricity ("gas + elec tech").

The Reference, noSAF and SAF100pct scenario definitions were consistent between the original set of GCAMv6 scenarios generated with the default GCAMv6 model and the subsequent GCAM-DECARB scenario generated after initial GCAM harmonization with the bottom-up assessment results described in Chapters 3–6. However, the original GCAMv6 scenarios included BF35bil.gal scenarios instead of BF50bil.gal. The initial DAC.Ref_BF35bil.gal scenario was designed to be consistent with the volumetric target for SAF from the Sustainable Aviation Fuel Grand Challenge[12] (estimated as 35 billion gallons of SAF in 2050) and was produced before we separated out aviation fuel (and SAF coproducts) in GCAM). The revised DAC.Ref_BF50bil.gal scenario was implemented after bottom-up modeling further clarified the production level of other biofuel coproducts during SAF production. The BF50bil.gal scenario refers to a total biofuels (SAF + coproducts) volumetric target consistent with the Sustainable Aviation Fuel Grand Challenge SAF target. Thus, the BF50bil.gal scenario entails a higher bioliquids target and thus is not directly comparable to the BF35bil.gal scenario utilized in Chapters 3–6.

2.3 Results and Discussion

2.3.1 Reference Scenario

The Reference scenario includes updates to biomass yields, processing, and refining, as do the net-zero scenarios, but includes no emissions reduction policy. Rather, changes in energy

[12] https://www.energy.gov/eere/bioenergy/sustainable-aviation-fuel-grand-challenge

technology deployments and bioenergy consumption are driven by standard technology costs and other parameters in GCAMv6.

Despite a lack of climate policy, bioenergy production expands in the Reference scenario, driven by growth in second-generation bioenergy crops (both shades of green in Figure 2.2a), which experience significant yield improvements. Second-generation crops increase to 3.6 EJ in 2050, representing 45% of bioenergy supply. This growth is somewhat balanced by a decrease in corn for ethanol (the Reference scenario does not include an explicit representation of the Renewable Fuel Standard or similar policies) and biomass from agricultural residues, leading to a total biomass supply increase of 2.9 EJ, or 57%, between 2020 and 2050.

The increased biomass supply is roughly evenly split between biofuel production and bioelectricity generation by 2050 (Figure 2.2Figure 2.2b). Demands for delivered biomass in buildings and industry, biomass for gasification, and biomass oil for biodiesel remain roughly constant after 2025. Consumption of corn for ethanol falls by 0.6 EJ, or 38%, between 2020 and 2050, but this drop is more than matched by increases of 1.3 EJ and 1.1 EJ in biomass for second-generation biofuels[13] and bioelectricity, respectively, between 2020 and 2050. Despite these increases, generation of bioelectricity only contributes 1.8% of total electricity generation in 2050 and total biofuel production, including biodiesel, corn ethanol, and second-generation biofuels, slightly decreases by 0.05 EJ between 2020 and 2050. Refined liquid production remains dominated by oil, with less than 8% of production originating from biomass feedstock in 2050.

[13] Second-generation bioenergy crops are not currently used to produce biofuels at commercial scale.

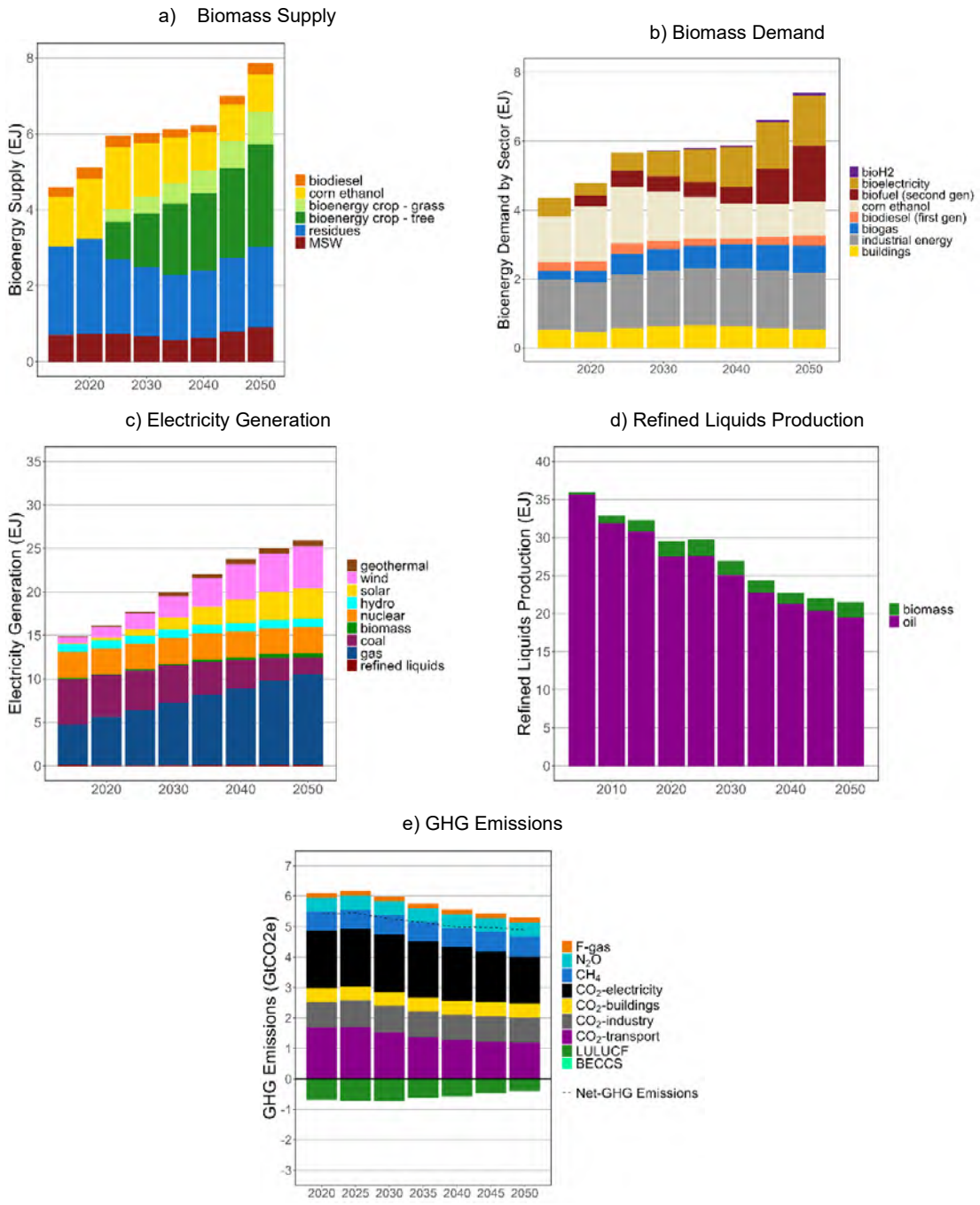

Figure 2.2. For the Reference scenario modeled in GCAM, a) Biomass supply by feedstock, b) Biomass demand by sector/energy conversion technology, c) Electricity generation by fuel,d) Refined liquids production by fuel, e) GHG emissions by gas and sector

2.3.2 Net-Zero Scenarios

All of the net-zero scenarios, by definition, reach net-zero GHG emissions in 2050, but they achieve this target through differing strategies (Figure 2.3). Non-CO_2 GHG emissions, which are harder to mitigate (U.S. EPA 2019), vary little between the six scenarios; the differences between the scenarios are dominated by the balance of positive and negative CO_2 emissions.

As the SAF target increases, total negative emissions decrease, and negative emissions come increasingly from BECCS rather than DAC and terrestrial carbon sequestration. By 2050, total carbon dioxide removal in the scenario is roughly 1.9 billion metric tons CO_2/yr in the DAC.Ref_noSAF scenario, which declines to about 1.7 billion metric tons CO_2/yr in the DAC.Ref_SAF100pct scenario. BECCS accounts for roughly 57% of the CDR in the DAC.Ref_SAF100pct scenario (sequestering 970 million metric tons CO_2/yr) compared with about 47% (890 million metric tons CO_2/yr) in the DAC.Ref_noSAF scenario. The SAF requirement leads to an overall increase in bioenergy use, and given the 2050 net-zero requirement, this is most efficiently combined with CCS, reducing demand for negative emissions from DAC. CDR from DAC decreases from roughly 360 million metric tons CO_2/yr in the DAC.Ref_noSAF scenario to roughly 120 million metric tons CO_2/yr in the DAC.Ref_SAF100pct scenario.

At the same time as the distribution of negative emissions changes, the distribution of positive CO_2 emissions also varies. Emissions from transportation, industry and buildings decrease in all net-zero scenarios, relative to Reference. Transportation emissions decrease more in scenarios with SAF targets relative to the scenario with no SAF target (due to greater biofuel utilization), while industry and buildings emissions decline slightly less in scenarios with SAF targets. (Because all scenarios reach the same emissions target, greater reductions in one sector correspond to lower reductions in other sectors.) Transportation emissions are lower with more SAF/biofuels because those biofuels displace oil in aviation fuel and other liquid fuels that are primarily consumed by the transportation sector. Annual transportation emissions in 2050 decrease from 520 million metric tons CO_2 in the DAC.Ref_noSAF scenario to 290 million metric tons CO_2 in the DAC.Ref_SAF100pct scenario. Within transportation, aviation accounts for virtually all the emission reductions in the DAC.Ref_SAF100pct scenario compared to the DAC.Ref_noSAF scenario, with only small changes in emissions from other transportation subsectors (e.g., passenger, freight, shipping). Specifically, aviation CO_2 emissions are roughly 230 million metric tons CO_2/yr in 2050 in the DAC.Ref_noSAF scenario and decline to zero when 100% of aviation fuel demand is met with SAF.

With more advanced and cheaper DAC technologies available, there is an increase in negative emissions from DAC, as well as an increase in total negative emissions. Advanced DAC technology increases total negative emissions by 480 million metric tons CO_2, relative to scenarios with the same SAF policy but reference DAC technology. As a side effect, across the range of SAF assumptions, more DAC usage is paired with higher positive CO_2 emissions across all end-use sectors, as there is greater headroom for positive CO_2 emissions when there are more negative emissions.

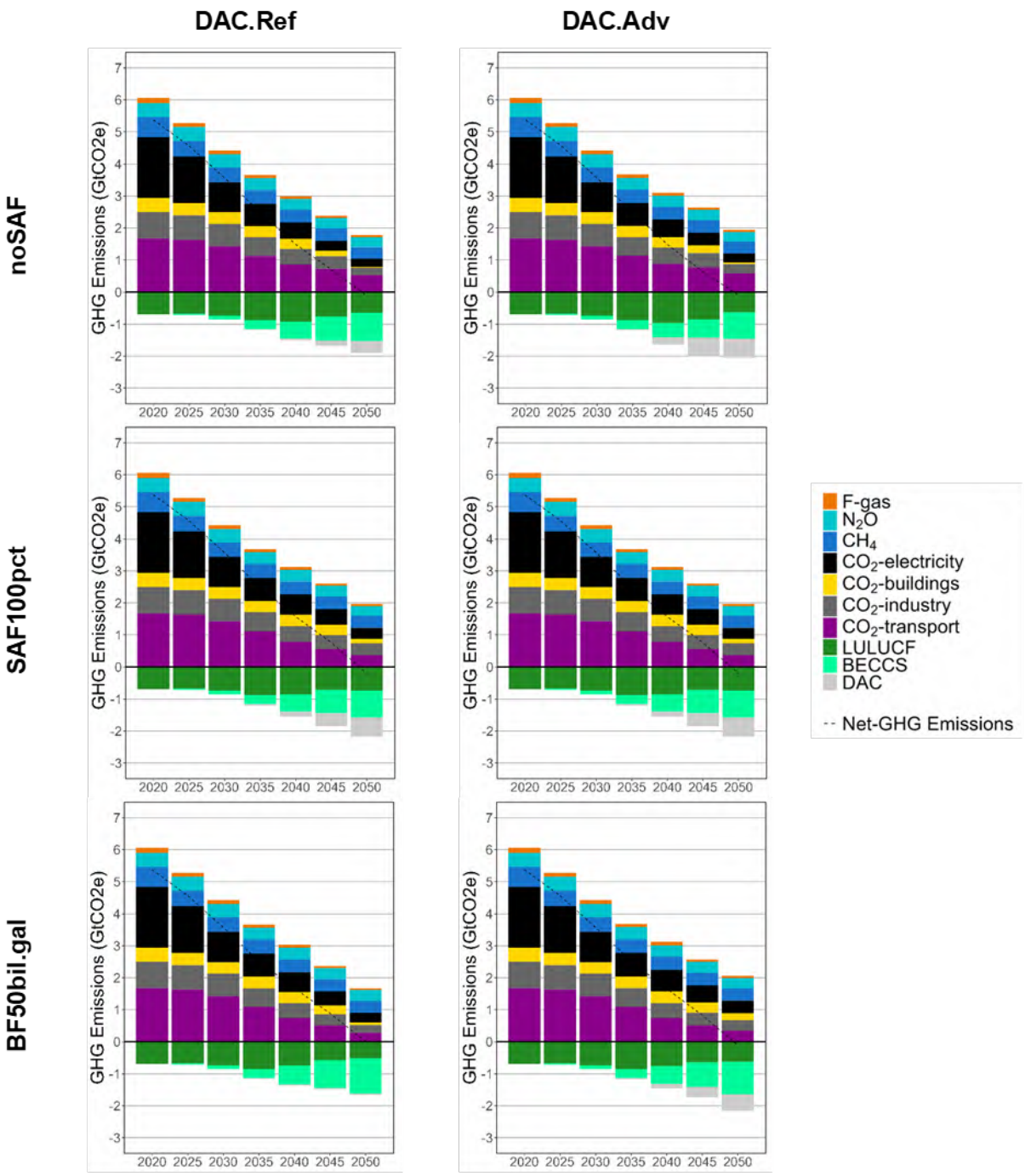

Figure 2.3. Greenhouse gas emissions by scenario in $GTCO_2e$, with either reference DAC technology (left column) or advanced DAC technology (right column) and increasing biofuel requirements moving from top to bottom

As SAF targets increase, so too does total biomass production and consumption. Total biomass supply increases from 5.0 EJ in 2020 to 14.8 EJ, 19.2 EJ, and 22.8 EJ for the DAC.Ref_noSAF, DAC.Ref_SAF100pct, and DAC.Ref_BF50bil.gal scenarios, respectively, in 2050 (Figure 2.4).

However, there is little variation between scenarios in biomass supply from MSW, crop residues, or first-generation biomass crops. The variation in total supply is primarily influenced by differences in second-generation grass and tree bioenergy crop supplies. Supplies of these second-generation crops reach 9.1 EJ, 13.5 EJ, and 16.8 EJ in 2050 in the DAC.Ref_noSAF, DAC.Ref_SAF100pct, and DAC.Ref_BF50bil.gal scenarios, respectively. Compared to the Reference case in 2050, 28%–36% less land is dedicated to cropland (for nonenergy crops) across the net-zero scenarios, with biomass and afforestation accounting for most of the change. For example, in the DAC.Ref_noSAF scenario, afforestation accounts for about 50% of the total change in land allocation in 2050 (relative to the Reference scenario), with second-generation bioenergy crops accounting for 46%.

Tree crops make up a larger proportion of this second-generation production than grass crops, with roughly a 70–30 split between tree and grass crops in all scenarios in 2050. Although yields in most water basins are higher for grass crops than for tree crops, nonland costs for growing biomass trees (most significantly fertilizer costs, with a smaller margin for other production costs) tend to be lower than those for grass crops in GCAM, driving the overall preference for tree crops in the model. It's important to note that other characteristics (beyond yield and cultivation cost) also impact their suitability for different conversion processes; at present, GCAM combines all feedstocks into a single biomass commodity and thus does not capture the impact of other factors which may influence these feedstocks' market potential. The bottom-up analyses in Chapters 4–6 explore some of these factors.

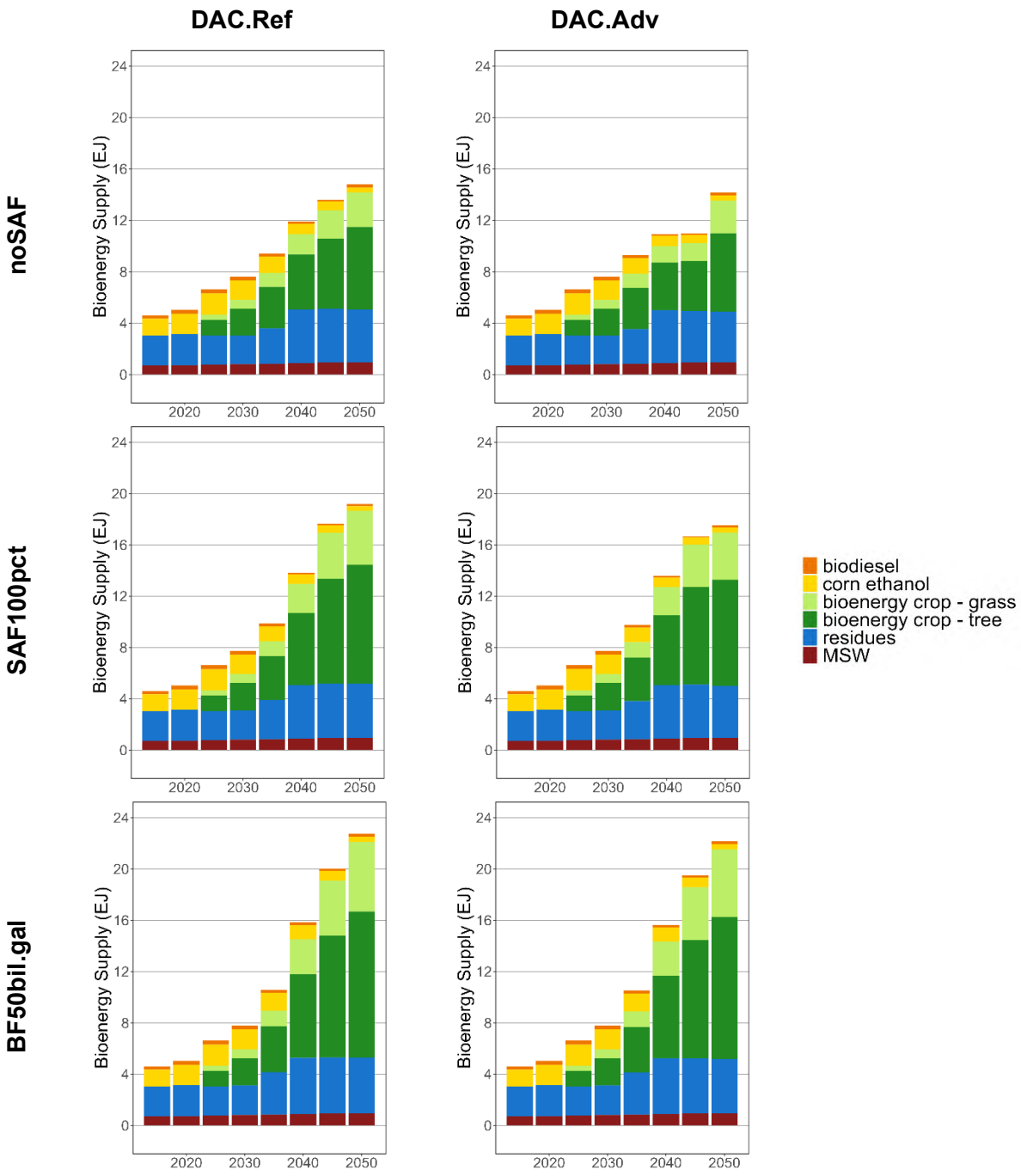

Figure 2.4. Biomass supply by feedstock in EJ, with either reference DAC technology (left column) or advanced DAC technology (right column) and increasing biofuel requirements moving from top to bottom

In addition to total bioenergy supply, the distribution of demand for biomass across sectors differs greatly depending on the SAF target (Figure 2.5). In the DAC.Ref_noSAF scenario, 3.1 EJ of biofuels are demanded to produce second-generation biofuels, compared with 9.5 EJ of combined demand for electricity and hydrogen generation. This preference for using biomass in

electricity and hydrogen generation is in part due to a greater ability to capture carbon when converting biomass into these secondary energy carriers. Whereas in biofuel production much of the carbon still remains in the fuel product and is released into the atmosphere by final consumers, for electricity or hydrogen all of the carbon in the feedstock is released during conversion, meaning more CO_2 is available to capture and store. Despite its importance for carbon sequestration, bioenergy accounts for a small portion (5%) of total electricity generation in the DAC.Ref_noSAF scenario (Figure 2.6); however, bioelectricity with CCS accounts for 50% of carbon sequestration from BECCS across all sectors (i.e., electricity, refined liquids, and hydrogen). In addition to the greater carbon capture capability of electricity and hydrogen production, there is much more investment opportunity in these energy carriers than in refined liquids. While electricity generation grows by 111% between 2020 and 2050 in the DAC.Ref_noSAF scenario, refined liquid production falls by 54% due to the electrification of end uses throughout the economy (Figure 2.7). In this scenario, there is little demand for new capacity build-out in refined liquids, whereas new electricity and hydrogen capacity are needed to meet the growing demands of a decarbonized economy. Additionally, bioelectricity with CCS may be a cost-effective way to produce power and offset emissions from uncaptured fossil fuel peak generators (especially gas) which can support important grid services such as resource adequacy (Mai et al. 2022).

As SAF requirements increase, bioenergy shifts from electricity and hydrogen generation to liquid fuel production. Biomass inputs to liquid fuel production in 2050 for DAC.Ref scenarios grow from 3.1 EJ in the noSAF case to dominate the biomass demand with 14.2 EJ and 19.1 EJ, respectively, in the SAF100pct and BF50bil.gal cases. The demand for biofuels in the SAF100pct and BF50bil.gal cases is mostly driven by the aviation sector, which requires 3.4 EJ of SAF in 2050. Meeting the aviation sector demand uses between 12.3 EJ and 14 EJ of biomass inputs across all SAF100pct and BF50bil.gal scenarios. This range reflects different distributions of bioliquid conversion pathways across scenarios, with the FT pathway producing more liquid fuel per unit of biomass feedstock but the cellulosic ethanol to jet pathway producing a higher proportion of SAF to other liquid fuels.

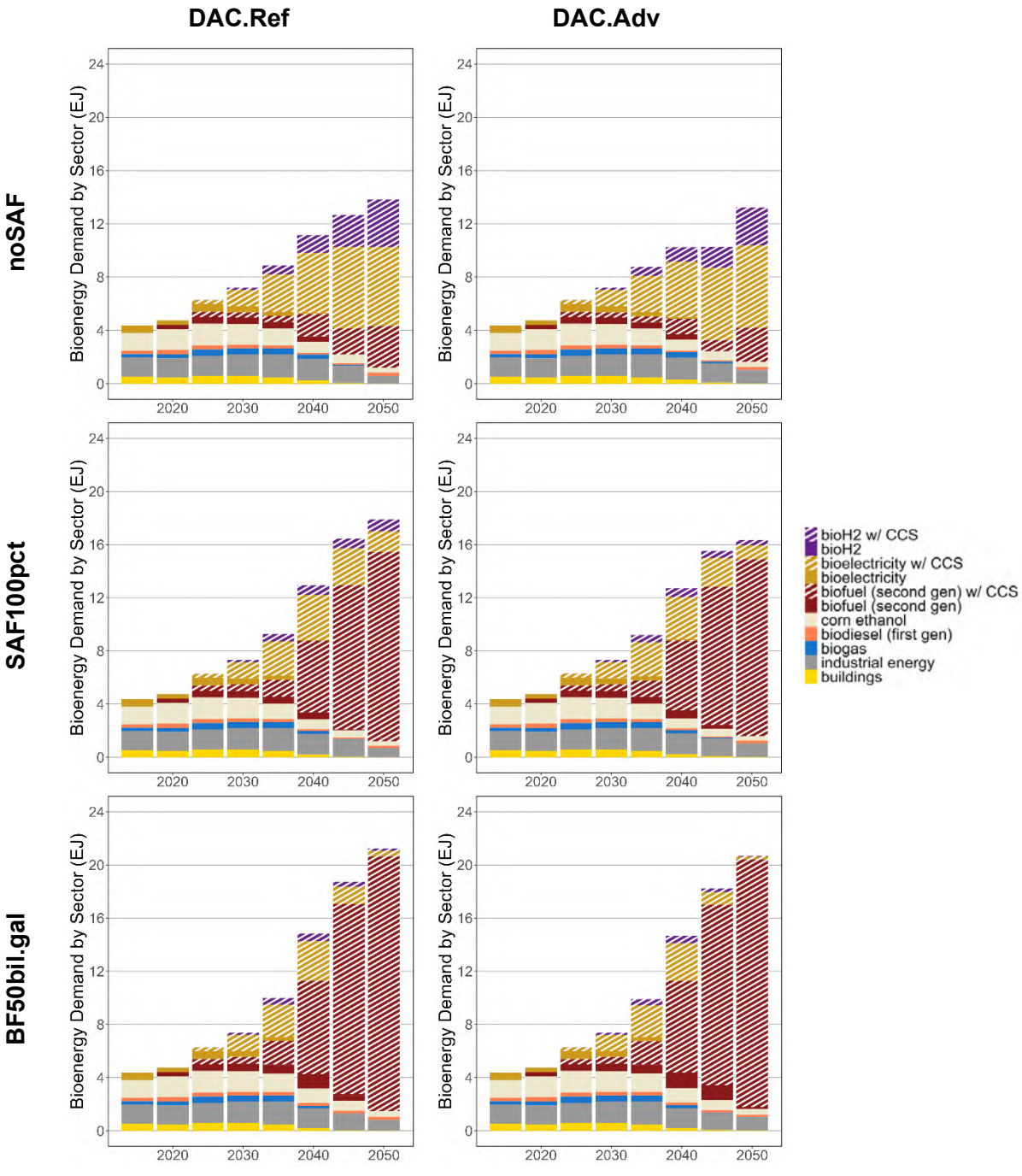

Figure 2.5. Biomass demand by sector in EJ, with either reference DAC technology (left column) or advanced DAC technology (right column) and increasing biofuel requirements moving from top to bottom

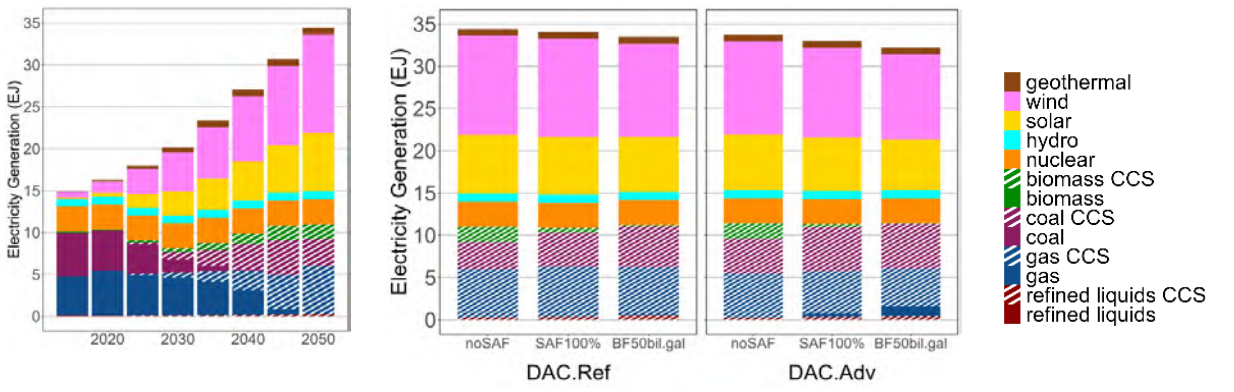

Figure 2.6. Electricity generation by fuel in EJ across time for the DAC.Ref_noSAF scenario (left) and in 2050 for all net-zero scenarios (right)

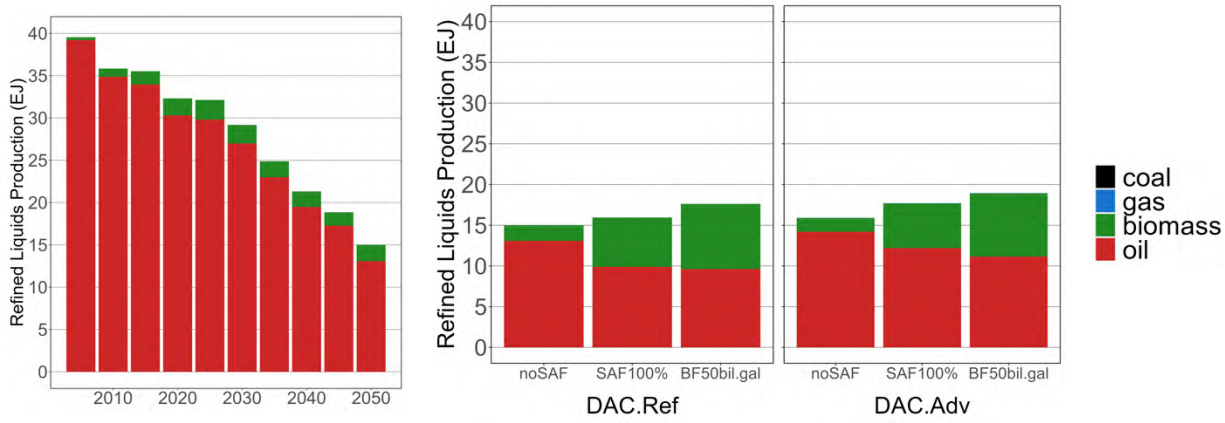

Figure 2.7. Refined liquids production by feedstock in EJ, including both aviation fuel and generic refined liquids

All years displayed for the DAC.Ref_noSAF scenario (left), and only 2050 displayed for all net-zero scenarios (right)

With more advanced DAC, the model can achieve net-zero GHG emissions with slightly less biomass compared to scenarios with reference DAC (see again Figure 2.4). With a less expensive alternative source for negative emissions, the overall demand for bioenergy decreases, although the reduction is relatively small (3%–9%, depending on SAF policy). However, this effect does not occur until 2040, as DAC deployment is near-zero through 2035 when ample lower-cost mitigation opportunities are available to meet the scenario's emissions target. In the SAF100pct case, total biomass demand is equivalent between the two DAC scenarios in 2030, but the DAC.Adv scenario has 0.23 EJ less demand than the DAC.Ref scenario in 2040 and 1.6 EJ less demand in 2050. This reduction in demand is split approximately evenly between a decrease in biomass inputs to liquid fuel production and a decrease in biomass inputs to electricity and hydrogen production. The reduction in biofuel inputs does not affect the production of aviation fuels, instead causing a shift to ethanol-to-jet (ETJ) pathways that produce a higher ratio of SAF to other liquid fuel products. A more detailed description of the various conversion processes is provided in Chapter 5.

2.3.3 Allocation of Biomass Across Competing Uses

As mentioned above, absent specific policies prioritizing biomass utilization for liquid fuels, GCAM allocates the greatest fraction of bioenergy in net-zero scenarios to the electricity sector, followed by hydrogen production and refining. But what factors drive electricity to be the dominant use of bioenergy in GCAM net-zero scenarios? In short, despite higher abatement costs for bioelectricity than for biohydrogen and biofuels, bioenergy deployment is led by bioelectricity because of rising demand for, and therefore greater opportunity for new investment in, electricity as more end uses electrify in the coming decades. However, these results are sensitive to assumptions about stock-turnover in the refining sector, grid decarbonization and availability of CDR. If existing fossil fuel refining capacity retires more rapidly, liquid biofuel deployment increases and becomes the predominant use of bioenergy economywide.

Table 2.3 (below) presents the technology costs and emissions intensities of bioenergy compared to select sectoral incumbent technologies for the DAC.Ref_noSAF scenario in 2030 and 2050. Both the technology costs and emissions factors are GCAM model outputs and thus vary across scenarios and across years within each scenario. Technology costs include both nonenergy (e.g., capital, operations and maintenance costs and fuel costs and vary mostly based on changes in fuel prices (e.g., oil, gas, biomass, electricity). Solar photovoltaic costs also include GCAM's variable renewable energy variable renewable energy integration costs, which reflect profile, intermittency, and other challenges associated with high levels of variable renewable energy penetration[14]. Solar photovoltaic module costs are based on NREL's Annual Technology Baseline and decrease from 2030 to 2050, although more significant cost improvements are observed between 2020 and 2030. Costs for all bioenergy technologies rise between 2030 and 2050 due to increasing demand for, and price of, biomass feedstocks. For hydrogen electrolysis, the cost increase from 2030 to 2050 is driven by rising electricity prices, which make up the bulk of the levelized costs. One important note is that GCAM's nonenergy (e.g., capital, operations and maintenance) costs are exogenously prescribed and are not a function of technology deployment and associated learning, supply-chain constraints or economies of scale; technologies with greater market share (such as solar photovoltaic energy) could experience different trajectory of cost reductions than assumed in this analysis.

Emissions intensities reflect carbon uptake during feedstock cultivation, indirect emissions from nitrogen fertilizer emissions (for bioenergy feedstocks) and electricity generation (for hydrogen production), direct emissions from conversion processes, carbon removal (for BECCS technologies), and end-use emissions (in the case of refined liquids, which produce emissions upon combustion in end-use sectors). One important omission is land-use change emissions from bioenergy production; our scenarios are not designed to solely perturb bioenergy feedstock demand and carefully measure all direct and indirect land-use change emissions. Similarly,

[14] Previous studies have compared GCAM's VRE integration approach to other models, such as the Regional Energy Deployment System (ReEDS) electricity-sector model. Section 3.4.2 of the following report contains a more detailed discussion of this approach and description of alternative approaches to representing VRE integration. Binsted, Matthew, Harry Suchyta, Ying Zhang, Laura Vimmerstedt, Matt Mowers, Catherine Ledna, Matteo Muratori, and Chioke Harris. 2022. Renewable Energy and Efficiency Technologies in Scenarios of U.S. Decarbonization in Two Types of Models: Comparison of GCAM Modeling and Sector-Specific Modeling. Golden, CO: National Renewable Energy Laboratory. NREL/TP-6A20-84243. https://www.nrel.gov/docs/fy23osti/84243.pdf

emissions from manufacturing the technologies (e.g., solar photovoltaic panels, electrolyzers) are not included in this analysis, although they are considered in the LCA in Chapter 6.

A few insights emerge from Table 2.3. First, bioelectricity with CCS, relative to solar photovoltaic energy, has both the greater abatement potential per unit of energy produced and the higher unit cost of emissions abatement. Second, hydrogen production from biomass with CCS has the lower cost of emissions abatement (across the three sectors analyzed in Table 2.3) relative to the sectoral incumbent (electrolysis). Note that this analysis assumes that electrolysis consumes grid electricity and pays the same electricity price as other large industrial users. Electricity prices (and grid electricity emissions) are key drivers of the relative abatement cost and potential of bioenergy in the hydrogen sector. Finally, FT biofuels with CCS (capturing both process and combustion emissions) have a low abatement cost compared with bioelectricity with CCS in 2030. However, by 2050, the abatement costs between FT biofuels and bioelectricity are similar, due mostly to declining oil demand and associated price drops, with oil prices down more than 40% in 2050 relative to 2020.

Table 2.3. Bioenergy Technology Cost and Emissions Intensity Compared to Select Alternative Technologies for the DAC.Ref_noSAF Scenario in 2030 and 2050

Sector	Technology		Year	Cost (2019$/GJ)	Emissions Factor (gCO2e/MJ)	Abatement Cost (2019$/tCO2e)
Electricity	bioenergy tech	Biomass w/ CCS	2030	$ 60.15	-284.67	
Electricity	alternative tech	PV	2030	$ 28.69	0	
Electricity	difference		2030	$ 31.46	-284.67	$ 110.51
Electricity	bioenergy tech	Biomass w/ CCS	2050	$ 75.65	-258.02	
Electricity	alternative tech	PV	2050	$ 33.90	0	
Electricity	difference		2050	$ 41.75	-258.02	$ 161.81
Hydrogen	bioenergy tech	Biomass to H2 w/ CCS	2030	$ 26.63	-188.61	
Hydrogen	alternative tech	Electrolysis	2030	$ 64.75	74.31	
Hydrogen	difference		2030	$ (38.12)	-262.92	$ (144.99)
Hydrogen	bioenergy tech	Biomass to H2 w/ CCS	2050	$ 38.13	-178.96	
Hydrogen	alternative tech	Electrolysis	2050	$ 78.36	7.69	
Hydrogen	difference		2050	$ (40.23)	-186.65	$ (215.54)
Refining	bioenergy tech	FT Biofuels w/ CCS (process & combustion CCS)	2030	$ 29.87	-106.69	
Refining	alternative tech	Oil Refining	2030	$ 21.51	77.09	
Refining	difference		2030	$ 8.36	-183.78	$ 45.49
Refining	bioenergy tech	FT Biofuels w/ CCS (process & combustion CCS)	2050	$ 41.05	-105.75	
Refining	alternative tech	Oil Refining	2050	$ 14.33	76.66	
Refining	difference		2050	$ 26.72	-182.41	$ 146.48

Technology costs in GCAM are a combination of exogenous capital and operations and maintenance costs and endogenous fuel costs. Thus, the levelized costs shown here are model outcomes and vary across scenario and model period. GCAM's electricity capital and operations and maintenance costs for this study are based on NREL's Annual Technology Baseline 2021 ("Moderate" case). GCAM uses a capital recovery factor of 13% for energy transformation sectors, so levelized costs will differ from those in the Annual Technology Baseline. GCAM's H_2 production technology capital and operations and maintenance costs are based on the NREL Hydrogen Analysis Model (H2A) (version 3) (a detailed description of GCAM's representation of hydrogen technologies is available at http://jgcri.github.io/gcam-doc/cmp/359-Hydrogen_and_transportation.pdf). Bioliquid capital and operations and maintenance technology costs in GCAM come from the NREL techno-economic analysis conducted as part of this study (Chapter 5).

Figure 2.8 presents these abatement costs as a function of carbon price; the x-intercept corresponds to the GHG abatement cost in Table 2.3. This reinforces the point that while FT bioliquids with CCS have a lower abatement cost than bioelectricity with CCS, the latter is more valuable at higher carbon prices because it sequesters more CO_2 (thus producing more negative emissions). In the DAC.Ref_noSAF scenario in 2030, GCAM's carbon price is higher than the breakthrough abatement price (carbon price where the technology's abatement cost relative to the sectoral incumbent is zero) for all three sectors, but lower than the point at which bioelectricity with CCS is more valuable.

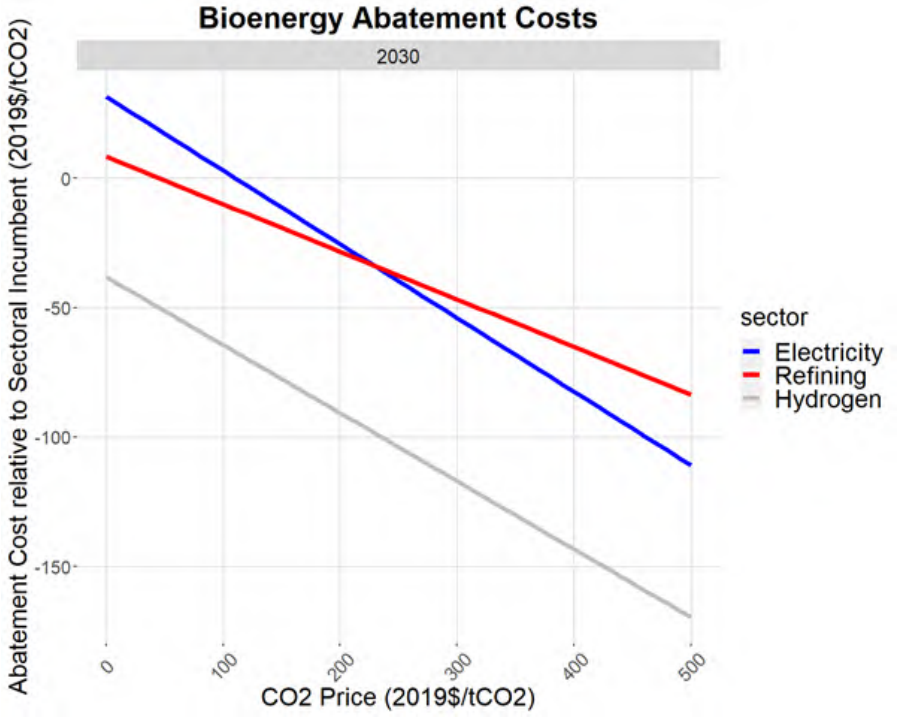

Figure 2.8. Bioenergy technology abatement costs compared to select sectoral incumbent technologies for the DAC.Ref_noSAF scenario in 2030

The question remains, then, why bioliquids (and biohydrogen) deployment is lower than that of bioelectricity in scenarios without explicit bioliquids policies. As Figure 2.9 demonstrates, this result is driven by the stock turnover dynamics within GCAM. In each of the energy transformation sectors (i.e., electricity generation, refining, and hydrogen production), technologies are assumed to have multidecadal lifetimes, with the technology stock accumulating over time. Existing capacity (e.g., technologies installed in previous model periods) retires at the end of its technical lifetime or when it becomes unprofitable to operate because of shifting economic conditions in a scenario.

Figure 2.9a shows the share of new investment in each sector captured by BECCS technologies for the DAC.Ref_noSAF scenario. Consistent with the relative abatement cost calculation, biohydrogen with CCS captures the largest investment share across the three sectors. Bioliquids with CCS capture the next highest investment share, with bioelectricity with CCS accounting for the lowest bioenergy share of new investment across sectors, rarely accounting for more than 5% of new power sector generation.

a)

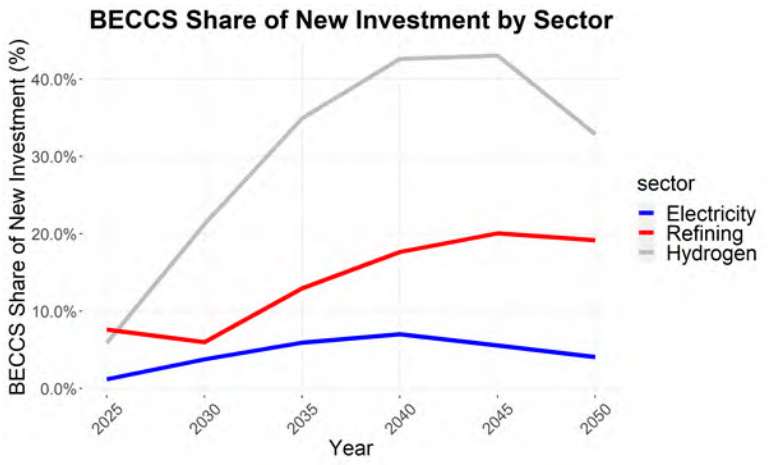

b)

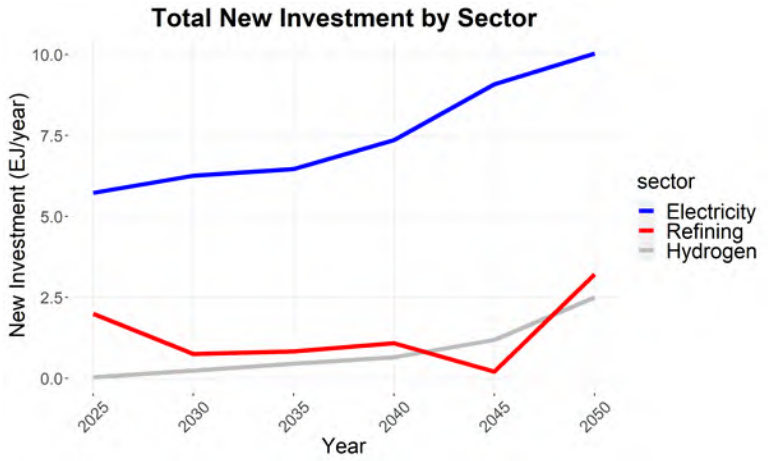

c)

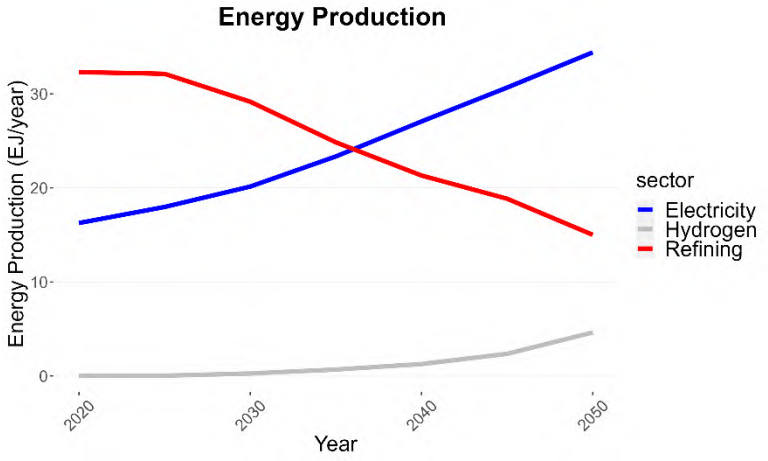

Figure 2.9. For the United States in the DAC.Ref_noSAF scenario, a) bioenergy with CCS technology shares of new investment by sector for key energy transformation sectors; b) total new investment (across all technologies) by sector; and c) total energy production by sector

Figure 2.9b shows the total new investment by sector (across all technologies), while Figure 2.9c shows total energy output for the electricity, refining, and hydrogen production sectors (for the DAC.Ref_noSAF scenario). From this, it is easy to observe that the greatest growth in these energy transformation sectors occurs in electricity generation, driven by rapid electrification of end uses like buildings and passenger vehicles. Hydrogen production and investment grows steadily but makes up a relatively small portion of secondary energy. Conversely, demand for refined liquids, the largest source of secondary energy historically, declines by more than 50% in 2050 relative to 2020. This significantly limits opportunities for investment in new refining capacity, and, therefore, the overall scale of bioliquids deployment.

One important caveat is that GCAM does not currently represent international trade of refined liquids products (only crude oil). In reality, the United States does currently export some (about 15%) of its refined liquids products abroad. If global market demand for U.S. refined liquids products grows in the future, that could create an opportunity for increasing U.S. refined liquid capacity and greater bioliquids production. However, our scenarios assume that the rest of the world is also decarbonizing their economies (though not necessarily as rapidly as the United States), resulting in a 17% decrease in global refined liquid consumption between 2020 and 2050 in the DAC.Ref_noSAF scenario.

Clearly, stock turnover in the refining sector is an important factor influencing the allocation of biomass resources across competing uses. Stock turnover in refining is uncertain because refineries tend to have very long lifetimes and are regularly updated and expanded. For example, the United States had 129 operational petroleum refineries at the start of 2023; more than 100 of those refineries (and more than 90% of the country's total refining capacity) were constructed before 1975 (EIA 2023a). Even for the country's relatively newer refineries (constructed in 1975 or later), their refining capacity has more than tripled since the facilities' initial operating dates (EIA 2023a). Additionally, refineries are relatively capital-intensive facilities; however, because of their long-lived nature, most existing refineries have amortized the majority of their capital investments and thus incur only operating costs (Favennec 2022). Conversely, building new biorefineries entails both new capital expenditures and operating costs, giving incumbent fossil fuel refineries an inherent advantage in a stagnant or declining fuels market. However, it is possible to transition facilities from refining petroleum to refining biofuels (e.g., the Phillips 66 Rodeo refinery in California [EIA 2023b]), potentially defraying some of the capital costs of expanding biorefining capacity.

To further probe the sensitivity of GCAM model results to assumptions about the rate of existing fossil fuel refining capacity stock turnover, we conducted a simple experiment where we shortened the maximum and average lifetimes for existing refineries from 50 years and 30 years (default), respectively, to 40 years and 20 years. The results of this experiment are shown in Figure 2.10 for the DAC.Ref_noSAF scenario. With a 10-year reduction in average and maximum lifetime of existing refineries, the "shorter lifetime" sensitivity leads bioliquids to become the largest source of bioenergy demand in the United States in 2050, consuming 45% of bioenergy inputs, followed closely by bioelectricity and then biohydrogen, which consume 33% and 18% of bioenergy inputs, respectively. However, the level of biomass allocated to bioliquids in the "shorter lifetime" sensitivity scenario (~6 EJ) is still significantly lower than in either of the SAF policy scenarios, regardless of DAC assumptions (see Figure 2.5).

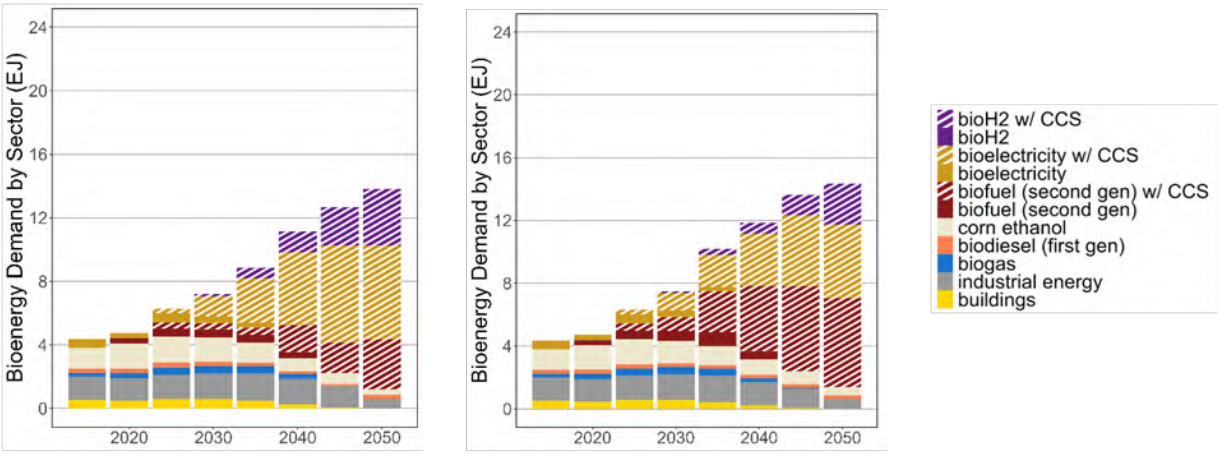

Figure 2.10. Biomass supply by sector in EJ for scenarios with default lifetimes (30-year average, 50-year maximum) vs. shorter lifetimes (20-year average, 40-year maximum) for existing U.S. refineries

2.3.4 Comparison With IPCC Scenario Database

To place these results within the context of the broader integrated assessment model literature, we compare our results to the International Panel on Climate Change's Sixth Assessment Report (AR6) scenario database (Byers et al. 2022). We find that the bioenergy results from this report fall within the range of AR6 scenarios, but with slightly more bias toward biofuel production rather than bioelectricity generation. The AR6 database contains results from 188 modeling frameworks related to climate change mitigation. For this comparison, we used only models with separate results for the United States and where net-CO_2 emissions in the United States reach zero by 2050. Note that many of these scenarios do not achieve net-zero GHG emissions (which is significantly more stringent than net-zero CO_2 emissions), but all represent significant decarbonization by midcentury. 86 scenarios in the AR6 database met the net-zero CO_2 target for the United States, across 15 modeling frameworks. However, not all variables are included for each model/scenario combination, so the number of AR6 lines vary in each comparison figure below. Since some GCAM scenarios are included in the AR6 database, we refer to the GCAM scenarios for this study as the GCAM-DECARB scenarios.

In terms of total U.S. bioenergy consumption and the percentage of primary energy produced by bioenergy (Figure 2.11), the GCAM-DECARB scenarios are well within the range of the AR6 scenarios. In 2050, U.S. bioenergy consumption in the AR6 database ranges from 3.3 EJ to 38.5 EJ with an average of 19.7 EJ, compared to the range for this study of 14.2 EJ to 22.8 EJ. In the AR6 database, bioenergy represents on average 25.4% of total 2050 primary energy production, compared with 20.5% in the GCAM-DECARB scenarios.

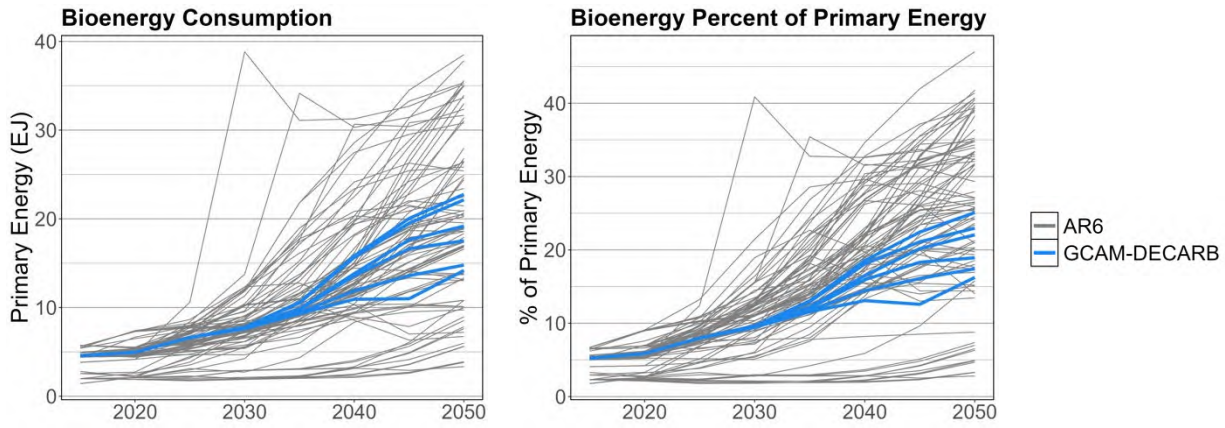

Figure 2.11. U.S. bioenergy consumption in EJ (left) and bioenergy percentage of primary energy (right) for the AR6 scenarios (gray) and the GCAM-DECARB scenarios (blue)

As in the GCAM-DECARB scenarios, the AR6 scenarios see an important role for bioenergy in combination with CCS. In all AR6 scenarios, at least 50% of U.S. bioenergy consumption is combined with CCS, with an average of 78%, compared with the GCAM-DECARB range of 88%–96% (Figure 2.12). Much of this difference is likely explained by the difference in the levels of negative emissions required to achieve net-zero GHG emissions in GCAM-DECARB versus the net-zero CO_2 filter we use for the AR6 scenario.

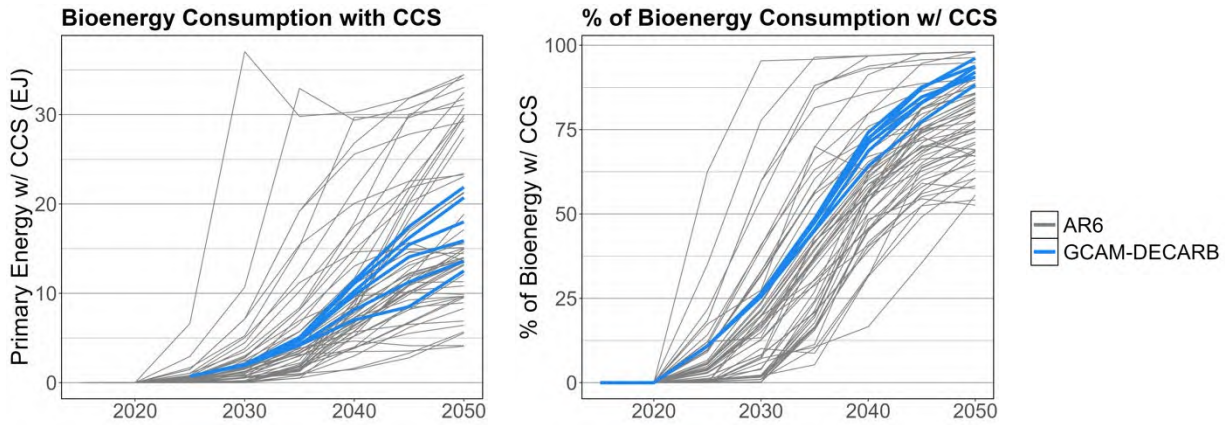

Figure 2.12. U.S. bioenergy with CCS consumption in EJ (left) and percentage of bioenergy used with CCS (right) for the AR6 scenarios (gray) and the GCAM-DECARB scenarios (blue)

To meet this demand for bioenergy, a large growth in biomass production occurs across most scenarios (Figure 2.13). Total U.S. energy crop production rises steeply between 2020 and 2050 in most, but not all, AR6 scenarios. Average production reaches 570 million dry metric tons in 2050, with a range of 30 to 1,760 million metric tons, compared to average GCAM-DECARB production of 730 million metric tons in 2050. Scenarios at the lower end of the AR6 range for U.S. bioenergy crop production may in part reflect greater imports of biomass rather than growing energy crops domestically (which we did not allow in GCAM-DECARB), rather than strictly lower U.S. bioenergy use.

Significant land area is required to cultivate the rapidly growing biomass supply. The GCAM-DECARB scenarios use between 28 and 53 million hectares (Mha) for dedicated bioenergy crops in 2050. For reference, about 12.5 Mha of U.S. cropland was allocated to corn crops for ethanol in 2022 (authors' calculations from U.S. Department of Agriculture Economic Research Service [USDA ERS 2023] data[15]), although replacing some grain in livestock diets with biorefinery coproducts like DDGS (distiller's dried grains with solubles) could lower the land area attributed to corn ethanol production (Mumm et al. 2014). The state of Colorado is 27 Mha, so the GCAM-DECARB range of U.S. land area allocated for dedicated bioenergy crops in 2050 roughly covers between one and two times the land area of Colorado. The AR6 range is 2050 is approximately 0 to 70 Mha, with an average of 29 Mha. In addition to the impact of trade, this difference likely reflects different assumptions about energy crop yields across models.

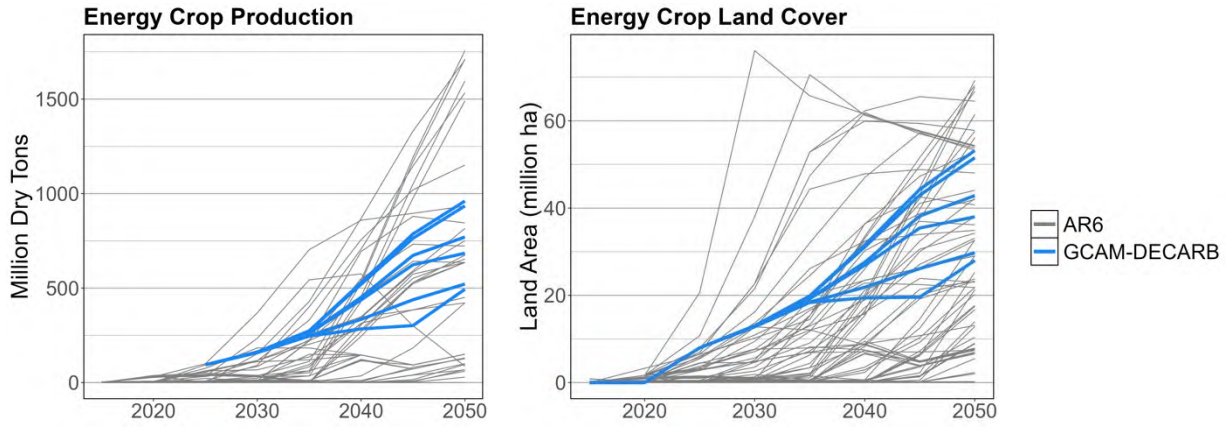

Figure 2.13. Total U.S. energy crop production in million dry metric tons (left) and energy crop land cover in million ha (right) for the AR6 scenarios (gray) and the GCAM-DECARB scenarios (blue)

Finally, we compare the production of liquid fuels, electricity, and hydrogen using biomass feedstocks (Figure 2.14). The GCAM-DECARB scenarios cover roughly the same range of biofuel production as the AR6 scenarios. GCAM-DECARB biofuel production is between 1.7 EJ and 8.0 EJ in 2050, compared with the AR6 range of 0.6 EJ to 11.6 EJ, with a mean of 4.2 EJ. In contrast, electricity and hydrogen production from bioenergy in the GCAM-DECARB scenarios fall in the lower end of the range from AR6. The scenario with the most bioelectricity production in GCAM-DECARB reaches 1.8 EJ in 2050, which is less than the AR6 average of 1.9 EJ. Similarly, maximum biohydrogen production in GCAM-DECARB is 1.5 EJ in 2050, less than the AR6 mean of 1.7 EJ.

[15] Of 13.9 trillion bushels of U.S. corn production in 2022, 5.3 trillion bushels (38%) were used for ethanol production. 80.8 million acres of U.S. land was dedicated to corn production in 2022 (harvested area); 28% of this is 30.8 million acres or 12.5 Mha.

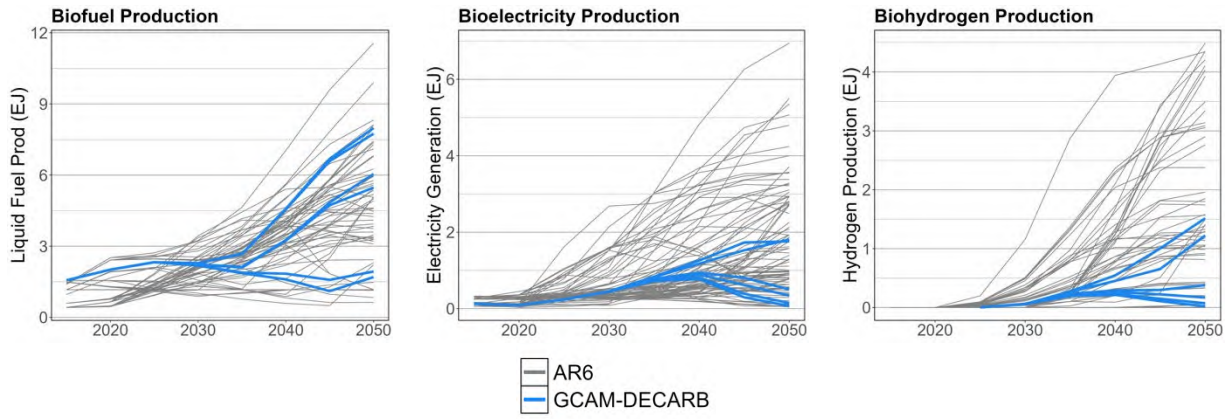

Figure 2.14. Total U.S. biofuel production (left), bioelectricity production (center), and biohydrogen production (right), all in EJ, for the AR6 scenarios (gray) and the GCAM-DECARB scenarios (blue)

The GCAM-DECARB scenarios with SAF targets prioritize bioenergy utilization for liquid fuel production and fall at the upper end of biofuel production from AR6. Conversely, GCAM-DECARB scenarios without SAF targets fall at the low end of AR6 biofuel production. This is re-enforced by Figure 2.15, which shows the fraction of total biomass feedstocks allocated to liquid biofuel production. Again, there is a clear separation between GCAM-DECARB scenarios with and without SAF targets. On average, AR6 scenarios allocate 55% of biomass to liquid fuel production, while GCAM-DECARB scenarios with biofuel targets all use 75% or more of total biomass for liquid fuels, and GCAM-DECARB scenarios without biofuel targets use less than 25% of biomass for liquid fuels. The GCAM-DECARB BF50bil.gal scenarios fall above the AR6 range in terms of percentage of biomass allocated to liquid biofuel production.

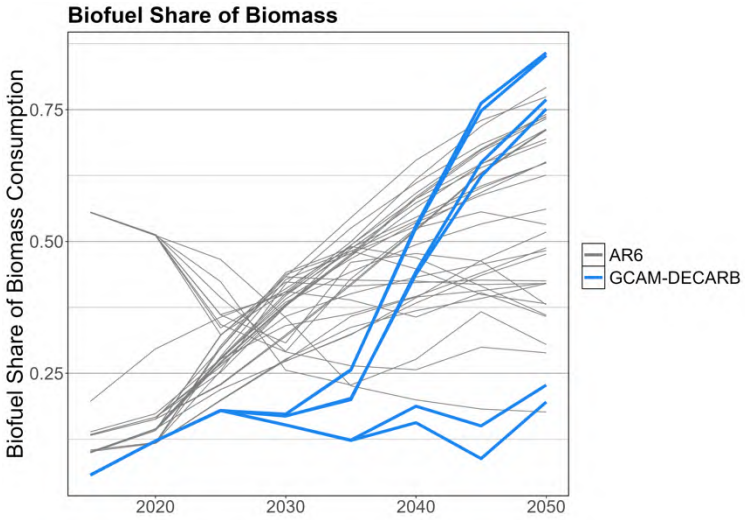

Figure 2.15. Share of total U.S. biomass feedstocks used for liquid biofuel production for the AR6 scenarios (gray) and the GCAM-DECARB scenarios (blue)

2.4 Summary and Key Insights

If the United States is to achieve its ambitious target of reducing economywide GHG emissions to net-zero by 2050, bioenergy is likely to play a major role. In the net-zero GHG scenarios explored for this analysis, economywide biomass feedstock demand ranged from 13.5 to 22.1 EJ (0.77 billion–1.26 billion metric tons) in 2050 across scenarios. CDR is an important strategy for reaching net-zero, helping offset non-CO_2 emissions and residual CO_2 emissions from hard-to-decarbonize sectors. Total CDR from all sources (i.e., land sink, BECCS, DAC) ranges from 1.6 to 2.1 Gt CO_2 across scenarios in 2050. BECCS is an important contributor to CDR, sequestering between 820 million metric tons CO_2 and 1,100 million metric tons CO_2 per year by 2050. In fact, in our scenarios, the vast majority (88%–96%) of bioenergy is used in combination with CCS. The availability of advanced DAC technologies slightly reduces demand for biomass compared to scenarios with reference DAC (Figure 2.4), although the change is relatively small (3%–9%, depending on SAF policy). Advanced DAC technology has a similarly small impact on how frequently CCS is paired with DAC (2-4% lower with advanced DAC vs. reference DAC, across SAF policy cases). This indicates that, in the context of deep decarbonization, the value of CO_2 removal from bioenergy significantly outweighs the cost of adding CCS to bioenergy facilities. It's important to note, however, that our technology representation and scenario design did not explicitly explore the competition between different biorefinery configurations that trade higher product yields (biomass conversion efficiency) for lower CDR. Further examining this tradeoff between energy provision and CDR in the context of bioenergy is an important area for continued research.

How biomass is utilized throughout the energy system depends heavily on assumptions about sustainable fuels policy and stock turnover in the refining sector. In scenarios with no SAF target, most of the available biomass feedstock is utilized to produce electric power (45%) and hydrogen (27%), with somewhat lower utilization in refined liquids production (24%). There are two main drivers of this result. First, production of bioelectricity with CCS and biohydrogen with CCS is more effective at creating negative emissions than production of liquid biofuels with CCS, and negative emissions are especially valuable for reaching deep decarbonization targets like net-zero GHG emissions. Second, across all scenarios, liquid fuel consumption decreases markedly to 2050 (Figure 2.7), while electricity and hydrogen demands increase significantly (Figure 2.6 and Figure 2.9). This limits opportunities for expansion of liquid biofuels while increasing opportunities for bioelectricity and biohydrogen to capture some of the new investment projected in GCAM. However, faster retirement of existing (fossil fuel) refining capacity can create more opportunities for deployment of liquid biofuels; stock turnover in refining is uncertain but an important factor in determining how finite bioenergy resources are utilized.

Sustainable fuel targets lead to several changes in bioenergy utilization. First, incentivizing use of bioenergy in liquid fuels increases overall biomass demand. With reference DAC assumptions, biomass demand in 2050 increases by 4.4 EJ (0.25 billion metric tons) in the scenario with 100% SAF requirements and by 8.0 EJ (0.46 billion metric tons) in the scenario with requirements for ~56 billion gallons of biofuel production relative to the scenario with no SAF or biofuel targets. Second, these targets require allocating the vast majority of all biomass feedstocks to production of liquid fuels (82% in the 100% SAF scenario and 93% in the ~56 billion gallon liquid biofuel scenario). Finally, these scenarios tend to rely less heavily on DAC

for CDR, with the ~56 billion gallon liquid biofuel scenario and the 100% SAF scenarios requiring only 50 million metric tons CO_2 and 117 million metric tons CO_2 respectively of sequestration from DAC in 2050, compared to 368 million metric tons CO_2 in the scenario without SAF targets.

This sprint study has provided an opportunity to compare and harmonize GCAM representations of bioenergy supply, transportation, conversion, and utilization with more detailed bottom-up analyses. This resulted in updates to many elements of GCAM's bioenergy system representation, including:

- Second-generation bioenergy crop yields and yield improvement (see Chapter 3, Section 3.3, subsection on Energy Crop Yield Data for GCAM Harmonization)
- Bioenergy transportation and preprocessing costs (see Chapter 4, Section 4.3.2, and especially Table 4.2, Table 4.3, Table 4.4, Table 4.5, Table 4.6, and Table 4.7)
- Bioenergy conversion pathway costs and efficiencies (see Chapter 5, Section 5.3, and especially Table 5.2 and Table 5.3)
- Separate tracking of aviation fuels.

Future efforts could build upon this work by:

- Understanding the synergies and trade-offs of bioenergy production versus using biomass for carbon sequestration.
- Evaluating the best use of biomass, including that for bioelectricity, biohydrogen, biofuels and CDR
- Sensitivity analysis around land use change for biomass cultivation
- Harmonizing bioenergy crop nonland production costs and nitrogen fertilizer inputs
- Separately representing preprocessing and/or conversion pathways for specific biomass feedstock types
- Adding additional bioenergy conversion pathways such as gasification, methanol, or catalytic fast pyrolysis

References

Browning, M., J. McFarland, J. Bistline, G. Boyd, M. Muratori, M. Binsted, C. Harris et al. 2023. "Net-zero CO_2 by 2050 scenarios for the United States in the Energy Modeling Forum 37 study." *Energy and Climate Change* 4: 100104. https://doi.org/10.1016/j.egycc.2023.100104.

Byers, E., V. Krey, E. Kriegler, K. Riahi, R. Schaeffer, J. Kikstra, R. Lamboll et al. 2022. "AR6 Scenarios Database hosted by IIASA." International Institute for Applied Systems Analysis. https://doi.org/10.5281/zenodo.5886911.

Calvin, K., P. Patel, L. Clarke, G. Asrar, B. Bond-Lamberty, R. Yiyun Cui, A. Di Vittorio et al. 2019. "GCAM v5.1: representing the linkages between energy, water, land, climate, and economic systems." *Geosci. Model Dev*. 12(2), 677–698. https://doi.org/10.5194/gmd-12-677-2019.

Clarke, L., Y.-M. Wei, A. De la Vega Navarro, A. Garg, A. N. Hahmann, S. Khennas, I. M. I. Azevedo et al. 2022. Energy Systems. In *Climate Change 2022: Mitigation of Climate Change." Contribution of Working Group III to the IPCC Sixth Assessment Report*. Cambridge, UK: Cambridge University Press. https://doi.org/10.1017/9781009157926.008.

EIA. 2021. *Annual Energy Outlook 2021*. Washington, D.C.: U.S. Energy Information Administration. https://www.eia.gov/outlooks/archive/aeo21/.

EIA. 2023a. "Frequently Asked Questions: When was the last refinery built in the United States?" U.S. Energy Information Administration. Accessed October 5, 2023. https://www.eia.gov/tools/faqs/faq.php?id=29&t=10.

EIA. 2023b. "Energy refinery capacity increased slightly for the first time since the COVID-19 pandemic. U.S. Energy Information Administration. Accessed October 5, 2023. https://www.eia.gov/todayinenergy/detail.php?id=57220.

FAA 2021. *United States 2021 Aviation Climate Action Plan.* Washington, DC: U.S. Department of Transportation Federal Aviation Administration. https://www.faa.gov/sites/faa.gov/files/2021-11/Aviation_Climate_Action_Plan.pdf.

Favennec, J. P. 2022. "Economics of Oil Refining." In *The Palgrave Handbook of International Energy Economics*. Edited by M. Hafner and G. Luciani. London, UK: Palgrave Macmillan, Cham. https://doi.org/10.1007/978-3-030-86884-0_3.

IEA. 2021. *Net Zero by 2050: A Roadmap for the Global Energy Sector* (4th revision). Paris, France: International Energy Agency. https://iea.blob.core.windows.net/assets/deebef5d-0c34-4539-9d0c-10b13d840027/NetZeroby2050-ARoadmapfortheGlobalEnergySector_CORR.pdf.

JGCRI. 2022. GCAM 6.0. College Park, MD: Joint Global Change Research Institute. https://github.com/JGCRI/gcam-core/releases/tag/gcam-v6.0.

Mai, T., P. Denholm, P. Brown, W. Cole, E. Hale, P. Lamers, C. Murphy et al. 2022. "Getting to 100%: Six strategies for the challenging last 10%." *Joule* 6(9) 1981–1994, ISSN 2542–4351. https://doi.org/10.1016/j.joule.2022.08.004.

Mumm, R. H., P. D. Goldsmith, K. D. Rausch, and H. H. Stein. 2014. Land usage attributed to corn ethanol production in the United States: sensitivity to technological advances in corn grain yield, ethanol conversion, and co-product utilization. *Biotechnol Biofuels* 7(61). https://doi.org/10.1186/1754-6834-7-61.

L. Uppink, M. Ganguli, and R. Riedel. 2023. "Making Net-Zero Aviation Possible: An industry-backed, 1.5°C-aligned transition strategy." Mission Possible Partnership. https://missionpossiblepartnership.org/wp-content/uploads/2023/01/Making-Net-Zero-Aviation-possible.pdf.

USDA ERS. 2023. "Feed Grains Sector at a Glance." U.S. Department of Agriculture Economic Research Service. https://www.ers.usda.gov/topics/crops/corn-and-other-feed-grains/feed-grains-sector-at-a-glance/. Accessed July 23, 2023.

U.S. DOE. 2016. *2016 Billion-Ton Report: Advancing Domestic Resources for a Thriving Bioeconomy, Volume 1: Economic Availability of Feedstocks*. M. H. Langholtz, B. J. Stokes, and L. M. Eaton (Leads). Oak Ridge, TN: Oak Ridge National Laboratory. ORNL/TM-2016/160. https://doi.org/10.2172/1271651.

U.S. DOE, U.S. DOT, USDA, U.S. EPA. 2022. *SAF Grand Challenge Roadmap: Flight Plan for Sustainable Aviation Fuel*. Washington, DC: U.S. Department of Energy, U.S. Department of Transportation, and U.S. Department of Agriculture, in collaboration with the U.S. Environmental Protection Agency. https://www.energy.gov/sites/default/files/2022-09/beto-saf-gc-roadmap-report-sept-2022.pdf.

U.S. DOS. 2021. *The Long-Term Strategy of the United States: Pathways to Net-Zero Greenhouse Gas Emissions by 2050*. Washington, DC: U.S. Department of State. https://www.whitehouse.gov/wp-content/uploads/2021/10/US-Long-Term-Strategy.pdf.

U.S. EPA. 2019. *Global Non-CO_2 Greenhouse Gas Emission Projections & Mitigation Potential: 2015–2050.* Washington, DC: Environmental Protection Agency Office of Atmospheric Programs. EPA-430-R-19-010. https://www.epa.gov/sites/default/files/2019-09/documents/epa_non-co2_greenhouse_gases_rpt-epa430r19010.pdf.

The White House. 2021. FACT SHEET: Biden Administration Advances the Future of Sustainable Fuels in American Aviation. Washington, DC: The White House. https://www.whitehouse.gov/briefing-room/statements-releases/2021/09/09/fact-sheet-biden-administration-advances-the-future-of-sustainable-fuels-in-american-aviation/.

2.5 Appendices

Table A.2.1. Comparison of GCAM Bioenergy Crop Yields Before/After Harmonization With ORNL Data

Region	Crop Type	Basin	Management Technology	Base Yield (2015)		Yield Improvement	
				Original	Updated	Original	Updated
USA	Grass	NelsonR	Rainfed – High Yield	0.0191	0.0235	0.0066	0.0098
USA	Grass	California	Rainfed – High Yield	0.0241	0.0065	0.0062	0.0098
USA	Grass	MissppRN	Rainfed – High Yield	0.0301	0.0357	0.0057	0.0098
USA	Grass	MissppRS	Rainfed – High Yield	0.0192	0.0436	0.0061	0.0098
USA	Grass	UsaColoRN	Rainfed – High Yield	0.0080	0.0062	0.0066	0.0098
USA	Grass	UsaColoRS	Rainfed – High Yield	0.0097	0.0097	0.0058	0.0098
USA	Grass	GreatBasin	Rainfed – High Yield	0.0098	0.0060	0.0066	0.0098
USA	Grass	MissouriR	Rainfed – High Yield	0.0214	0.0184	0.0065	0.0098
USA	Grass	ArkWhtRedR	Rainfed – High Yield	0.0229	0.0273	0.0057	0.0098
USA	Grass	TexasCst	Rainfed – High Yield	0.0293	0.0259	0.0062	0.0098
USA	Grass	UsaCstSE	Rainfed – High Yield	0.0163	0.0381	0.0062	0.0098
USA	Grass	GreatLakes	Rainfed – High Yield	0.0219	0.0293	0.0066	0.0098
USA	Grass	OhioR	Rainfed – High Yield	0.0240	0.0371	0.0057	0.0098
USA	Grass	UsaPacNW	Rainfed – High Yield	0.0261	0.0095	0.0066	0.0098
USA	Grass	TennR	Rainfed – High Yield	0.0198	0.0374	0.0057	0.0098
USA	Grass	RioGrande	Rainfed – High Yield	0.0158	0.0098	0.006	0.0098
USA	Grass	UsaCstNE	Rainfed – High Yield	0.0199	0.0311	0.0067	0.0098
USA	Grass	UsaCstE	Rainfed – High Yield	0.0188	0.0310	0.0057	0.0098
USA	Tree	NelsonR	Rainfed – High Yield	0.0191	0.0149	0.0066	0.0098
USA	Tree	California	Rainfed – High Yield	0.0241	0.0072	0.0062	0.0098
USA	Tree	MissppRN	Rainfed – High Yield	0.0301	0.0236	0.0057	0.0098

Region	Crop Type	Basin	Management Technology	Base Yield (2015)		Yield Improvement	
				Original	Updated	Original	Updated
USA	Tree	MisspRS	Rainfed – High Yield	0.0192	0.0234	0.0061	0.0098
USA	Tree	UsaColoRN	Rainfed – High Yield	0.0080	0.0057	0.0066	0.0098
USA	Tree	UsaColoRS	Rainfed – High Yield	0.0097	0.0050	0.0058	0.0098
USA	Tree	GreatBasin	Rainfed – High Yield	0.0098	0.0047	0.0066	0.0098
USA	Tree	MissouriR	Rainfed – High Yield	0.0214	0.0132	0.0065	0.0098
USA	Tree	ArkWhtRedR	Rainfed – High Yield	0.0229	0.0142	0.0057	0.0098
USA	Tree	TexasCst	Rainfed – High Yield	0.0293	0.0138	0.0062	0.0098
USA	Tree	UsaCstSE	Rainfed – High Yield	0.0163	0.0247	0.0062	0.0098
USA	Tree	GreatLakes	Rainfed – High Yield	0.0219	0.0206	0.0066	0.0098
USA	Tree	OhioR	Rainfed – High Yield	0.0240	0.0264	0.0057	0.0098
USA	Tree	UsaPacNW	Rainfed – High Yield	0.0261	0.0077	0.0066	0.0098
USA	Tree	TennR	Rainfed – High Yield	0.0198	0.0245	0.0057	0.0098
USA	Tree	RioGrande	Rainfed – High Yield	0.0158	0.0046	0.006	0.0098
USA	Tree	UsaCstNE	Rainfed – High Yield	0.0199	0.0228	0.0067	0.0098
USA	Tree	UsaCstE	Rainfed – High Yield	0.0188	0.0232	0.0057	0.0098

NOTE: Base Yield units are GJ/m.^{2} Yield Improvement is represented as an annual improvement rate (i.e., 0.0098 is equivalent to a 0.98% annual improvement).

Table A.2.2. Updates to Bioenergy Refining Efficiency, Costs, Carbon Removal, and Byproduct Production

GCAMv6 includes improvement in most variables over time, so we include the 2020 and 2050 end-point values. The updated values do not change between 2020 and 2050.

Variable	Units	Conversion Pathway	GCAMv6 - 2020	GCAMv6 - 2050	Updated (generic liquid fuels)	Updated (aviation fuel)
biomass I/O coefficient[1]	GJ in/GJ out	cellulosic ethanol	2.057	1.95	2.62	2.82
		cellulosic ethanol CCS level 1	2.139	2.028	2.62	2.82
		cellulosic ethanol CCS level 2	2.263	2.145	2.62	2.82
		FT biofuel	1.961	1.878	2.18	2.18
		FT biofuel CCS level 1	2.039	1.953	2.18	2.18
		FT biofuel CCS level 2	2.157	2.066	2.18	2.18
non-energy cost[2]	2021$/GJ	cellulosic ethanol	17.33	14.84	19.21	21.84
		cellulosic ethanol level 1	18.17	15.49	19.82	22.46
		cellulosic ethanol level 2	24.36	20.29	21.47	24.11
		FT biofuel	28.52	24.42	15.85	15.85
		FT biofuel level 1	30.90	26.27	17.33	17.33
		FT biofuel level 2	32.43	27.45	21.02	21.02
carbon capture rate[3]	% carbon captured	cellulosic ethanol CCS level 1	26%	26%	23%	23%
		cellulosic ethanol CCS level 2	90%	90%	96%	96%

Variable	Units	Conversion Pathway	GCAMv6 - 2020	GCAMv6 - 2050	Updated (generic liquid fuels)	Updated (aviation fuel)
		FT biofuel CCS level 1	82%	82%	35%	35%
		FT biofuel CCS level 2	90%	90%	99%	99%
SAF to other fuels production	ratio of SAF production : other fuel production	cellulosic ethanol	N/A*	N/A*	0:1	4.1:1
		cellulosic ethanol CCS level 1	N/A*	N/A*	0:1	4.1:1
		cellulosic ethanol CCS level 2	N/A*	N/A*	0:1	4.1:1
		FT biofuel	N/A*	N/A*	0.7:1	0.7:1
		FT biofuel CCS level 1	N/A*	N/A*	0.7:1	0.7:1
		FT biofuel CCS level 2	N/A*	N/A*	0.7:1	0.7:1

[1] biomass I/O coefficient represents the ratio of biomass feedstock inputs (in energy terms) to biofuel output

[2] non-energy costs include levelized, annualized capital costs and fixed and variable operations and maintenance (O&M)

[3] carbon capture rate is the percentage of carbon dioxide produced by the conversion process that's captured and stored

[4] SAF to other fuels production ratio is the ratio of sustainable aviation fuel to other liquid fuel types produced by the conversion pathway

* by default, GCAM does not distinguish among different types of liquid fuel products. A separate market for aviation fuels was added as part of this analysis. N/A indicates that fuel types (e.g., SAF vs. other fuels) are not explicitly represented / tracked.

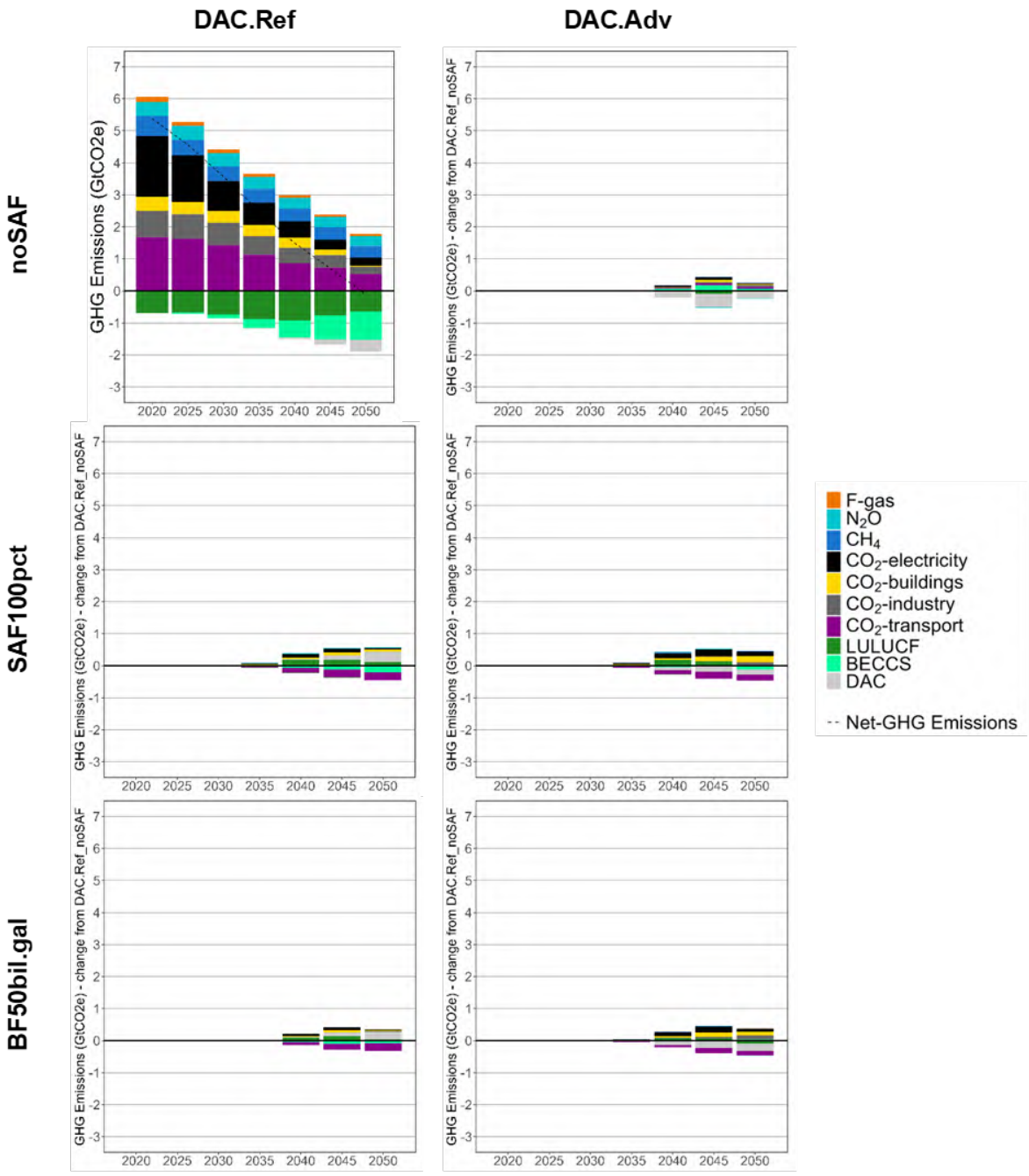

Figure A.2.1. Greenhouse gas emissions by scenario in $GTCO_2e$ for the DAC.Ref_noSAF scenario; change in emissions in $GTCO_2e$ relative to DAC.Ref_noSAF for all other scenarios. Scenarios vary by DAC technology assumptions across columns; scenarios vary by biofuel requirements across rows.

3 Feedstock Resource Assessment

3.1 Background

The objective of this analysis was to better contextualize the likely location, cost, and viability of the different levels of lignocellulosic biomass feedstock production implied in select GCAM decarbonization scenarios (Chapter 2), translating those top-down projections to more specific changes "on the ground" and ensuring that scenario analysis is well-aligned with recent DOE-supported advancements in energy crop productivity and other innovations. This analysis used the detailed bottom-up biomass resources assessment conducted in the DOE-supported BT16 to predict which regions are most likely to meet the biomass demand projected in the decarbonization scenarios, using which specific resources, and at what costs. This work provides an external point of comparison to the endogenous feedstock models built into GCAM, with increased spatial resolution, and considering a more comprehensive set of regionally appropriate candidate feedstock crops.

In addition, this chapter also calculated the rates of change in land use, crop management practices, and fertilizer consumption implied in the different decarbonization scenarios, which are practical scale-up considerations that are not always explicitly modeled or constrained during scenario development. Previous analyses have shown that bioenergy-heavy decarbonization scenarios can imply rates of new crop adoption (Turner et al. 2018) or agricultural input manufacturing (Richard 2010) that greatly exceed historical precedents. These analyses are thus useful for identifying potential pinch-points in future bioeconomy scale-up and informing the overall plausibility of the decarbonization scenarios. Together, these data provide an alternative bottom-up perspective against which to compare the GCAM-derived biomass feedstock estimates and establish a foundation for iterative harmonization across GCAM and bottom-up assessments. Over the course of the current study, total biomass production data from the default GCAMv6 model was used as a basis for feedstock resource cost analysis using bottom-up methods, and then select results from that bottom-up modeling (e.g., per-area energy crop yields) were integrated back into GCAM, contributing to the new GCAM-DECARB model. Additional future iterations of data exchange (e.g., re-running the bottom-up feedstock resource assessment using fertilizer price data from GCAM) would serve to further harmonize these top-down and bottom-up assessment approaches.

3.2 Methods

3.2.1 Types of Biomass Feedstock Considered

This feedstock resource assessment focused on the various lignocellulosic and waste-derived feedstocks detailed in Table 3.1. Since biofuels from first-generation feedstocks comprise a small and declining share of total biobased feedstock consumption across the scenarios developed in Chapter 2 (Figure 2.5), those feedstocks were excluded from this bottom-up resource assessment. Lignocellulosic and waste-derived feedstocks can be classified as forest resources, agricultural resources, wastes, and algae, following the categories used by the Billion-Ton Report. Forest resources include logging residues and whole-tree biomass. Agricultural resources include agricultural residues (corn stover; cereal straws from wheat, oats, and barley; and sorghum stubble) and dedicated energy crops, including herbaceous energy crops (switchgrass,

miscanthus, biomass sorghum, and energy cane) and short-rotation woody crops (poplar, pine, willow, and eucalyptus). Wastes include agricultural secondary wastes (sugarcane residues, soybean hulls, rice hulls and rice field residues, grain dust and chaff [from corn, wheat, sorghum, barley, oats, and soybeans], orchard and vineyard prunings, animal fats and yellow grease, cotton gin trash and cotton field residues, and animal manure), MSW (paper and paperboard, food waste, and yard trimmings), forestry and wood wastes (other removal residues, thinnings from other forestland, unused primary and secondary mill processing residues, urban wood waste, wood waste liquids, and black liquor), and other supplies (wastewater biosolids; used cooking oils; brown and trap greases; industrial, institutional, and commercial food processing wastes; landfill gas; and utility tree trimmings).

The GCAM model considers more aggregate groupings of these feedstocks—specifically agricultural residues, herbaceous biomass crops, woody biomass crops, and MSW—as indicated with the color shading in Table 3.1. Algae, including both micro- and macro-algae, could be a significant biomass source in the future. However, it was considered out of scope for the current study and was not included in the analysis described in this chapter or the GCAM results described in the previous chapter. Similarly, the Billion-Ton Report methods could be expanded in the future to consider other novel feedstocks such as cover crops grown during the off-season, but that was also considered out of scope here.

Table 3.1. Biomass Resources Considered in This Analysis

Biomass Feedstock	Category	Biomass Source	Data Source
Ag residues (corn, sorghum, oats, barley, winter/spring wheat)	Herbaceous cellulosics	Existing annual cropland	BT16 Ch. 4
Secondary ag residues (e.g., soy hulls, rice husk)	Herbaceous cellulosics	Processing facilities	BT16 Ch. 5.2
Logging residues & mill residues	Woody biomass	Timberland; lumber mills	BT16 Ch. 3 & 5.4
Biomass sorghum	Herbaceous cellulosics	Dedicated energy crops grown on permanent pasture, cropland pasture, and annual cropland	BT16 Ch. 4
Energy cane			
Miscanthus			
Switchgrass			
Eucalyptus	Woody biomass		
Pine			
Poplar			
Willow			
MSW–yard trimmings	Herbaceous cellulosics	MSW	BT16 Ch. 5.3
MSW–food waste	Wet waste		
Whole-tree biomass & wood waste from thinning	Woody biomass	Existing timberland	BT16 Ch. 3 & 5.4
Manure	Wet waste	Animal facilities	BT16 Ch. 5.2

Biomass Feedstock	Category	Biomass Source	Data Source
Wastewater sludge	Wet waste	Wastewater treatment/ Water resource recovery facilities s	BT16 Ch. 5.5
Landfill gas	Landfill gas	Landfills	BT16 Ch. 5.5
Used cooking oils	Fats, oils, and greases	Processing facilities	BT16 Ch. 5.5

Different biomass resources modeled endogenously in BT16 and GCAM, with row colors aligned with subsequent Figure 3.3 and Figure 3.5. Agricultural residues (blue), forestry residues (orange), herbaceous biomass crops (green), woody biomass crops (red), and MSW (purple) are included in both data sets. Whole-tree harvest (brown) and manure (pink) are included in BT16 but not in GCAM. BT16 also includes nonspatial data for other select bioresources shown in white, though these are not included in the current study.

3.2.2 Billion-Ton Report Data

The primary data source used for this bottom-up feedstock resource assessment was the most recently published report in the Billion-Ton study series, the ORNL-led 2016 Billion-Ton Report (Langholtz et al. 2016). BT16 is a spatially and temporally explicit assessment of potential biomass supply in the contiguous United States from agricultural residues, forestry residues, dedicated energy crops, and various waste sources at different biomass price points over the years 2015 to 2040, under economic and sustainability constraints. BT16 estimated the lignocellulosic biomass potential at the farmgate (i.e., including all operations associated with growing, harvesting, and bailing, but excluding transport from the farm to the point of intermediate storage or use) from agricultural residues and dedicated energy crops as affected by conventional crop land requirements, environmental limitations, equipment limitations, and other sustainability constraints. The cost of on-farm use of seed, fertilizer, other agricultural chemicals, fuel, etc., is considered in BT16 via regionally specific crop production budgets (associated emissions are considered separately in Chapter 6). BT16 includes separate assessment models for forest-derived and waste feedstocks.

Agricultural feedstocks (i.e., crop residues and dedicated energy crops produced on former annual crop or range land) were modeled with the POLYSYS linear program partial equilibrium model (Ugarte and Ray 2000) to project the adoption of crop residue harvesting and land conversion to dedicated energy crops. POLYSYS was run under fixed assumptions of conventional crop yields and agricultural land use extrapolated from USDA agricultural projections (e.g., Dohlman et al. 2021). The USDA projects the planted area, per-area yield, production total, and prices of various major agricultural commodity crops a decade into the future based on a unified set of macroeconomic, policy, and trade assumptions. This approach enables estimation of the amount of surplus cropland that may become available for future energy crop production while meeting demands for food, feed, and fiber. POLYSYS allows energy crops to be grown on former annual cropland that has been spared through food crop yield increases, and on pastureland. Aggregate state- and county-scale BT16 output data are available for download in tabular format from the DOE Bioenergy Knowledge Discovery Framework.[16]

Spatial estimates of energy crop yields in BT16 were derived from the PRISM–EM model, which combines field trial data from the Sun Grant Regional Feedstock Partnership with historical weather data, soil data, and expert elicitation (Daly et al. 2018). PRISM–EM produces

[16] https://bioenergykdf.net/bt16-2-download-tool/county

high-spatial-resolution estimates of both herbaceous (Lee et al. 2018) and woody (Volk et al. 2018) energy crop yields. Data on PRISM-estimated energy crop yields aggregated to the county scale (i.e., input to the BT16 workflow) are also available for visualization and download via the Tableau tool on Knowledge Discovery Framework (interactive versions of Figures C-4 through C-9).[17] PRISM–EM and POLYSYS both assume that energy crop production will be rainfed, which result in very low yield potentials in the arid interior western United States. Energy crop plantings are modeled as competing with existing conventional crop production at the county scale, rather than being targeted specifically on discreet areas of degraded, abandoned, or marginal land (e.g., areas of unfavorable topography or soils). BT16-projected energy crop production potential is thus concentrated in the southern Great Plains and other areas of lower current agricultural intensity, avoiding areas like the Corn Belt where conventional crops are more profitable than biomass alternatives, and also avoiding the arid interior west where low energy crop yields preclude economically viable production.

Note that this analysis does not account for any potential effects of future climate change on agricultural productivity and land use patterns. There is evidence that climate change is already causing shifts in conventional crop cultivation ranges (e.g., Sloat et al. 2020), a trend that could conceivably free up existing cropland for other uses (while leading to cropland expansion in other regions). Higher levels of climate change could also affect dedicated energy crop yields and reduce the effectiveness of bioenergy as a climate mitigation approach (Xu et al. 2022). Such impacts are still very speculative, and they are generally not included in IAM-based scenario analyses, though they are an important area for future research (Wagner and Schlenker 2022).

BT16 identifies a maximum domestic lignocellulosic biomass supply potential of 1,030 million dry short tons annually in the base case scenario under a mature industry (i.e., projection year 2040, after 25 years of growth in the sector) at the highest farmgate biomass price (100 USD/short ton), excluding the small categories of nonspatial data and noncellulosic resources described in Table 5.3. Applying the same assumed biomass heating value used in GCAM (17.5 GJ per metric ton), this corresponds to 16.4 exajoules of primary bioenergy annually (EJ y^{-1}). Note that this is an estimate of raw biomass potential before any considerations of supply-chain losses or stranded resources located far from potential processing facilities (see next chapter). About 59% of that supply (9.6 EJ) comes from agricultural residues, forestry residues, and various waste streams—biomass resources that exist already independent of an advanced bioenergy industry. That estimate reflects the anticipated future size of the forestry and agricultural sectors, sustainability constraints to limit erosion and maintain soil organic matter in annual cropping systems, and stover harvest equipment limitations. The other 41% of this supply (6.8 EJ y^{-1}) is anticipated to come from future plantings of dedicated energy grasses and trees. The ultimate size of the energy crop resource is limited by conventional crop land requirements, and by exclusion of forest or other nonagricultural land conversion to energy crops.

BT16 also includes scenarios premised on more rapid increases in per-area crop yields, which both increases the productivity of energy crops and expands the land base on which they can be grown (by reducing the land requirements for conventional agricultural production). Under the most optimistic scenario of 4% per year energy crop yield increases, raw biomass potential increases by 50% over the base case scenario, to 1,500 million short tons per year (23.9 EJ y^{-1}).

[17] https://bioenergykdf.net/farmgate

These scenarios provide important context on the maximum potential size of biomass supply for scenarios heavy in bioenergy use. However, initial BT16–GCAM harmonization efforts focused on the BT16 base case scenario (1% per year productivity improvements), as detailed in the next section.

3.2.3 BT16–GCAM Alignment

Differences in the temporal scope, spatial granularity, feedstock types, and management and technology assumptions represented in the BT16 resource assessment versus the GCAM biomass module had to be reconciled for this analysis (Table 3.2). BT16 covers the 2015–2040 period, with availability of different types of biomass resources reported in either 5- or 10-year increments. BT16 provided projections of biomass availability as a function of time, which reflects dynamic limits on the amount of land that can be converted to energy crops in any given year (representative of short-term barriers to new crop adoption) and the rate of scale-up of crop residue harvest (representative of harvest equipment limitations). Note that this temporal component of the analysis is meant to capture the maximum rate at which maximum potential supply could grow subject to equipment, sustainability, and technology limitations. It is not, however, a specific prediction of how this sector will evolve, since it does not attempt to capture noneconomic factors in landowner decision-making, or a variety of other potential real-world constraints on growth. For the purposes of this comparison, we used linear interpolation to represent all BT16 resources on a common 5-year increment.

The GCAM scenarios from Chapter 2 cover the 2015–2050 period in 5-year increments. Since the temporal scope of the two models overlaps over the 2015–2040 period, we could make direct comparisons across the two models for that period. We then treated the 2040 BT16 results as representative of a "mature" biomass industry that would be directly comparable to the year 2045 and 2050 data points in GCAM. Extrapolation of biomass supply trends beyond 2040 is not possible since land and crop residue availability have upper limits, though the underlying POLYSYS simulations and other assessment models could be extended through 2050 in future work. BT16 includes representation of specific herbaceous and woody energy crop species, whereas GCAM considers more aggregate representation of generic "energy grass" and "energy tree" crops. The process for aggregating individual BT16 energy crops into the generic GCAM energy crop categories is further detailed in the Results and Discussion section below.

Table 3.2. Different Scopes of the Biomass Resource Assessments From GCAM and BT16

	GCAM	BT16	This Comparison
Time range	2015–2050 (5-year increments)	2015–2040 (5- or 10-year increments*)	Linearly interpolate all BT16 resources to a common 5-year increment Align BT16 & GCAM over 2015–2040 Treat BT16 2040 as "mature" case comparable to 2045 & 2050 GCAM results
Spatial scale	HUC2 major river basin (U.S. Geological Survey two-digit hydrological unit code, defining major river basins)	County	Aggregate BT16 data to county-delimited HUC2 resolution
Feedstocks	1st-generation crops and cellulosic biomass from: • Crop residues • Forestry residues • Generic energy grass • Generic energy trees • MSW	Cellulosic biomass only (under a fixed level of demand for 1st-generation crops) from: • Crop residues • Forestry residues • Whole-tree harvest • Specific energy grasses (switchgrass, miscanthus, energycane, sorghum) • Specific energy trees (poplar, willow) • MSW • Manures	Aggregate biomass into various higher-level category groupings (e.g., herbaceous/woody/waste) for comparison Be aware that certain BT16 feedstocks (e.g., whole-tree harvest) are not directly represented in GCAM
Scenarios	Reference scenario and decarbonization scenarios with various levels of biofuel mandates and DAC technology maturity (see Chapter 2)	Four different assumptions around future yield improvement rate for conventional and energy crops (1%, 2%, 3%, and 4%/year)	Focus on a limited subset of GCAM scenarios: • Reference (no climate policy) • DAC.Ref_noSAF (no specific SAF mandate) • DAC.Ref_BF35bil.gal (specific SAF mandate) Use most conservative BT16 "base case" scenario of 1%/year yield improvement

*Some biomass types are available in 5-year increments, others on 10-year increments.

GCAM models feedstock supply at the scale of major river basins, as defined by a two-digit U.S. Geological Survey hydrological unit code (HUC2).[18] Basic GIS work was undertaken in ArcGIS

[18] https://water.usgs.gov/GIS/regions.htmlhttps://www.usgs.gov/national-hydrography/watershed-boundary-dataset

using HUC2 watershed boundary shapefiles available from the U.S. Geological Survey.[19] Each county in the contiguous United States (the resolution of the BT16 resource assessment data) was sorted into an associated HUC2 river basin (Figure 3.1). In cases where counties are divided across two or more HUC2 watersheds, the entire county is assigned to the watershed covering the greatest area of the county. This county-to-basin mapping scheme was then used to aggregate fine-scale BT16 results up to the appropriate basin scale for comparison with and harmonization of the GCAM biomass module.

Figure 3.1. Sorting individual counties into 18 different HUC2 river basins

Importantly, BT16 and GCAM take fundamentally different approaches to representing the potential for increased energy crop production over time in the face of higher demand. In BT16, increased yield potential from improved genotypes is considered for both energy crops and conventional crops (which determines the amount of surplus agricultural land available for bioenergy crops), modeled as a linear increase over time. BT16 includes four scenarios: a "base case" of 1% annual yield improvements (applied linearly, not compounded), as well as cases of 2%, 3%, and 4% annual improvement. However, BT16 only considers rainfed energy crop production, and management intensity (e.g., fertilizer application) is modeled as uniform in space and constant over time. In contrast, GCAM does not directly represent genotypic improvements or equipment limitations over time, but it does consider four different levels of management intensity for dedicated energy crops (irrigated or nonirrigated, and high- or low-fertilizer, in combination). As biomass prices increase in the model, more intensive management (irrigation and high fertilizer application) is adopted and the total amount of biomass production increases.

In the interest of making a conservative initial comparison to GCAM, we considered only the BT16 1% yield improvement base case, excluding the more optimistic yield scenarios. We also used the corresponding conservative scenario for forestry feedstocks,[20] though these forestry feedstocks make up only a relatively small component of total biomass supply and show little

[19] https://www.usgs.gov/national-hydrography/watershed-boundary-dataset
[20] The "medium housing, high energy demands" scenario features the lowest amount of sawmill residues and the highest level of competition for wood feedstocks for other energy applications.

variability between scenarios. The energy crop management assumptions in BT16 correspond most closely to the nonirrigated, high fertilizer rate case in GCAM.

3.2.4 Analysis Code

All data analysis was coded in Python using JupyterLab notebooks for transparency, repeatability, and portability. A repository containing all raw data, analysis code, and intermediate and final results used in this analysis is available through the externally facing ORNL GitLab server[21] (non-ORNL users must follow the link to register for an XCAMS account to gain access). The markdown README displayed on the landing page of the repository provides additional details around how the underlying raw BT16 and PRISM–EM data can be accessed, how different individual BT16 feedstock resources are aggregated for display purposes and comparison to GCAM, and the organization of the various analysis code notebooks.

3.3 Results and Discussion

3.3.1 Biomass Consumption Targets and Prices From GCAM

Our first step was to select a subset of the GCAM scenarios that reflect a range of total U.S. biomass consumption and prices for further bottom-up analysis. At the time of this bottom-up assessment work, we had access to the original set of GCAMv6 scenarios, as described in the previous chapter. The following subset of GCAMv6 scenarios were selected for further analysis since they cover a relatively wide range of biomass consumption:

- The no-policy "Reference" scenario
- The net-zero-by-2050 scenario with DAC costs at their default reference level and no specific SAF mandate ("DAC.Ref_noSAF")
- The net-zero-by-2050 scenario with DAC costs at their default reference level and a mandate of 35 billion gallons (Bgal) of annual liquid biofuels production by 2050 ("DAC.Ref_BF35bil.gal"), consistent with the SAF Grand Challenge volumetric target for meeting U.S. jet fuel demand, excluding coproducts.

Figure 3.2 shows the total level of lignocellulosic biomass consumption and associated biomass price over time for each of the selected GCAMv6 scenarios. In the Reference scenario, U.S. biomass use more than doubles from 2015 to 2050, reaching an annual biomass consumption rate of 440 million dry short tons by 2050. Biomass price declines slightly over time in this scenario, from approximately 70 to 60 U.S. dollars (USD; 2014 basis) per dry short ton. The 2050 rate of biomass consumption Is 1.9 times greater in the net-zero scenario without specific biofuel mandates (DAC.Ref_noSAF; 843 million dry short tons/y) and 2.3 times greater in the biofuel-mandate net-zero scenario (DAC.Ref_BF35bil.gal; 1,030 million dry short tons/y). In those net-zero scenarios, the price of biomass grows sharply as biomass consumption exceeds ~500 million dry short tons per year around 2035, eventually reaching as high as $183 per dry short ton in the DAC.Ref_BF35bil.gal scenario.

[21] https://code.ornl.gov/fieldjl/decarb_ornl

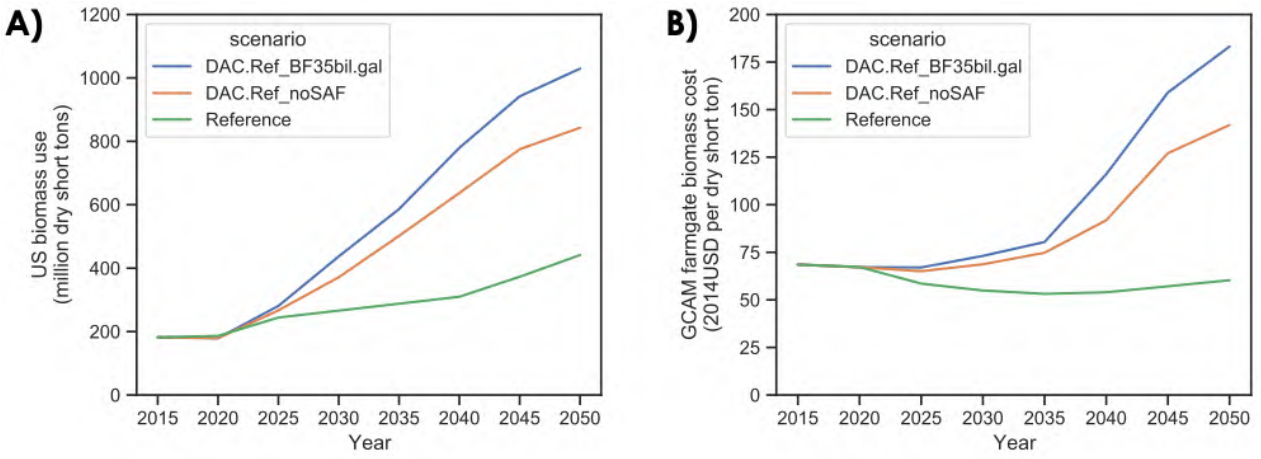

Figure 3.2. U.S. lignocellulosic biomass A) consumption and B) price over the 2015–2050 period in three selected GCAMv6 scenarios

First-generation biofuels (e.g., from corn and soybean feedstocks) are excluded here (although they were illustrated previously in Figure 2.4).

3.3.2 BT16 Biomass Supply Costs

Next, we used bottom-up BT16 data to determine the specific biomass supply mix that could meet the biomass consumption levels specified in these three GCAMv6 scenarios at the lowest possible cost. The associated analysis sequence is illustrated in Figure 3.3. The total amount of U.S. biomass consumption in a given year is extracted from the GCAM scenario curve (Figure 3.3A, which is the same as Figure 3.2A). BT16 data for that same year are aggregated up to the broad biomass categories considered in GCAM (Table 3.1) and arranged into a supply curve showing biomass supply versus price in 10-USD increments (Figure 3.3B). Finally, the associated biomass mix and price meeting the biomass demand in each GCAMv6 scenario can then be linearly interpolated from the BT16 supply curve. This procedure is repeated for each time point over the 2015–2050 period. Specific BT16 data on biomass supply and cost are available for the years 2015, 2020, 2025, 2030, 2035, and 2040. For the years 2045 and 2050, BT16 data from the year 2040 is used as a proxy representing a mature biomass supply technology case.

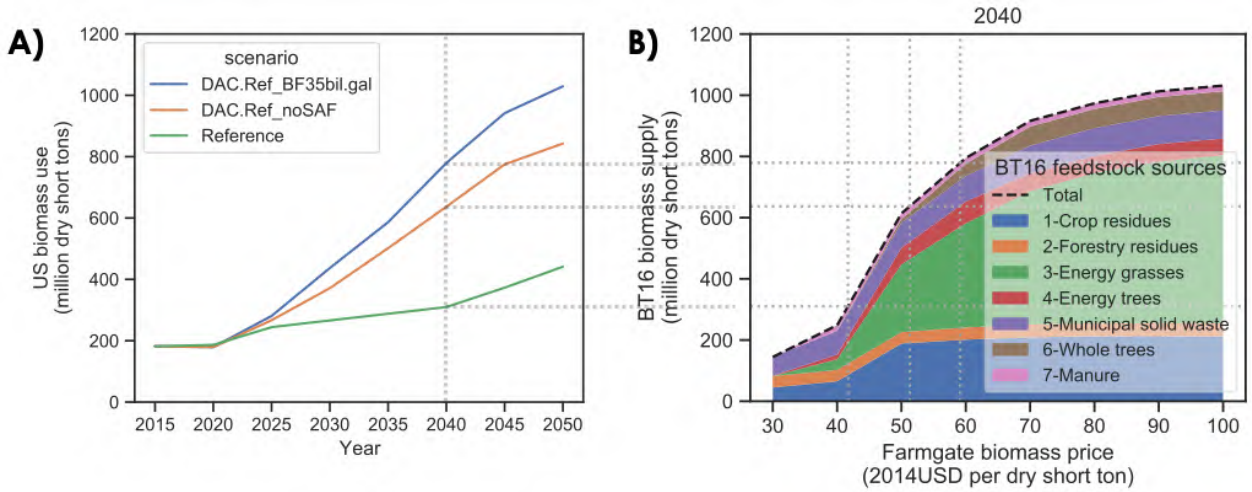

Figure 3.3. Example of BT16 biomass supply interpolation. A) The total amount of U.S. biomass consumption for a given year (e.g., 2040) is extracted from the GCAM scenario curve. B) BT16 data for that year are aggregated into broad source categories and arranged into a supply curve.

The total BT16 biomass price and supply mix can then be interpolated for the particular level of biomass consumption specified in each GCAM scenario for that given year. This procedure was repeated for years 2015, 2020, 2025, 2030, 2035, 2040, 2045, and 2050.

The resulting BT16-derived biomass prices for each scenario are compared to the original GCAMv6-predicted prices in Figure 3.4. The BT16-estimated prices are systematically lower than those from GCAMv6, by a factor of ~40% in 2015 and by 46%–55% in 2050 for the net-zero scenarios (DAC.Ref_noSAF and DAC.Ref_BF35bil.gal). As discussed later in this chapter and in Chapter 7, this is attributable in part to BT16's assumptions of higher per-area energy crop yields and lower nutrient requirements compared with assumptions in GCAMv6. The maximum biomass price estimated from BT16 is $99 per dry short ton for 1.03 billion short tons of biomass production in 2050 under the 35 Bgal biofuels scenario; the corresponding biomass price in GCAMv6 is $183 per dry short ton. Note that the highest farmgate price considered in BT16 is $100 per dry short ton, so almost all available cellulosic biomass in the bottom-up BT16 base case scenario needs to be mobilized to fulfil the demand specified in the top-down GCAMv6 35 Bgal biofuels scenario.

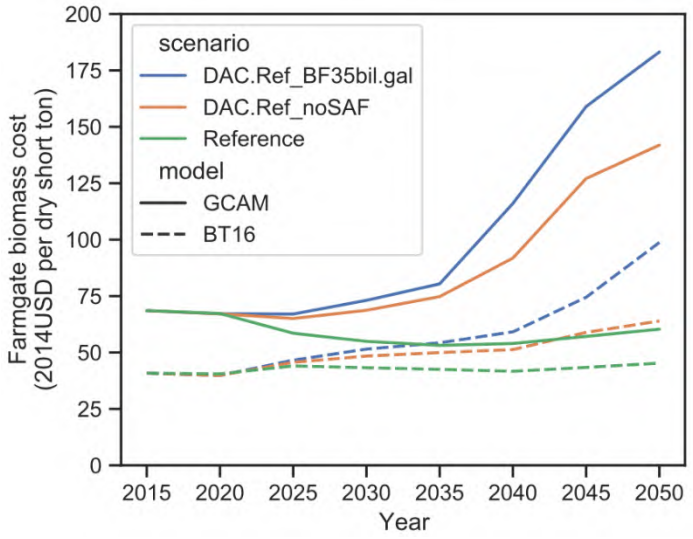

Figure 3.4. Biomass prices over time for the select scenarios as per the top-down GCAMv6 and bottom-up BT16 assessments

3.3.3 BT16 Biomass Supply Categories and Regions

Compared with the original GCAMv6 scenario modeling, BT16 data suggest that biomass demand will most likely be met by a somewhat different mix of biomass sources. Figure 3.5 shows the different mixes of biomass supply projected by the bottom-up and top-down assessments for the scenario of net-zero-by-2050 with 35 Bgal of annual biofuels production (DAC.Ref_BF35bil.gal). BT16 and GCAMv6 project broadly similar levels of biomass supply from crop residues (212 million dry short tons/y and 202 million dry short tons/y, respectively) and forestry residues (42 million dry short tons/y and 65 million dry short tons/y) in 2050. However, the models differ substantially in their projections of dedicated energy crops. GCAMv6 shows a much greater role for energy trees (539 million dry short tons/y) than energy grasses (163 million dry short tons/y), whereas BT16 shows substantial production of energy grasses (547 million dry short tons/y) but much lower production (43 million dry short tons/y) of energy trees. Also note that BT16 includes potential biomass supplies from whole-tree harvest and manure that are not included in GCAMv6, though these make up only a small share of the total BT16-estimated biomass supply for these scenarios.

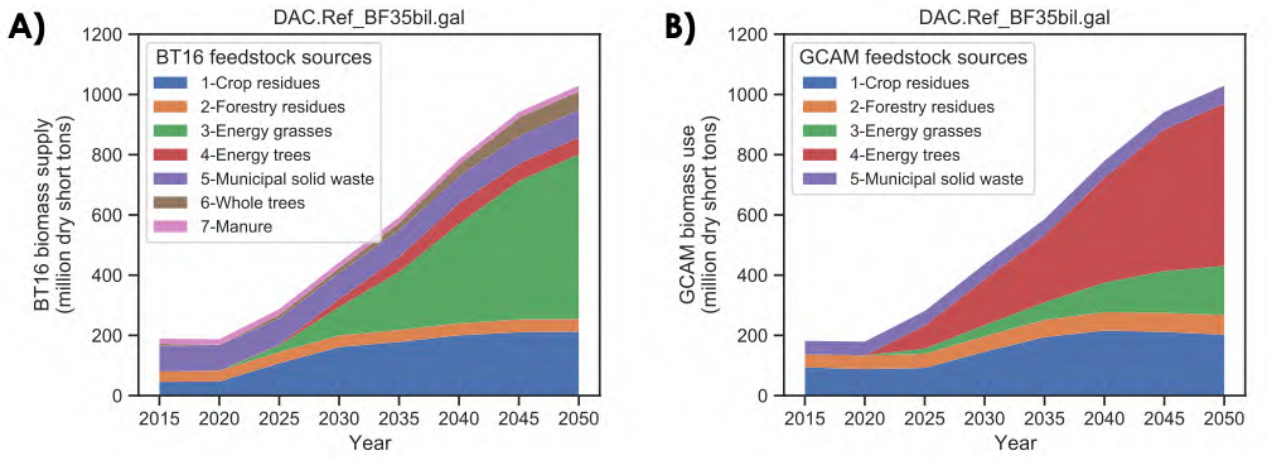

Figure 3.5. Biomass supply mixes projected A) from BT16, and B) from GCAMv6 under the scenario of net-zero-by-2050 and with 35 Bgal of annual biofuels production mandated by 2050 (DAC.Ref_BF35bil.gal)

These different biomass supply mixes correspond to different regional sources. Figure 3.6 shows projected biomass supply at the basin scale in units of EJ biomass per billion acres (i.e., giga-acres, or Gacres), reflecting both per-area biomass yields and the total area within each basin on which biomass is produced within a given scenario. Both GCAMv6 and BT16 show the Upper Mississippi, Lower Mississippi, Missouri, and Ohio River Basins as important for the supply of agricultural residues. BT16 suggests a large supply of dedicated energy grasses cultivated in the Arkansas–White–Red River Basin, the Texas–Gulf Basin, and the Missouri River Basin. Note that these are not necessarily the areas where these energy grasses achieve maximum yield, but rather the areas in which these crops compete most favorably with current-day land uses. In contrast, GCAM projects much smaller levels of energy grass production in the Arkansas–White–Red River and Texas–Gulf Basins, and virtually none in the Missouri River Basin. GCAM projects moderate levels of dedicated energy tree cultivation in California and the Pacific Northwest, while BT16 does not show any significant production in those regions.

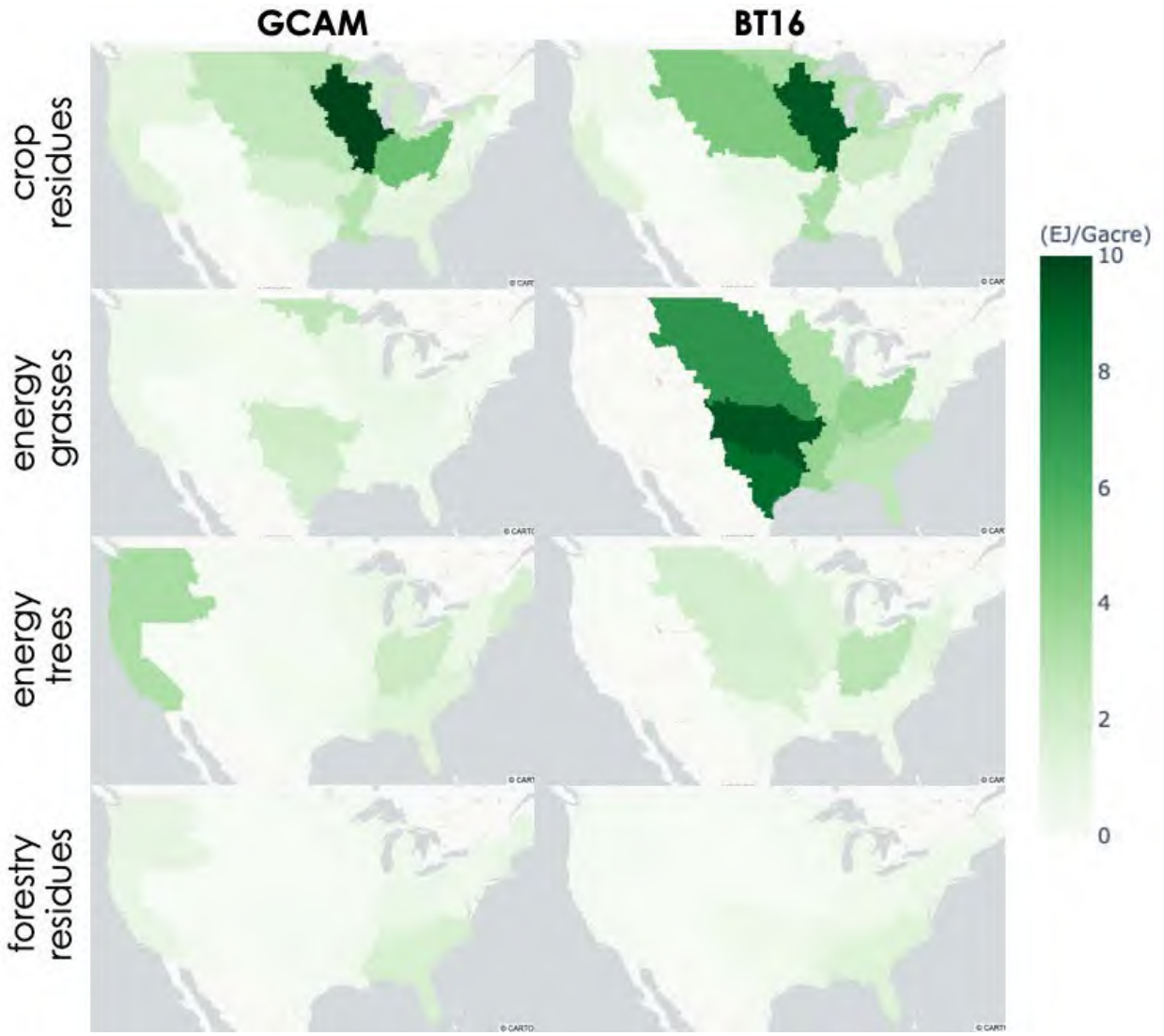

Figure 3.6. Basin-scale projections of biomass sourcing as per GCAMv6 and BT16 in 2040. Biomass supply density is shown in units of exajoules per billion acres (Gacres). In the case of agricultural feedstocks, this metric integrates both the fraction of the landscape from which the resource is collected or cultivated, plus the per-area yield of resource on that land. Dedicated energy crop cultivation is zero at the beginning of the BT16 data set, but by 2040 it accounts for 59% of total supply. Energy crop cultivation is highly concentrated in the Arkansas–White–Red River Basin, the Texas–Gulf Basin, and the Missouri River Basin. BT16 projects no significant production of dedicated energy crops in the Great Basin, California, and Upper and Lower Colorado River Basins, where nonirrigated yield rates are too low to be economically viable.

Figure 3.7 shows finer county-scaled results from BT16 for crop residues and energy grasses. Dedicated energy grasses are generally cultivated in regions with less conventional crop (and crop residue) production. However, both types of biomass feedstock are produced in certain counties in the Lower Mississippi River Basin.

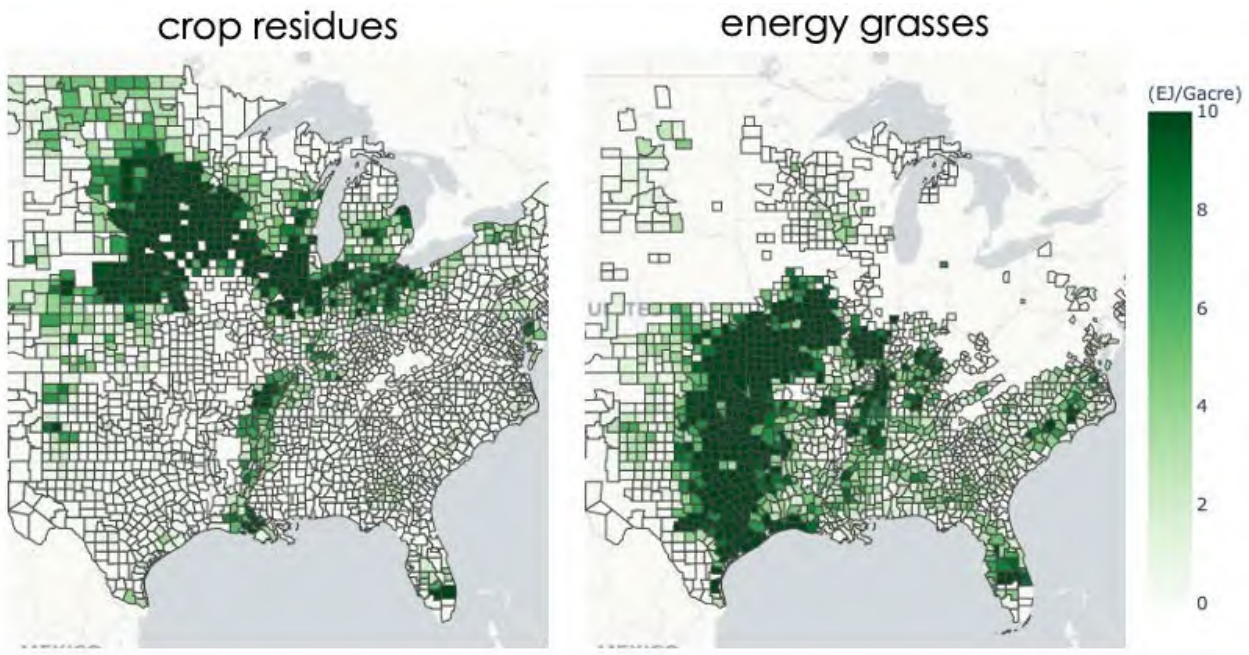

Figure 3.7. County-scale supply of crop residues and dedicated energy grasses in 2040 as per BT16, focusing on the region between 75 degrees and 105 degrees longitude.

3.3.4 Energy Crop Yield Data for GCAM Harmonization

BT16 considers a more diverse set of candidate energy crops than does GCAMv6, and its yield estimates reflect recent DOE-supported advancements in crop breeding and management. Data on energy crop yield potential was therefore compiled from BT16 for use in the new GCAM-DECARB model, which represents a first iteration toward a harmonization between the top-down and bottom-up assessment perspectives explored in this project.

This required aggregating the individual second-generation energy crop species modeled in BT16 (based on data from PRISM–EM) into a single representative or composite energy grass and a single representative or composite energy tree since that is the level of detail expected in the GCAM data input. One possible approach would be to select a single species of grass (e.g., miscanthus) and tree (e.g., poplar) as broadly representative of those crop categories, compile yield data for those particular species in each county, and then aggregate to the GCAM HUC2 basin scale. While straightforward, this method would underestimate the true yield potential of energy crops since the granular PRISM–EM data show certain species to be most productive in one region and different species to be most productive in another. Instead, we adopted a more granular approach to GCAM–BT16 energy crop harmonization by selecting the highest-yielding BT16 energy grass and energy tree species within each county, and then combining the yields for those optimal crop selections into composite energy grass and composite energy tree yield maps. This approach, which is consistent with farmers making their own regionally appropriate crop selections, maximizes total biomass production potential.

The set of highest-yielding energy grass and energy tree species in each county are mapped in Figure 3.8A and Figure 3.8C. The associated continuous maps of yield potential based on these selections are shown in Figure 3.8B and Figure 3.8D. The composite herbaceous energy grass

crop reaches yields of 25–30 dry metric tons per hectare in the Mississippi River Valley and Gulf Coast regions. The composite woody energy tree crop reaches yields above 15 dry metric tons per hectare in the Corn Belt and along the Gulf Coast. Future yields of both food crops and energy crops are threatened by climate change. This introduces a potentially important time-dependent constraint on bioenergy effectiveness for mitigation (Xu et al. 2022), though such effects are not explored in the relatively short time horizon of the BT16 assessment.

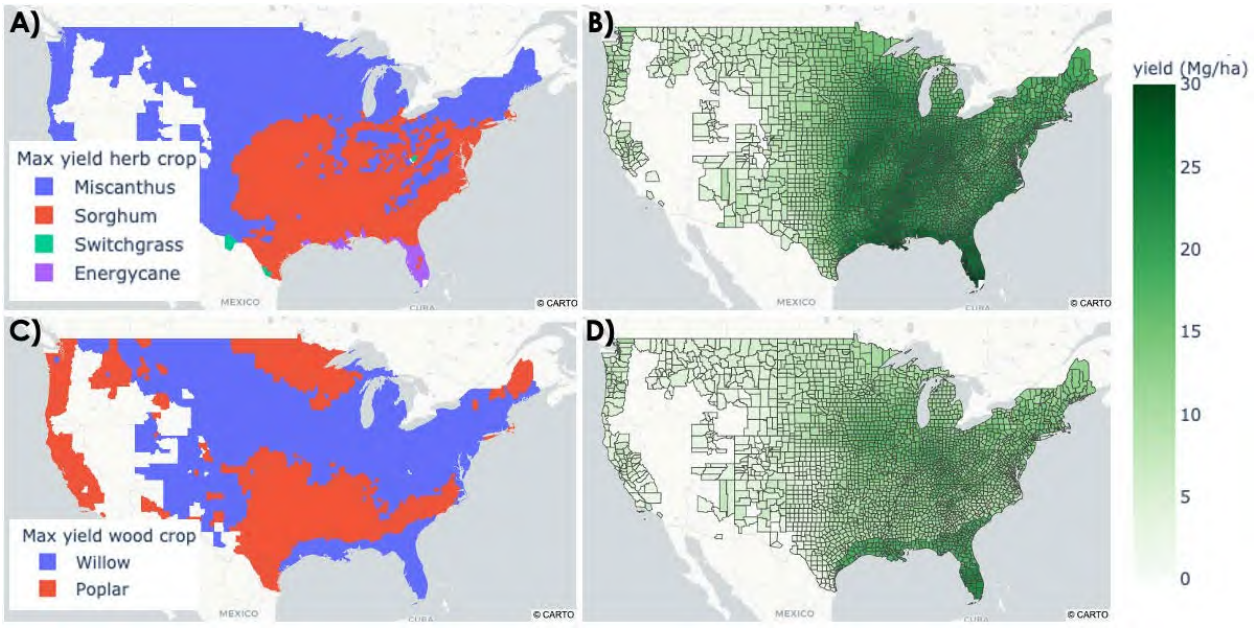

Figure 3.8. Highest-yielding A) herbaceous and C) woody energy crops in each county as per the PRISM–EM data set, and associated composite B) herbaceous (i.e., grass) and D) woody (i.e., tree) energy crop yield maps. Missing counties in the arid interior western United States reflect areas that lack significant existing agricultural land appropriate for energy crop cultivation (e.g., mountainous areas), and areas of excessively low projected energy crop yields that were excluded from the analysis.

The per-area annualized yield potential of energy grasses and energy trees as represented in GCAMv6 and for the selected BT16 crop composites is shown in Figure 3.9. This figure shows the underlying yield potential of these different crops, whereas Figure 3.6 showed where they are mostly likely to be grown (which also depends on the yields and profitability that could be achieved with conventional crops there instead). The GCAMv6 data reflect management intensification as biomass prices increase over time in the net-zero scenarios, and they show little difference between crop type (i.e., grass versus tree). The BT16 data reflect yield data from PRISM–EM for the base year 2015, plus annual yield increases of 1% from 2015 to 2040 as per the BT16 "base case." Energy grass yields are substantially higher in BT16 than in GCAMv6, and they show a very different spatial pattern, reaching their highest values in the Upper and Lower Mississippi and Ohio River Basins and the South Atlantic–Gulf Region. BT16 energy tree yields show a similar spatial pattern but are much lower than the BT16 energy grass yields and somewhat lower than the GCAMv6 energy tree yields.

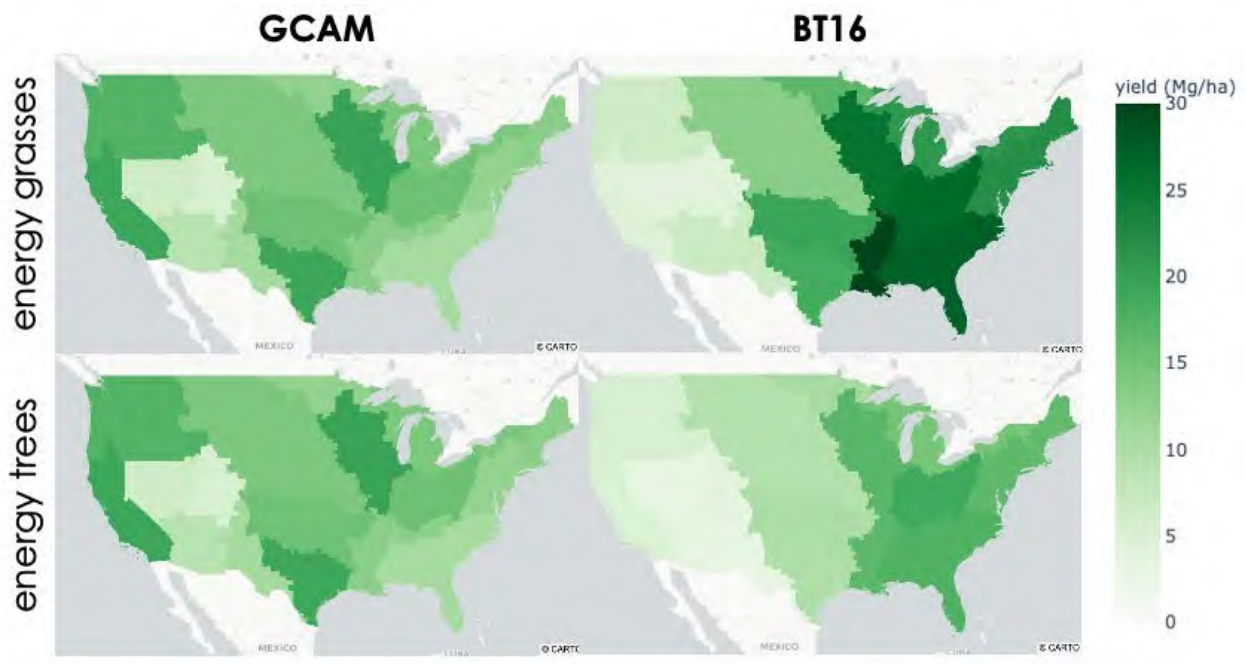

Figure 3.9. Per-area annualized yield potential of dedicated energy crops in GCAMv6 and BT16 in the year 2040

The BT16-modeled production costs for these composite energy grass and energy tree crops are illustrated in Figure 3.10 in 2015 USD per dry metric ton of biomass. These cost estimates include inputs of seed, fertilizer, and herbicide; farm operations associated with planting, management, and harvest; and land rental rates. Discontinuities in the production cost maps occur at the boundaries between different crop ranges. These BT16 bioenergy crop costs are compared to the costs in GCAM in detail in Chapter 7.

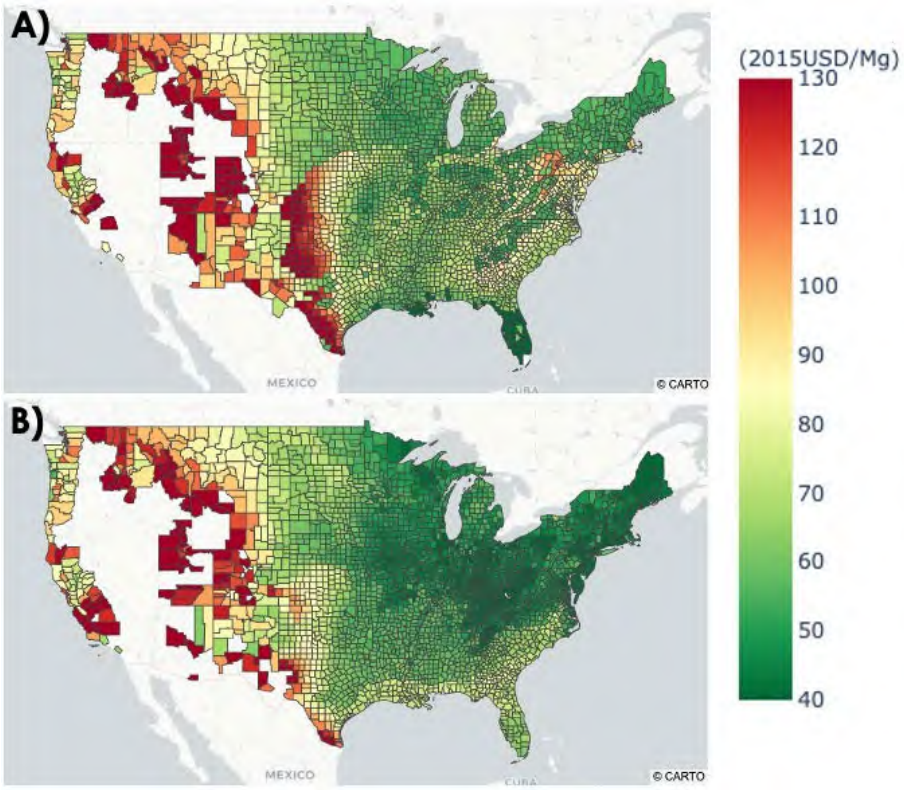

Figure 3.10. BT16-derived cost estimates for the composite A) herbaceous and B) woody energy selections illustrated above in Figure 3.8

3.3.5 Rates of Land Use Change and Fertilizer Consumption

Finally, the rates of land use change, crop management changes, and increases in nitrogen fertilizer consumption implied in the selected GCAM decarbonization scenarios can be compared to historical analogues to judge their plausibility. Where possible, we focus on the original scenario modeling results from GCAMv6, as that model's lower per-area energy crop yields and higher nutrient requirement assumptions make those results more conservative compared to BT16 results. Figure 3.11A shows the rate of agricultural land-use change from conventional food crop cultivation to energy crop cultivation modeled in GCAMv6, which accounts for changes in food crop demand and per-area yield over time. The average annual rates of land-use change to energy crop cultivation in the no-policy (Reference), net-zero with no SAF mandate (DAC.Ref_noSAF), and 35 Bgal biofuels net-zero (DAC.Ref_BF35bil.gal) scenarios are 0.5, 1.1, and 1.5 Mha per year, respectively, over the period from 2025 to 2050 (i.e., the period of widespread energy crop cultivation). The highest rate of land-use change modeled in any 5-year GCAM modeling time step was 1.9 Mha/y for the 35 Bgal biofuels net-zero scenario in 2035–2040.

Since GCAM results are reported in 5-year time steps, we converted historical annual data on analogous land-use changes to 5-year rolling averages for consistency. Soybeans, first introduced at wide scales in the middle of the last century, provide a useful historical analogue for realistic rates of adoption of a novel and profitable new crop. Data on soybean planting area are available

from the USDA National Agricultural Statistics Service QuickStats database[22] for the 1924–2022 period. The long-term average rate of soybean expansion over this period of almost a century was 0.89 Mha/y. However, the 5-year rolling average rate of soybean adoption exceeded 1.9 Mha/y during most of the 1960s, 1970s, and 1990s. Similarly, the establishment of the Conservation Reserve Program (CRP) provides another example of how quickly land use can change with the introduction of new incentives (USDA n.d.). Under CRP, landowners can enroll cropland in 10- or 15-year contracts under which they agree to remove the land from active production and adopt certain restoration practices, in exchange for being paid a yearly rental payment. The total level of enrollment each year is ultimately limited by the USDA budget for rental payments, and landowners' demand for CRP participation has often exceeded supply. The average rate of annual new enrollments from the start of the program in 1986 through 2020 was 2.1 Mha/y, and the 5-year rolling average rate exceeded 1.9 Mha/y for the first 9 years in which a rolling average could be calculated. Thus, the rate of agricultural land-use change from conventional food crop cultivation to dedicated energy crop cultivation in all the GCAMv6 scenarios is less than the historical rate of CRP enrollment over the lifetime of that conservation program and less than the rate of soybean cultivation expansion observed during multiple historical periods.

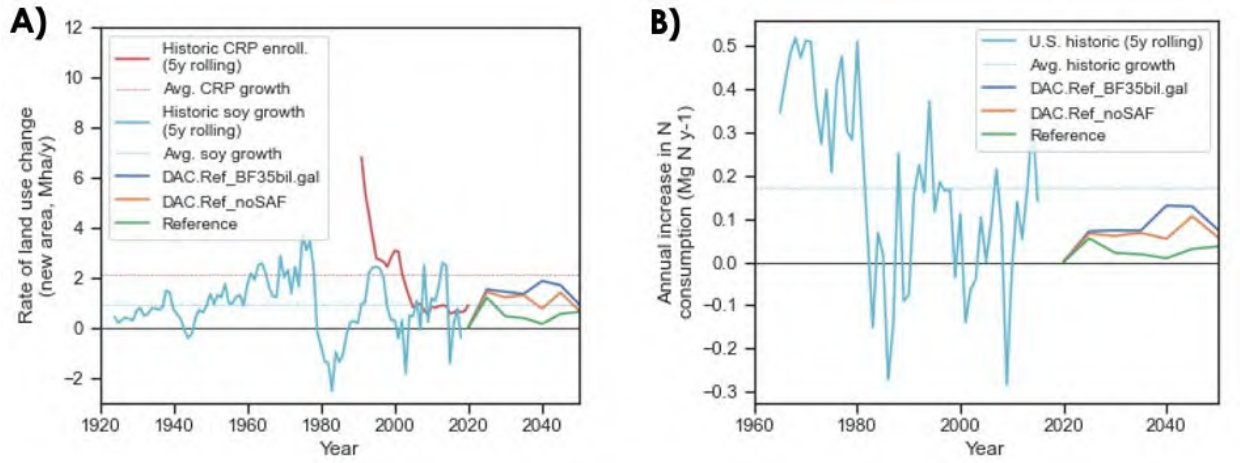

Figure 3.11. Rates of GCAM-projected A) land-use change from conventional food crop cultivation to dedicated bioenergy crop cultivation, and B) increases in nitrogen fertilizer consumption, as compared to historical analogues

Similar comparisons can be made for the expansion of crop residue harvest implied in the decarbonization scenarios. Assuming a constant biomass price of $50 per dry short ton (roughly representative of the no-SAF-mandate BT16 net-zero scenario; see Figure 3.4), the BT16 data set suggests that the area of cropland with crop residue harvest will expand at a rate of ~1.5 Mha/y. For context, that can be compared to the rate of adoption of conservation agriculture practices such as cover cropping and conservation tillage. While detailed historical crop management data is sparse (Nguyen et al. 2022), the USDA Economic Research Service estimates that cover cropping was adopted on U.S. cropland at approximately the same rate of 1.5 Mha/y over the period from 2012 to 2017, during which that information was collected through the U.S. Census of Agriculture (Wallander et al. 2021). Similarly, data on conservation tillage adoption was available for much of the 1990s from the National Crop Residue Management Survey

[22] https://quickstats.nass.usda.gov/results/5BF2EB90-3D96-3E5B-AFAA-5753D66D2EB6

administered by the Conservation Tillage Information Center.[23] From 1990 to 1998, conservation tillage was adopted in the United States at an average annual rate of ~4 Mha/y, far greater than the rate of expansion in crop residue harvesting projected in the BT16 data.

In addition, the widespread cultivation of dedicated energy crops implies a significant new demand for agricultural chemical inputs (e.g., fertilizers, pesticides) and equipment, and expanded crop residue collection also removes the nutrients in those residues, which then would require replacement through additional fertilizer application. The rate of bioenergy-induced increase in U.S. nitrogen fertilizer use modeled by GCAMv6 ranges from 24,000 Mg N y^{-1} in the no-policy reference scenario to 79,000 Mg N y^{-1} in the net-zero scenario requiring production of 35 Bgal of biofuels (Figure 3.11B). For comparison, the long-term rate of increase in U.S. nitrogen consumption over the 1960–2015 period, according to USDA Economic Research Service data,[24] was 173,000 Mg N y^{-1}.

3.4 Summary and Key Insights

All the GCAMv6 scenarios selected for detailed bottom-up assessment—specifically the no-policy "Reference" scenario and the net-zero-by-2050 scenarios with and without biofuels mandates ("DAC.Ref_noSAF" and "DAC.Ref_BF35bil.gal," respectively)—call for substantial growth in biomass consumption by 2050 compared with current levels. GCAMv6 projects that biomass consumption will more than double in the reference scenario, with production of bioelectricity, second generation biofuels, and biogas expanding (and corn ethanol production contracting) on a cost-competitive basis alone, even in the absence of carbon pricing. In the net-zero scenarios, additional demand for low-emissions energy sources and CDR drives biomass consumption to increase by a factor of 4–5 to as much as 1030 million dry short tons of biomass per year by 2050 (Figure 3.2), with uncertainties depending on whether specific SAF mandates are adopted and the state of alternative CDR methods (e.g., direct air capture). Our bottom-up resource assessment based on the BT16 base case scenario was able to identify sufficient raw biomass feedstock resources to meet the level of feedstock consumption specified in each of these three GCAMv6 scenarios, but just barely in the case of the biofuels mandate scenario ("DAC.Ref_BF35bil.gal"). Such production would be contingent on continued improvements in conventional crop yields in line with USDA projections, and sustained high rates of land use change and expanded fertilizer production (Figure 3.11). Further harmonization efforts could expand this current bottom-up assessment to incorporate the supply-chain losses and stranded resources modeled in Chapter 4, and consider the newer GCAM-DECARB scenario with total biofuel demand expanded to 50 billion gallons annually ("DAC.Ref_BF50bil.gal"). Doing so could show that insufficient biomass is produced under the BT16 base case, and that investments in agricultural crop technology to achieve the higher yield levels explored in the other BT16 scenarios would be required to fully satisfy future demand.

Both GCAMv6 and BT16 show similar levels of biomass supply coming from crop and forestry residues, and both project that dedicated energy crops will contribute most of the growth in biomass supply in the net-zero-by-2050 scenarios (Figure 3.5), though they disagree about whether energy grasses or energy trees will be most widely adopted. Bottom-up BT16 assessment suggests that the Corn Belt could play an important role in supplying crop residues;

[23] https://www.ctic.org/crm
[24] https://www.ers.usda.gov/data-products/fertilizer-use-and-price/

that energy grasses could be produced in a broad swath of lower-value land from northern Missouri through eastern Kansas, Oklahoma, and Texas; and that the Lower Mississippi River Basin could be important for both energy grasses and energy trees (Figure 3.7).

Furthermore, the bottom-up BT16 data suggest that the large expansion in biomass production called for in the origin GCAMv6 net-zero scenarios could be achieved while keeping farmgate biomass prices below $100 per dry short ton, substantially lower than projected in GCAMv6 (Figure 3.4). This discrepancy is due in part to more optimistic assumptions of per-area energy crop yields (Figure 3.9), as well as lower assumed fertilizer requirements (see Chapter 7). This expansion of biomass supply over a relatively short time frame implies substantial cropland management change for residue collection, conversion of idle cropland and pasture to energy crop cultivation, and increases in fertilizer consumption. However, the rates of land-use and land-management change implied in these scenarios are comparable to the historically observed rates of soybean expansion, CRP enrollment, and conservation agriculture practice adoption, and the increase in U.S. nitrogen fertilizer use is likewise well within historical rates.

References

Daly, C., M. D. Halbleib, D. B. Hannaway, and L. M. Eaton. 2018. "Environmental limitation mapping of potential biomass resources across the conterminous United States." *GCB Bioenergy* 10(10): 717–734. https://doi.org/10.1111/gcbb.12496.

Dohlman, E., J. Hansen, and D. Boussios. 2021. *USDA Agricultural Projections to 2030.* Washington, DC: U.S. Department of Agriculture. OCE-2021-1. http://www.ers.usda.gov/publications/pub-details/?pubid=100525.

Langholtz, M. H., B. J. Stokes, and L. M. Eaton. 2016. *2016 Billion-ton Report: Advancing Domestic Resources for a Thriving Bioeconomy, Volume 1: Economic Availability of Feedstock.* Oak Ridge, TN: Oak Ridge National Laboratory. ORNL/TM-2016/160. https://doi.org/10.2172/1271651.

Lee, D. K., E. Aberle, E. K. Anderson, W. Anderson, B. S. Baldwin, D. Baltensperger, M. Barrett et al. 2018. "Biomass production of herbaceous energy crops in the United States: Field trial results and yield potential maps from the multiyear regional feedstock partnership." *GCB Bioenergy* 10(10): 698–716. https://doi.org/10.1111/gcbb.12493.

Nguyen, T. H., J. L. Field, H. Kwon, T. R. Hawkins, K. Paustian, and M. Q. Wang. 2022. "A multi-product landscape life-cycle assessment approach for evaluating local climate mitigation potential." *Journal of Cleaner Production* 354: 131691. https://doi.org/10.1016/j.jclepro.2022.131691.

Richard, T. L. 2010 "Challenges in scaling up biofuels infrastructure." Science 329: 793-796. https://doi.org/10.1126/science.1189139.

Sloat, L.L., S.J. Davis, J.S. Gerber, F.C. Moore, D.K. Ray, P.C. West, and N.D. Mueller. 2020. "Climate adaptation by crop migration." *Nature Communications* 11: 1243. https://doi.org/10.1038/s41467-020-15076-4.

Turner, P. A., K. J. Mach, D. B. Lobell, S. M. Benson, E. Baik, D. L. Sanchez, and C. B. Field. 2018. "The global overlap of bioenergy and carbon sequestration potential." *Climatic Change* 148: 1-10. https://doi.org/10.1007/s10584-018-2189-z.

Ugarte, D. G. D. L. T., and D. E. Ray. 2000. "Biomass and bioenergy applications of the POLYSYS modeling framework." *Biomass and Bioenergy* 18(4): 291–308. https://doi.org/10.1016/S0961-9534(99)00095-1.

USDA. n.d. *The Conservation Reserve Program: A 35-Year History* Washington, DC: U.S. Department of Agriculture. https://www.fsa.usda.gov/Assets/USDA-FSA-Public/usdafiles/Conservation/PDF/35_YEARS_CRP_B.pdf.

Volk, T. A., B. Berguson, C. Daly, M. D. Halbleib, R. Miller, T. G. Rials, L. P. Abrahamson et al. 2018. "Poplar and shrub willow energy crops in the United States: Field trial results from the multiyear regional feedstock partnership and yield potential maps based on the PRISM-ELM model." *GCB Bioenergy* 10(10): 735–751. https://doi.org/10.1111/gcbb.12498.

Wagner, G., and W. Schlenker. 2022. "Declining crop yields limit the potential of bioenergy." *Nature* 609(7926): 250–251. https://doi.org/10.1038/d41586-022-02344-0.

Wallander, S., D. Smith, M. Bowman, and R. Claassen. 2021. "Cover Crop Trends, Programs, and Practices in the United States." Washington, DC: U.S. Department of Agriculture Economic Research Service. EIB 222. https://ers.usda.gov/webdocs/publications/100551/eib-222.pdf?v=7190.5.

Xu, S., R. Wang, T. Gasser, P. Ciais, J. Peñuelas, Y. Balkanski, O. Boucher et al. 2022. "Delayed use of bioenergy crops might threaten climate and food security." *Nature* 609(7926). https://doi.org/10.1038/s41586-022-05055-8.

4 Economic Analysis of Feedstock Logistics and Preprocessing

4.1 Background

The objective of this analysis was to model transportation and preprocessing by simulating the flow of biomass along the supply chain for a set of biomass-to-X pathways as a way to verify the feasibility of the projections made by GCAM. Specifically, the analysis was performed to identify the number of biorefineries that can be supported and the range of costs to prepare the biomass for conversion. Data from the supply curves developed by ORNL (Chapter 3) for the most important feedstock categories (i.e., crop residues, energy crops, woody residues, and short rotation woody crops [SRWC]) were used to evaluate the logistics and preprocessing requirements for a set of biomass-to-X pathways identified by NREL (Chapter 5). The suite of tools developed by INL's supply chain and logistics research and development team were adapted to model the chosen feedstock conversion pathway combinations. The modeled logistics system accounted for the transportation and handling of selected biomass feedstocks, from multiple source locations, supplied to the biorefinery. Moreover, the quantity of biomass procured was estimated after accounting for systemwide losses of biomass during harvest, storage, and preprocessing, and the preprocessing system was designed to ensure that the processed feedstock met downstream conversion specifications for critical material attributes.

The primary results of the analysis were as follows:

1. The herbaceous-biomass-to-ethanol pathway supplied 227 biorefineries with a total of approximately 723 million dry short tons per year of biomass at an average delivered cost between $118 and $159 per dry ton. The two feedstock logistics scenarios, dry/baled logistics and wet/chopped logistics, supplied 176.4 million dry short tons per year and 546.4 million dry short tons per year, respectively.
2. The woody-biomass-to-gasification pathway supplied 152 biorefineries with a total of 162 million dry short tons per year of biomass at an average delivered cost between $103 and $132 per dry short ton. The woody-biomass-to-pyrolysis pathway supplied 109 biorefineries with 95 million dry short tons per year of biomass at an average delivered cost between $110 and $129 per dry short ton.
3. Feedstock availability and transportation costs vary by region, and depending on the quality specifications for downstream conversion, the preprocessing system design needs to be modified to ensure that the processed biomass meets defined critical material attributes. Mitigating variability in feedstock quality, through removal of inorganic elements and manipulating the moisture and size of particles to meet quality specifications, will increase cost and energy requirements during preprocessing.
4. Preliminary spatial analysis of selected biorefinery locations compared with disadvantaged census tracts identified by the DOE's Disadvantaged Communities Reporter mapping tool shows substantial overlap. Although conducting a regional impact analysis was beyond the scope of this study, future research could evaluate regional economy/community impacts and the economic, social, and environmental trade-offs of biorefinery location choice.

This chapter presents an overview of the methodology for estimating the economic and energy performance of logistics and preprocessing systems. We identified flexible supply-chain systems, which are modified based on the properties of the biomass being sourced (e.g., wet /chopped logistics for herbaceous biomass with high moisture and baled/dry logistics for herbaceous biomass with low moisture), to determine the maximum potential feedstock supply that could be mobilized for different end uses. For the herbaceous supply chain, we include both dry/baled logistics and wet/chopped logistics to account for regional variation in feedstock supply systems for agricultural residues and energy crops. The woody biomass supply chain is designed to accommodate differences in logistics and preprocessing system designs for logs, forestry residues, and SRWC. We also include a preliminary assessment of equipment needs and identify spatial overlap between selected biorefinery locations and disadvantaged regions and communities in the United States.

4.2 Methods

4.2.1 Feedstock Logistics

Mixed-integer linear programming (MILP) is a method of mathematical optimization in which some of the decision variables are restricted to integer values (e.g., to represent whether resources are used). For this project, a MILP model was developed to allocate the biomass supply from areas of production to locations of final use. Through this approach, available resources were chosen based on net transportation cost, quantity, and quality considerations. To determine the maximum potential feedstock supply that could be mobilized, the optimization model was developed as a dual, lexographic objective that first maximized the amount of feedstock material and then minimized the delivered cost to deliver the maximized supply. Following NREL's feedstock conversion design cases (Davis et al. 2013, Dutta et al. 2011), the minimum designed capacity for the biorefinery was set at 725,000 dry short tons per year but was allowed to vary in multiples of 725,000 short tons based on feedstock availability in a region. The total supply delivered to a location is constrained by biomass supply in surrounding locations and by the quality characteristics of the material. Delivered cost is the summation of the farmgate cost and transportation costs. The grower payment, which reflects the quantity of a feedstock purchased at a location at a specific price, is the farmgate cost as listed in the 2016 Billion-Ton Report (Langholtz et al. 2016) for a specific feedstock supply minus the harvesting and collection cost. Transportation cost, which is based on truck transportation from a feedstock supply location to the biorefinery, is made up of two parts. The first part is the variable cost based on the distance travelled and takes into account fuel consumption, maintenance cost of the truck, labor, and the bulk density of the material being transported. The second component is a fixed cost per short ton for loading and unloading activities and includes the fixed cost of the truck and trailer.

The MILP model is bound by several constraints on the solution. The supply constraint limits the amount of a biomass feedstock type, purchased at a specific price, that can be shipped from a supply location. An associated constraint specifies that only a single price can be selected for a biomass type at a location, thus limiting the access to each biomass feedstock type from a supply location to what is available at a single grower payment point along the supply curve. Additionally, a feedstock demand constraint enforces that the total quantity of all delivered feedstock, accounting for losses, must at minimum meet the required demand of the biorefinery.

Finally, a feedstock quality constraint requires that the delivered feedstock, after accounting for compositional changes due to dry-matter loss in the supply chain, meets the minimum specified quality requirements. The quality requirements were derived from the conversion specifications to be presented in Chapter 5, which identified feedstock utilization for specific feedstock-to-X pathways.

4.2.2 Feedstock Preprocessing

Feedstock quality is vital and can adversely influence the efficiency of downstream conversion processes. In addition, variability in feedstock quality—specifically moisture, ash, and carbohydrate content, as well as particle size specifications—necessitates additional preprocessing, which has implications for the delivered feedstock cost and energy requirements of the preprocessing system. As a first step, we collected feedstock-related critical material attributes (CMAs), i.e., feedstock properties that can influence downstream conversion processes. Three conversion pathways were identified, each having distinct CMAs (see Table 4.1): 1) herbaceous feedstocks to ethanol, 2) woody feedstocks for gasification, and 3) woody feedstocks for pyrolysis. The approach for feedstock preprocessing encompasses a range of system designs that can be used to achieve desired CMA specifications for downstream conversion. Some modifications might be necessary based on the specific characteristics of the feedstock, e.g., moisture and ash content, which can vary depending on the region or local weather conditions during or after harvest.

Table 4.1. Feedstock Preprocessing

Feedstock Category	Logistics System	Conversion Process
Herbaceous	Agricultural residue collection and processing	Ethanol pathway
Herbaceous	Herbaceous energy crop harvest, collection, and processing	Ethanol pathway
Woody	Forest residue collection and processing	Gasification/pyrolysis pathway
Woody	Traditional forest harvest, collection, and processing	Gasification/pyrolysis pathway
Woody	Short-rotation woody crop harvest, collection, and processing	Gasification/pyrolysis pathway

For herbaceous feedstocks, we considered two preprocessing system designs: 1) dry/baled logistics (a conventional form of feedstock logistics) and 2) wet/chopped logistics (Wendt et al. 2018). Under both systems, the specified CMAs for downstream conversion were a particle size between ¾ inch and 1 inch, with ash content below 10 wt%, moisture below 50 wt%, and total carbohydrate content above 50 wt%.

4.2.2.1 Dry/Baled Logistics System for Ethanol Pathway

For the dry/baled logistics system, the preprocessing operations encompass the unit processes within the dashed box in Figure 4.1. The stored bales undergo a first-stage size reduction in a bale processor. The bale processor has the capability to feed two bales at separate feed rates,

which could be an advantage for blending bales with different moisture contents or biomass types (Lin et al. 2020). After the first-stage size reduction, the material is air-classified to remove soil contaminants and then undergoes second-stage size reduction using a rotary shear. After these operations are completed, the CMA requirements for downstream conversion are achieved and the biomass is transferred to covered storage prior to use in the conversion process.

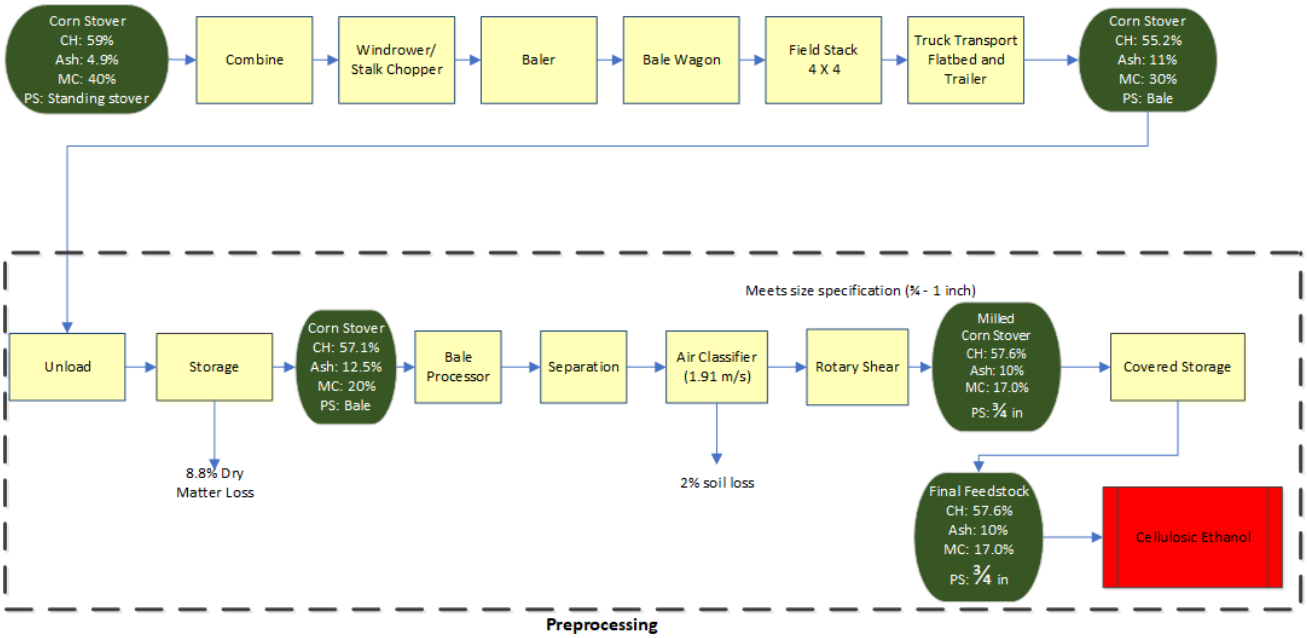

Figure 4.1. Preprocessing configuration for baled feedstock (corn stover example)

CH = carbohydrate content, MC = moisture content, PS = particle size

4.2.2.2 Wet/Chopped Logistics System for Ethanol Pathway

For the wet/chopped logistics system, the preprocessing operations encompass the unit processes within the dashed box in Figure 4.2. The main difference compared to the dry/baled logistics system is that the biomass is size-reduced to ¾ inch in the field itself using a forage chopper. The chopped biomass is bagged and ensiled in silage bags at the field side (Wendt et al. 2018). These operations result in lower dry matter losses in storage, and since the biomass is already size-reduced, preprocessing requirements at the refinery are minimal, comprising primarily a magnetic separation process and a washing step to eliminate soil contamination and meet the specified CMAs.

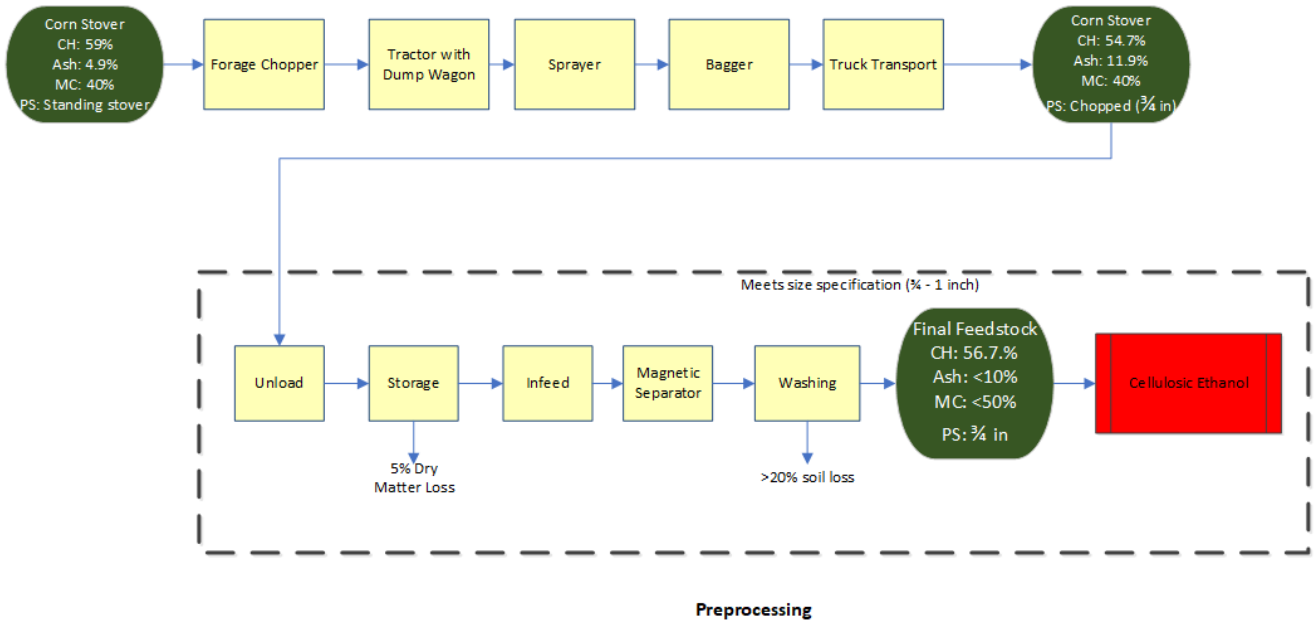

Figure 4.2. Preprocessing configuration for chopped feedstock (corn stover example)

CH = carbohydrate content, MC = moisture content, PS = particle size

Akin to the approach adopted for herbaceous feedstocks, the woody preprocessing systems encompass a range of designs that can be used to achieve desired CMA specifications for downstream conversion. We considered two different conversion pathways, gasification and pyrolysis, in conjunction with woody biomass from traditional forest harvest (logs), logging residues, and SRWC. The preprocessing operations for logging residues and SRWC are assumed to be identical, as the feedstocks are transported from the harvest sites in a chipped format for additional preprocessing at the biorefinery.

4.2.2.3 Woody Biomass for Gasification Pathway

For the gasification pathway, the CMAs for downstream conversion were particle size between 1 mm and 2 inches, low ash content (5–25 wt%), and moisture content between 3 wt% and 15 wt%. For traditional forest harvest, operations at the biorefinery include debarking and chipping the logs to an approximate size of 2 inches, as shown in the dashed box in Figure 4.3. On the other hand, logging residues and SRWC are delivered to the biorefinery in chipped form (see Figure 4.4). Chips from either material are conveyed to storage piles, where they are held until drying. For the gasification pathway, the materials are dried to 10% moisture content with waste heat from the conversion process using a rotary dryer and then held in covered storage (Hartley et al. 2020). The chips from each pile can be blended to meet the desired ash specification based on the type of reactor.

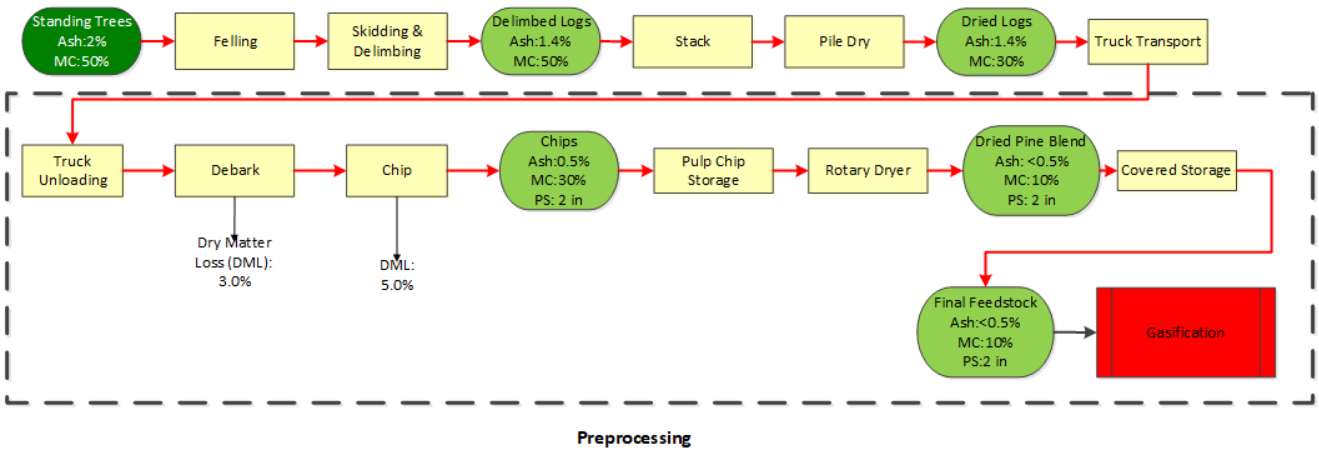

Figure 4.3. Preprocessing configuration for traditional harvest (pine logs example)

MC = moisture content, PS = particle size

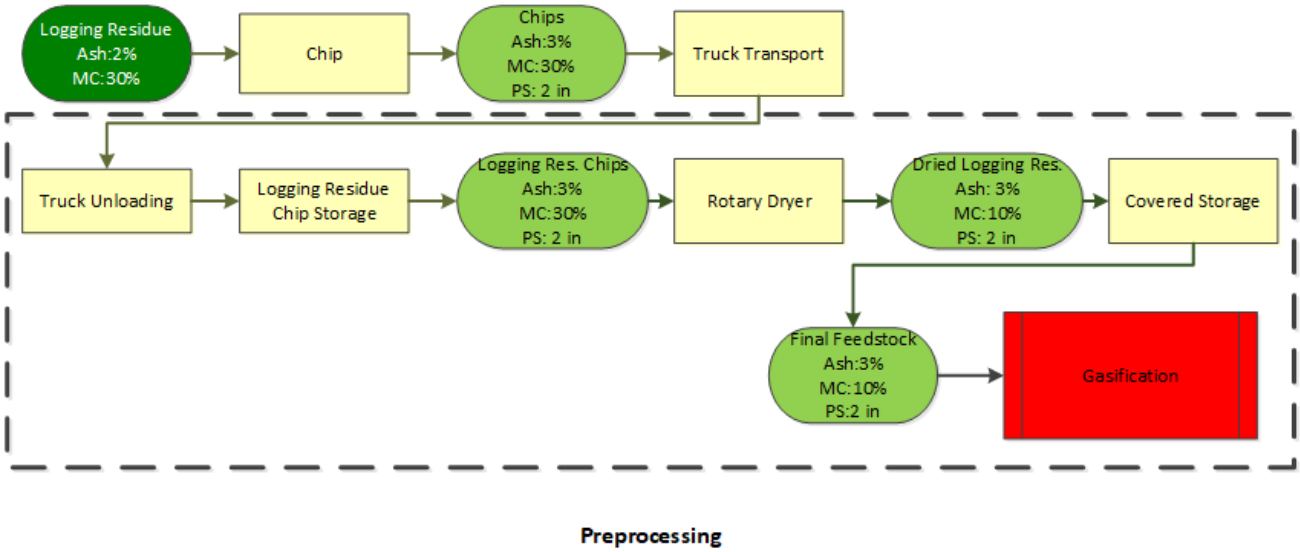

Figure 4.4. Preprocessing configuration for residues/SRWC (logging residues example)

MC = moisture content, PS = particle size

4.2.2.4 Woody Biomass for Pyrolysis Pathway

For the pyrolysis pathway, the CMAs for downstream conversion were particle size between 1 mm and 6 mm, moisture between 3 wt% and 15 wt%, and a much more stringent ash constraint of between 0 wt% and 1.5 wt%. The smaller particle size specification necessitates the inclusion of an additional comminution step during preprocessing. The initial steps are analogous to those described in the gasification pathway. For traditional forest harvest, operations at the biorefinery include log debarking and chipping to an approximate size of 2 inches, as shown in the dashed box in Figure 4.5. Logging residues and SRWC are delivered to the biorefinery in a chipped form (see Figure 4.6). Chips from either material are conveyed to storage piles, followed by secondary size reduction using a rotary shear. Unlike the gasification process, this system configuration has no waste process heat for use in the drying step. The material is dried to 10%

moisture content using a rotary dryer, but because the material is rotary sheared prior to drying, it requires less energy for drying than chips do (Hartley et al. 2020). The dried material is then held in covered storage until it is fed to the conversion process.

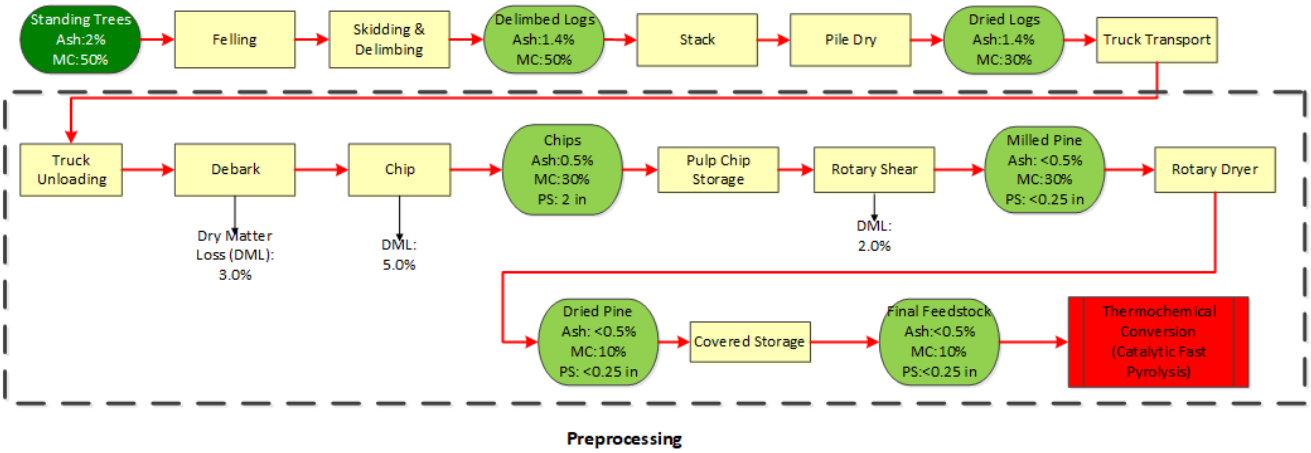

Figure 4.5. Preprocessing configuration for traditional harvest (pine logs example)

MC = moisture content, PS = particle size

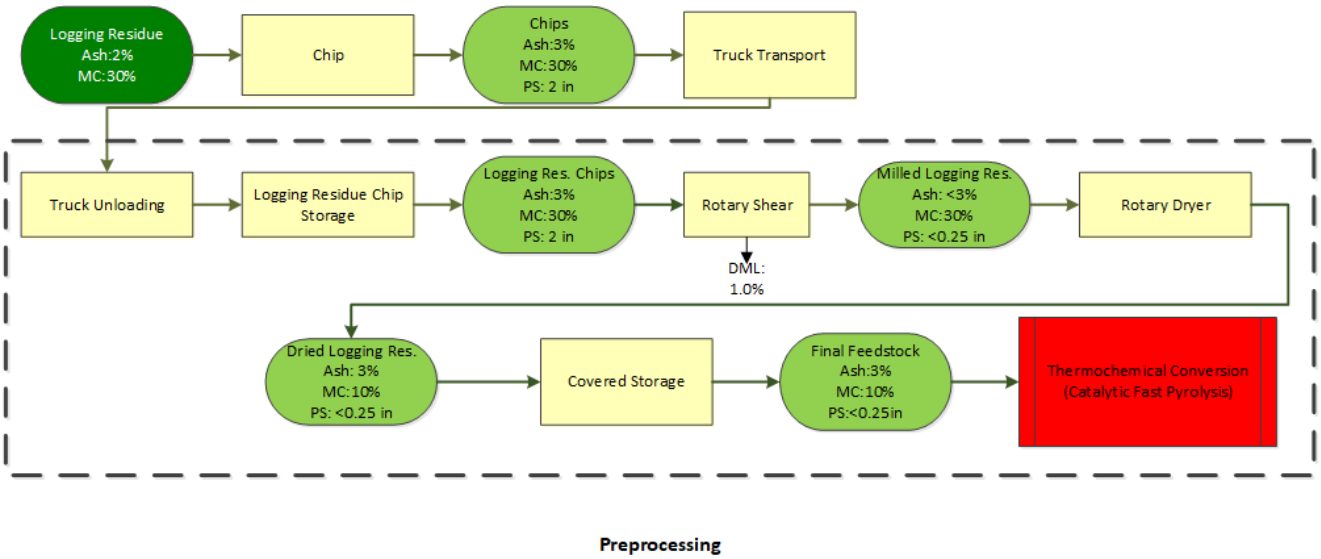

Figure 4.6. Preprocessing configuration for residues/SRWC (logging residues example)

MC = moisture content, PS = particle size

4.3 Results and Discussion

4.3.1 Feedstock Logistics

To limit computational complexities, we overlaid a grid of approximately 400 points spaced approximately 200 miles apart over the contiguous United States to simulate potential biorefinery locations that could be selected in the optimization analysis. The MILP model

allocated biomass supply from areas of production to locations of final use by maximizing the amount of material that could be mobilized and minimizing the delivered cost. The maximized supply at locations was also constrained by biomass supply at surrounding locations and the quality characteristics of the material. The delivered cost incorporated farmgate cost and transportation costs.

4.3.1.1 Herbaceous Biomass

Out of the approximately 400 potential locations, 227 were selected as refinery locations for herbaceous biomass, most of which were located toward the eastern half of the country. We estimated that these refineries could together receive around 723 million dry short tons of biomass. The Missouri, Upper Mississippi, and Arkansas–White–Red HUC2 regions receive the highest supply of herbaceous biomass and each could receive more than 100 million dry short tons per year (Figure 4.7). The source-to-refinery distance varied from 30 miles to around 146 miles, and the weighted average (based on distance) total delivered cost of herbaceous biomass varied from $118 to $159 per dry short ton of delivered biomass (2016$). Overall, the delivered costs of biomass were lower in regions with large biomass supply (Figure 4.8).

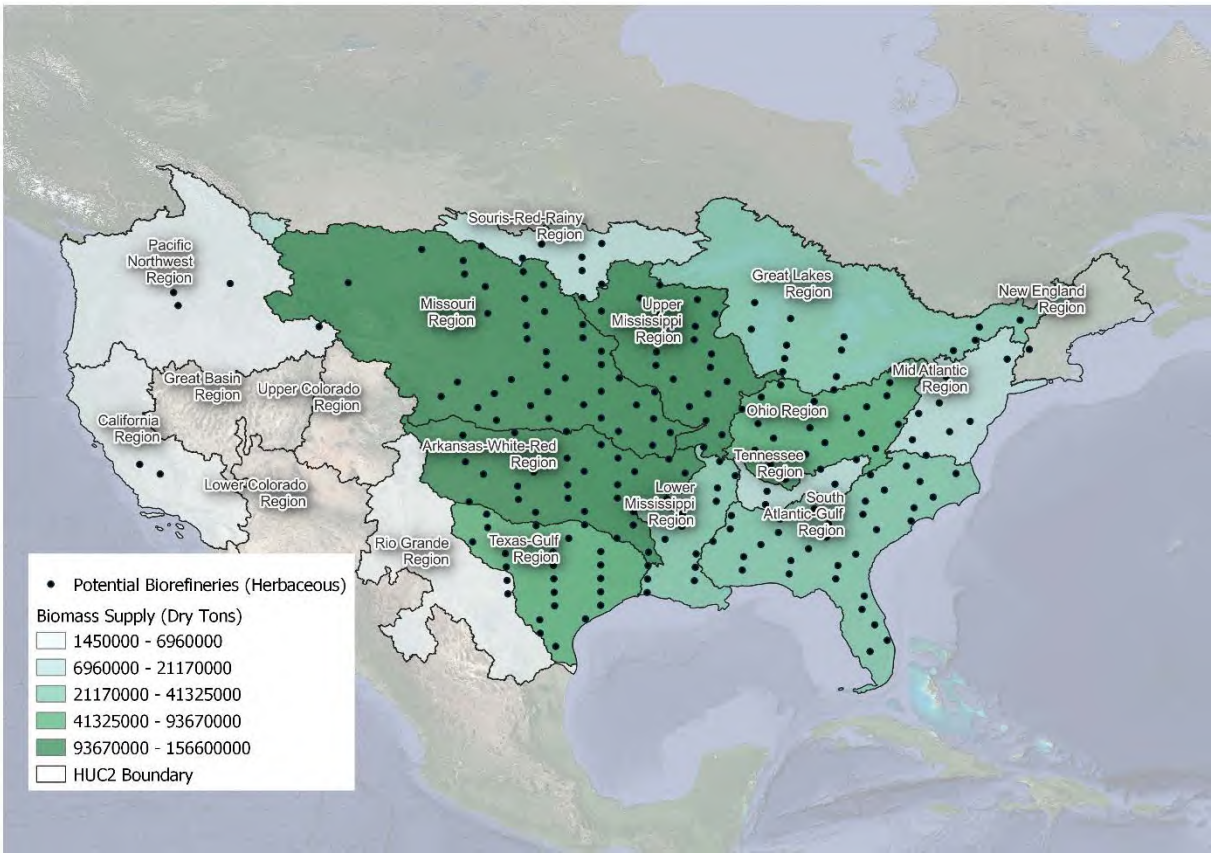

Figure 4.7. Herbaceous refineries with potential biomass supply at HUC2 region level (short tons)

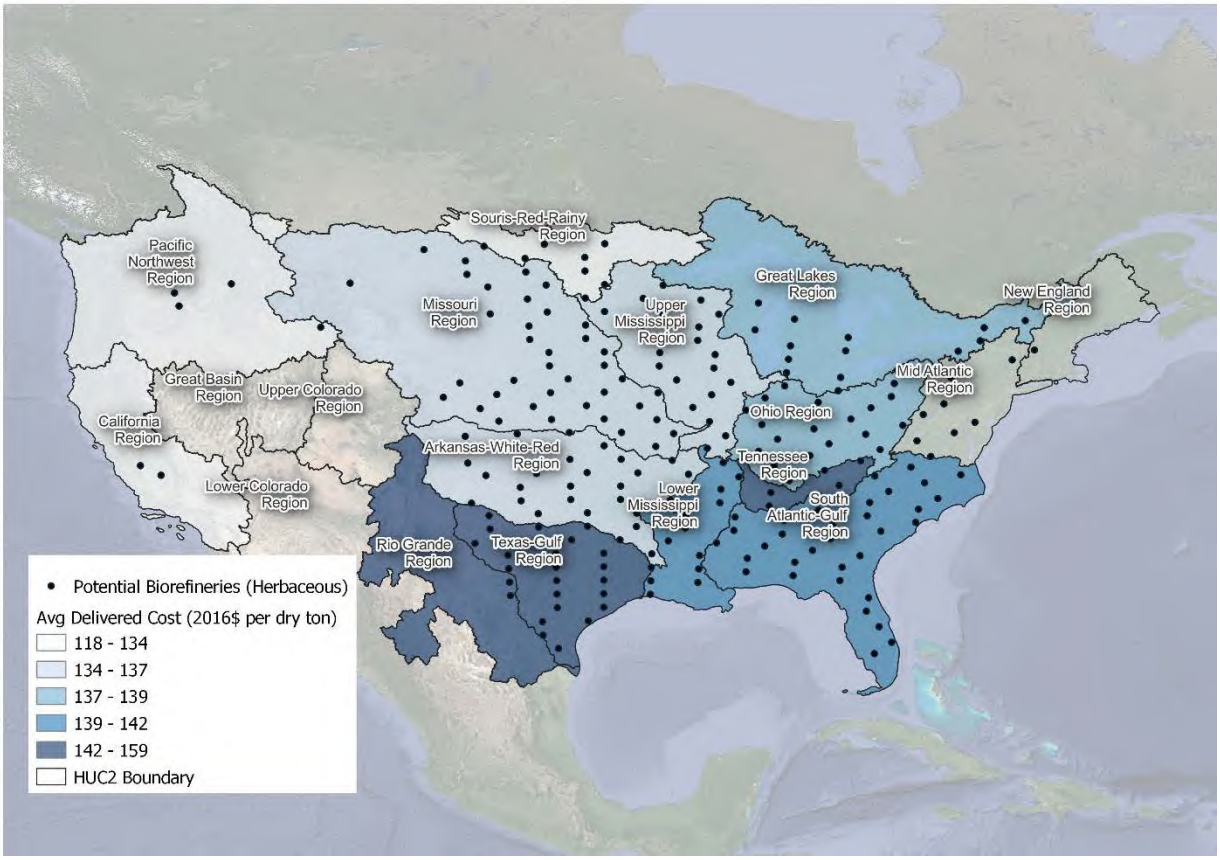

Figure 4.8. Source to refinery average delivered cost for herbaceous biomass (short tons)

4.3.1.2 Woody Biomass for Gasification Pathway

For the woody biomass gasification pathway, we selected 152 biorefinery locations, located mostly in southeastern and northern United States. The total quantity of biomass supplied to the biorefineries was estimated at around 162 million dry short tons (Figure 4.9). The Ohio, Mid-Atlantic, and South Atlantic–Gulf HUC2 regions had the highest biomass supply. The estimated average source-to-refinery distance ranged from approximately 79 miles to more than 260 miles for trees, 50 miles to more than 151 miles for residue, and 49 miles to more than 267 miles for SRWC. The average delivered cost ranged from around $103 to almost $132 per dry short ton of delivered biomass (2016$). The Missouri, Upper Colorado, and New England HUC2 regions had the highest costs (Figure 4.10).

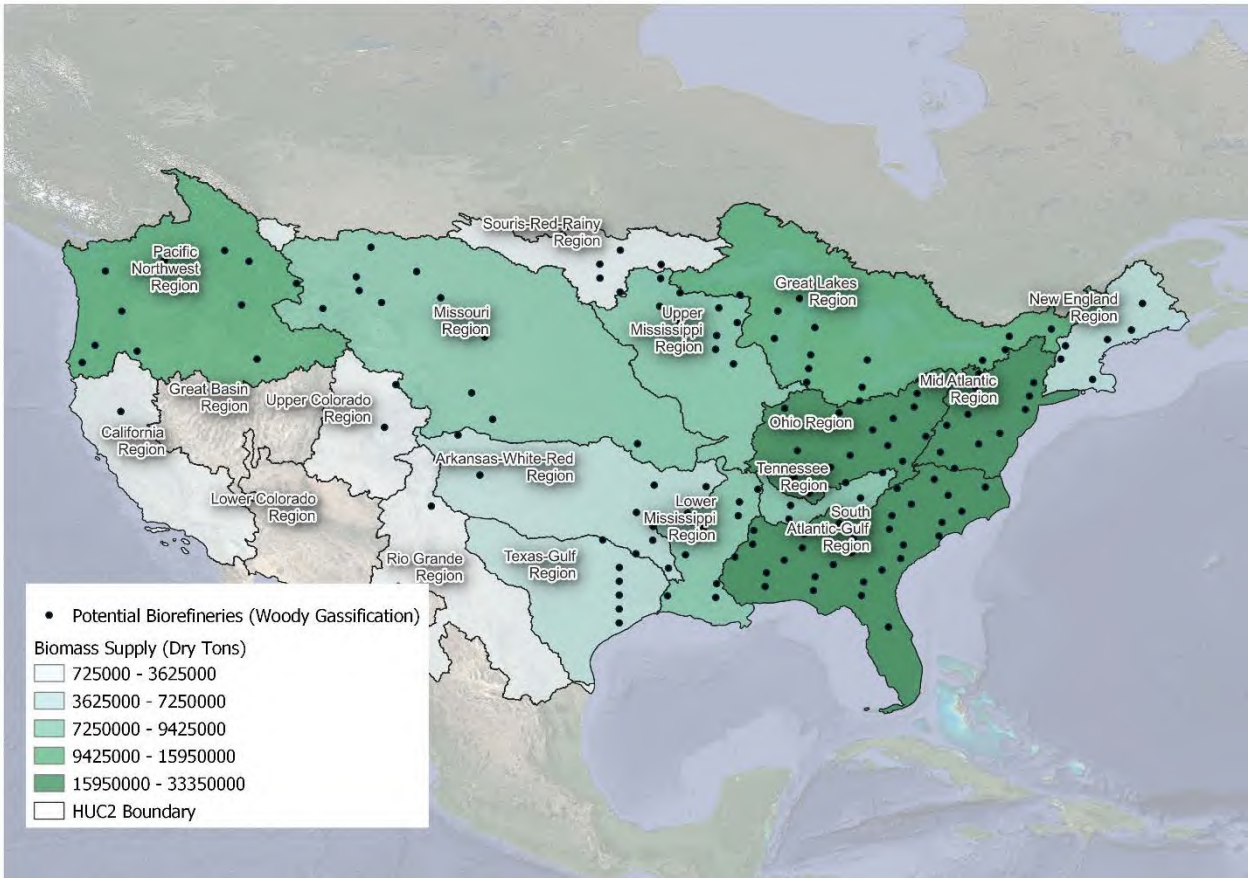

Figure 4.9. Woody biomass refineries (gasification pathway) with potential biomass supply at HUC2 region level

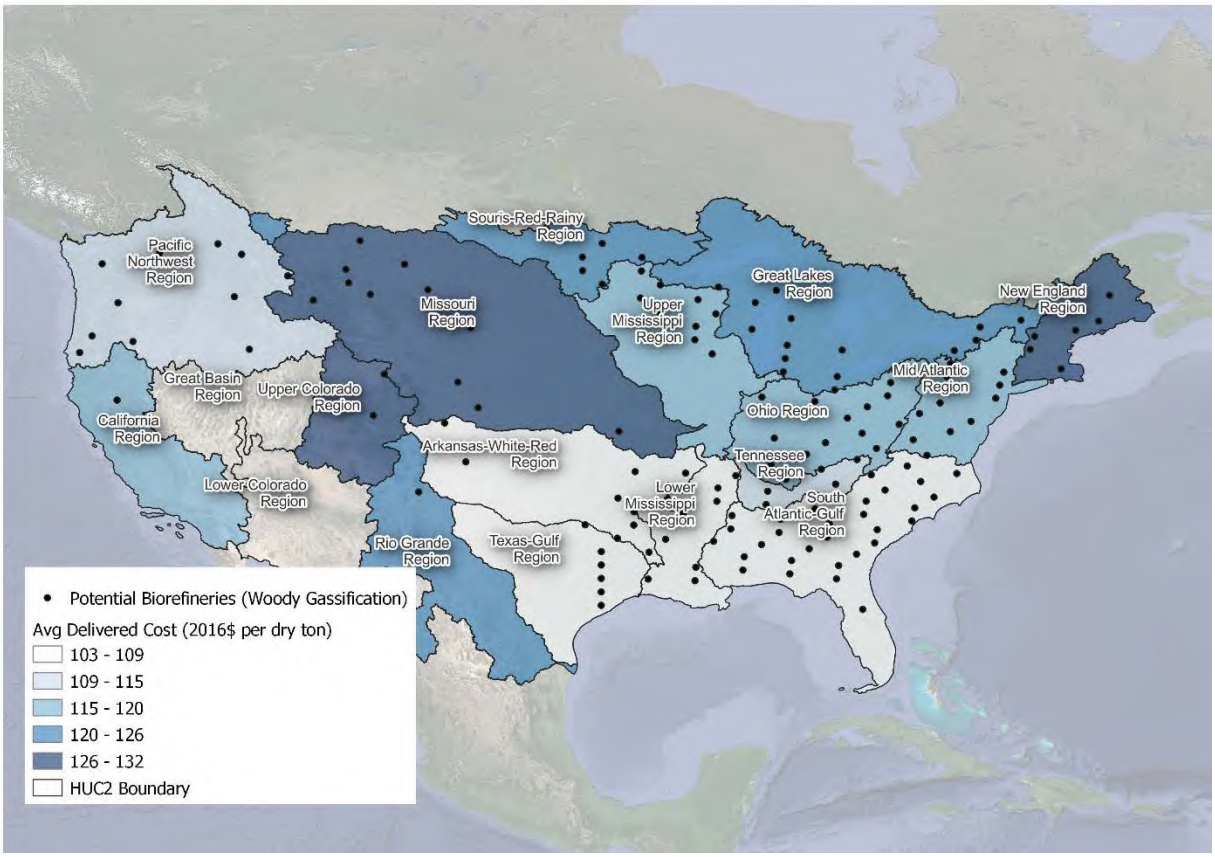

Figure 4.10. Source to refinery average delivered cost for woody biomass (gasification pathway)

4.3.1.3 Woody Biomass for Pyrolysis Pathway

For the woody biomass pyrolysis pathway, we selected 109 potential refinery locations, most of which were located toward the eastern side of the United States. We estimated that these refineries could receive a combined 95 million dry short tons of woody biomass for this pathway. The Mid-Atlantic and South Atlantic–Gulf HUC2 regions had the highest supply of woody biomass (Figure 4.11). The source-to-refinery distance ranged from 10 miles to around 140 miles for SRWC, 43 miles to 95 miles for residue, and 55 miles to 148 miles for trees. The average delivered cost of woody biomass varied from $110 to $128 per dry short ton (2016$). The Upper Colorado and Ohio regions had the highest costs (Figure 4.12).

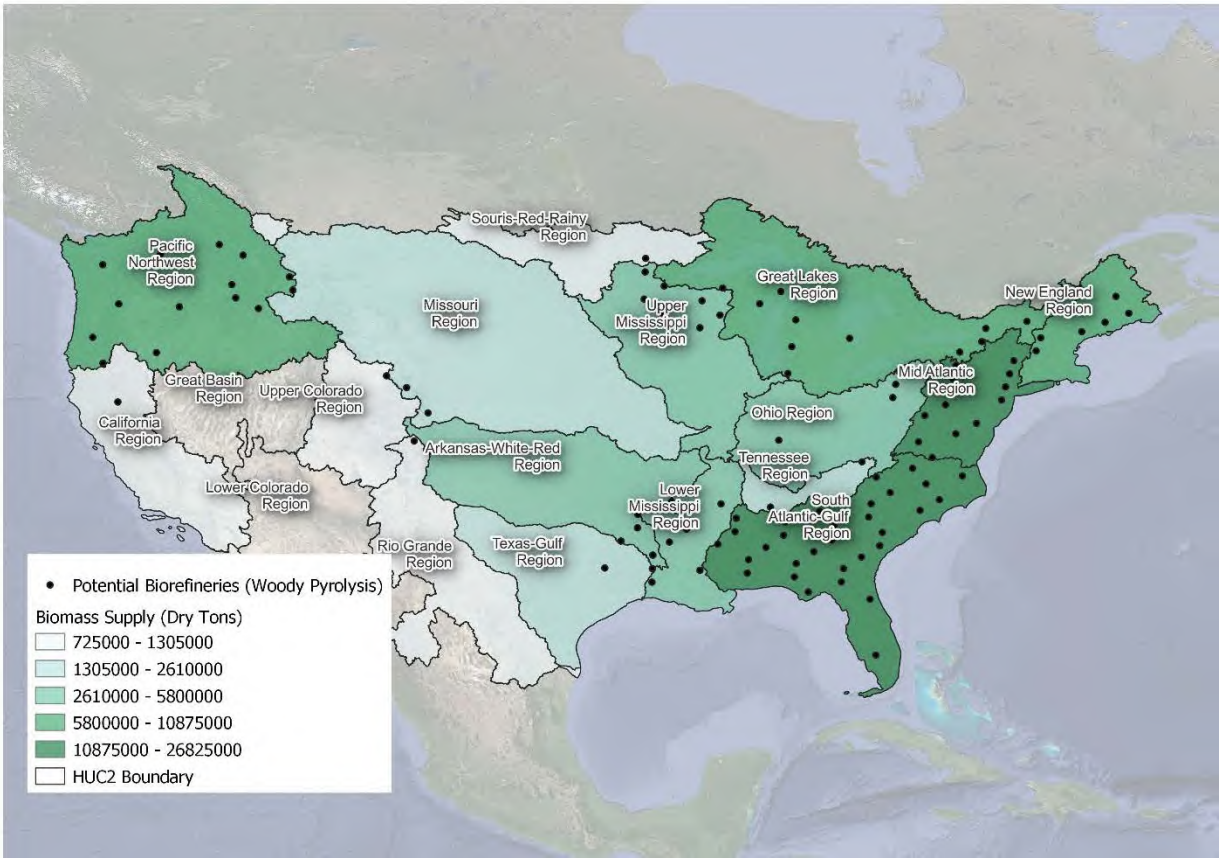

Figure 4.11. Woody refineries (pyrolysis pathway) with potential biomass supply at HUC2 region level (short tons)

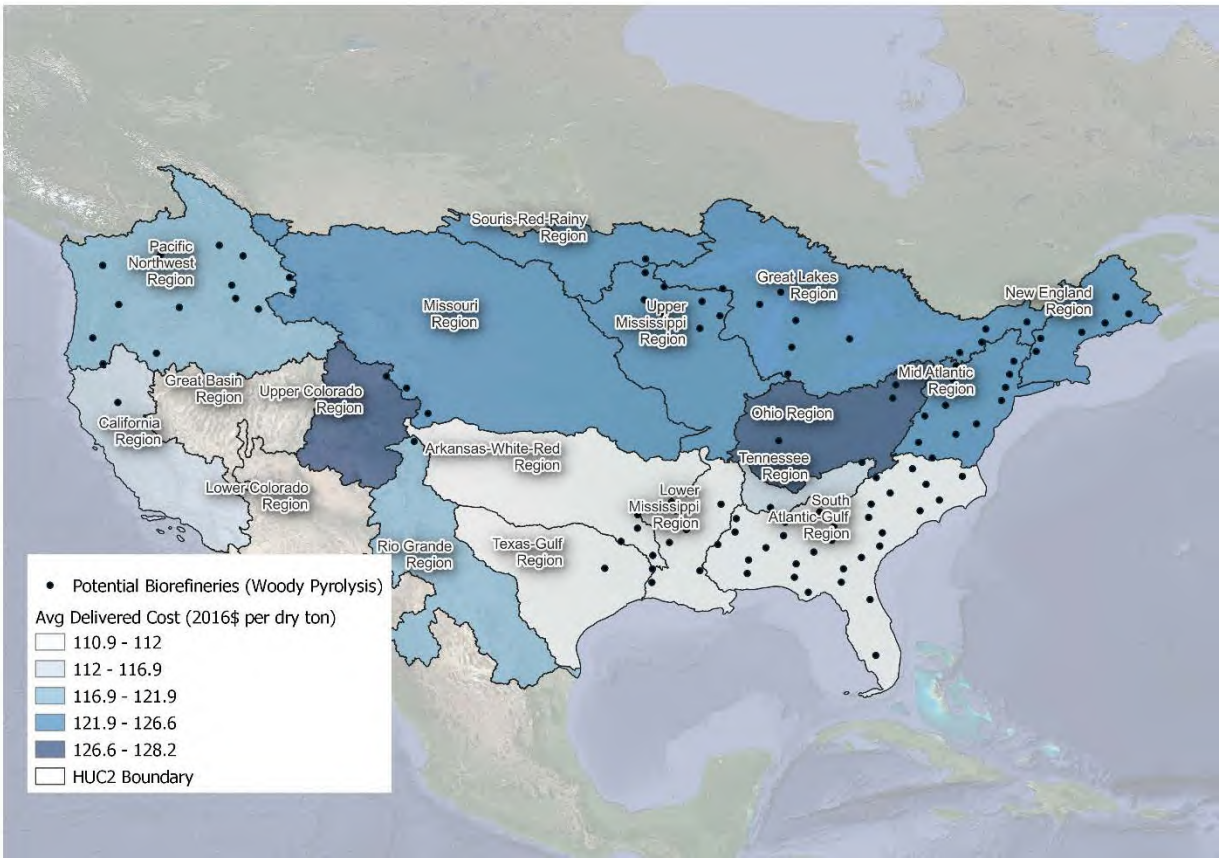

Figure 4.12. Source to refinery average delivered cost for woody biomass for pyrolysis pathway (short tons)

4.3.2 Feedstock Preprocessing

Variability in the incoming biomass is one of the main factors that influences the complexity of feedstock supply systems. As a result, a range of preprocessing operations become necessary to transform raw biomass into a format that is suitable for downstream conversion. Typically, preprocessing operations include steps like washing or air classification to remove contaminants, drying to reduce the moisture content of the feedstock, or size reduction to achieve a standardized feedstock particle size. Figure 4.13 provides a summary of preprocessing costs for the delivered feedstocks for different conversion pathways, and subsequent tables provide a detailed breakdown.

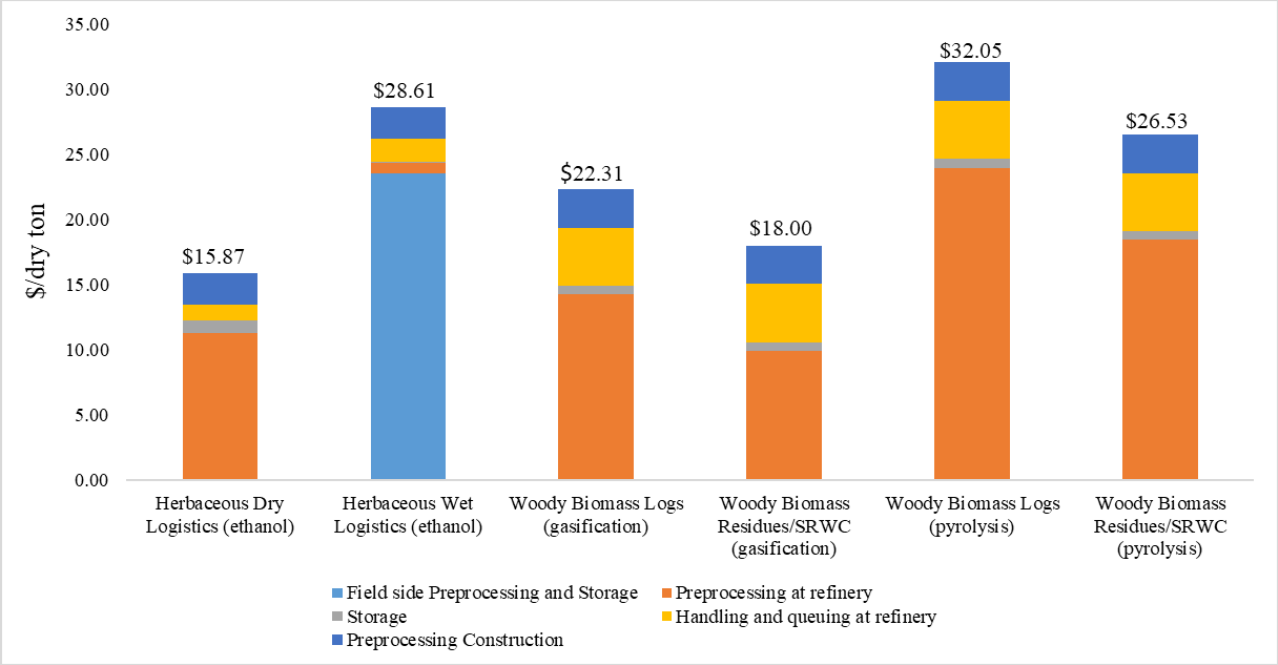

Figure 4.13. Preprocessing costs per dry short ton for delivered feedstocks for different conversion pathways (2016$)

4.3.2.1 Dry/Baled Logistics System for Ethanol Pathway

The cost of preprocessing 725,000 dry short tons per year in the baled logistics system was estimated at $15.87/dry short ton (2016$) (Table 4.2). The unit processes contributing most to the preprocessing cost were air classification and size reduction, which cost $4.83/dry short ton (2016$) and $3.48/dry short ton (2016$), respectively. However, the estimated preprocessing costs do not account for costs associated with dry matter losses, as costs associated with the loss of dry matter depend on upstream processes. Since the upstream costs associated with harvesting, field preprocessing, and transportation can differ based on the region the feedstock is sourced from, this analysis restricts the cost of preprocessing to the operations at the biorefinery itself. The primary unit process contributing to the energy consumption of preprocessing is rotary shearing, followed closely by dust collection and bale. Finally, we estimate dry matter losses (DML) at 12.75% for the preprocessing operations, as delineated in Table 4.2, with the largest losses, 8.8%, occurring during storage.

Table 4.2. Preprocessing Cost and Energy Breakdown for Dry/Baled Logistics System

	Cost ($/dry short ton) (2016$)				
	Ownership Cost	**Operational Cost**	**Total Cost ($/dry short ton)**	**DML (%)**	**MBtu/Dry Ton**
Preprocessing at refinery	2.45	8.84	11.28	3.95	127.35
Bale processor	0.32	1.49	1.80	0.00	28.36
Air classifier	0.62	4.20	4.83	2.45	2.13
Rotary shear	1.05	2.43	3.48	1.50	55.98
Conveyors	0.15	0.03	0.18	0.00	1.08
Dust collection	0.11	0.62	0.73	0.00	30.11
Surge bin	0.03	0.01	0.04	0.00	0.36
Misc. equipment	0.17	0.05	0.22	0.00	1.62
Storage	0.14	0.80	0.95	8.80	-
Handling and queuing at refinery	0.24	0.95	1.19	0.00	7.71
Preprocessing construction	2.44		2.44		
Total preprocessing cost			**15.87**		

4.3.2.2 Wet/Chopped Logistics System for Ethanol Pathway

In the wet/chopped logistics system, preprocessing costs at the refinery are relatively small since the biomass is already size reduced in the field. The total preprocessing costs were estimated at $28.61/dry short ton (2016$), a majority ($23.52/dry short ton (2016$)) of which are incurred in field-side preprocessing and storage (Table 4.3). Field-side preprocessing and storage also contributed the largest share of the energy consumption for the wet/chopped logistics system. While the overall cost of preprocessing was higher for the wet/chopped logistics system, dry matter losses were lower, at 5.75%, compared to the dry/baled logistics system. It is estimated that about 50% of the corn stover available in the United States is too wet to be stored properly in bales, and in such regions the wet/chopped logistics system could be advantageous as a feedstock management approach that reduces the risk of aerobic degradation of the biomass (Wendt et al. 2018).

Table 4.3. Preprocessing Cost and Energy Breakdown for Wet/Chopped Logistics System

	Cost ($/dry short ton) (2016$)				
	Ownership Cost	**Operational Cost**	**Total Cost ($/dry short ton)**	**DML (%)**	**Mbtu/Dry Short Ton**
Field-side preprocessing and Storage	7.52	15.99	23.52	0.75	285.01
Preprocessing at refinery	0.11	0.71	0.82	0.00	22.35
Infeed	0.04	0.01	0.05	0.00	0.21
Magnetic separator	0.05	0.69	0.74	0.00	13.65
Washing	0.01	0.01	0.02	0.00	0.21
Conveyors	0.00	0.01	0.01	0.00	0.28
Storage	0.09	0.00	0.09	5.00	-
Handling and queuing at refinery	0.24	1.50	1.74	0.00	8.21
Preprocessing construction	2.44		2.44		
Total preprocessing cost			**28.61**		

4.3.2.3 Woody Biomass Logs for Gasification Pathway

For woody biomass logs for the gasification pathway, preprocessing costs were estimated at $22.32/dry short ton (2016$) (Table 4.4). Since the gasification process can accept a particle size of around 2 inches, we did not include any additional size reduction of the chips. While the chipping process contributes $4.81/dry ton (2016$) to the overall preprocessing costs, the costs associated with the drying step are more than twice as large, at $8.81/dry short ton (2016$). The gasification process utilizes waste heat for the drying step, resulting in some savings in the energy required to power the rotary dryer.

Table 4.4. Preprocessing Cost and Energy Breakdown for Logs for Gasification Pathway

	Cost ($/dry short ton) (2016$)				
	Ownership Cost	**Operational Cost**	**Total Cost ($/dry short ton)**	**DML (%)**	**MBtu/Dry Short Ton**
Preprocessing at refinery	4.92	9.31	14.23	8.00	310.30
Debarker	0.07	0.29	0.36	3.00	3.04
Chipper	1.48	2.71	4.18	5.00	86.66
Rotary dryer	3.16	5.65	8.81	0.00	132.24
Conveyors	0.02	0.01	0.04	0.00	0.56
Misc. equipment	0.04	0.00	0.04	0.00	0.00
Dust collection	0.14	0.65	0.79	0.00	26.73
Surge bin	0.01	0.00	0.01	0.00	0.00
Storage	0.25	0.42	0.67	0.00	8.64
Handling and queuing at refinery	1.16	3.28	4.44	0.00	52.43
Preprocessing construction	2.96		2.96	0.00	
Total preprocessing cost			**22.31**		

4.3.2.4 Woody Biomass Residues/SRWC for Gasification Pathway

For logging residues/SRWC for the gasification pathway, preprocessing costs were estimated at $18.00/dry short ton (2016$) (Table 4.5). Since the biomass is delivered in the form of chips (approximately 2 inches), the only preprocessing step required at the refinery is drying of the biomass to 10% moisture content. While the drying step utilized waste heat, it was nevertheless the primary contributor to energy usage. We assumed no dry matter losses during preprocessing for this pathway.

Table 4.5. Preprocessing Cost and Energy Breakdown for Residues/SRWC for Gasification Pathway

	Cost ($/dry short ton) (2016$)				
	Ownership Cost	Operational Cost	Total Cost ($/dry short ton)	DML (%)	MBtu/Dry Short Ton
Preprocessing at refinery	3.43	6.49	9.92	0.00	220.58
Rotary dryer	3.26	5.82	9.08	0.00	132.24
Conveyors	0.02	0.01	0.04	0.00	0.54
Dust collection	0.14	0.65	0.79	0.00	26.73
Surge bin	0.01	0.00	0.01	0.00	0
Storage	0.25	0.42	0.67	0.00	8.64
Handling and queuing	1.16	3.28	4.44	0.00	52.43
Preprocessing construction	2.96		2.96	0.00	
Total preprocessing cost			**18.00**		

4.3.2.5 Woody Biomass Logs for Pyrolysis Pathway

The CMAs for the pyrolysis pathway were more stringent than those for the gasification pathway. As a result, we included an additional size reduction step to ensure that the particle size was under 6 mm. Furthermore, there is no source of waste process heat that can be used for the drying step, which resulted in higher drying costs and energy requirements. The total preprocessing costs for woody biomass for the pyrolysis pathway were estimated at $32.05/dry short ton (2016$). The rotary dryer contributed the highest, at $13.08/dry short ton (2016$), followed by the rotary shear at $5.60/dry short ton (2016$) (Table 4.6). Handling and queuing and the chipping process were the other large contributors to preprocessing costs, at $4.44/dry short (2016$) ton and $4.09/dry short ton (2016$), respectively. The rotary dryer accounted for a majority of the energy consumption at the preprocessing stage, followed by the chipper and rotary shear, which each consumed less than one-tenth of the energy of the dryer on a per-ton basis. We assumed approximately 10% dry matter losses during preprocessing; however, costs associated with the losses are not included in the cost estimates in Table 4.6.

Table 4.6. Preprocessing Cost and Energy Breakdown for Logs for Pyrolysis Pathway

	Cost ($/dry short ton) (2016$)				
	Ownership Cost	**Operational Cost**	**Total Cost ($/dry short ton)**	**DML (%)**	**MBtu/Dry Short Ton**
Preprocessing at refinery	8.84	15.14	23.98	10.00	1145.58
Debarker	0.07	0.27	0.35	3.00	3.08
Chipper	1.48	2.62	4.09	5.00	87.98
Rotary shear	2.26	3.34	5.60	2.00	68.92
Rotary dryer	4.82	8.27	13.08	0.00	896.83
Conveyors	0.02	0.01	0.04	0.00	0.56
Misc. equipment	0.04	0.00	0.04	0.00	0.00
Dust collection	0.14	0.62	0.76	0.00	27.14
Surge bin	0.01	0.00	0.01	0.00	0.00
Storage	0.25	0.42	0.67	0.00	8.64
Handling and queuing	1.16	3.28	4.44	0.00	52.43
Preprocessing construction	2.96		2.96	0.00	
Total preprocessing cost			**32.05**		

4.3.2.6 Woody Biomass Residues/SRWC for Pyrolysis Pathway

The preprocessing costs of woody biomass residues/SRWC for the pyrolysis pathway were estimated at $26.53/dry short ton (2016$) (Table 4.7). As for the woody biomass logs, the rotary dryer and rotary shear were the two largest contributors to the preprocessing costs, at $11.70/dry short ton (2016$) and $5.95/dry short ton (2016$), respectively. The rotary dyer and rotary shear were also the main contributors to the energy consumption of preprocessing. Since we adopted an approach that developed preprocessing system designs for different biomass feedstocks independently, the biomass can be blended based on the downstream CMA requirements. For example, in the current setup, a feedstock blend comprising 60% clean pine and 40% residues will achieve all the CMAs specified for the pyrolysis pathway. We have not included any air classification steps in the preprocessing system design and thus have assumed minimal dry matter losses during preprocessing.

Table 4.7. Preprocessing Cost and Energy Breakdown for Residues/SRWC for Pyrolysis Pathway

	Cost ($/dry short ton) (2016$)				
	Ownership Cost	Operational Cost	Total Cost ($/dry short ton)	DML (%)	MBtu/Dry Short Ton
Preprocessing at refinery	5.31	13.15	18.46	1.00	1,100.64
Rotary shear	1.87	4.07	5.95	1.00	115.5
Rotary dryer	3.26	8.44	11.70	0.00	896.83
Conveyors	0.02	0.01	0.04	0.00	0.51
Dust collection	0.15	0.62	0.77	0.00	26.73
Surge bin	0.01	0.00	0.01	0.00	0
Storage	0.25	0.42	0.67	0.00	8.64
Handling and queuing	1.16	3.28	4.44	0.00	52.43
Preprocessing construction	2.96		2.96	0.00	
Total preprocessing cost			26.53		

4.3.3 Biorefinery Locations and Disadvantaged Communities

The current administration has made a commitment to address inequity and inequality through several initiatives. DOE developed a working definition of disadvantaged communities based on cumulative burden, which includes information on 36 burden indicators mapped at the census tract level.[25] The 36 indicators are grouped into four categories (each with a different number of indicators): fossil dependence, energy burden, environmental and climate hazards, and socio-economic vulnerabilities. A census tract is classified as a disadvantaged community if:

1. It ranks in the 80th percentile of the cumulative sum of the 36 burden indicators *and*
2. Has at least 30% of the households classified as low-income.

Using data accessed in August 2022 from DOE's Disadvantaged Communities Reporter mapping tool, 13,978 census tracts were identified as disadvantaged in the contiguous United States (Figure 4.13a), which represents nearly 20% of the more than 72,000 census tracts in the contiguous United States. We assessed the extent of spatial overlap between the identified biorefinery locations (highlighted by the blue dots in Figure 4.13b–d) and disadvantaged communities (census tracts highlighted in red in Figure 4.13a–d).

As the source-to-refinery distance for herbaceous biomass is approximately 50 miles, we estimated the number of disadvantaged census tracts that fall within a 50-mile radius of the 227 locations identified as potential locations for biorefineries using herbaceous biomass. 6,493 census tracts (approximately 46% of all disadvantaged communities) lie within a 50-mile radius of these potential biorefinery locations (Figure 4.13b). Meanwhile, since the average source-to-refinery distance of woody biomass is larger than that of herbaceous biomass, an expanded

[25] https://www.energy.gov/diversity/justice40-initiative

buffer distance of 100 miles was used to identify disadvantaged communities near potential woody biomass biorefinery locations (Figure 4.14). We found that around 8,929 disadvantaged census tracts lie within a 100-mile radius of 109 potential biorefinery locations using woody biomass (pyrolysis pathway) Figure 4.13c) and around 10,792 disadvantaged census tracts lie within a 100-mile radius of 152 potential biorefinery locations using woody biomass (gasification pathway (Figure 4.13d). These results indicate a greater spatial overlap between potential supply regions for the woody biomass pathways and disadvantaged census tracts. The southern and southeastern United States have overlapping regions for biorefinery locations in the herbaceous scenario and both the woody scenarios. However, we observe spatial overlap between the disadvantaged tracts and potential biorefinery locations in the Pacific Northwest primarily for the woody scenarios.

Biorefinery operations can potentially introduce a range of negative externalities in the form of environmental burdens. Emissions of air pollutants, including particulate matter and GHGs, as well as noise and odors, during the operation of a biorefinery can result in adverse impacts from a health standpoint. Furthermore, the operation of a biorefinery is likely to require substantial quantities of water for processing. As a result, adequate safeguards for handling wastewater are necessary to prevent contamination of water resources, which can have detrimental consequences for drinking water, agriculture, or recreational use. Meanwhile, the transportation of biomass resources can increase truck traffic, causing congestion and air pollution in neighborhoods located near biorefineries, and changes in zoning and land use can disrupt local ecosystems. Assessing these externalities during the planning process can help incorporate mitigation mechanisms for some of the localized adverse impacts of biorefinery operations, and addressing concerns adequately can result in broader support from the community and participation from stakeholders along the supply chain. The establishment of biorefineries in proximity to disadvantaged communities can also present economic opportunities. The associated trade-offs between social, economic, and environmental repercussions of location choice could be evaluated in future research.

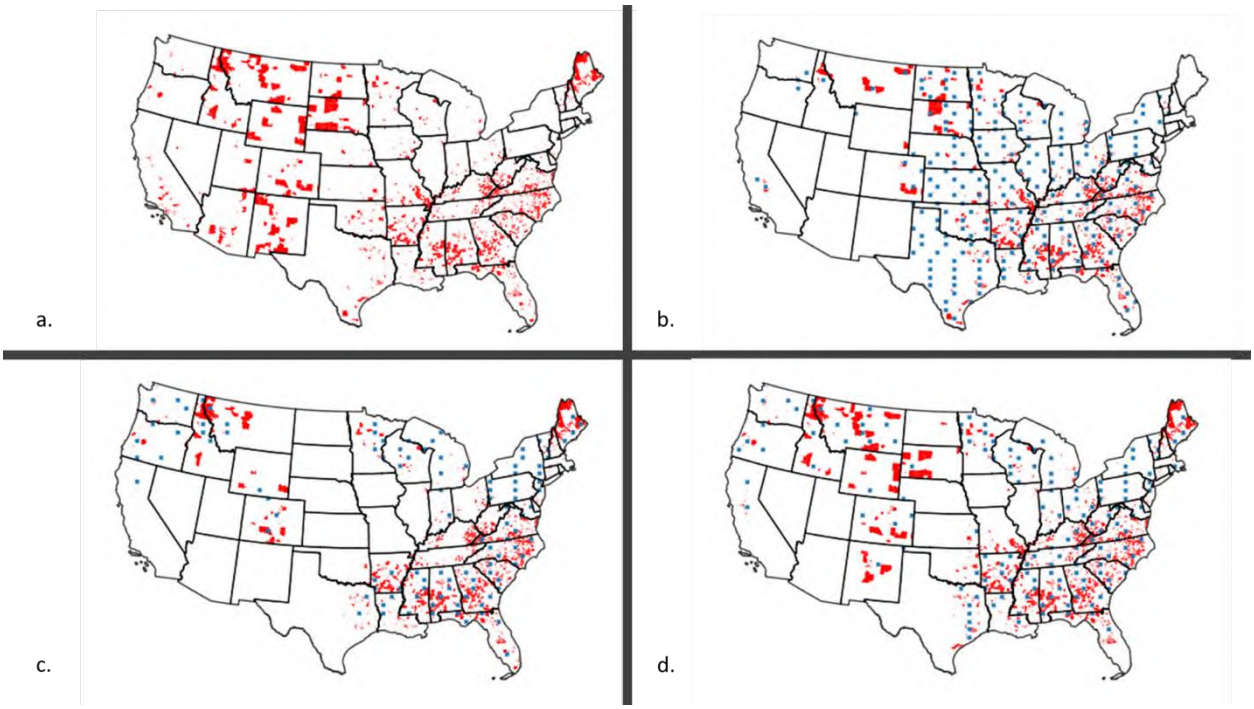

Figure 4.14. a) Disadvantaged census tracts (in red); disadvantaged census tracts b) within 50 miles of biorefinery locations for herbaceous biomass and within 100 miles of biorefinery locations for c) woody biomass (pyrolysis pathway) and d) woody biomass (gasification pathway)

Blue dots indicate biorefinery locations.

4.3.4 Equipment Estimates for Harvesting and Preprocessing Operations

The analysis on feedstock logistics and preprocessing evaluated the mobilization of biomass from the sources of production to the refinery throat. However, adequate agricultural equipment, transportation, and machinery to facilitate preprocessing operations are also necessary to ensure that the biomass supply chain can meet the cost, quality, and quantity requirements that enable the biorefinery/industry to produce fuels and products competitively. Following from the supply-chain logistics systems designs described earlier, we estimated equipment requirements for their harvesting and preprocessing operations. We use biorefinery-level estimates for equipment requirements from Mann et al. (2019) and equipment capacity from Hartley et al. (2021). Our approach relies on scaling equipment requirements and adapting system designs to arrive at estimates for the 2040 supply quantities and preprocessing system configurations, as described in Sections 4.3.1 and 4.3.2, respectively.

Herbaceous Biomass for Ethanol Pathway

Table 4.8 shows the estimated number of machines required to harvest and transport herbaceous biomass. The dry/baled and wet/chopped logistics systems require around 194,024 and 246,584 machines, respectively. This equipment can handle around 176.4 million dry short tons of dry/baled biomass and 546.4 million dry short tons of wet/chopped biomass.

Given these logistics systems' differences in harvesting and collection, they require different equipment. In the dry/baled logistics system, windrowed biomass is baled using round or square balers and collected using self-propelled stringer stackers and wagons. In the wet/chopped

logistics systems, the biomass is chopped in the field using forage harvesters and then ensiled. Both systems use a combination of trucks and trailers to transport the biomass from the field to the refinery.

Table 4.8. Estimated Machinery for Herbaceous Biomass Supply Chains

Equipment	Estimated Equipment for Herbaceous Biomass Mobilized in 2040	
	Baled Logistics	Chopped Logistics
Shredder/windrower	33,072	-
Round and square balers	26,458	-
Bale collectors/stackers	26,458	-
Forage harvester	-	16,394
Dump wagons	-	49,863
Silage/dump trucks	-	32,787
Loaders	6,615	10,246
Trucks and trailers	28,663	87,431
Tractors	72,758	49,863
Total	**194,024**	**246,584**

Baled biomass arrives on flatbed trucks that are weighed and emptied in the staging area of the biorefinery. The bales are placed in stacks or on drag chain conveyors, using telehandlers, which feed into destackers or destringers as required. The bale processor is then used to break the baled biomass, after which it is air-classified to remove contaminants (mainly soil). The air-classified biomass is conveyed to a second-stage grinding step. The preprocessing system also includes a dust collection system to minimize risk of fire or explosion. Size-reduced biomass is stored in bins from which it can be reclaimed and conveyed to the pretreatment reactor plug screw feeder.

The logistics system is different for chopped biomass, as this system is typically used to minimize losses from degradation during storage and reduce the risk of fire, which is greater in the dry/baled system. Ensiled biomass is delivered to the biorefinery and stored in piles using front-end loaders and compactors. The biomass is then reclaimed from these ensiled storage piles and screened using magnetic separators to remove metals. Screened materials are conveyed to day storage piles and reclaimed onto a belt conveyor into the live bottom surge bin, after which point the pretreatment reactor feeder is the same as that for the baled system. The estimated required numbers of each type of equipment are delineated in Table 4.9.

Table 4.9. Estimated Preprocessing Equipment for Herbaceous Biomass

Equipment	Estimated Equipment for Herbaceous Biomass Mobilized in 2040	
	Baled Logistics	Chopped Logistics
Truck scale	403	1,298
Telehandler	805	-
Front-end loader	403	1,298
Bale destacker	805	-
Pile compactor	-	2,596
Truck unloading system	-	1,298
Ensiled storage and stacker/reclaimer	-	1,298
Drag chain conveyor	3,419	-
Destringer	805	-
Bale processor	805	-
Air classifier	805	-
Magnetic separator	-	2,596
Grinder/rotary shear	805	-
Dust collection system	2,413	-
Fire and dust explosion suppression system	2,413	-
Pneumatic conveyor	1,609	-
Cyclone separator	1,609	-
Belt conveyor	805	12,979
Feedstock silo	805	-
Feedstock reclaimer	805	1,298
Live bottom surge bin	-	2,596
Dust silo	202	-
Metering weight belt	805	2,596
Screw conveyor	1,609	7,787
Plug screw feeder	1,609	2,596
Total	**23,739**	**40,236**

4.3.4.1 Woody Biomass (Trees/Residues/SRWC) for Gasification Pathway

The harvesting operations for trees are similar to those evaluated in the Woody Feedstocks 2020 State of Technology Report (Hartley et al. 2021), wherein the system uses a tracked feller buncher with a high-speed shear for felling the clean pine-sized materials. The grapple skidder is used for primary transportation, and the feller-buncher and grapple skidder are estimated to achieve 65% utilization rates at 49 dry short tons and 40 dry short tons, respectively. For the

clean pine, a delimbing operation is undertaken at the landing prior to stacking for storage. Meanwhile, the forest residues are chipped to a 2-inch chip size using a mobile disk chipper at the landing site and are loaded into the chip trailer through the outfeed. Estimates for SRWC follow from biorefinery level estimates in Mann et al. (2019). For each feedstock, we adjusted the required number of trucks and trailers to account for the source-to-refinery transportation distances analyzed in Section 4.3.1.2. The average transportation distance was 138 miles for trees, 65 miles for residues, and 98 miles for SRWC, far higher than the 50 miles in the reference case in Mann et al. (2019). To account for the associated additional time required for biomass-to-refinery delivery, we included scaling factors of 4×, 1×, and 2× to estimate truck and trailer requirements for trees, residues, and SRWC, respectively, compared to the reference case. Table 4.10 presents the estimated numbers for each type of equipment required to mobilize 83.15 million dry short tons of trees, 19.72 million dry short tons of logging residues, and 58.80 million dry short tons of SRWC for the gasification pathway.

Table 4.10. Estimated Machinery for Woody Biomass Supply Chains (Gasification Pathway)

	Estimated Equipment for Woody Biomass Mobilized in 2040		
Equipment	**Trees**	**Residues**	**SRWC**
Feller buncher (rated capacity 75.38 short tons/hr, utilization 65%)	849	-	-
Grapple skidder (rated capacity 62 short tons/hr, utilization 65%)	1,032	-	-
Delimber (rated capacity 50 short tons/hr)	832	-	-
Chipper (rated capacity 79.8 short tons/hr)	-	124	-
Forage harvester	-	-	1,471
Dump wagons	-	-	4,337
Silage/dump trucks	-	-	2,867
Loaders	550	131	1,103
Trucks and trailers	53,215	3,156	18,818
Tractors	-	-	4,337
Total	**56,478**	**3,411**	**32,933**

At the biorefinery, logs are delivered to the rotary head debarker and are then conveyed to the chipper to produce approximately 2-inch chips. Since logging residues and SRWC are delivered in a chipped format that meets the particle size specifications for the gasification pathway, there is no requirement for additional size reduction during preprocessing. Table 4.11 presents the estimated required numbers of each type of equipment, adjusted for the delivered quantities of each type of feedstock in this analysis compared to the reference case from Mann et al. (2019).

Table 4.11. Estimated Preprocessing Equipment for Woody Biomass (Gasification Pathway)

	Estimated Equipment for Woody Biomass Mobilized in 2040		
Equipment	**Trees**	**Residues**	**SRWC**
Truck scale	208	50	148
Front-end loader	208	50	148
Truck unloading system	208	50	148
Storage and stacker/reclaimer system	208	50	148
Belt conveyor	416	99	295
Debarker	832	-	-
Chipper	832	-	-
Drag chain conveyor	1,663	198	589
Rotary dryer	416	99	295
Storage silo and reclaimer	416	99	295
Pneumatic conveyor	1,248	296	883
Dust collection system	832	198	589
Dust silo	104	25	74
Fire and dust explosion suppression system	832	198	589
Screw conveyor	416	99	295
Metering weight belt	416	99	295
Material feeder	416	99	295
Total	**9,671**	**1,709**	**5,086**

4.3.4.2 Woody Biomass (Trees/Residues/SRWC) for Pyrolysis Pathway

The harvest and collection system for woody biomass for the pyrolysis pathway is identical to that described in Section 4.3.4.2, albeit with lower quantities of mobilized biomass owing to the more stringent feedstock quality requirements. The average transportation distance was 127 miles for trees, 63 miles for residues, and 101 miles for SRWC, and we used similar scaling factors to estimate truck and trailer requirements as described in Section 4.3.4.2 above. Table 4.12 presents the estimated numbers for each type of equipment required to mobilize 79.64 million dry short tons of trees, 11.46 million dry short tons of logging residues, and 3.15 million dry tons of SRWC for the pyrolysis pathway.

Table 4.12. Estimated Machinery for Woody Biomass Supply Chains (Pyrolysis Pathway)

Equipment	Estimated Equipment for Woody Biomass Mobilized in 2040		
	Trees	Residues	SRWC
Feller buncher (rated capacity 75.38 short tons/hr, utilization 65%)	813	-	-
Grapple skidder (rated capacity 62 short tons/hr, utilization 65%)	989	-	-
Delimber (rated capacity 50 short tons/hr)	797	-	-
Chipper (rated capacity 79.8 short tons/hr)	-	72	-
Forage harvester	-	-	79
Dump wagons	-	-	233
Silage/dump trucks	-	-	154
Loaders	527	76	60
Trucks and trailers	50,968	1,834	1,009
Tractors	-	-	233
Total	**54,094**	**1,982**	**1,768**

The types of equipment required for the preprocessing system are similar to those described in Section 4.3.4.2. However, given the smaller particle size requirement for the pyrolysis pathway, Table 4.13 incorporates an additional grinding step for all the biomass types. Since the quantity of mobilized biomass is lower, the estimated numbers of equipment required for preprocessing are also fewer than those for the gasification pathway.

Table 4.13. Estimated Preprocessing Equipment for Woody Biomass (Pyrolysis Pathway)

Equipment	Estimated Equipment for Woody Biomass Mobilized in 2040		
	Trees	Residues	SRWC
Truck scale	200	29	8
Front-end loader	200	29	8
Truck unloading system	200	29	8
Storage and stacker/reclaimer system	200	29	8
Belt conveyor	399	58	16
Debarker	797	-	-
Chipper	797	-	-
Grinder	797	115	32
Drag chain conveyor	2,390	115	32
Rotary dryer	399	58	16
Storage silo and reclaimer	399	58	16
Pneumatic conveyor	1,195	172	48
Dust collection system	797	115	32
Dust silo	100	15	4
Fire and dust explosion suppression system	797	115	32
Screw conveyor	399	58	16
Metering weight belt	399	58	16
Material feeder	399	58	16
Total	**10,864**	**1,111**	**308**

4.4 Summary and Key Insights

Mitigating variability in biomass quality necessitates additional/alternate preprocessing designs that impact the cost and preprocessing requirements, as demonstrated in Section 4.3.2, which depends on the specific quality requirements of downstream processes. Our analysis used data from the BT16 database at a county resolution to maximize the utilization of biomass subject to certain feedstock quality constraints for conversion. The optimization model accounted for costs up to the refinery throat, including cost of biomass, harvesting, collection and field-side preprocessing, transportation, and preprocessing at the refinery. In the herbaceous biomass-to-ethanol pathway, a total of approximately 723 million dry short tons of biomass per year were supplied to 227 biorefineries at an average delivered cost of $118 to $159 per dry short ton. In the woody biomass-to-gasification pathway, 152 biorefineries received a combined 162 million dry short tons of biomass per year at average delivered cost of $103 to $132 per dry short ton. In the woody biomass-to-pyrolysis pathway, 109 biorefineries received a combined 95 million dry tons of biomass per year at an average cost of $110 to $129 per dry short ton. As expected, feedstock availability and transportation distances vary by region depending on the feedstock types and downstream quality specifications for selected conversion pathways, which influence

the delivered feedstock cost at the throat of the refinery. Furthermore, feedstock quality can also vary depending on the region, feedstock type, harvest method, and climatic conditions during harvest and postharvest, which can have an impact on the preprocessing requirements at the refinery. Together these factors influence the quantities of usable feedstock that can be delivered from available biomass. Spatial analysis of potential biorefinery locations and disadvantaged communities shows substantial overlap. Although conducting a regional impact analysis was beyond the scope of this study, future research could evaluate the economic, social, and environmental trade-offs of biorefinery location choice and regional economy/community impacts.

References

Davis, R., L. Tao, E. C. D. Tan, M. J. Biddy, G. T. Beckham, C. Scarlata, J. Jacobson et al. 2013. *Process Design and Economics for the Conversion of Lignocellulosic Biomass to Hydrocarbons: Dilute-Acid and Enzymatic Deconstruction of Biomass to Sugars and Biological Conversion of Sugars to Hydrocarbons.* Golden, CO: National Renewable Energy Laboratory. NREL/TP-5100-60223. https://doi.org/10.2172/1107470.

Dutta, A., M. Talmadge, J. Hensley, M. Worley, D. Dudgeon, D. Barton, P. Groendijk. 2011. *Process design and economics for conversion of lignocellulosic biomass to ethanol: thermochemical pathway by indirect gasification and mixed alcohol synthesis*. Golden, CO: National Renewable Energy Laboratory. NREL/TP-5100-51400. https://doi.org/10.2172/1015885.

Hartley, D. S., D. N. Thompson, and H. Cai. 2021. *Woody Feedstocks 2020 State of Technology Report*. Idaho Falls, ID: Idaho National Laboratory. NL/EXT-20-59976-Rev000. https://doi.org/10.2172/1782211.

Langholtz, M. H., B. J. Stokes, and L. M. Eaton. 2016. *2016 Billion-ton report: Advancing domestic resources for a thriving bioeconomy, Volume 1: Economic availability of feedstock.* Oak Ridge, TN: Oak Ridge National Laboratory. ORNL/TM-2016/160. https://doi.org/10.2172/1271651.

Lin, Y., M. S. Roni, D. N. Thompson, D. S. Hartley, M. Griffel, and H. Cai. 2020. *Herbaceous Feedstock 2020 (State of Technology Report*). Idaho Falls, ID: Idaho National Laboratory. INL/EXT-20-59958-Rev.1. https://doi.org/10.2172/1785122.

Mann, Margaret K., Mary J. Biddy, Chad R. Augustine, Quang Nguyen, Hong Hu, Mahmood Ebadian, and Erin Webb. 2019. *Evaluation of Agricultural Equipment Manufacturing for a Bio-Based Economy*. Golden, CO: National Renewable Energy Laboratory. NREL/TP-6A20-71570. https://doi.org/10.2172/1530715.

Wendt, L. M., W. A. Smith, D. S. Hartley, D. S. Wendt, J. A. Ross, D. M. Sexton, J. C. Lukas et al. 2018. "Techno-economic assessment of a chopped feedstock logistics supply chain for corn stover." *Frontiers in Energy Research* 6, 90. https://doi.org/10.3389/fenrg.2018.00090.

5 Conversion Modeling and Integration of Economic Analysis

5.1 Background

5.1.1 Overview

The objective of this chapter is to provide data and analysis insights on selected feedstock-to-X scenarios for this study and align with more big-picture perspectives on best use of feedstocks and potential benefits and complications across various analysis strategies. The project team conducted analysis that directly compares biomass utilization by differing pathways across multiple metrics of interest.

5.1.2 Scope

In this chapter, NREL leverages existing TEA approaches and generates cost evaluations for the feedstock-to-X pathways. The project team compares different uses of biomass—for fuels, chemicals, or power—via quantitative understanding of cost, energy, and environmental trade-offs as a particular market barrier for biomass utilization and large-scale deployment. Cost evaluations include the feedstock economic analysis of Chapter 4 and result in revised supply curves that consider feedstock resource, logistics, and preprocessing costs as well as conversion costs to final end uses. Furthermore, process-level analysis data are fed into the LCA work of Chapter 6 and inform the various inputs for each pathway and the relative shares of the various coproducts. Assessing alternative biomass conversion pathway combinations, taking into account potential end-use demands, costs, and resource constraints, provides a thorough understanding of incorporating integrated analysis data to provide bigger-picture perspectives on the best use of feedstocks and the potential benefits and complications across various analysis strategies. Note that nonfuel/power products were outside the scope of this study.

The conversion pathways are summarized in Table 5.1. For herbaceous feedstocks, one typical pathway is biochemical conversion to fermentation intermediates (such as ethanol, butanol, 2,3-butanediol, farnasene, etc.) and upgrading of the intermediates to SAF or other chemicals (such as building block chemicals and/or end-use chemicals, not considering nonfuel/power products). Gasification and pyrolysis pathways are typically used for thermochemical conversion of both herbaceous and woody biomass. Intermediate products from these processes can either be catalytically upgraded to hydrocarbon fuels or ammonia or be coprocessed through existing refineries to a variety of fuel products. BECCS was holistically analyzed to compare utilization of biomass for power with utilization for liquid fuel. Similarly, biofuel production with CCS is within the scope of this study. For instance, waste CO_2 from fermentation off-gas is known to have relatively high purity, so incorporating CCS would likely require reasonably low capital investment. Carbon capture and utilization is, however, a relatively low-technology-readiness-level (TRL) technology area whose potential contribution to decarbonization is still uncertain (Kleijne 2022), and it is therefore omitted from the scope of this sprint study.

Product and chemical pathways considered in scope include conversion of biogenic feedstocks to products that offset carbon-intensive fossil pathways and to long-lived products with carbon

removal potential (Patrizio 2021). In the initial analyses, this project team performed both TEA and LCA studies using representative pathways and leveraging existing capabilities. Pathway selection was based on a set of clear criteria, including at least 1) potential market size based on existing deep decarbonization scenarios, 2) GHG emissions avoided or sequestered, 3) TRL (or other similar indicator of technology readiness) relative to the anticipated market size over time, and 4) leveraging of previous pathway analysis funded by the DOE Bioenergy Technologies Office. Based on these selection criteria, the list of pathways selected for this study is summarized in Table 5.1. The selected pathways include conversion of cellulosic ethanol to hydrocarbon fuels (5.3.1), FT Pathway (5.3.2), Biomass Gasification to Methanol Pathway (5.3.3), and Catalytic Fast Pyrolysis Pathway (5.3.4). For each pathway, the conceptual process design of each base-case pathway is based on previously established TEA efforts without consideration of CCS. An alternative scenario including CCS is studied for each pathway as a decarbonization strategy. Note that CCS might not work for all the biofuel production pathways, and this study (especially conversion pathway and cost analysis) only considers CO_2 purification and compression costs; pipeline transportation and regional aspects are not included in this work.

5.2 Methods

We use a rigorous process modeling approach for conversion of feedstocks to fuels and products for the technology pathways shown in Table 5.1 below. We use the material and energy balances from the process models to estimate the production cost of hydrocarbon fuels, also known as minimum fuel selling price (MFSP), using a discounted cash flow rate of return analysis at a discount rate of 10% and net present value of zero (Davis et al. 2013, Dutta et al. 2011).

Table 5.1. Selected Conversion Pathways Considered for Decarbonization Strategies

Feedstock Category	Conversion Process	Intermediates	Products	Use Sector
Herbaceous	Biochemical conversion	Ethanol	Jet fuel ethanol & ethylene	Aviation, HDVs & chemical
Herbaceous and woody	Gasification and Fischer-Tropsch (FT) synthesis	Syngas	Jet fuel, FT diesel, & naphtha ammonia	Aviation and HDVs Chemical
Herbaceous and woody	Gasification and synthesis	Methanol	Methanol	Marine or HDVs Chemical
Herbaceous and woody	Catalytic fast pyrolysis and upgrading	Pyrolysis oil	Jet fuel & CFP Diesel	Aviation and HDVs
Herbaceous and woody	Bioelectricity with CCS	N/A	Electricity	Electric grid

5.3 Results and Discussion

5.3.1 Cellulosic Ethanol to Hydrocarbon Fuels

This process uses a biochemical conversion pathway that converts herbaceous biomass into ethanol (Humbird et al. 2011) via anaerobic fermentation and then upgrades the ethanol to hydrocarbon fuels, as illustrated in the process flow diagram shown in Table 5.1. There are two

process vent streams that provide opportunities for decarbonization through CCS. One is the fermentation off-gas vent stream, which consists of 96.8% CO_2 (mass basis), and the second is the combustion off-gas stream, which consists of 19% CO_2 (mass basis).

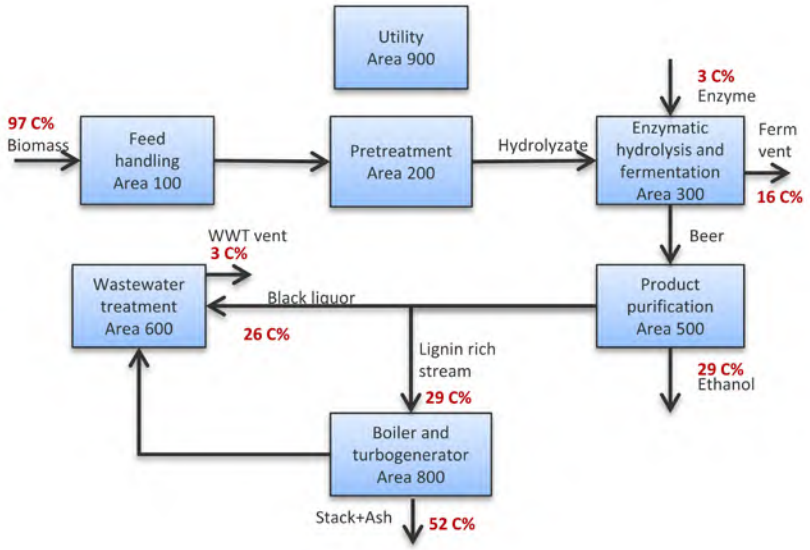

Figure 5.1. Process block diagram for base case cellulosic ethanol to hydrocarbon fuels

Without CCS, the cellulosic ethanol process produces hydrocarbon fuels with an MFSP of $4.6 per gallon of gasoline equivalent (GGE) for a facility processing 2,000 dry metric tons per day (dmtd) of herbaceous biomass feedstock. This corresponds to a fuel yield of 310 lb/dry ton of biomass or 49 GGE/dry ton of biomass, equivalent to 6 GJ/dry ton of biomass on an energy basis. Because no CO_2 is being captured and sequestered, the biogenic CO_2 emissions from this process are estimated to be 396 lb/GJ of hydrocarbon fuels.

We consider two CCS cases for this process: a) CO_2 captured and sequestered from the fermentation vent stream (CCS1) and b) CO_2 captured and sequestered from the fermentation and combustion off-gas vent streams (CCS2, refer to Figure 5.2). Incorporating CCS from the fermentation vent stream (i.e., CCS1) would increase the MFSP of the produced hydrocarbon fuels to $4.7/GGE, with a CO_2 yield of 0.21 tons of CO_2 per ton of biomass. As this vent stream primarily contains CO_2, equivalent to 15% carbon from biomass, no compression and purification step is needed, so the MFSP increases by only 2%. This strategy reduces the overall CO_2 emissions of this process to 311.9 lb/GJ, a 22% decrease relative to the base case.

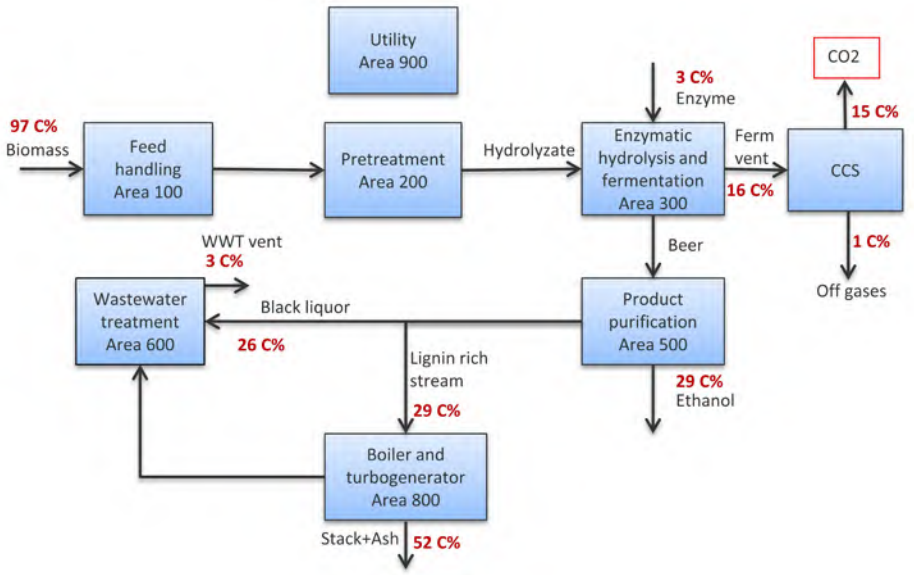

a.

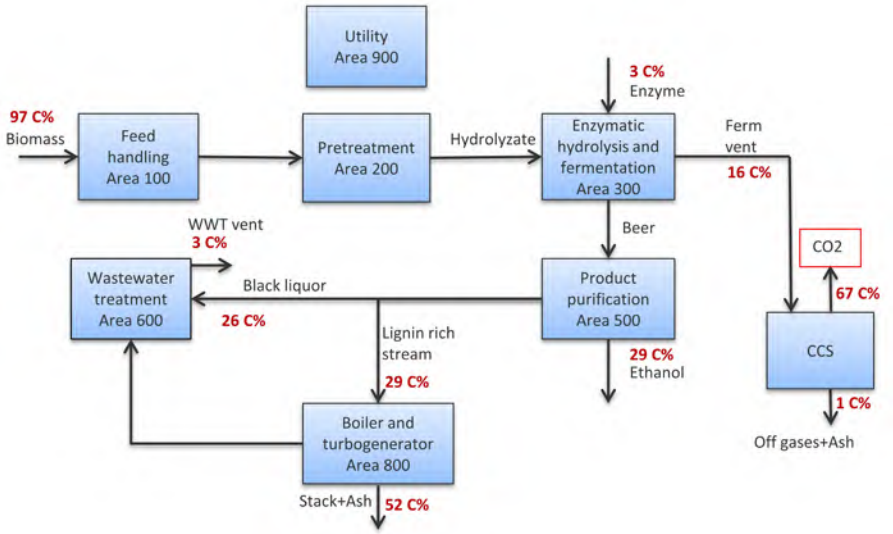

b.

Figure 5.2. Process block diagram for cellulosic ethanol to hydrocarbon fuels with carbon capture and sequestration option, a) partial CCS of fermentation CO_2 and b) full CCS of fermentation and combustion CO_2

Incorporating CCS from combustion off-gases along with the fermentation vent stream (i.e., CCS2) would increase the MFSP of the produced hydrocarbon fuels to $5.0/GGE, with a CO_2 yield of 0.91 tons of CO_2 per ton of biomass. As this stream contains a mixture of off-gases, a compression and purification step is needed to separate CO_2 from the mixture, increasing the MFSP by 8.7%. This CCS strategy reduces the overall CO_2 emissions of the process to 17.1 lb/GJ, a 96% reduction relative to the base case. Table 5.2 below summarizes the TEA parameters for these two CCS cases compared to the base case.

Table 5.2. Summary of TEA Parameters for the Cellulosic Ethanol to Hydrocarbon Fuels Process With CCS as Compared to Base Case

Cellulosic Ethanol to Hydrocarbons	Units	Base Case	Base Case w/ CCS Ferm Off-gas (CCS1)	Base Case w/ CCS All Flue Gases (CCS2)
Throughput capacity	dt/day	2,205	2,205	2,205
Feedstock type		herbaceous	herbaceous	herbaceous
Fixed capital investment	$	461,225,000	481,400,000	544,300,000
Fixed operating cost	$/yr	12,420,000	12,560,000	13,000,000
Other (nonfeedstock) variable operating cost	$/yr	25,730,000	25,730,000	26,060,000
Imported hydrogen	$/yr	3,790,000	3,790,000	3,790,000
Coproducts sales revenue	$/yr	N/A	N/A	N/A
Power sales revenue	$/yr	2,000,000	1,860,000	N/A
Imported electricity	$/yr	N/A	N/A	(3,450,000)
MFSP	$/GGE	4.6	4.7	5.0
Feedstock cost	$/dt	84.45	84.45	84.45

Based on projected herbaceous biomass feedstock availability in 2030, potential hydrocarbon fuel production from the cellulosic ethanol pathway ranges from 1 billion GGE/yr with a feedstock price of $70/dry ton to 26 billion GGE/yr with a feedstock price of $140/dry ton. Similarly, based on projected herbaceous biomass feedstock availability in 2040, potential hydrocarbon fuel production ranges from 2 billion to 34 billion GGE/yr with feedstock prices of $70 to $140/dry ton, respectively. Assuming a facility scale of 2,205 dmtd, the number of cellulosic ethanol to hydrocarbon fuels production facilities that could be built ranges from 32 to 725 in 2030 and from 56 to 953 in 2040. Figure 5.3 below shows the hydrocarbon fuel potential and number of facilities based on 2030 and 2040 feedstock data.

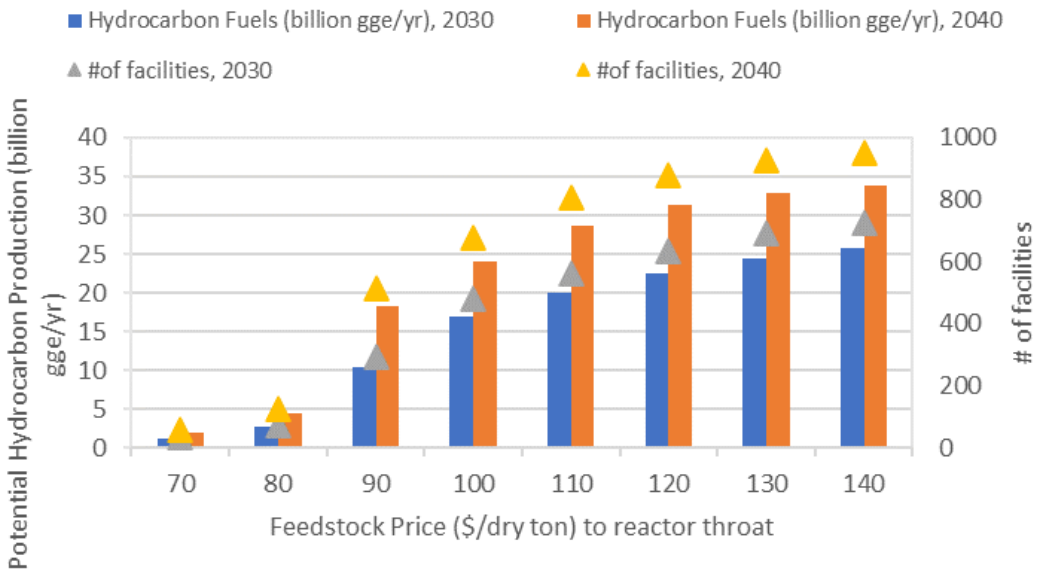

Figure 5.3. Potential hydrocarbon fuel production from the cellulosic ethanol to hydrocarbon fuels process

The total CO_2 sequestered per 2205 dmtd cellulosic ethanol facility is estimated to be 86.6 lb/GJ for CCS1 (CCS on the fermentation vent stream) and 379 lb/GJ for CCS2 (CCS on the fermentation and combustion off-gas streams). For CCS1, this corresponds to total CO_2 sequestration of 2,771–62,785 lb/GJ in 2030 and 4,850–82,530 lb/GJ in 2040 with feedstock prices of $70 to $140/dry ton, respectively. For CCS2, CO_2 sequestration totals 12,128–274,775 lb/GJ in 2030 and 21,224–361,187 lb/GJ in 2040 with feedstock prices of $70 to $140/dry ton, respectively. Figure 5.4 shows total CO_2 sequestration for both CCS options considering 2030 and 2040 feedstock supply data.

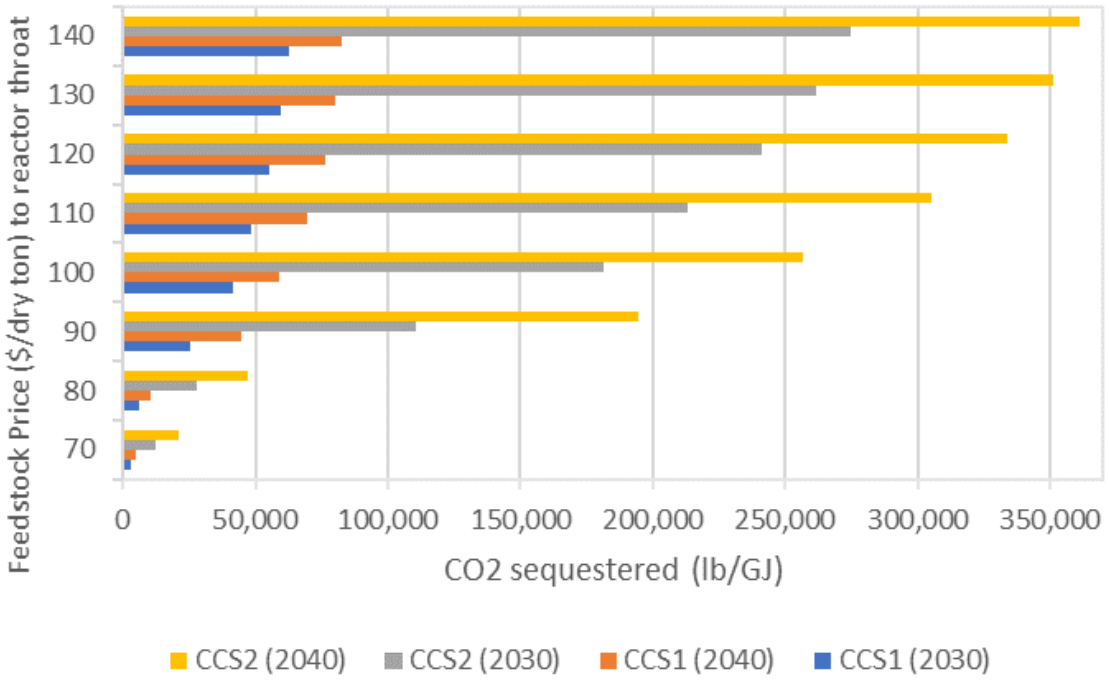

Figure 5.4. Total CO_2 sequestration for the cellulosic ethanol to hydrocarbon fuels process

5.3.2 Fischer-Tropsch Pathway

This process uses a thermochemical conversion pathway that converts woody biomass into hydrocarbon fuels via synthesis of syngas and conversion of syngas to hydrocarbons through the FT catalyst oligomerization process (Tao et al. 2022), as illustrated in the process block diagram in Figure 5.5. This pathway has two process vent streams that provide opportunities for decarbonization through CCS: the FT flue gas stream and the gasification off-gas stream, both of which consist of approximately 11% CO_2 (mass basis).

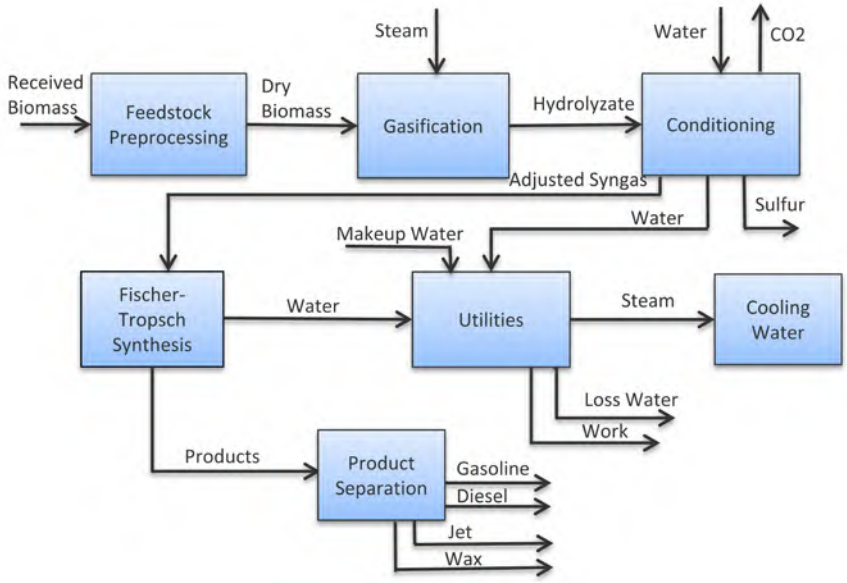

Figure 5.5. Process block diagram for the base-case FT process

Without CCS, the FT process produces hydrocarbon fuels with an MFSP of $2.6/GGE for a facility processing 2,000 dmtd of woody biomass feedstock. This corresponds to a fuel yield of 398 lb/dry ton of biomass or 63 GGE/dry ton of biomass, equivalent to 7.7 GJ/dry ton of biomass on an energy basis. Because no CO_2 is being captured and sequestered, the biogenic CO_2 emissions from this process are estimated to be 303.6 lb/GJ of hydrocarbon fuels.

We consider two CCS cases for this process: a) CO_2 is captured and sequestered from the FT flue gas stream (CCS1), and b) CO_2 is captured and sequestered from all flue gases, including the FT flue gas and the gasification off-gas stream (CCS2, refer to Figure 5.6). Incorporating CCS from the FT flue gas stream (i.e.,CCS1) would increase the MFSP of hydrocarbon fuels to $2.9/GGE, with a CO_2 yield of 0.29 tons of CO_2 per ton of biomass. This stream contains 22.4% carbon from biomass in the form of CO_2. Adding a CCS unit would increase the MFSP by 11.5% due to capital and operating costs associated with acid gas removal, compression,and purification. These processing steps are needed to first recover CO_2 from the flue gas stream, then compress purified CO_2 stream to the pressure rating to pipeline quality. This strategy reduces overall CO_2 emissions to 196.6 lb/GJ, a 35% decrease relative to the base case.

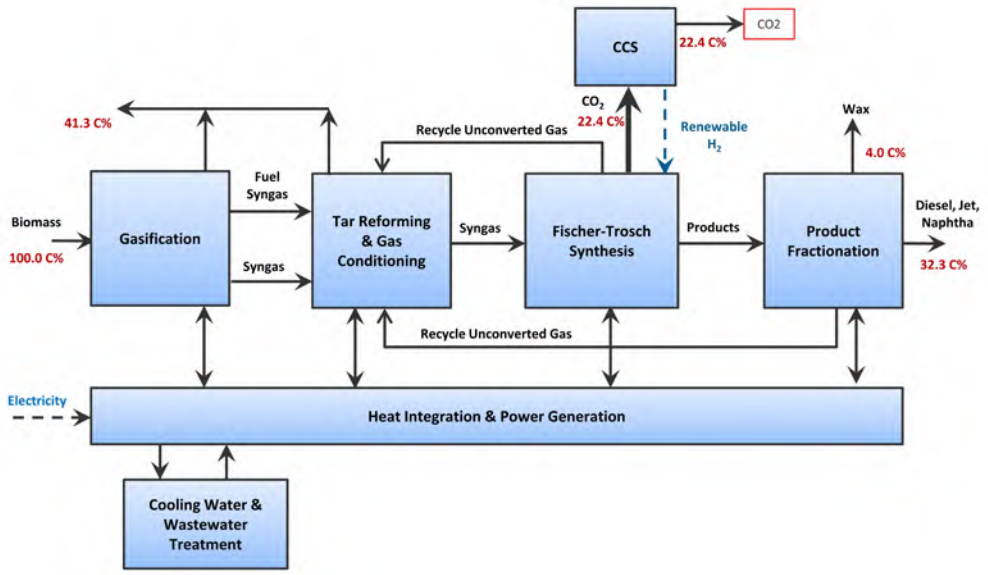

a.

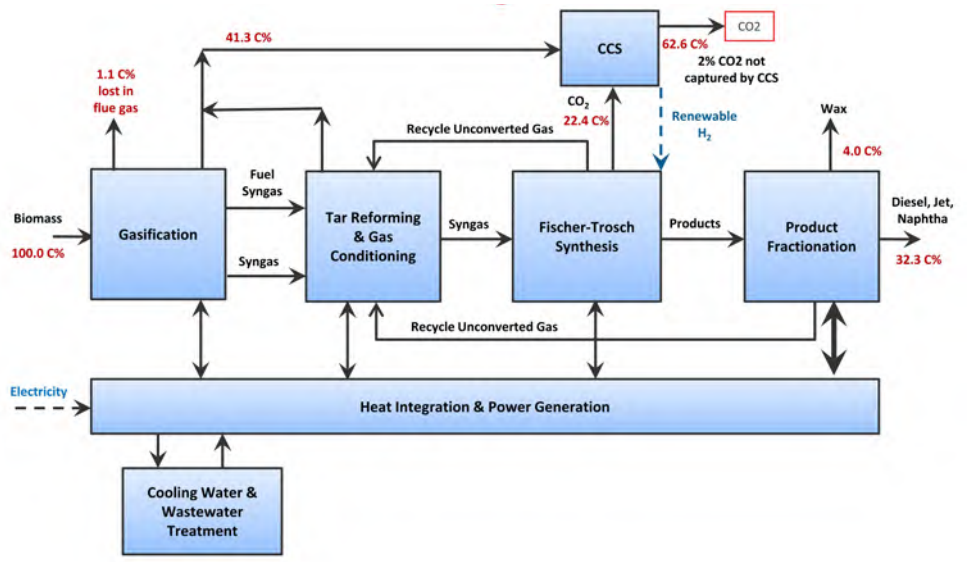

b.

Figure 5.6. Process block diagram for the FT process with CCS cases CCS1 (top) and CCS2 (bottom)

Incorporating CCS from all flue gases (i.e., CCS2) would increase the MFSP of the produced hydrocarbon fuels to $3.4/GGE, with a CO_2 yield of 0.81 tons of CO_2 per ton of biomass. As this stream contains a mixture of off-gases, a compression and purification step is needed to separate CO_2 from the mixture, which is equivalent to 63% carbon from biomass, thus increasing the MFSP by 30.8%. This CCS strategy reduces the overall CO_2 emissions of the process to 4.4 lb/GJ, a 99% reduction compared to the base case. Table 5.3 below summarizes the TEA parameters for these two CCS cases compared to the base case.

Table 5.3. Summary of TEA Parameters for the FT Process With CCS as Compared to Base Case (All Cost Numbers Are in 2016 U.S. Dollars Without Tax Incentives)

Fisher-Tropsch	Units	Fischer-Tropsch SPK	Fischer-Tropsch SPK w/CCS AGR CO2 (CCS1)	Fischer-Tropsch SPK w/CCS All Flue Gases (CCS2)
Throughput capacity	dt/day	2,205	2,205	2,205
Feedstock type		Woody	Woody	Woody
Fixed capital investment	$	448,333,000	507,919,000	654,825,000
Fixed operating cost	$/yr	22,530,000	22,530,000	30,170,000
Other (nonfeedstock) variable operating cost	$/yr	5,450,000	5,450,000	5,540,000
Imported hydrogen	$/yr	N/A	N/A	N/A
Coproducts sales revenue	$/yr	18,720,000	18,720,000	18,720,000
Power sales revenue	$/yr	N/A	N/A	N/A
Imported electricity	$/yr	N/A	(2,070,000)	(5,870,000)
MFSP	$/GGE	2.6	2.9	3.4
Feedstock cost	$/dt	63	63	63

Based on projected woody biomass feedstock availability in 2030, potential hydrocarbon fuel production from the FT pathway ranges from 5.7 billion GGE/yr with a feedstock price of $70/dry ton to 11.8 billion GGE/yr with a feedstock price of $140/dry ton. Similarly, based on projected woody biomass feedstock availability in 2040, potential hydrocarbon fuel production ranges from 5.8 billion to 10.9 billion GGE/yr with feedstock prices of $70 to $140/dry ton, respectively. Assuming a facility scale of 2205 dmtd, the number of FT production facilities that could be built ranges from 125 to 257 in 2030 and 126 to 239 in 2040. Figure 5.7 below shows the hydrocarbon fuel potential and number of facilities based on 2030 and 2040 feedstock data.

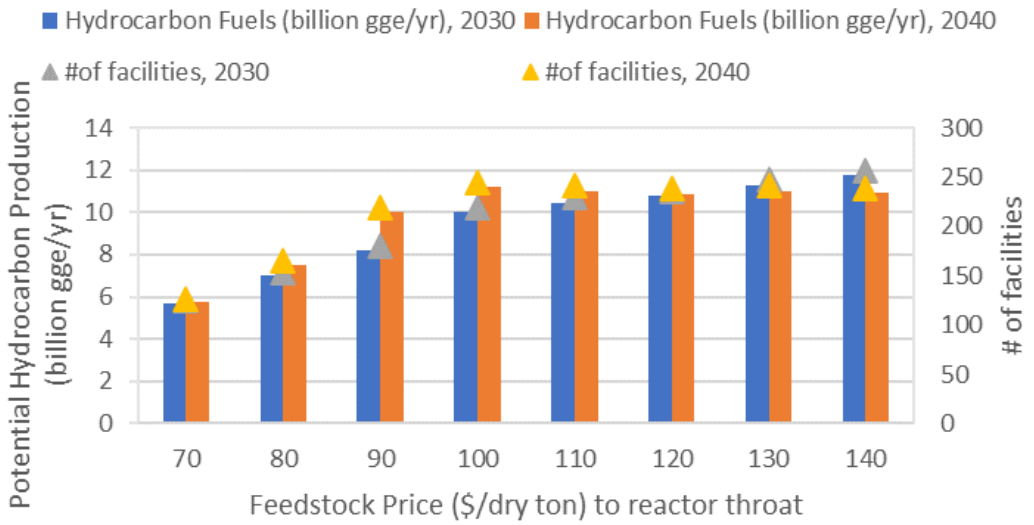

Figure 5.7. Potential hydrocarbon fuel production from the FT process

The total CO_2 sequestered per 2205 dmtd FT facility is estimated to be 106.9 lb/GJ for CCS1 (CCS on the FT flue gas stream) and 299.2 lb/GJ for CCS2 (CCS on the FT flue gas and gasification off-gas streams. For CCS1, this corresponds to total CO_2 sequestration of 13,363–27,473 lb/GJ in 2030 and 13,469–255,49 lb/GJ in 2040 with feedstock prices of $70 to $140/dry ton. For CCS2, CO_2 sequestration totals 37,400–76,894 lb/GJ in 2030 and 37,699–71,509 lb/GJ in 2040 with feedstock prices of $70 to $140/dry ton, respectively. Figure 5.8 shows total CO_2 sequestration for both CCS options considering 2030 and 2040 feedstock supply data.

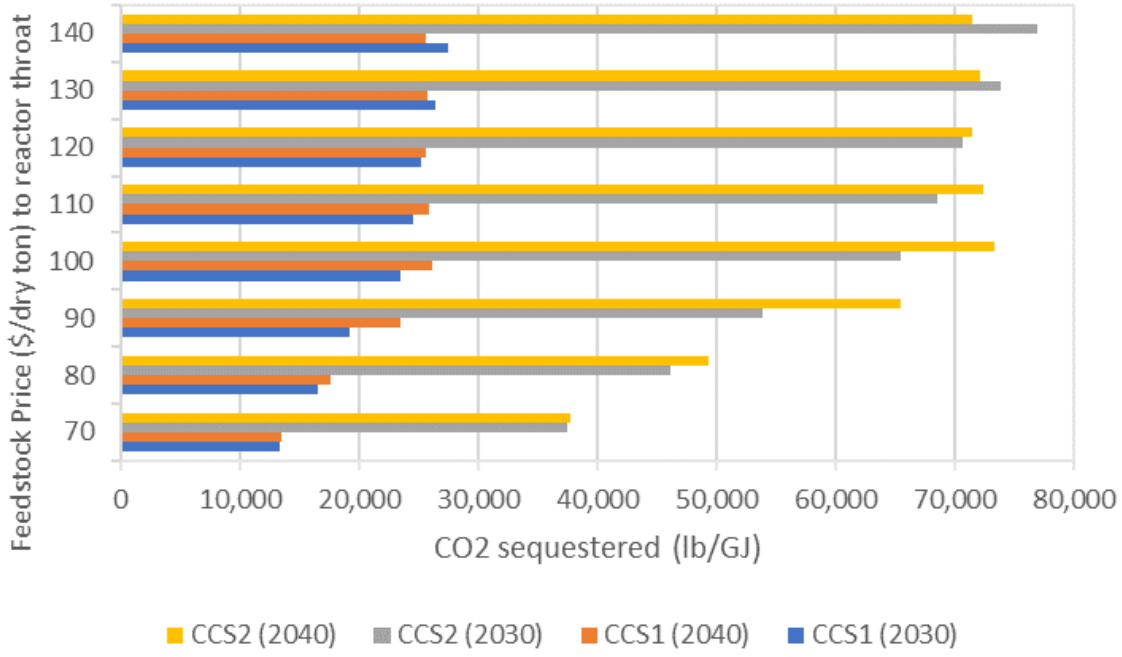

Figure 5.8. Total CO_2 sequestration for the FT process

5.3.3 Biomass Gasification to Methanol Pathway

This process uses a thermochemical conversion pathway that converts woody biomass into methanol via a gasification process (Harris et al. 2021). Refer to Figure 5.9 for the process block diagram. This pathway has two process vent streams that provide opportunities for decarbonization through CCS. The first is the methanol synthesis flue gas stream, which consists of low-purity CO_2, and the second is a gasification off-gas stream, which consists of 19% CO_2 (mass basis).

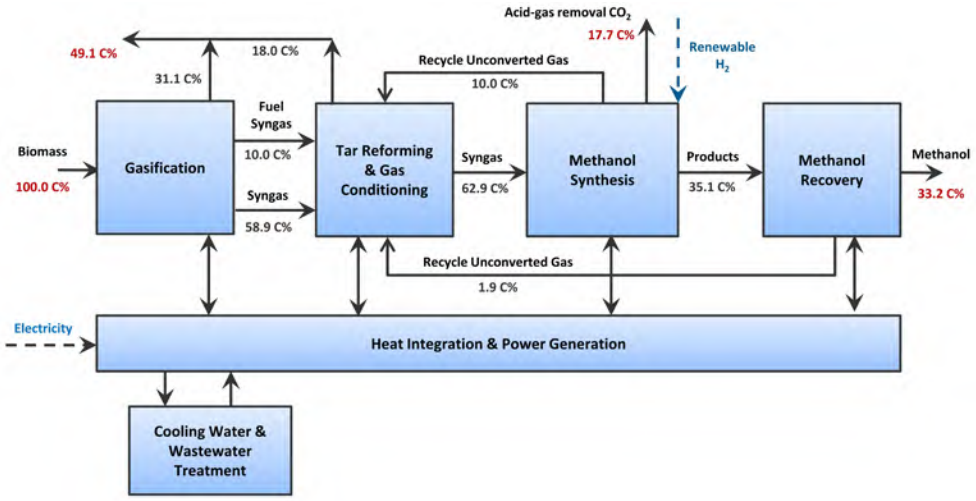

Figure 5.9. Process block diagram for the base-case biomass gasification to methanol process

Without CCS, the gasification process produces methanol with an MFSP of $2.4/GGE for a facility processing 2,000 dmtd of woody biomass feedstock. This corresponds to a methanol yield of 884 lb/dry ton of biomass or 65 GGE/dry ton of biomass (133 gal of methanol/dry ton biomass), equivalent to 7.9 GJ/dry ton of biomass on an energy basis. Because no CO_2 is being captured and sequestered, the biogenic CO_2 emissions from this process are estimated to be 308.2 lb/GJ of hydrocarbon fuels.

We consider two CCS cases for this process: a) CO_2 is captured and sequestered from the methanol synthesis flue gas stream (CCS1), and b) CO_2 is captured and sequestered from all flue gases, including the methanol synthesis flue gas and gasification off-gas streams (CCS2, refer to Figure 5.10). Incorporating CCS from the methanol synthesis flue gas stream (i.e., CCS1) would increase the MFSP of the produced methanol to $2.6/GGE, with a CO_2 yield of 0.23 ton of CO_2 per ton of biomass. This stream contains 17.7% carbon from biomass in the form of CO_2. Adding a CCS unit would increase the MFSP by 8.2% due to the capital and operating costs associated with acid gas removal, compression, and purification. This strategy reduces overall CO_2 emissions to 226.5 lb/GJ, a 26.5% decrease relative to the base case.

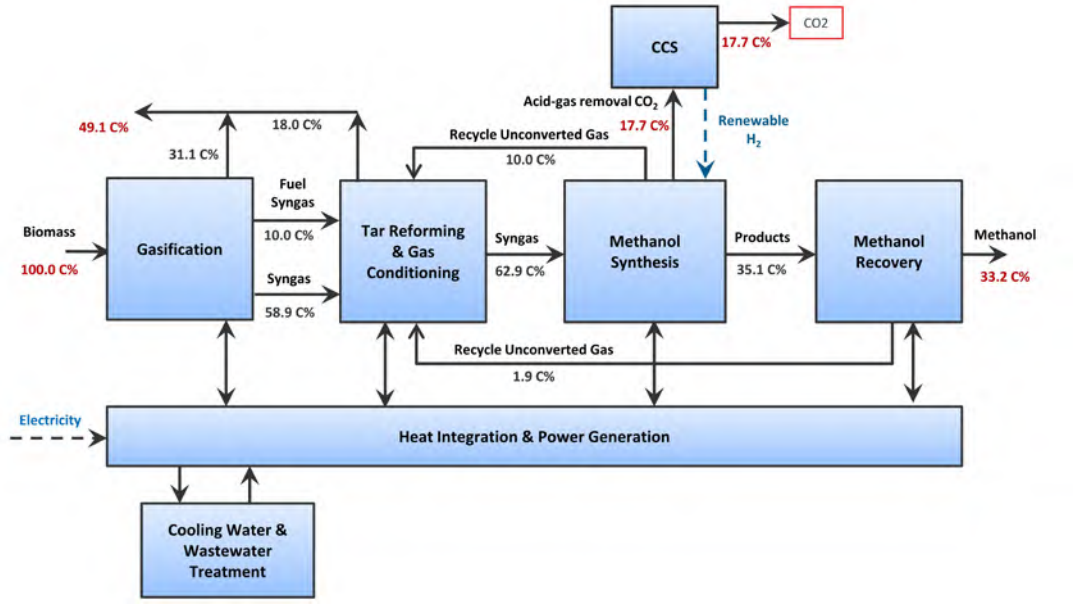

a.

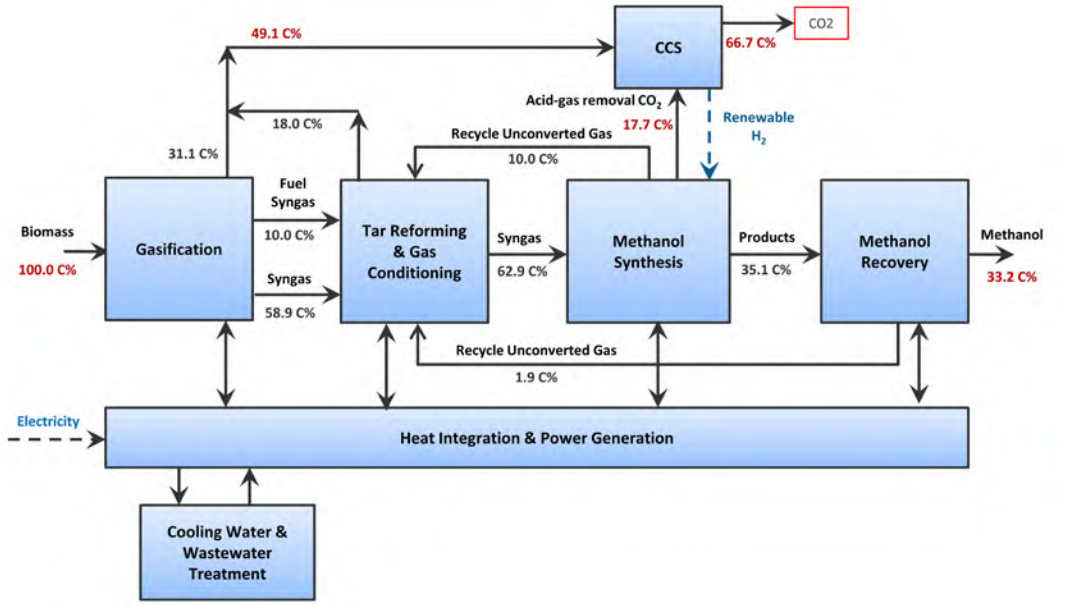

b.

Figure 5.10. Process block diagram for the biomass gasification to methanol process with CCS cases CCS1 (up) and CCS2 (down)

Additionally, considering CCS from all flue gases (i.e., CCS2) would increase the MFSP of the produced methanol to $3.2/GGE, with a CO_2 yield of 0.85 ton of CO_2 per ton of biomass. As this stream contains a mixture of off-gases, a compression and purification step is needed to separate CO_2 from the mixture, which is equivalent to 67% carbon from biomass, thus increasing the MFSP by 33.3%. This strategy reduces overall CO_2 emissions to 4.5 lb/GJ, a 99% reduction relative to the base case. Table 5.4 below summarizes the TEA parameters for these two CCS cases compared to the base case.

Table 5.4. Summary of TEA Parameters for the Biomass Gasification to Methanol Process With CCS as Compared to Base Case

Gasification Methanol	Units	Gasification Methanol	Gasification Methanol w/CCS AGR CO2 (CCS1)	Gasification Methanol w/CCS All Flue Gas CO_2 (CCS2)
Throughput capacity	dt/day	2,205	2205	2205
Feedstock type		Woody	Woody	Woody
Fixed capital investment	$	331,625,537	369,577,000	487,193,000
Fixed operating cost	$/yr	17,865,000	19,270,000	23,621,000
Other (nonfeedstock) variable operating cost	$/yr	5,420,000	5,420,000	5,520,000
Imported hydrogen	$/yr	N/A	N/A	N/A
Coproducts sales revenue	$/yr	16,000	16,000	16,000
Power sales revenue	$/yr	N/A	N/A	N/A
Imported electricity	$/yr	N/A	(2,770,000)	(10,440,000)
MFSP	$/GGE	2.4	2.6	3.2
Feedstock cost	$/dt	60.58	60.58	60.58

Based on woody biomass feedstock availability in 2030, potential hydrocarbon fuel production from the gasification to methanol pathway ranges from 5.9 billion GGE/yr (methanol production using the GGE basis) with a feedstock price of $70/dry ton to 12.1 billion GGE/yr with a feedstock price of $140/dry ton. Similarly, based on biomass feedstock availability in 2040, potential hydrocarbon fuel production ranges from 5.9 billion to 11.2 billion GGE/yr with feedstock prices of $70 to $140/dry ton, respectively. Assuming a facility scale of 2205 dmtd, the number of gasification to methanol production facilities that could be built ranges from 125 to 257 in 2030 and from 126 to 239 in 2040. Figure 5.11 below shows the methanol potential and number of facilities based on 2030 and 2040 feedstock data.

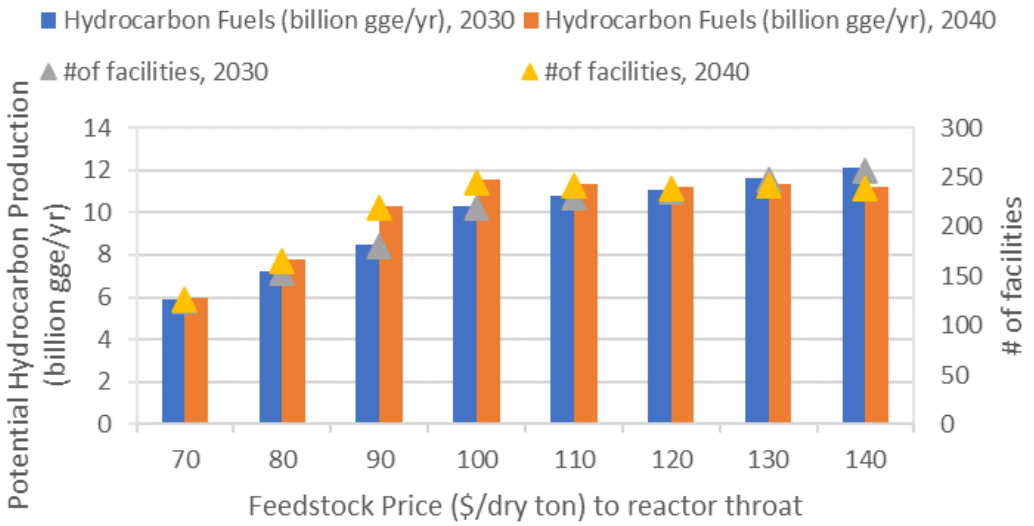

Figure 5.11. Potential hydrocarbon fuel production from the biomass gasification-to-methanol process

The total CO_2 sequestered per 2205 dmtd gasification to methanol facility is estimated to be 82 lb/GJ for CCS1 (CCS on the methanol synthesis flue gas stream) and 304 lb/GJ for CCS2 (CCS on the methanol synthesis and gasification off-gas streams). For CCS1, this corresponds to total CO_2 sequestration in the range of 10,250–21,074 lb/GJ in 2030 and 10,332–19,598 in 2040 with feedstock prices of $70 to $140/dry ton, respectively. For CCS2, CO_2 sequestration totals 38,000–78,128 lb/GJ in 2030 and 38,304–72,656 lb/GJ in 2040 with feedstock prices of $70 to $140/dry ton, respectively. Figure 5.12 shows the total CO_2 sequestered for both CCS options considering 2030 and 2040 feedstock supply data.

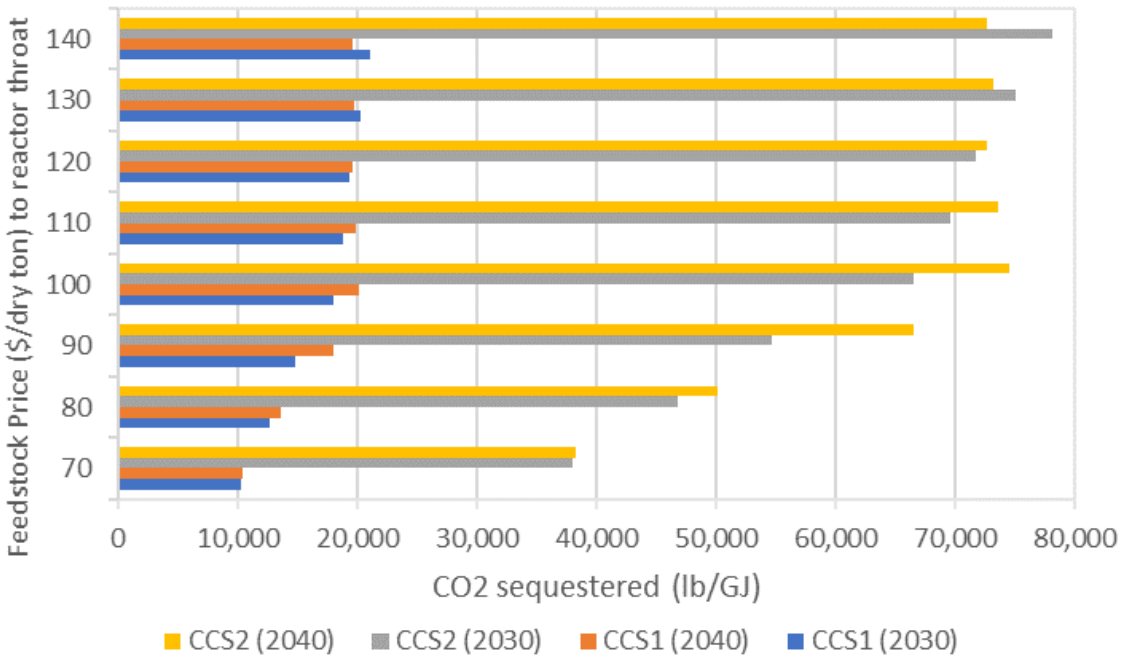

Figure 5.12. Total CO_2 sequestration for the biomass gasification to methanol process

5.3.4 Catalytic Fast Pyrolysis Pathway

This process uses a thermochemical conversion pathway that converts woody biomass into hydrocarbon fuels via catalytic fast pyrolysis. Refer to Figure 5.13 for the process block diagram. The one process vent stream that provides opportunities for decarbonization through CCS is the flue gas stream, which consists of 62% CO_2 by mass.

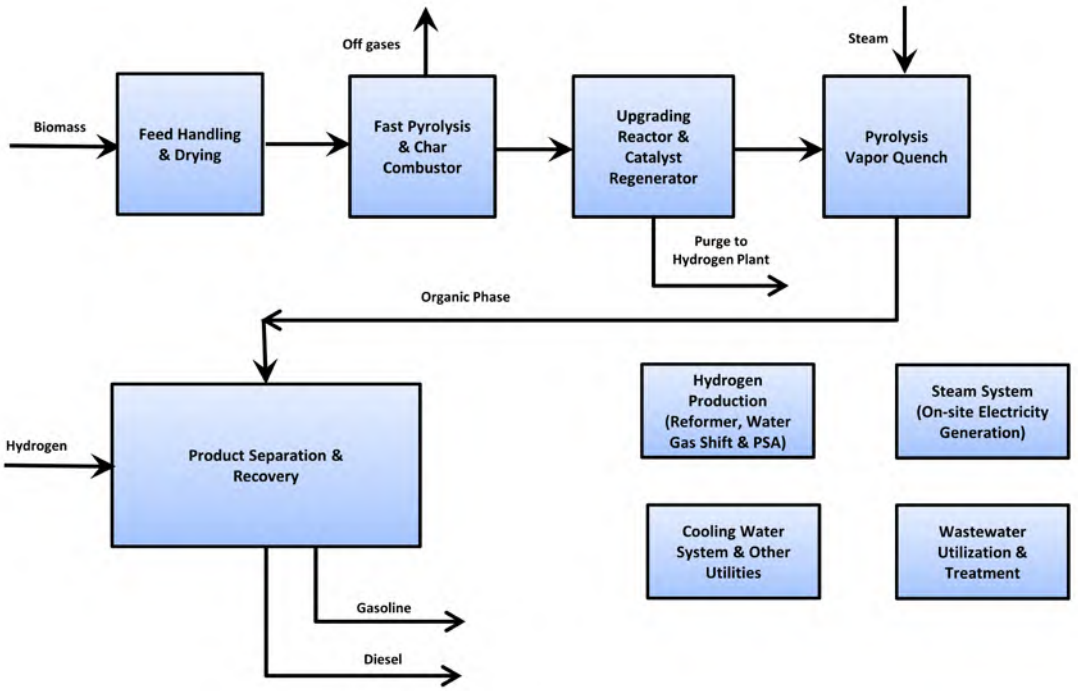

Figure 5.13. Process block diagram for the base-case catalytic fast pyrolysis process

Without CCS, the catalytic fast pyrolysis process produces hydrocarbon fuels with an MFSP of $2.8/GGE for a facility processing 2,000 dmtd of woody biomass feedstock. This corresponds to a hydrocarbon fuel yield of 392 lb/dry ton of biomass or 61 GGE/dry ton of biomass, equivalent to 7.5 GJ/dry ton of biomass on an energy basis. Because no CO_2 is being captured and sequestered, the biogenic CO_2 emissions from this process are estimated to be 304.8 lb/GJ of hydrocarbon fuels.

We consider one CCS case for this process, in which CO_2 is captured and sequestered from the flue gas (refer to Figure 5.14). Incorporating CCS would increase the MFSP of the produced hydrocarbon fuels to $3.6/GGE, with a CO_2 yield of 0.9 ton of CO_2 per ton of biomass. As this vent stream contains a mixture of off-gases, a compression and purification step is needed to separate CO_2 from the mixture, which consists of 62% carbon from biomass, thus increasing the MFSP by 28.6%. This strategy reduces overall CO_2 emissions to 61 lb/GJ, an 80% reduction relative to the base case. Table 5.5 below summarizes the TEA parameters for this CCS case compared to the base case.

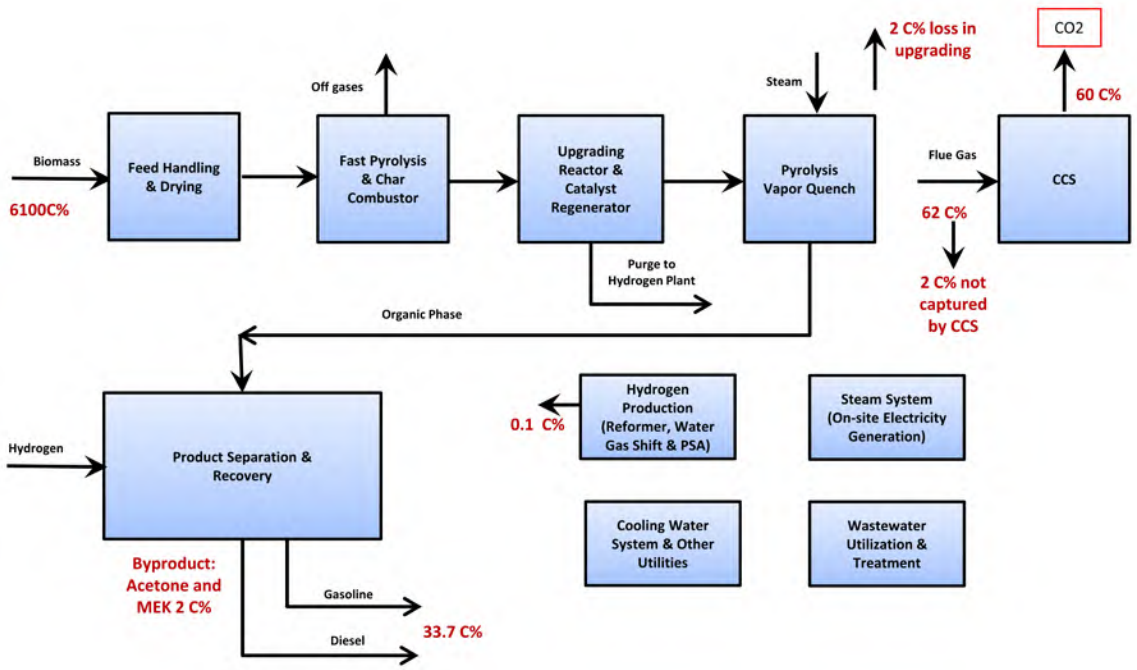

Figure 5.14. Process block diagram for catalytic fast pyrolysis process with carbon capture and sequestration (Dutta et al. 2021). Note that the CCS unit captures from all areas of the facility, flue gas from all sources is depicted as a single flow to the CCS unit on the right.

Table 5.5. Summary of TEA Parameters for the FT Process With CCS as Compared to Base Case

Catalytic Fast Pyrolysis	Units	CFP	CFP w/CCS All Flue Gas CO_2
Throughput capacity	dt/day	2,205	2,205
Feedstock type		Woody	Woody
Fixed capital investment	$	517,923,273	697,095,000
Fixed operating cost	$/yr	25,690,000	32,319,000
Other (nonfeedstock) variable operating cost	$/yr	3,506,000	3,603,000
Imported hydrogen	$/yr	N/A	N/A
Coproducts sales revenue	$/yr	24,330,000	24,330,000
Power sales revenue	$/yr	12,180,000	6,430,000
Imported electricity	$/yr	N/A	N/A
MFSP	$/GGE	2.8	3.7
Feedstock cost	$/dt	67.03	67.03

Based on woody biomass feedstock availability in 2030, potential hydrocarbon fuel production from the catalytic fast pyrolysis pathway ranges from 5.5 billion GGE/yr with a feedstock price of $70/dry ton to 11.4 billion GGE/yr with a feedstock price of $140/dry ton. Similarly, based on

biomass feedstock availability in 2040, potential hydrocarbon fuel production ranges from 5.6 billion to 10.5 billion GGE/yr with feedstock prices of $70 to $140/dry ton, respectively. Assuming a facility scale of 2205 dmtd, the number of catalytic fast pyrolysis to hydrocarbon fuel production facilities that could be built ranges from 125 to 257 in 2030 and from 126 to 239 in 2040. Figure 5.15 below shows the hydrocarbon fuel production potential and number of facilities based on 2030 and 2040 feedstock data.

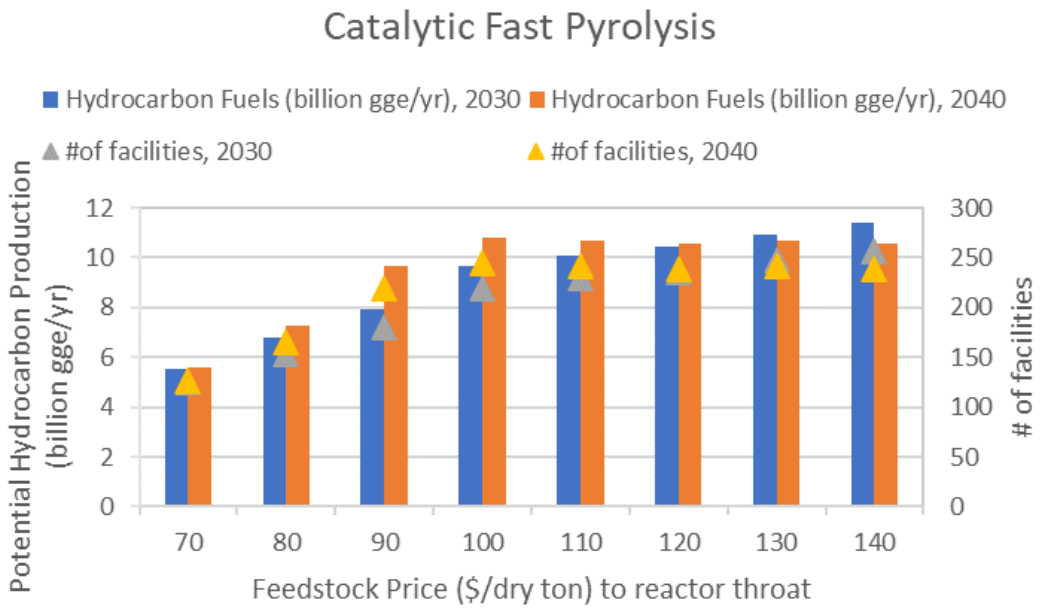

Figure 5.15. Potential hydrocarbon fuel production from the catalytic fast pyrolysis process

Incorporating CCS from the flue gas stream would sequester an estimated 298.7 lb/GJ per 2205 dmtd catalytic fast pyrolysis facility. This corresponds to total CO_2 sequestration of 37,337.5–76,766 lb/GJ in 2030 and 37,636–71,389 lb/GJ in 2040 with feedstock prices of $70 to $140/dry ton, respectively. Figure 5.16 shows total CO_2 sequestration considering 2030 and 2040 feedstock supply data.

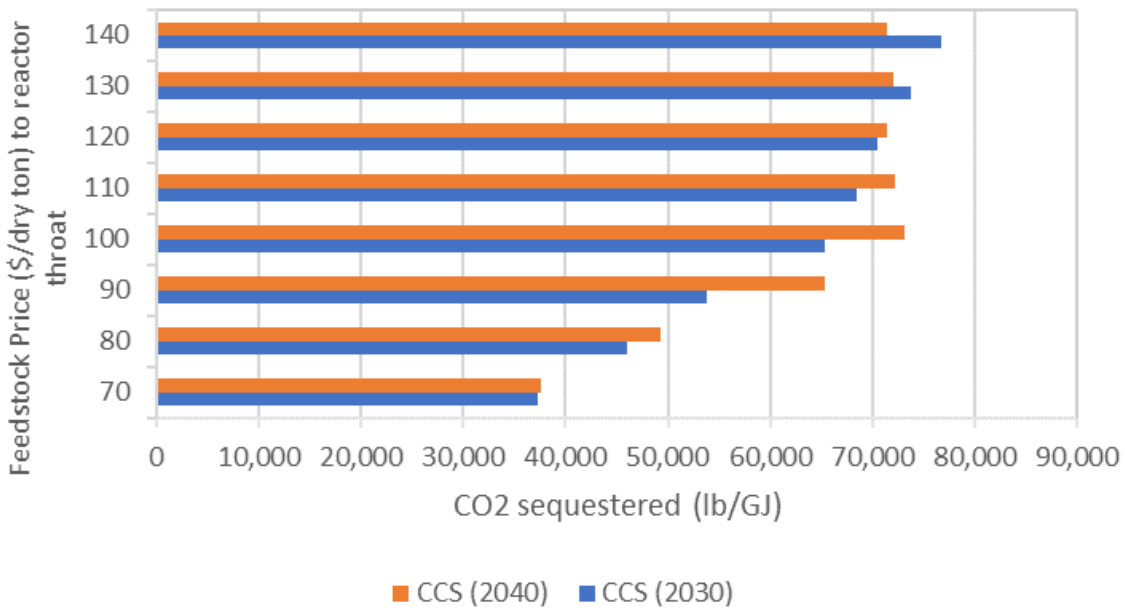

Figure 5.16. Total CO_2 sequestration for the catalytic fast pyrolysis process

5.4 Summary and Key Insights

We find that all the pathways analyzed here have MFSP values ranging from $2.6/GGE to $5.7/GGE with feedstock price varying between $70/dry ton and $140/dry ton, which is close to the existing fossil incumbent costs (Chapter 7). Several pathways emit high-purity CO_2 streams which may be captured at nominal (<10%) additional costs. While the above costs are comparable to existing fossil incumbents, availability of other transport/industry decarbonization options (e.g., electrification) may compete with these pathways.

Biochemical conversion to alcohols combined with alcohol-to-jet technologies is cost-effective for conversion of agricultural residues and herbaceous feedstocks to SAF. Thermochemical conversion is competitive for conversion of woody biomass to SAF. For the four biomass conversion pathways analyzed here, Figure 5.17 shows the change in the MFSP of their products as a function of feedstock price (to the reactor throat) for the base-case scenarios (without CCS integration). Because feedstock price is the key variable affecting production cost, it is important to analyze its impact on the overall process economics. This study is not intended to compare the MFSP of these pathways because the uncertainty associated with the lower-TRL pathways is significant.

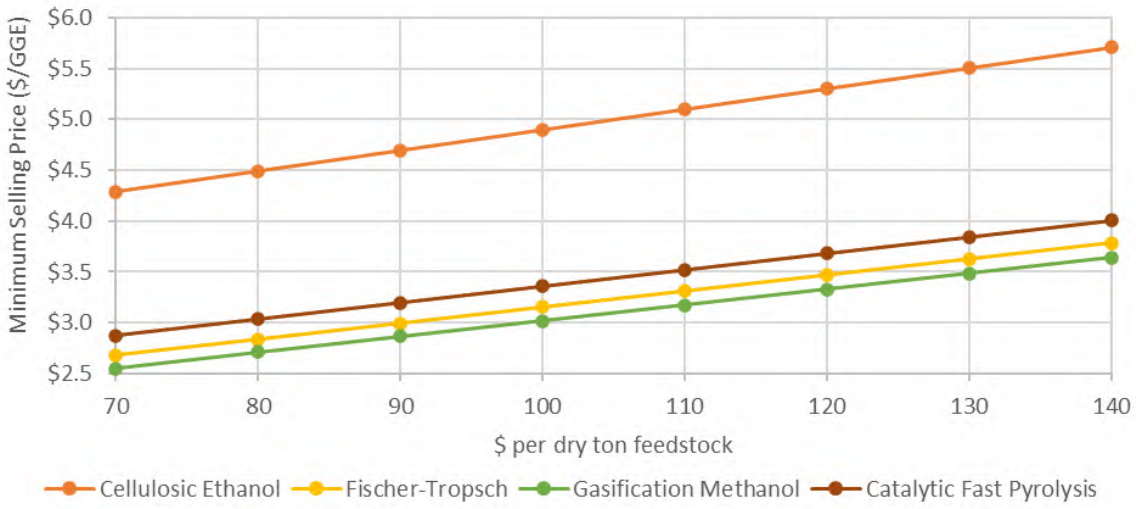

Figure 5.17. Summary of change in MFSP across varying feedstock prices for the base case

Based on the estimated availability of feedstocks in 2030 and 2040, we find that with feedstock prices of at least $90/dry ton, hydrocarbon fuel production potential (on a GGE basis) is highest for the cellulosic ethanol process, which utilizes herbaceous biomass feedstocks, primarily due to the greater availability of herbaceous biomass compared to woody biomass (refer to Figure 5.18). With lower feedstock prices ($70 and $80/dry ton), hydrocarbon fuel production potential is highest for the FT, gasification, and catalytic fast pyrolysis pathways, which utilize woody biomass feedstocks, due to the higher availability of woody biomass at these prices.

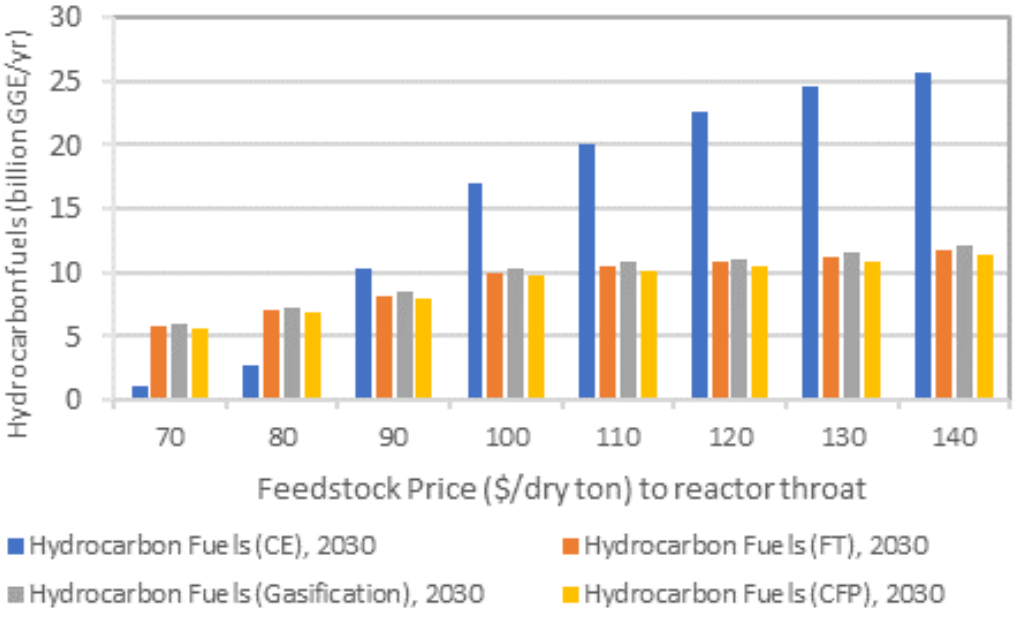

a)

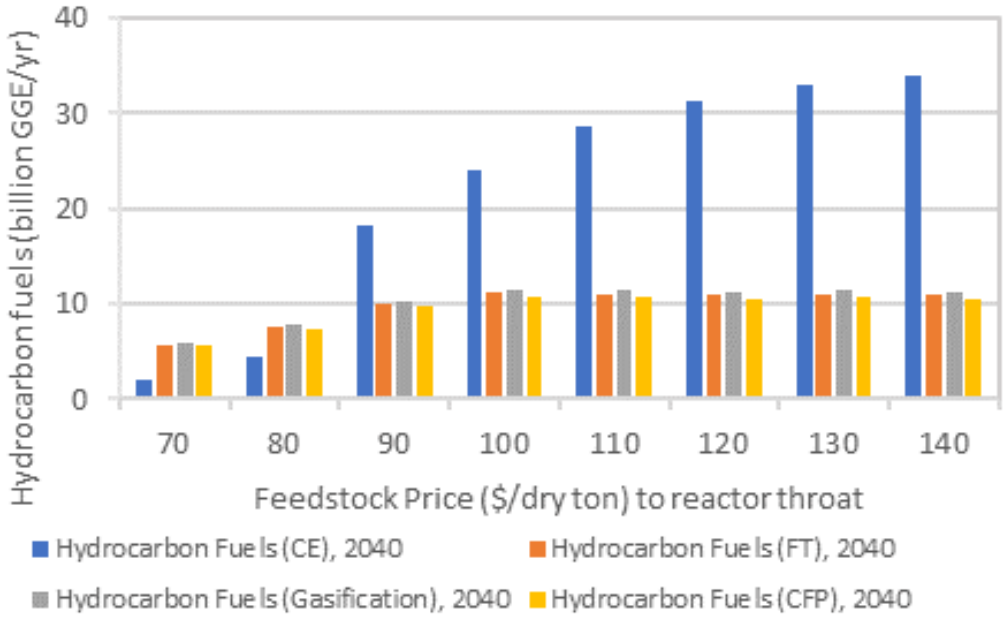

b)

Figure 5.18. Hydrocarbon fuel production potential based on a) 2030 and b) 2040 feedstock supplies

While most of these biomass conversion pathways have multiple flue gas streams available for CCS, some of these streams have low CO_2 purity, necessitating additional cleanup steps, including compression and purification, that make CCS costly and can increase the MFSP by more than 25% relative to the base case in some cases. For example, the fermentation off-gas stream has high CO_2 purity, making it inexpensive to pair with CCS; however, if flue gas from the boiler combustion stream is also considered, a compression and purification step is needed to purify CO_2, increasing the MFSP of the produced hydrocarbons by more than 25%. Figure 5.19 shows the carbon distribution between hydrocarbon fuels and the CCS1 and CCS2 options (outlined previously—see Figure 5.2, Figure 5.6, Figure 5.10, and Figure 5.14) for the four conversion pathways.

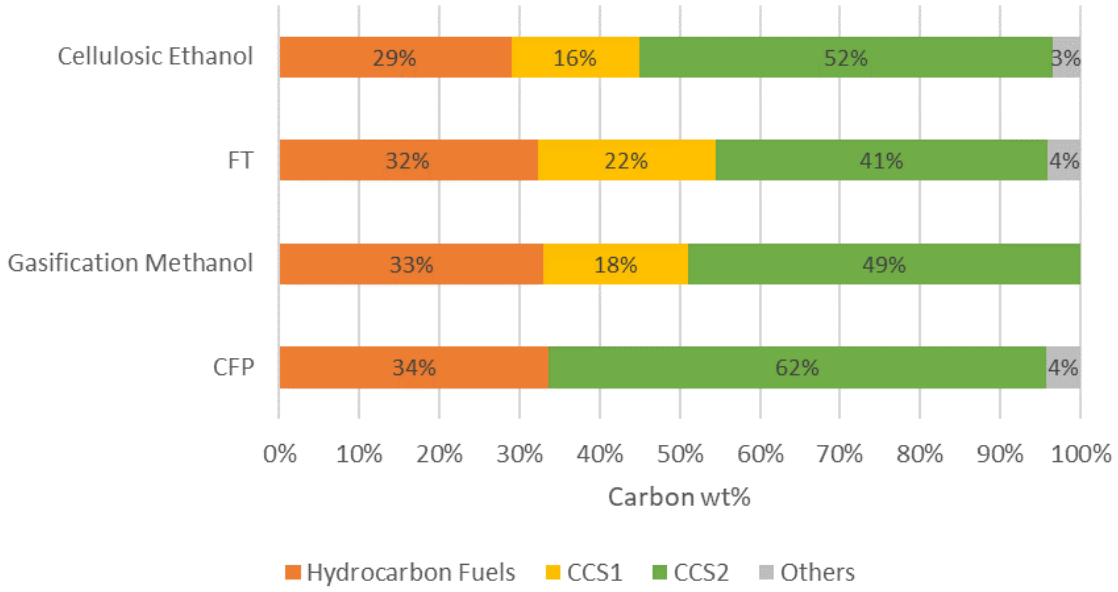

Figure 5.19. Carbon distribution between hydrocarbon fuels and CCS options considered in this analysis

As shown in Figure 5.19, incorporating CCS to capture CO_2 from all flue gases in the catalytic fast pyrolysis process could yield the maximum carbon emission reduction, whereas for the FT process integrating CCS with all flue gases, only 41% carbon is attributed to CO_2. However, trade-offs between the cost of integrating CCS and the resulting reduction in carbon emissions should be carefully considered to make informed decisions. The amount of CO_2 sequestered would be highest when CCS is integrated to capture CO_2 from all flue gases. Of the analyzed conversion process designs, the cellulosic ethanol to hydrocarbon fuels pathway has the highest CCS potential, capturing and sequestering 379 lb CO_2 per GJ of hydrocarbon fuels. The maximum CCS potential of the other three pathways is around 300 lb CO_2 per GJ of hydrocarbon fuels. In comparison, the incremental cost of CCS is low because of the high-purity streams of CO_2 from biorefining in the cellulosic ethanol pathway.

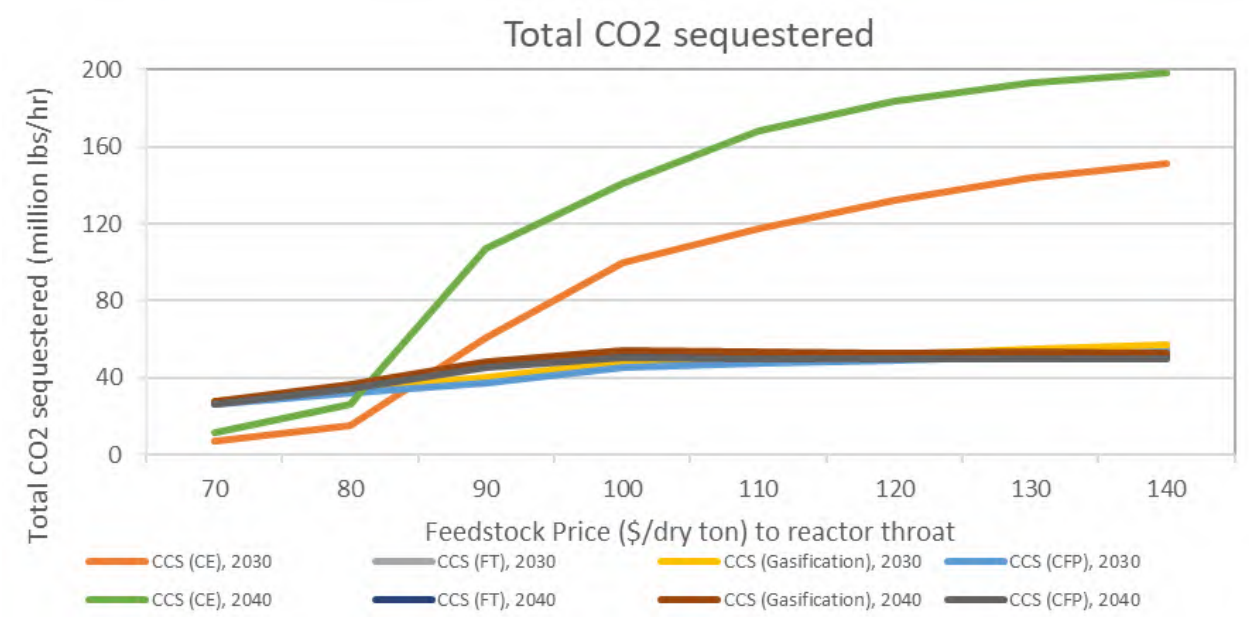

Figure 5.20. Potential for total CO_2 sequestration based on feedstock supply data

As shown in Figure 5.20, integrating CCS to capture CO_2 from all flue gases in the cellulosic ethanol process has the potential to capture up to 151 million lb/yr of CO_2, equivalent to 0.27 million lb/GJ of hydrocarbon fuels, based on 2030 herbaceous feedstock supply data. Based on 2040 herbaceous feedstock data, the CO_2 sequestration potential of this process could reach 199 million lb/yr, equivalent to 0.36 million lb/GJ. Based on 2030 and 2040 woody biomass feedstock data, the FT pathway could sequester up to 54.7 million lb CO_2/yr in 2030 and 50.9 million lb CO_2/yr in 2040, the gasification pathway could sequester up to 56.8 million lb CO_2/yr in 2030 and 52.8 million lb CO_2/yr in 2040, and the catalytic fast pyrolysis pathway could sequester up to 53 million lb CO_2/yr in 2030 and 49.3 million lb CO_2/yr in 2040. Overall, coupling bioenergy with CCS can achieve net-negative GHG emissions capable of offsetting other hard-to-decarbonize sources (see Section 7.2 for additional discussion on this).

References

Davis, R., L. Tao, E. C. D. Tan, M. J. Biddy, G. T. Beckham, C. Scarlata, J. Jacobson et al. 2013. *Process Design and Economics for the Conversion of Lignocellulosic Biomass to Hydrocarbons: Dilute-Acid and Enzymatic Deconstruction of Biomass to Sugars and Biological Conversion of Sugars to Hydrocarbons.* Golden, CO: National Renewable Energy Laboratory. NREL/TP-5100-60223. https://doi.org/10.2172/1107470.

Dutta, A., M. Talmadge, J. Hensley, M. Worley, D. Dudgeon, D. Barton, P. Groendijk. 2011. *Process design and economics for conversion of lignocellulosic biomass to ethanol: thermochemical pathway by indirect gasification and mixed alcohol synthesis*. Golden, CO: National Renewable Energy Laboratory. NREL/TP-5100-51400. https://doi.org/10.2172/1015885.

Dutta, A., C. Mukarakate, K. Iisa, H. Wang, M. Talmadge, D. Santosa, K. Harris et al. 2021. *Ex Situ Catalytic Fast Pyrolysis of Lignocellulosic Biomass to Hydrocarbon Fuels: 2020 State of Technology*. Golden, CO: National Renewable Energy Laboratory. NREL/TP-5100-80291. https://doi.org/10.2172/1805204.

Harris, K., R. G. Grim, Z. Huang, and L. Tao. 2021. "A comparative techno-economic analysis of renewable methanol synthesis from biomass and CO_2: Opportunities and barriers to commercialization." *Applied Energy* 303: 117637. https://doi.org/10.1016/j.apenergy.2021.117637.

Humbird, D., R. Davis, L. Tao, C. Kinchin, D. Hsu, A. Aden, P. Schoen, J. Lukas, B. Olthof, and M. Worley. 2011. *Process design and economics for biochemical conversion of lignocellulosic biomass to ethanol.* Golden, CO: National Renewable Energy Laboratory. NREL/TP-5100-47764. https://doi.org/10.2172/1013269.

Kleijne, K., S. Hanssen, L. van Dinteren, M. Huijbregts, R. van Zelm, and H. de Coninck. 2022. "Limits to Paris compatibility of CO_2 capture and utilization." *One Earth* 5(2): 168–185.

Tao, L., K. Harris, U. Lee, and E. Yoo, 2022. *Techno-Economic Evaluation of Strategies to Approach Net-Zero Carbon Sustainable Aviation Fuel via Woody Biomass Gasification and Fischer-Tropsch Synthesis.* Golden, CO: National Renewable Energy Laboratory. NREL/PR-5100-82703. https://www.osti.gov/biblio/1865606.

6 Life Cycle Analysis and Decarbonization Scenario Analysis

6.1 Background

The objective of this chapter is to provide environmental life cycle analysis and screening-level, process-based decarbonization scenario analysis for selected pathways to produce power, fuel, and products from biomass feedstocks. The scope of the analysis presented in this chapter includes the full life cycle of the products, avoided emissions from conventional waste management, and a combination of allocation and system expansion to address coproducts. The metrics presented are life cycle/systemwide GHG emissions and fossil energy consumption, including consideration of the permanence of CO_2 sequestration (Terlouw 2021). The LCA is conducted using the GREET model. The LCA outputs are used as inputs to decarbonization scenario analysis performed using the Bioeconomy AGE model, which brings together LCA outputs, scenario information, and feedstock supply to calculate environmental metrics for renewable technology/decarbonization scenarios. Bioeconomy AGE places LCA modeling results in the context of scenarios and provides a streamlined framework for screening scenarios. The LCA outputs inform the decarbonization potential for the selected pathways as well as potential trade-offs between environmental metrics, potential synergies or conflicts between decarbonization strategies, and the best use of biomass feedstocks.

6.2 Methods

This section describes the methods in two parts. First, LCA of the pathways considers system expansion in line with the International Organization for Standardization standards (ISO 14044:2006) which provide the best practice guidance for carrying out LCA consistently and transparently. This approach provides results per unit of a target fuel or energy product, but results can be complicated by coproduct effects and presenting results outside the context of economywide effects. Pathway LCA results are placed in the context of economywide decarbonization scenarios using the Bioeconomy AGE model.

The analyses described in this chapter incorporate inputs from previous chapters. From the GCAM analysis described in Chapter 2, this analysis considers the feedstock amounts, preprocessing/conversion technology, and fuel/product amounts for decarbonization scenarios by end use. The land area for feedstock production (yield) and irrigation water use are incorporated from the feedstock supply analysis described in Chapter 3. The energy and other input requirements for feedstock harvesting, feedstock transportation modes and distances to preprocessing/conversion, energy and other input requirements for feedstock preprocessing, and fuel and product transportation modes and distances to end use are incorporated from the analysis described in Chapter 4. The mass and energy balances for conversion processes are incorporated from the process modeling described in Chapter 5.

The outputs from the LCA also feed back into the analyses presented in other chapters. The life cycle GHG emissions were also considered in establishing the models/design for the pathways described in Chapters 4 and 5, and the LCA and Bioeconomy AGE results informed the parameterization of the GCAM runs presented in Chapter 2.

The results from the LCA presented in this chapter include life cycle GHG emissions, water consumption, and fossil energy consumption presented on a per-unit energy basis (kg carbon dioxide equivalent (CO_2e)/megajoule [MJ]). Results for biomass flows and GHG emissions are presented for the scenario analysis as economywide totals.

6.2.1 Life Cycle Analysis

LCA is performed for the four pathways described in detail in association with the process modeling and TEA presented in Chapter 5, as well as for bioelectricity generation, which is modeled separately. These pathways are 1) jet fuel via biochemical ethanol production from cellulosic feedstocks and ethanol-to-jet, 2) synthetic paraffinic kerosene via FT synthesis, 3) methanol via biomass gasification, 4) gasoline via catalytic fast pyrolysis, and 5) bioelectricity. Each pathway was simulated with and without CCS. Combining geologic CO_2 sequestration with the feedstocks' biological CO_2 capture (during photosynthesis) could lead to net-negative emissions. In fact, past work shows that pathways such as biochemical ethanol production are the lowest-hanging fruit for achieving net-negative emissions (Sanchez et al. 2018). Pathways 1–3 offer particularly high concentrations of CO_2 from some off-gas streams, which can be captured at low cost and energy investments.

The functional unit of Pathways 1–4 is 1 MJ of finished liquid biofuels. The functional unit for Pathway 5 is 1 kWh of electricity, enabling comparison with other published electricity and bioelectricity LCAs with and without CCS.

The system boundary for the LCAs encompasses feedstock cultivation and collection; feedstock preprocessing, transportation, conversion, and intermediate upgrading (as necessary); CO_2 capture, compression, transport, and storage for selected pathways; and product end use as transportation fuels. For fuel products (jet fuel, gasoline, diesel, wax, methyl ethyl ketone, acetone), the net emissions were allocated based on energy content. We have noted that when biogenic CO_2 emissions are captured and stored in the geosphere, they could become a carbon sink and provide negative emissions. As such, negative emissions in our analysis connote biogenic CO_2 emissions captured and sequestered through CCS (Singh and Dunn 2022, Terlouw et al. 2021). When CCS is not incorporated, biogenic CO_2 emissions from fuel combustion are considered carbon-neutral. For all GHGs in this LCA, including CO_2, CH_4, and N_2O, the Intergovernmental Panel on Climate Change Sixth Assessment Report global warming potential values have been used to convert them to CO_2 equivalent units. While LCA results are presented considering today's electricity grid, no displacement credit is assigned to the coproduced electricity, as it is assumed the electricity grid will be decarbonized as these biofuel production pathways scale up (Chapter 2).

For the pathways producing liquid fuels, the output data—inventory of feedstock, energy and chemicals, and biofuel yields and coproducts—from Chapter 5 was used as the input data for the LCA. The GREET model (ANL, 2022) developed at Argonne National Laboratory was configured to estimate the GHG emissions, fossil energy consumption, and water consumption for each pathway. The feedstocks were corn stover for Pathway 1 and forest residues for Pathways 2–4.

Pathway 5 leveraged recent GREET LCA work on bioelectricity generation from forest biomass (Xu et al. 2021) and added CO_2 capture, compression, transport, and storage to bioelectricity

generation without CCS (Figure 6.1). We assumed a CO_2 capture efficiency of 90%, which imposes an energy penalty of 38.7% for CCS at bioelectricity power plants based on the estimates suggested by past GCAM analysis (Muratori et al. 2017). This energy penalty included capture and compression. Net plant efficiency was adjusted accordingly. For pipeline transport, CO_2 needs to be compressed to a pressure of 2,000 psi, or 13.8 MPa (Rubin and Rao 2002). For CO_2 transport and storage, additional energy consumption of 0.1 J/t-CO_2/km and 0.68 kWh/t-CO_2 were applied, respectively (Zang et al. 2021, Melara et al. 2020).

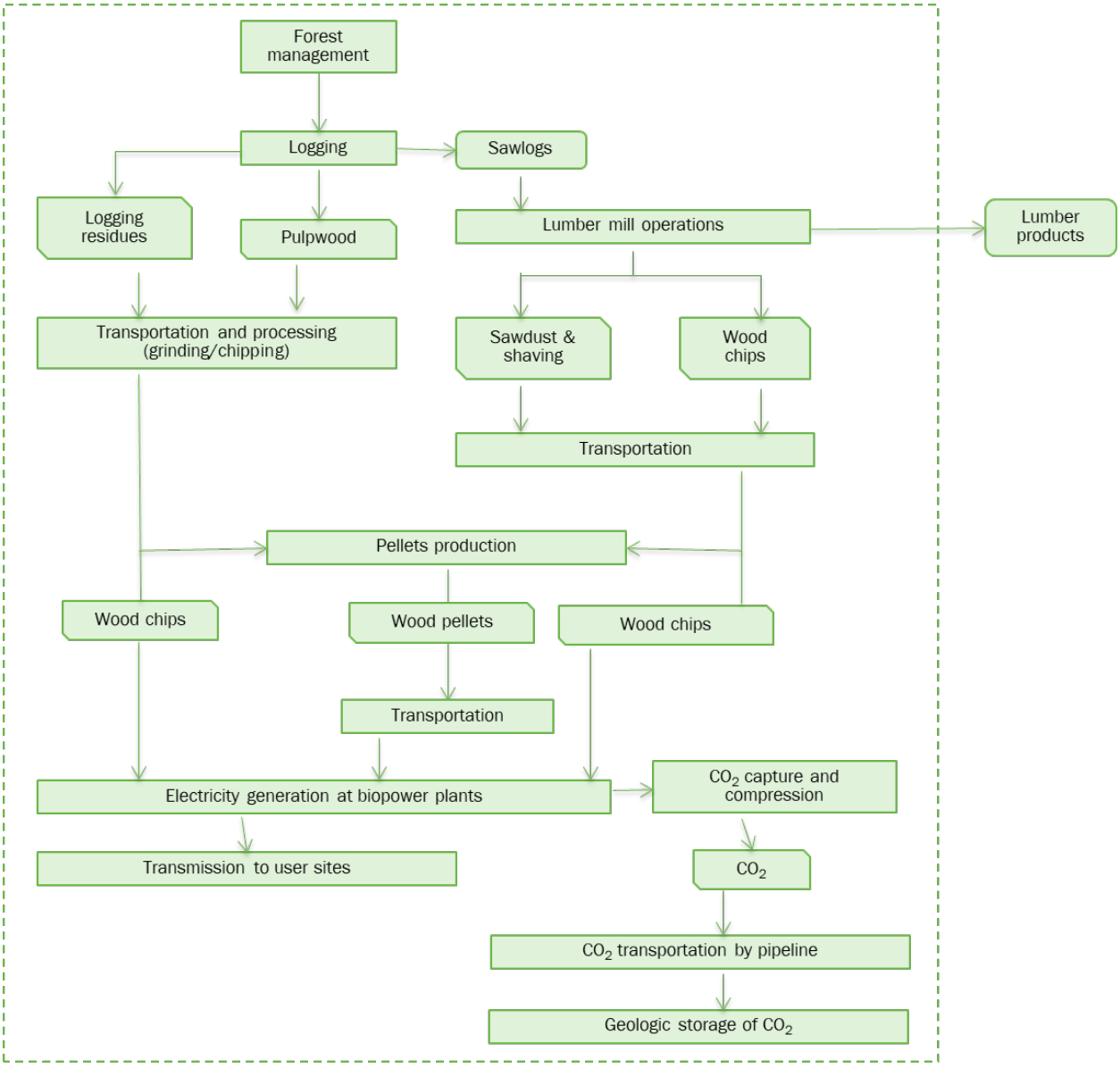

Figure 6.1. System boundary for estimating life cycle emissions and resource use for bioelectricity generation with CCS

6.2.2 Decarbonization Scenario Analysis

6.2.2.1 Bioeconomy Air Emissions, Greenhouse Gas Emissions, and Energy Use

Bioeconomy AGE is a scenario-based spreadsheet model that estimates the energy and environmental impacts of biotechnology deployment at scale. It can evaluate the energy and environmental effects of large-scale deployment of a wide range of bioenergy, bioproducts, and biochemical technologies. Bioeconomy AGE has been used to analyze the development and deployment of biotechnology pathways across a range of technologies and scenarios (Rogers et al. 2016, Oke et al. 2022, Dunn et al. 2020, Oke et al. 2023, Kar et al. 2022).

The data input into Bioeconomy AGE includes biomass resource supply and pathways for producing fuels, products, and electricity (Figure 6.2). It integrates temporally explicit life cycle profiles of the five pathways modeled with the inventory data provided by the GREET model and the analysis in Chapter 5, and with scenario information and feedstock supply and demand from Chapter 2 (Pacific Northwest National Laboratory) to calculate energy and environmental metrics for the decarbonization scenarios out to 2050.

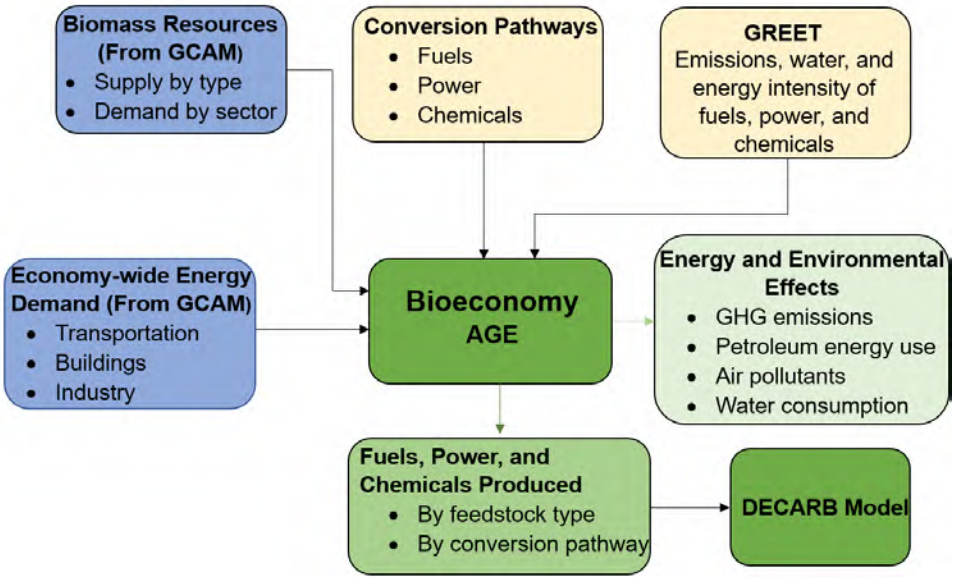

Figure 6.2. Data flow into the Bioeconomy AGE model

We extract key metrics from three specific scenarios' GCAM output—including biomass supply and demand and energy demand across transportation, building, and industry—for screening-level analyses in Bioeconomy AGE modeling. The GCAM scenarios considered include the reference case, the scenario where novel biofuel conversion technologies become available but no SAF production targets are represented (DAC.Ref_noSAF), and the scenario that requires the production of 35 billion gallons of liquid biofuels in 2050, consistent with the SAF Grand Challenge volumetric target for meeting U.S. jet fuel demand, excluding coproducts (DAC.Ref_BF35bil.gal).

Note that the scenarios presented here are based on GCAMv6 defaults and differ somewhat from the GCAM scenarios used in Chapter 2. Details about the differences among these scenarios are provided in Chapter 2 (Section 2.1).

The metrics extracted from GCAM are aggregated data that require further disaggregation before being used in Bioeconomy AGE modeling. For example, GCAM, by default, does not track different types of liquid fuels but rather a homogenous blend of liquid fuels produced from all feedstocks (oil, biomass, etc.) and conversion pathways. However, Bioeconomy AGE explicitly tracks specific liquid fuel pathways together with their biomass supply and demand. We leveraged the effort of ORNL in Chapter 3 to disaggregate biomass supply from GCAM by category into more explicit types (e.g., "Biomass Supply|2nd Gen Crops|biomassGrass" disaggregated into switchgrass, miscanthus). In addition, the homogenous blend of liquid fuels in GCAM was disaggregated for explicit representation of gasoline vs. diesel vs. jet fuel, etc., based on the Annual Energy Outlook 2022 energy demand projection for different sectors (EIA 2022).

The available biomass resources are allocated to various end uses such as building heating, industrial energy and process heat, electricity, and liquid fuel production, as specified in GCAM output. However, the allocation of biomass to liquid fuel production is based on the selected pathways in this study as represented in Chapter 5 (Table 5.1) and not based on GCAMv6 pathways modeling economywide changes. We use the "fuel pool" concept to allocate various biomass types to different conversion pathways rather than favoring a particular sector. For example, all sectors using diesel, including transportation, building, and industry, will have the same blending level of biofuel in the decarbonization scenarios. However, we note that this assumption may not always hold considering differences in fuel quality/specification/blending requirement for use in different sectors.

In addition, to estimate the ramp-up of biofuel, Bioeconomy AGE uses a technology adoption curve based on the logistic equation to predict biofuel market penetration for the emerging pathways (Oke et al. 2022). In allocating biomass to liquid fuel production, four main factors, including the target fuel, fuel yield per unit biomass, carbon intensities of fuels, and TRL of the conversion pathway are considered in Bioeconomy AGE modeling. Overall, how biomass is utilized in each scenario depends on its assumptions about SAF production. Amongst the selected liquid biofuel pathways with SAF output, the FT-SPK pathway appears favorable considering the TRL, carbon intensities of fuels, and the overall fuel yield (diesel, gasoline, and jet fuel). However, because its yield is low for jet fuel, this pathway will require more biomass to meet a specific jet target compared to the ethanol-to-jet pathway. Hence, we start with the FT-SPK pathway with high TRL in 2020 and gradually move to the ETJ pathway with low TRL but higher SAF yield from 2030 to 2050. The model provides a level playing field to all pathways unless a specific pathway is preferred. For instance, in scenarios where the SAF pathway is incentivized, the minimum biofuels constraint is applied to the model in line with the SAF Grand Challenge target.

Figure 6.3 provides an overview of biomass flow to biofuels and bioelectricity through various conversion pathways. For the Reference case (Figure 6.3a), we allocate biomass to buildings, industry, and bioelectricity based on the amount allocated in GCAM. The remaining biomass resources go to biofuels, with corn and soybean allocation also based on their allocations in

GCAM. For cellulosic ethanol, we use the Bioeconomy AGE adoption curve to set the production target in 2050 based on the amount of biomass used in GCAM for cellulosic ethanol in 2050. While GCAM allocates resources to gasification and FT-SPK pathways in the reference case, Bioeconomy AGE assumes the selected pathways in this study (ETJ, FT-SPK, CFP, gasification to methanol) are not in use in the reference case.

For the DAC.Ref_noSAF scenario (Figure 6.3b), allocation in GCAM favors bioelectricity over biofuel since no target is placed on SAF production. Biomass for building, industry, and bioelectricity is as used in GCAM, while the remaining biomass resources are converted to biofuels based through the selected pathways. Because the technology adoption curve is characterized by four growth stages—early slow growth in market share, fast growth in market share, late-stage slow growth, and no growth in market share—there are periods when the biomass designated for biofuel production is not used up. In these periods, any leftover biomass is redirected to bioelectricity.

The DAC.Ref_BF35bil.gal targets annual production of 35 billion gallons of liquid biofuels, including SAF, in 2050, consistent with the SAF Grand Challenge volumetric target for meeting U.S. jet fuel demand, excluding coproducts. After allocation of biomass to buildings and industry according to GCAM allocations, the remaining biomass resources are allocated to produce enough biofuels to meet the 35-billion-gallon target, followed by bioelectricity (Figure 6.3c).

In each scenario, GCAM allocates some biomass to biohydrogen production. This is not considered in Bioeconomy AGE modeling, since biomass-to-biohydrogen is not a pathway considered in this study. Instead, using the electricity generation mix from GCAM for each scenario, Bioeconomy AGE assumes hydrogen production from electrolysis.

a)

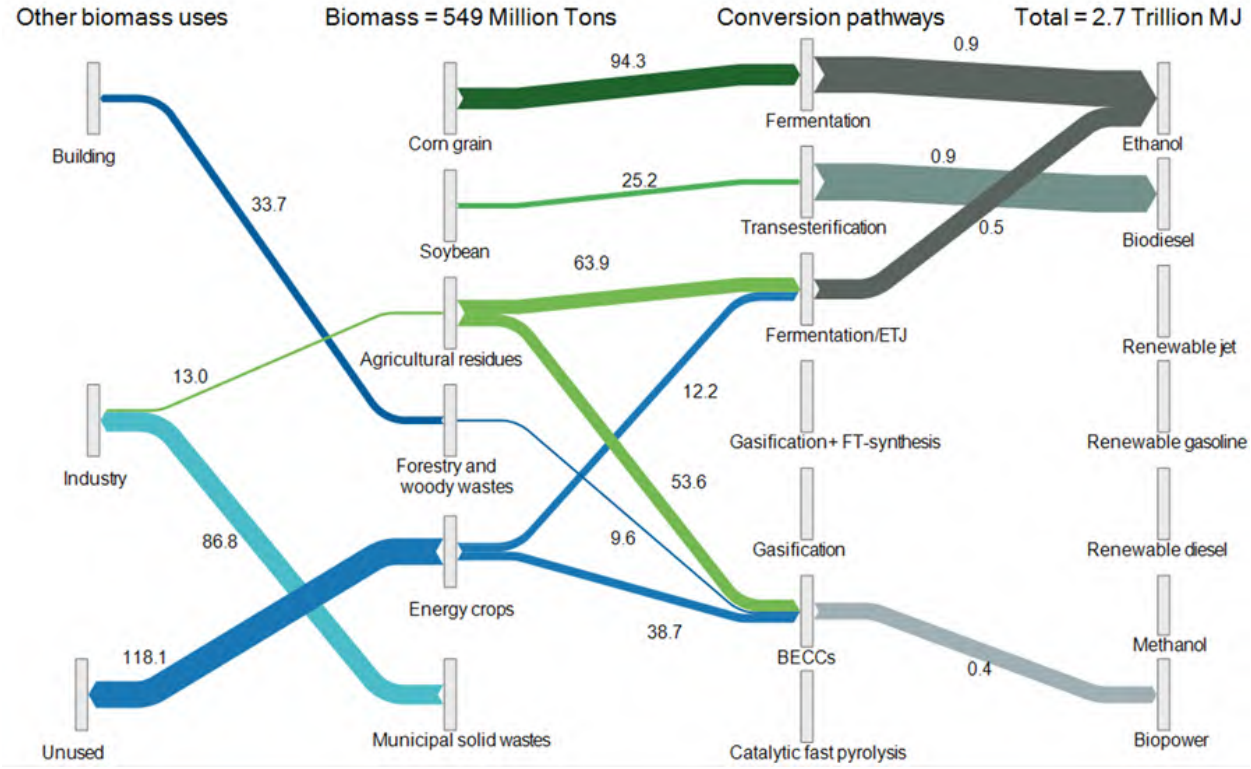
Other biomass uses
Biomass = 549 Million Tons
Conversion pathways
Total = 2.7 Trillion MJ
Building
Industry
Unused
Corn grain
Soybean
Agricultural residues
Forestry and woody wastes
Energy crops
Municipal solid wastes
Fermentation
Transesterification
Fermentation/ETJ
Gasification+ FT-synthesis
Gasification
BECCs
Catalytic fast pyrolysis
Ethanol
Biodiesel
Renewable jet
Renewable gasoline
Renewable diesel
Methanol
Biopower
33.7
13.0
86.8
118.1
94.3
25.2
63.9
53.6
9.6
12.2
38.7
0.9
0.9
0.5
0.4

b)

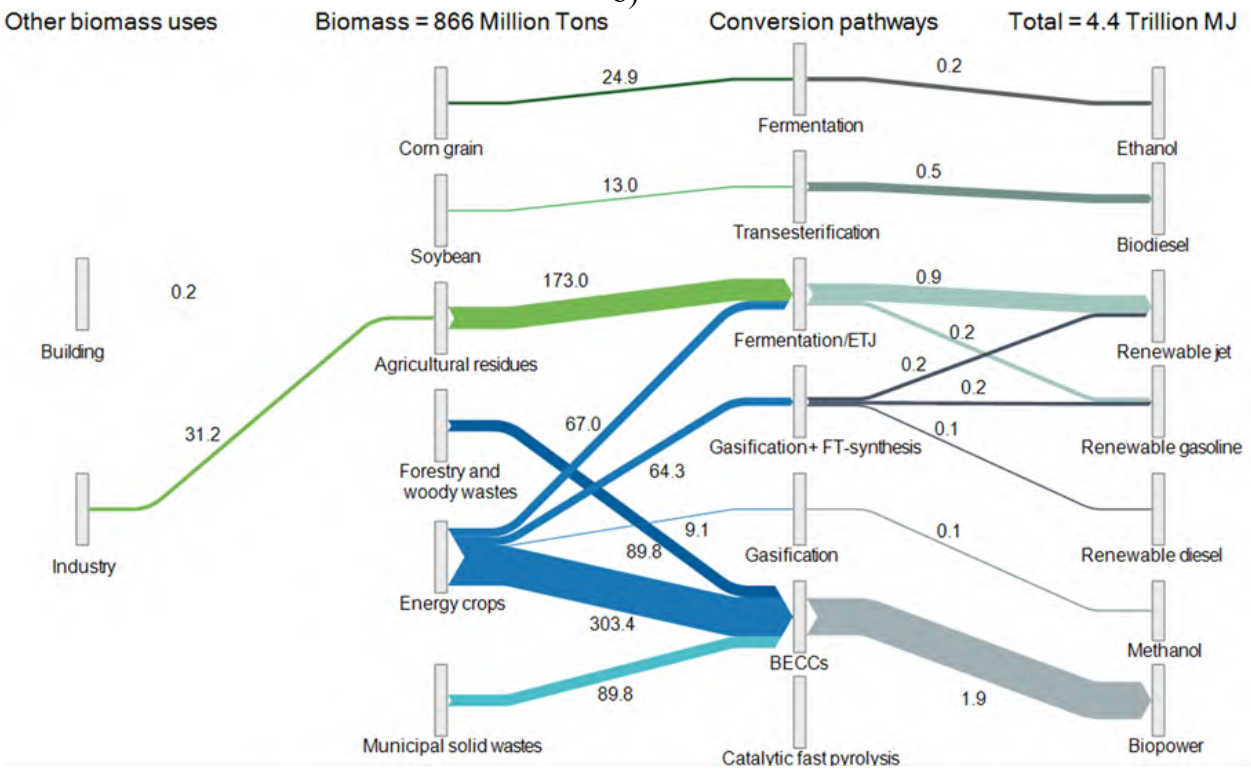
Other biomass uses
Biomass = 866 Million Tons
Conversion pathways
Total = 4.4 Trillion MJ
Building
Industry
Corn grain
Soybean
Agricultural residues
Forestry and woody wastes
Energy crops
Municipal solid wastes
Fermentation
Transesterification
Fermentation/ETJ
Gasification+ FT-synthesis
Gasification
BECCs
Catalytic fast pyrolysis
Ethanol
Biodiesel
Renewable jet
Renewable gasoline
Renewable diesel
Methanol
Biopower
0.2
31.2
24.9
13.0
173.0
67.0
64.3
9.1
89.8
303.4
89.8
0.2
0.5
0.9
0.2
0.2
0.2
0.1
0.1
1.9

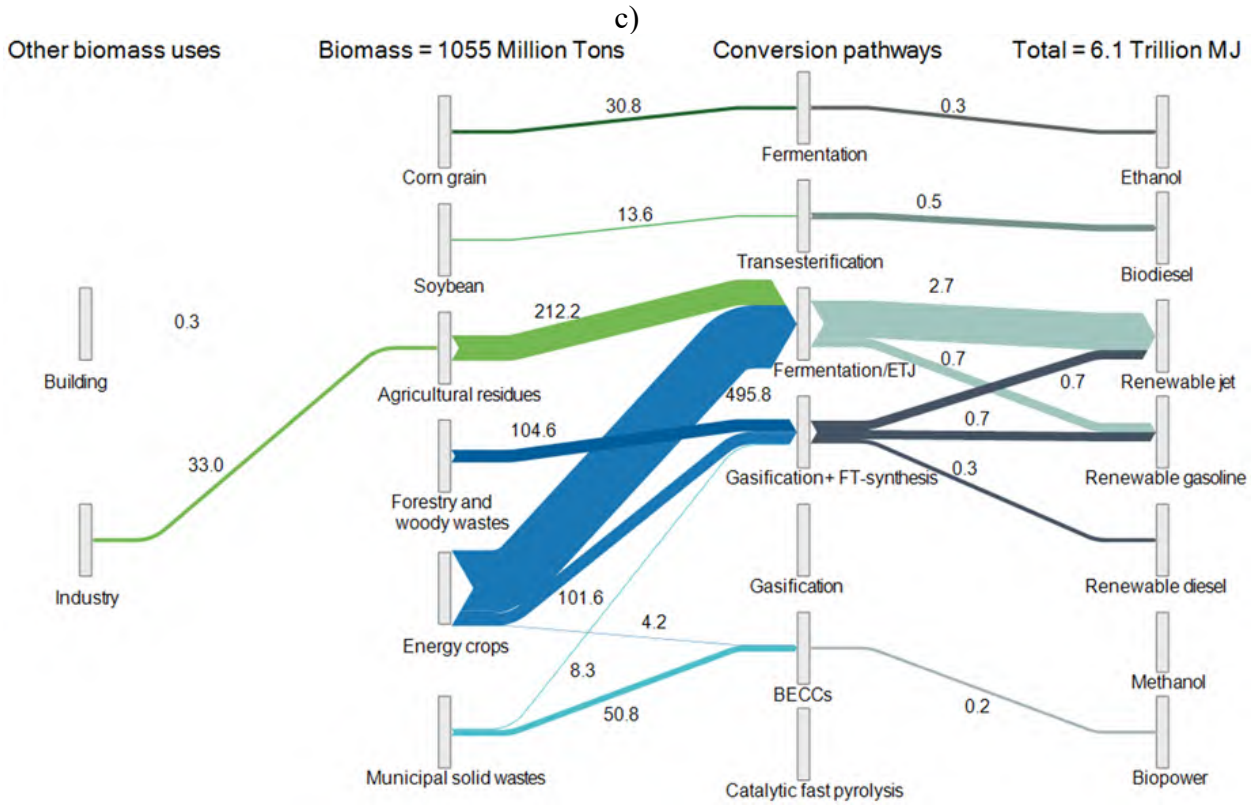

Figure 6.3. Biomass allocation to end uses in the a) Reference case, b) DAC.Ref_noSAF, and c) DAC.Ref_BF35bil.gal scenarios

Biofuels and bioelectricity produced by each feedstock type and conversion pathway are integrated with LCA data to evaluate each scenario's environmental and energy impacts. In addition, the environmental impact of each scenario is assessed based on two levels of CCS for the liquid fuel conversion pathways.

6.3 Results and Discussion

6.3.1 Life Cycle Analysis

6.3.1.1 Results for Liquid Biofuels

Pathways 1–4 focused on production of different types of liquid biofuels, and Pathways 1–3 were each modeled with two distinct levels of CO_2 capture. In the first level ("Partial CCS" in Figure 6.4), only the high-purity process CO_2 stream was captured, which imposes a minimal parasitic energy requirement (illustrated in Figure 6.4 as "Energy for CCS" in gray). For example, this included the CO_2 resulting from ethanol fermentation, which has almost 99% purity and, as such, can be directly compressed and sequestered. In the second level ("Full CCS" in Figure 6.4), CO_2 was captured from both the high-purity process emissions and the combustion emissions, which have lower CO_2 purity and therefore impose additional parasitic energy loss for capture. Figure 6.4 shows the net GHG emissions for the four liquid biofuel pathways.

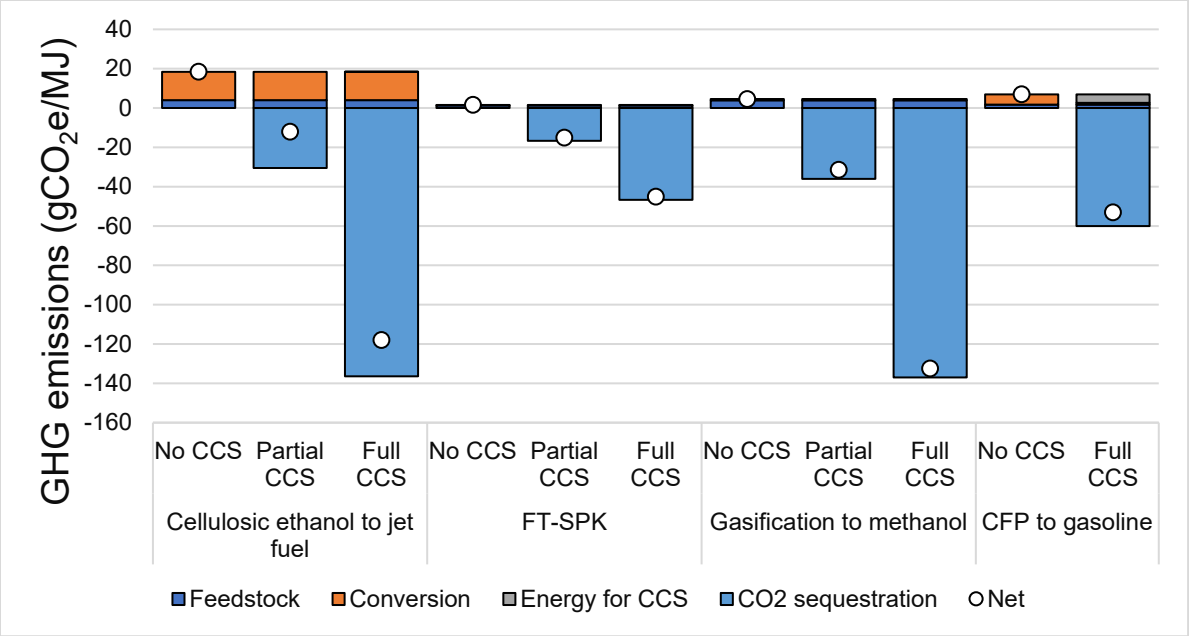

Figure 6.4. Net GHG emissions for the liquid biofuel pathways (ETJ, FT-SPK, gasification to methanol, and CFP, from left to right)

The negative emissions entail carbon flow from the atmosphere to the geosphere via CCS. The emissions shown in the "credits" stack are displacement benefits from coproducts. These are differentiated in accordance with the DOE/FECM methodology for CCS LCA.

For Pathway 1, the baseline emissions without CCS were 18 g CO_2e/MJ. Here, the conversion of biomass to ethanol and upgrading to jet fuel was emission-intensive, particularly due to input of hydrogen from the current U.S. hydrogen mix (which is 95% from natural gas steam reforming) and significant consumption of corn steep liquor and glucose. Corn stover, the feedstock for this pathway, is associated with low emissions, as GREET allocates higher emissions to corn grain (Canter et al. 2016). As such, this feedstock contributed only 4 g CO_2e/MJ of GHG emissions.

When partial CCS was adopted, i.e., from the fermentation off-gas, it did not require significant energy input for capture because it is a high-pressure, high-purity source (Ou et al. 2021). About 31 g CO_2e/MJ of CO_2 is sequestered from the fermentation process, more than offsetting the 18 g CO_2e/MJ of emissions from the conversion process, resulting in net emissions of -12 g CO_2e/MJ. Capturing CO_2 from the entire conversion process (full CCS) resulted in additional energy penalties in the form of natural gas (for sorbent regeneration) and electricity (for CO_2 compression), which does not result in any additional GHG emissions in a decarbonized electricity grid. The total CO_2 sequestered in this case was substantially higher, i.e., -136 g CO_2/MJ, resulting in net emissions of -112 g CO_2e/MJ (Figure 6.4).

Pathway 2 produces jet fuel via the FT process. The key advantage of this pathway from the LCA perspective, relative to Pathway 1, is that the conversion process is less emission-intensive, emitting only 0.3 g CO_2e/MJ. Thus, the emissions—even in the baseline case—are very close to zero, i.e., 2 g CO_2e/MJ. Inclusion of CCS on the acid gas removal (AGR) process stream, which contains relatively high-purity but not completely pure CO_2, results in gross sequestration of 17 g CO_2e/MJ. The emissions associated with CO_2 capture are zero since the electricity grid is assumed to be decarbonized. Thus, the net emissions in the pathway with CCS only on AGR are

-15 g CO_2e/MJ. After capturing CO_2 streams from the entire process, the net emissions are reduced to -47 g CO_2e/MJ (Figure 6.4).

The gross emissions from feedstock and conversion for Pathway 3 are similar to those for Pathway 2. However, there are no additional displacement credits, as methanol is the only product produced. This results in baseline emissions of 5 g CO_2e/MJ without CCS. As in the case of Pathway 2, CCS on the AGR stream gives rise to considerable gross emissions, resulting in net emissions of -31 g CO_2e/MJ. Capturing CO_2 from all process streams offers gross CO_2 sequestration of 137 g CO_2e/MJ, resulting in net emissions of -132 g CO_2e/MJ. Pathway 4 involves catalytic fast pyrolysis. As opposed to slow pyrolysis, which prioritizes biochar production for carbon sequestration, fast pyrolysis favors production of liquid fuels, which in our study is assumed to be further upgraded to "drop-in" gasoline. The emissions for CFP without CCS are 7 g CO_2e/MJ. There is no relatively high-purity stream of CO_2 in this pathway, so CO_2 capture imposes an energy penalty of 4 g CO_2e/MJ. However, the negative emissions of -60 g CO_2e/MJ more than offset this increase, resulting in net emissions of -53 g CO_2e/MJ. In addition to GHG emissions, we also estimated the total energy use, fossil energy use, water consumption, and criteria air pollutant emissions associated with the liquid biofuel pathways. These results are shown in Table 6.1. Some criteria air pollutant emissions, such as sulfur oxide emissions, are considerably lower for Pathway 1 because this pathway uses only cellulosic feedstock.

Table 6.1. LCA Metrics for Liquid Biofuel Pathways

		Energy		Water
Pathway	**GHG (g CO_2e/MJ)**	Total (BTU/MJ)	Fossil (BTU/MJ)	Consumption (L/MJ)
Cellulosic ethanol to jet	18	396	230	0.140
with CCS of fermentation gas	-12	408	230	0.140
with CCS fermentation gas and combustion emissions	-118	492	230	0.140
FT-SPK jet	2	25	21	0.028
with CCS of higher concentration gas	-15	49	21	0.028
with CCS of all flue gases	-45	92	21	0.028
Gasification to methanol	5	71	60	0.047
with CCS AGR CO_2	-31	102	60	0.047
with CCS of all flue gases	-132	185	60	0.047
Pyrolysis bio-oil to gasoline	7	-46	74	0.020
with CCS of all flue gases	-53	35	66	0.018

6.3.1.2 Results for Bioelectricity

LCA results for bioelectricity generation, shown in Table 6.2, were obtained by leveraging recent GREET analysis. Because of lack of technological specificity, we did not account for emission reductions via specialized equipment such as SO_2 polishers.[26] The results show that while net GHG emissions are close to zero without CCS, incorporating CCS reduces net emissions to -2 kg CO_2e/kWh.

Table 6.2. LCA Results for Bioelectricity Pathway With and Without CCS

Emissions	Without CCS	With CCS
CH_4 (g CH_4/kWh)	0.113	0.156
N_2O (g N_2O/kWh)	0.060	0.083
CO_2 (g CO_2/kWh)	-2.27	-2,030
GHGs (g CO_2e/kWh)	18.8	-2,000

Values reflect emissions to the atmosphere; higher values in the "with CCS" case reflect the additional energy requirements for CCS. The last row includes selected GHGs only (CH_4, N_2O, CO_2).

6.3.2 Marginal Cost of GHG Avoidance

One of the most referred-to metrics for the overall cost of decarbonization is the marginal cost of GHG avoidance. Estimation of this metric has several key advantages. First, it helps in evaluating whether a particular technology may be economically viable under a given policy scenario. When the cost of GHG avoidance is lower than the carbon price, it means available policy incentives and/or market mechanisms could be adequate to make the technology profitable (Clarke et al. 2022). Second, it helps in prioritizing particular sectors or products for preferential investments and identifying low-hanging fruits. In other words, if the cost of GHG avoidance for a technology is negative or close to zero, it shows that adoption of the mitigation measure may not pose a significant economic challenge. Third, arranging the costs of GHG avoidance in ascending order when their mitigation potential has also been assessed (as in prior chapters of this report) allows for the construction of a marginal abatement cost curves. These curves are universally used in policymaking since the area under the curve results in the total monetary investments needed for decarbonizing the economy.

$$\text{Cost of GHG avoidance} = \frac{\left(\text{Cost of new product}, \frac{\$}{MJ}\right) - \left(\text{Cost of reference product}, \frac{\$}{MJ}\right)}{\left(\text{GHG intensity of reference product}, \frac{gCO_2e}{MJ}\right) - \left(\text{GHG intensity of new product}, \frac{gCO_2e}{MJ}\right)}$$

One challenge with computing this metric is that the values in the numerator and denominator are inconsistently calculated across different system boundaries. This challenge is solved herein by harmonizing across the LCA and TEA to ensure their evaluations have a common system boundary. This approach illustrates an advantage of this project (Chapter 7).

[26] For some CO_2 capture technologies, it is essential to remove air pollutants, failing which the equipment may break down due to the formation of heat-stable salts. This study does not go into that particular level of detail around the type of capture technology (Singh and Rao 2014).

Table 6.3. Cost of GHG Avoidance for Pathways 1–4 Relative to Replacement of Reference Product

Pathway	Reference Fuel	GHG Emissions (gCO2e/MJ)	Cost (or MFSP)[a] (USD2016/GGE)	Cost of GHG Avoidance[b] (USD2016/ t-CO2e)
Cellulosic ethanol with jet upgrading	Jet fuel	18	4.60	202
with CCS of fermentation off-gas	Jet fuel	-12	4.70	147
with CCS fermentation off-gas and combustion stack off-gas	Jet fuel	-118	5.00	82
FT-SPK	Jet fuel	2	2.60	-38
with CCS of higher concentration off-gas	Jet fuel	-15	2.90	-7
with CCS of all flue gases	Jet fuel	-45	3.40	27
Gasification to methanol	Diesel	5	2.40	-85
with CCS AGR off-gas	Diesel	-31	2.60	-46
with CCS of all flue gases	Diesel	-132	3.20	-3
Gasoline from upgraded pyrolysis bio-oil	Gasoline	7	2.80	-4
with CCS of all flue gases	Gasoline	-53	3.70	50

[a] The life cycle GHG emissions and minimum fuel selling prices of the reference fuels used for the cost of GHG avoidance analysis for jet fuel, diesel and gasoline are 84.5, 90.3, and 89.9 g CO_2e/MJ and 2.98, 3.28, and 2.84 USD2016/GGE respectively. The costs of the CO_2 transport and storage for the liquid fuel pathways with partial and full CCS were out of scope for the cost analysis performed for this study; therefore, the marginal costs of GHG avoidance are artificially low. On average, CO_2 transport and storage costs are estimated to be around \$10/t-CO_2 but may have substantial variation based on geography and geology.

[b] Conventional gasoline and diesel MFSPs are indicated as the costs of crude oil and refining (but excluding taxes, distribution and marketing) based on the September 2023 EIA Gasoline and Diesel Fuel Update. Similarly, the MFSP of conventional jet fuel is the average price in North America paid at the refinery based on the Jet Fuel Price Monitor of the International Air Transport Association for the week ending Oct. 20, 2023.

Table 6.3 shows the costs of marginal GHG avoidance for the various liquid fuel pathways studied in this analysis. This leverages the costs computed in Chapter 5 and the emission factors computed in this chapter. Note that it is important to define a suitable reference product for estimating the cost of avoidance. Thus, we have considered that methanol produced in the gasification pathway will replace diesel. However, a parallel analysis could assume that methanol would be used to replace light diesel oil as an industrial fuel, which could give markedly different results.

The cost of avoidance for the cellulosic ethanol pathway is \$202/t-CO_2e. When partial and full CCS are added, the cost of avoidance reduces to \$147/t-CO_2e and \$82/t-CO_2e, respectively. The reduction of the cost of avoidance when only the fermentation off-gas is captured (i.e., partial CCS) is intuitive as the cost per gallon of ethanol production remains nearly same while the GHG emissions reduce by 30 g CO_2e. This is clearly seen in the literature and several operational projects where capture at ethanol facilities is practiced and recommended (Singh et al. 2023, Gollakota and McDonald 2012). Interestingly, the cost of avoidance for capturing CO_2 across the entire facility (i.e., full CCS) also decreases because the marginal GHG reduction is

substantial. This shows that if a shift from conventional jet fuel to the ethanol variant is undertaken, it may be economically viable to include CCS in the process design.

For all other pathways, this pattern is reversed, i.e., the cost of avoidance for CCS progressively increases as more CO_2 is captured from the flue gas. With full CCS, the cost for producing jet fuels through the FT-SPK pathway is \$27/t-CO_2e, while that for producing gasoline substitute via pyrolysis is \$0/t-CO_2e. The cost with CCS is lowest for producing methanol via gasification (-\$-3/t-CO_2e) because the current price of the reference product (i.e., diesel) is higher than the cost of the biomethanol pathway. Ultimately, these costs are all lower than the consensus carbon prices estimated by the Intergovernmental Panel on Climate Change Sixth Assessment Report for the 1.5°C pathways in 2030, which are a median \$100/t-CO_2. Thus, the pathways here are consistent with decarbonization pathways as projected in the IAM literature (Clarke et al. 2022). In the synthesis chapter (Chapter 7), we have also compared these with the carbon prices as estimated by GCAM for this specific project.

6.3.3 Decarbonization Scenario Analysis

6.3.3.1 Bioenergy Production

Figure 6.5 shows the fuel share across different liquid fuel pools and bioelectricity for different scenarios. Overall, bioenergy (i.e., biofuels and bioelectricity) accounts for 4.1%, 8%, and 11% of the total energy demand in 2050 in the Reference, DAC.Ref_noSAF, and DAC.Ref_BF35bil scenarios, respectively (Figure 6.6).

The Reference scenario does not include the new biomass conversion pathways from Table 6.3. As such, 118 million metric tons of dry biomass are left unused. This shows that use of the entirety of available waste biomass resources in the United States requires development and deployment of new commercial-scale biofuel technologies. In the absence of these technologies, biodiesel, corn ethanol, and cellulosic ethanol are the major biofuels in the Reference scenario, accounting for 8% and 17% of diesel and gasoline fuel pools, respectively, in 2050. While corn ethanol production decreases by 0.2 EJ from 2020 to 2050, cellulosic ethanol production increases from near-zero in 2020 to 0.5 EJ. Bioelectricity also accounts for 1.8% of total electricity demand in 2050.

Absence of a defined biofuels target prioritizes bioelectricity production in the DAC.Ref_noSAF scenario. This is because the SAF pathways in Table 6.3 also coproduce supplemental renewable gasoline and diesel. In the absence of a policy target for SAF, about 61% of available biomass is directed to bioelectricity generation, so fewer SAF coproducts are available for light-duty vehicles to use and, as such, there is a greater demand for electrification of the road transport sector. This bioelectricity generation accounts for 6.5% of electricity demand in 2050. Even without a stated SAF target, this scenario still sees an increase in biofuel production, with 1.1 EJ of SAF in 2050, accounting for 33% of jet fuel demand. 0.43 EJ of renewable gasoline and 0.09 EJ of renewable diesel are coproduced with SAF. Although no preference is given to either FT-SPK or ETJ, SAF production from FT-SPK increased from 0.03 to 0.2 EJ in 2050, while output from ETJ reached 0.92 EJ. Because ETJ produces a higher ratio of SAF to other hydrocarbons than FT-SPK, there is a significant shift to the ETJ pathway from 2030 onward. Finally, the high yield of the gasification to methanol pathway allows for 0.07 EJ of methanol to be produced in 2050, accounting for 10% of total residual fuel oil demand.

The presence of a 35-billion-gallon biofuels target within the DAC.Ref_BF35bil scenario in 2050 gives rise to a shift in biomass use from bioelectricity to biofuel production. In this scenario, 3.4 EJ of SAF is produced in 2050, with 1.7 EJ of other liquid biofuels (renewable diesel and gasoline) coproduced. In total, SAF and other coproduced biofuels reached 40 billion gallons in 2050, with an additional 7.5 billion gallons from biodiesel and corn ethanol. Bioelectricity generation reduced to 0.2 EJ in this scenario, compared to 1.9 EJ in the DAC.Ref_noSAF scenario.

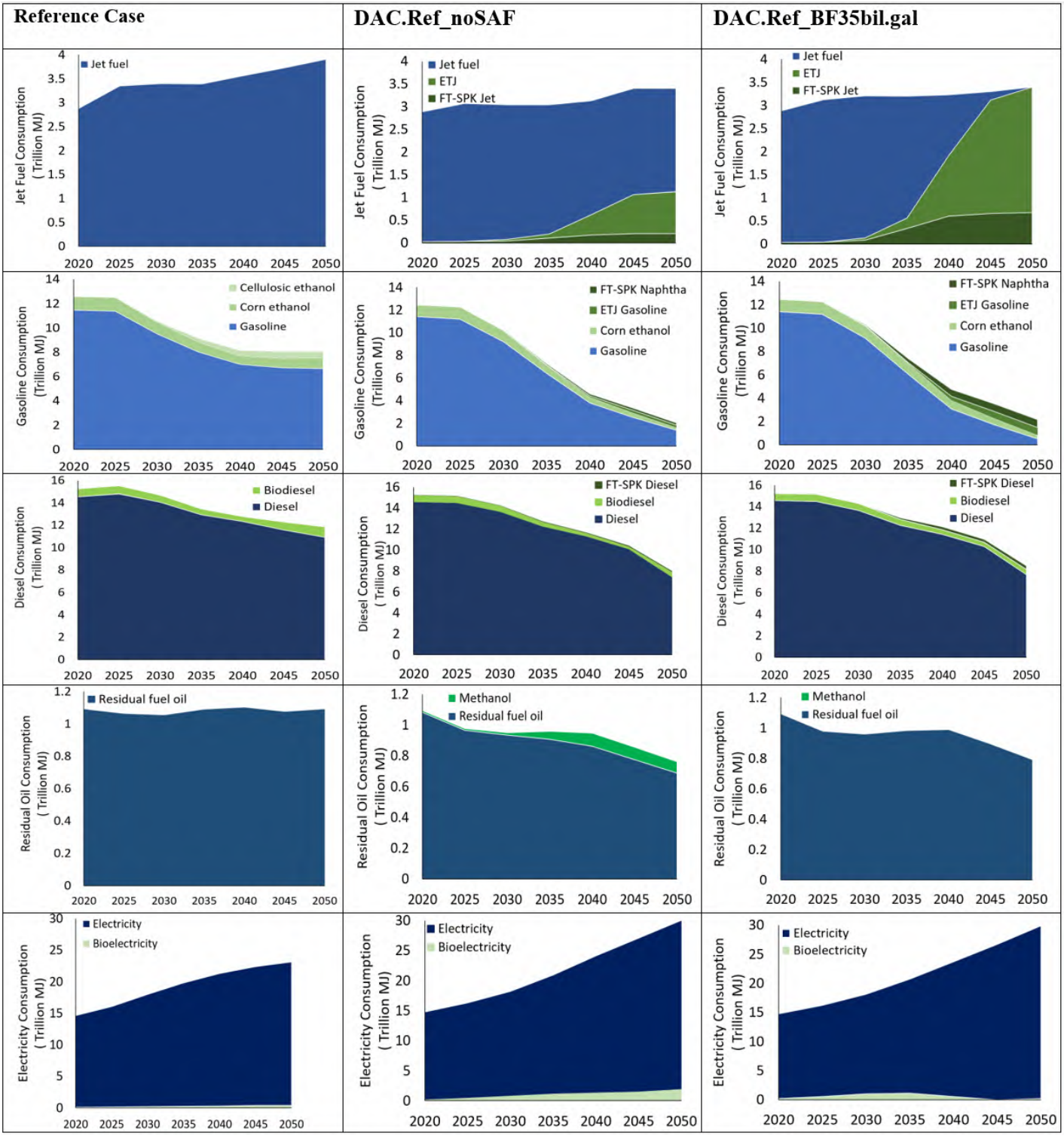

Figure 6.5. Fuel share across different liquid fuel and electricity pools in 2050

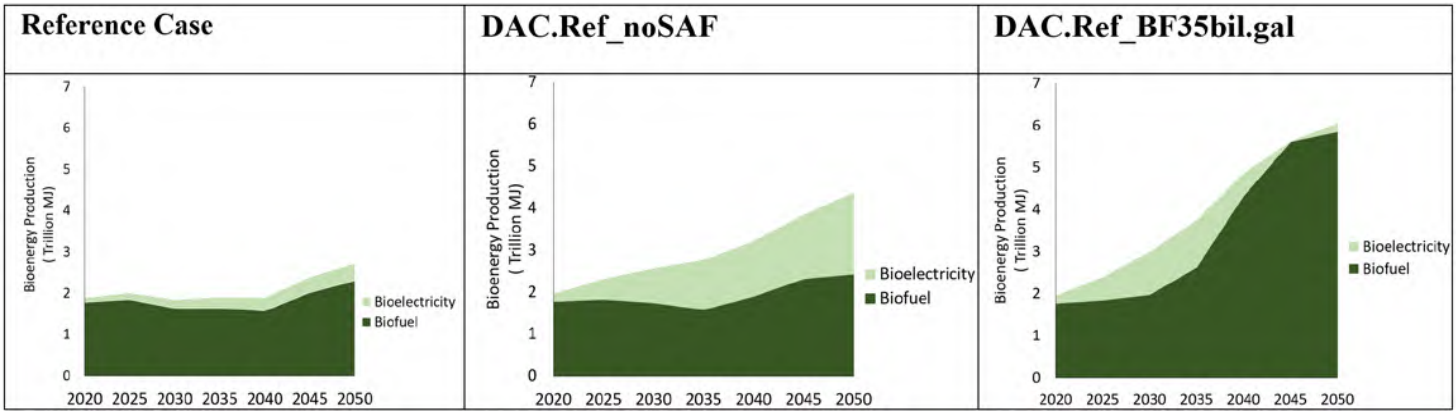

Figure 6.6. Overall bioenergy production

6.3.3.2 GHG Emissions

Bioeconomy AGE represents each liquid biofuel pathway without and with two levels of CCS. We assume technologies begin without CCS in 2020 and gradually introduce CCS technologies to integrate with the bioenergy technologies over time. We then analyze the impact of partial and full CCS in facilitating CDR and reaching net-zero GHG emissions in 2050 (Figure 6.7).

Both decarbonization scenarios assessed in Bioeconomy AGE show substantial GHG emissions reduction by coupling bioenergy with CCS. The scenario with no stated SAF target (DAC.Ref_noSAF) is projected to have CDR of 1.1 and 1.2 Gt-CO_2 annually by 2050 with partial and full CCS, respectively. This primarily comes from bioelectricity production because BECCS constitutes >6% of the electricity mix in this scenario. Cumulatively, this scenario converges to net-zero emissions without the need for widespread DAC deployment. With full CCS, the negative emissions from biofuels with CCS increase while the negative emissions from bioelectricity with CCS remain unchanged as bioelectricity has only one level of CCS.

The scenario with a 35-billion-gallon biofuels target in 2050 (DAC.Ref_BF35bil.gal) is accompanied by 0.2 and 0.6 Gt-CO_2 of CO_2 sequestration via BECCS with partial and full CCS, respectively. With full CCS, the primary driver of CO_2 sequestration (0.5 Gt-CO_2) is the production of jet fuels with full CCS. Additional CO_2 reduction corresponds to replacement of conventional gasoline and diesel for road transport with the renewable counterparts coproduced during the SAF production process. This scenario, accordingly, requires >0.6 Gt CDR from other engineered means (e.g., DAC or enhanced weathering).

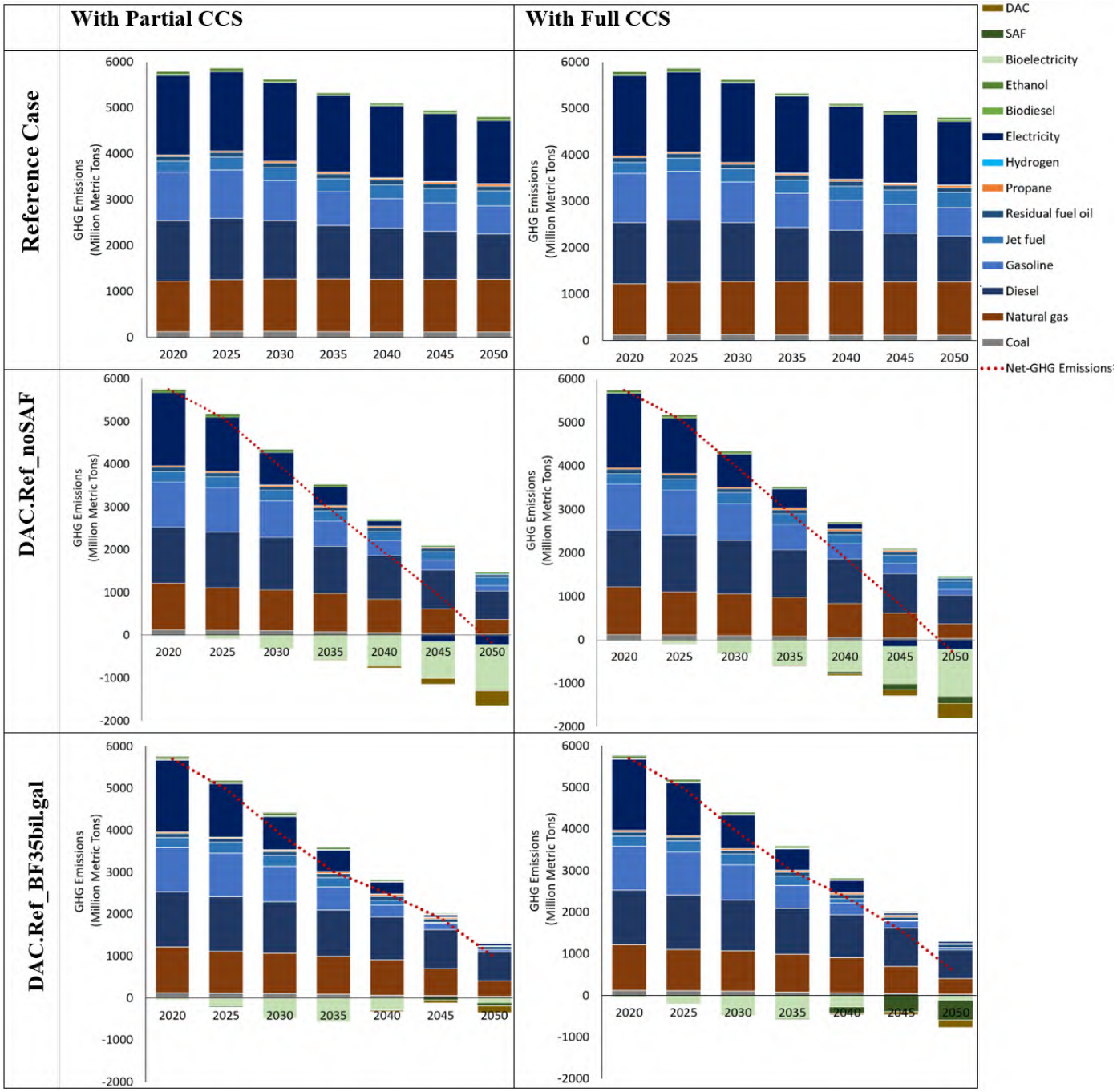

Figure 6.7. GHG emissions (in million metric tons CO_2e) across different scenarios with partial CCS

6.3.4 Limitations of the Study

The caveat to these results is that the large magnitude of negative emissions in bioelectricity are a function of the low combustion efficiency of 22% assumed in the current GREET analysis (Xu et al. 2021). A lower plant efficiency increases the carbon sequestration per kWh because it requires more biological feedstock, which prioritizes carbon storage over energy efficiency. In future iterations of the DECARB analyses, this estimate may change by incorporating

technologies better suited to bioelectricity generation with CCS, e.g., biomass gasification combined cycle plants or power plants with chemical looping capture (Bhave et al. 2017). The costs of the liquid fuel pathway with partial and full CCS were calculated in Chapter 5 without including the transport and storage cost components. On average, these costs are estimated to be around an additional \$10/t-CO_2 but may have substantial variation based on geography and geology. Some basins in the United States, for example the Tuscaloosa basin in the Southeast, can offer storage costs as low as \$2/t-CO_2 owing to optimal storage conditions, while other basins can result in higher costs where depth is high or porosity/permeability is lower (Singh et al. 2020). Sensitivities around land use change parameters may also affect results significantly. These considerations were outside the scope of this analysis.

6.4 Summary and Key Insights

The pathways evaluated focus on liquid fuel production (cellulosic ethanol to jet fuel, SPK, methanol, and gasoline) and electricity. These pathways are evaluated with and without CCS. The net GHG emissions across pathways for liquid fuels without CCS range from 2 g to 18 g CO_2e/MJ. Adding CCS to some or all CO_2 vent streams offers the opportunity to achieve CDR and offers net emissions of -45 to -118 g CO_2e/MJ (for full CCS). Based on current state of the art, the net GHG emissions for bioelectricity generation are close to zero without CCS and could drop to -1.9 kg CO_2e/kWh with CCS. Bioenergy is anticipated to play a key role in the decarbonization scenarios considered here and may account for 4%–11% of the total energy mix. In the scenario adhering to the SAF Grand Challenge target of producing 35 billion gallons of liquid biofuels by 2050, SAF coproducts (renewable diesel and gasoline) play a key role in displacing fossil fuel use for road transport. Contrastingly, the absence of a specific biofuels target results in increased production of bioelectricity, which can be used to electrify transportation, heat for buildings, and industrial processes.

References

ANL. 2022. “The Greenhouse Gases, Regulated Emissions, and Energy Use in Transportation Model.” Argonne National Laboratory. https://greet.es.anl.gov/.

Bhave, A., R. H. S. Taylor, P. Fennell, W. R. Livingston, N. Shah, N. Mac Dowell, John Dennis et al. 2017 "Screening and techno-economic assessment of biomass-based power generation with CCS technologies to meet 2050 CO2 targets." *Applied Energy*: 190: 481-489. https://doi.org/10.1016/j.apenergy.2016.12.120

Canter, C. E., J. B. Dunn, J. Han, Z. Wang, and M. Wang. 2016. “Policy implications of allocation methods in the life cycle analysis of integrated corn and corn stover ethanol production.” *BioEnergy Research* 9(1): 77–87. https://doi.org/10.1007/s12155-015-9664-4.

Clarke, L., Y.-M. Wei, A. De la Vega Navarro, A. Garg, A. N. Hahmann, S. Khennas, I. M. I. Azevedo et al. 2022. Energy Systems. In *Climate Change 2022: Mitigation of Climate Change. Contribution of Working Group III to the IPCC Sixth Assessment Report*. Cambridge, UK: Cambridge University Press. https://doi.org/10.1017/9781009157926.008.

Dunn, J. B., E. Newes, H. Cai, Y. Zhang, A. Brooker, L. Ou, N. Mundt et. al. 2020. "Energy, economic, and environmental benefits assessment of co-optimized engines and bio-blendstocks." *Energy and Environmental Science* 13(8): 2262–2274. https://doi.org/10.1039/D0EE00716A.

EIA. 2022. Annual Energy Outlook 2022. Washington, D.C.: U.S. Energy Information Administration. https://www.eia.gov/outlooks/aeo/narrative/introduction/sub-topic-01.php.

Gollakota, S., and S. McDonald. 2012. "CO_2 capture from ethanol production and storage into the Mt Simon Sandstone. Greenhouse Gases." *Science and Technology* 2(5): 346–351. https://doi.org/10.1002/ghg.1305.

Kar, S., T. Hawkins, G. Zaimes, D. Oke, H. Kwon, X. Wu, G. Zhang et al. 2022. *Decarbonization Scenario Analysis Model: Evaluation of a Scenario for Decarbonization of the United States Economy Energy Systems and Infrastructure Analysis* Argonne, IL: Argonne National Laboratory. ANL-22/40.

Melara, A. J., U. Singh, and L. M. Colosi. 2020. "Is aquatic bioenergy with carbon capture and storage a sustainable negative emission technology? Insights from a spatially explicit environmental life-cycle assessment." *Energy Conversion and Management* 224: 113300. https://doi.org/10.1016/j.enconman.2020.113300.

Muratori, M., H. Kheshgi, B. Mignone, L. Clarke, H. McJeon, and J. Edmonds. 2017. "Carbon capture and storage across fuels and sectors in energy system transformation pathways." *International Journal of Greenhouse Gas Control* 57: 34–41. https://doi.org/10.1016/j.ijggc.2016.11.026.

Oke, D., J. B. Dunn, and T. R. Hawkins. 2022. "The contribution of biomass and waste resources to decarbonizing transportation and related energy and environmental effects." *Sustainable Energy and Fuels* 6(3): 721–735. https://doi.org/10.1039/D1SE01742J.

Oke, D., L. Sittler, H. Cai, A. Avelino, E. Newes, G. G. Zaimes, Y. Zhang et al. 2023. "Energy, economic, and environmental impacts assessment of co-optimized on-road heavy-duty engines and bio-blendstocks." *Sustainable Energy and Fuels* 7(18): 4580–4601. https://doi.org/10.1039/D3SE00381G.

Ou, L., S. Banerjee, H. Xu, A. M. Coleman, H. Cai, U. Lee, M. Wigmosta, and T. Hawkins. 2021. "Utilizing high-purity carbon dioxide sources for algae cultivation and biofuel production in the United States: Opportunities and challenges." *Journal of Cleaner Production* 321: 128779. https://doi.org/10.1016/j.jclepro.2021.128779.

Rogers, J. N., B. Stokes, J. Dunn, H. Cai, M. Wu, Z. Haq, and H. Baumes. 2016. "An Assessment of the Potential Products and Economic and Environmental Impacts Resulting from a Billion Ton Bioeconomy." *Biofuels Bioprod. Biorefining* 2017 11(1): 110–128. https://doi.org/10.1002/bbb.1728.

Rubin, E. S., and A. B. Rao. 2002. "A technical, economic, and environmental assessment of amine-based CO_2 capture technology for power plant greenhouse gas control." United States. https://doi.org/10.2172/804932.

Sanchez, D. L., N. Johnson, S. T. McCoy, P. A. Turner, and K. J. Mach. 2018. "Near-term deployment of carbon capture and sequestration from biorefineries in the United States." *Proceedings of the National Academy of Sciences* 115(19): 4875–4880. https://doi.org/10.1073/pnas.1719695115.

Singh, U., S. Banerjee, and T. R. Hawkins. 2023. "Implications of CO_2 Sourcing on the Life-Cycle Greenhouse Gas Emissions and Costs of Algae Biofuels." *ACS Sustainable Chemistry and Engineering* 11(39): 14435–14444. https://doi.org/10.1021/acssuschemeng.3c02082.

Singh, U., and J. B. Dunn. 2022. "Shale Gas Decarbonization in the Permian Basin: Is It Possible?" *ACS Engineering Au* 2: 248–256. https://doi.org/10.1021/acsengineeringau.2c00001.

Singh, U., E. M. Loudermilk, and L. M. Colosi. 2020. "Accounting for the role of transport and storage infrastructure costs in carbon negative bioenergy deployment." *Greenhouse Gases Science and Technology* 11(1): 144–164. https://doi.org/10.1002/ghg.2041.

Singh, U., and A. B. Rao. 2014. "Estimating the environmental implications of implementing carbon capture and storage in Indian coal power plants." In *2014 International Conference on Advances in Green Energy (ICAGE)* IEEE Xplore: 226–232. https://doi.org/10.1109/ICAGE.2014.7050169.

Terlouw, T., C. Bauer, L. Rosa, and M. Mazzotti. 2021. "Life cycle assessment of carbon dioxide removal technologies: a critical review." *Energy and Environmental Science* 14(4): 1701–1721. https://doi.org/10.1039/D0EE03757E.

Xu, H., G. Latta, U. Lee, J. Lewandrowski, and M. Wang. 2021. "Regionalized life cycle greenhouse gas emissions of forest biomass use for electricity generation in the United States." *Environmental Science & Technology* 55(21): 14806–14816. https://doi.org/10.1021/acs.est.1c04301.

Zang, G., P. Sun, E. Yoo, A. Elgowainy, A. Bafana, U. Lee, M. Wang, and S. Supekar. 2021. Synthetic Methanol/Fischer–Tropsch Fuel Production Capacity, Cost, and Carbon Intensity Utilizing CO_2 from Industrial and Power Plants in the United States. *Environmental Science and Technology* 55(11): 7595–7604. https://doi.org/10.1021/acs.est.0c08674.

7 Integration and Synthesis of Analysis Results

The previous chapters of this report detailed the many data exchanges between the modeling tools employed in this study and highlighted the insights that each tool can provide about the role, challenges, and opportunities for bioenergy in a deeply decarbonized U.S. economy. This chapter seeks to tie these threads together to highlight the robust findings and unique perspectives brought to bear by the study's top-down and bottom-up modeling approaches. In integrating the findings from this analysis, we seek to answer the following questions:

- How consistent are integrated assessment model scenarios with bottom-up, spatially resolved assessment data?
- What are the benefits of soft-linking IAMs with process models, and where are the opportunities to harmonize these models deeply in the future?
- In which sectors and applications are limited sustainable biomass feedstocks put to their best use for supporting net-zero greenhouse gas emissions by 2050?
- What are the key equity questions related to future bioeconomy build-out? How could bioenergy create economic development opportunities for rural communities and those adversely affected by persistent poverty and disproportionate environmental burdens (e.g., air and water pollution impacts)?

This chapter is structured in two segments. The first segment (Sections 7.1–7.3) explores key aspects of the bioenergy life cycle (e.g., feedstock production, transportation and preprocessing, conversion, end-use demand) and quantitatively compares and contrasts the findings from the top-down and bottom-up modeling approaches. The second segment (Sections 7.4–7.5) summarizes the key insights, uncertainties, opportunities, challenges, and future research needs related to the bioeconomy in a deeply decarbonized United States.

A note about scenarios: This analysis was conducted over the course of six months with the goal of demonstrating how top-down and bottom-up modeling approaches could be deployed in a consistent framework to address important questions about the role of bioenergy in a deeply decarbonized U.S. economy. This condensed timeline provided limited opportunity for multiple iterations across the entire modeling framework. Thus, the GCAM scenarios analyzed by the bottom-up models are slightly different than those presented in Chapter 2. The main difference is that the scenarios in Chapter 2 (referred to as GCAM-DECARB) entailed harmonization with assumptions from bottom-up models across a range of inputs, including second-generation bioenergy crop yields, bioenergy transportation and preprocessing costs, and bioenergy conversion pathway costs and efficiencies. The scenarios analyzed by the bottom-up models (referred to as GCAMv6) predated this harmonization.

Additionally, while the definitions of two of the scenarios (DAC.Ref_noSAF and DAC.Ref_SAF100pct) were largely unchanged between GCAMv6 and GCAM-DECARB, the highest bioliquids scenario was changed from DAC.Ref_BF35bil.gal in GCAMv6 to DAC.Ref_BF50bil.gal in GCAM-DECARB. This is because the initial DAC.Ref_BF35bil.gal scenario was designed to be consistent with the volumetric target for SAF from the Sustainable Aviation Fuel Grand Challenge (i.e., 35 billion gallons per year by 2050), whereas the revised DAC.Ref_BF50bil.gal scenario was designed to target the total biofuels (SAF + coproducts) volumetric target from the Sustainable Aviation Fuel Grand Challenge. Thus, the

DAC.Ref_BF50bil.gal scenario entails a higher bioliquids target and is not directly comparable to the DAC.Ref_BF35bil.gal scenario.

7.1 Factors Affecting Feedstock Supply and Price

7.1.1 Feedstock Production To Meet Overall Demand

Biomass is a substantial, cost-effective, and energy-rich feedstock that we have demonstrated could be a pillar of the United States' decarbonization strategy. Our detailed top-down projection supports bottom-up assessments that more than 18 EJ (1 billion metric tons) of biomass can be sustainably produced annually within the United States by 2050 under different decarbonization scenarios. Amongst the GCAM scenarios run for this analysis, bioenergy supply increases steeply, from 5 EJ in 2020 to between 14 EJ and 23 EJ in 2050 in those that reach net-zero GHG emissions by mid-century. The production costs (excluding distribution, marketing, and taxes) for biofuel pathways ranged from $2.4 to $5.0/GGE, with CCS adding a small cost margin (<10%) for the liquid biofuel pathways (excluding transport and storage infrastructure costs). This is comparable to the current U.S. average gasoline price of $2.7/GGE. The range here corresponds to different technology pathways with and without CCS. The incremental cost of CCS is lower than that of power sector CCS because of the high-purity streams of CO_2 from biorefining in the intermediate ethanol pathway (Table ES.1).

Integrating more recent trends in energy crop yield improvement, the 2016 Billion-Ton Report suggests these large quantities of biomass may be produced at lower cost, on a smaller land footprint, and with fewer inputs than estimated in many top-down assessments (Daioglou et al. 2020, Bauer et al. 2020). Future yields of both food crops and energy crops are threatened by climate change. This introduces a potentially important time-dependent constraint on bioenergy effectiveness for mitigation (Xu et al. 2022), though such effects are not explored in the relatively short time horizon of the BT16 assessment. Biomass fills at least two important roles in decarbonization scenarios: the provision of low-carbon fuels and energy carriers for aviation and other difficult-to-electrify sectors, and a means of achieving CDR to offset remaining emissions from other hard-to-abate sectors (Butnar et al. 2020a). As such, IAMs tend to project high levels of biomass consumption growth into the future, as illustrated previously in Figure 2.11. In 2016, the U.S. bioenergy sector consumed approximately 6.3 EJ (360 million dry metric tons) of plant-based feedstocks, mostly in the form of using corn for ethanol production and mill wastes for electricity generation. All scenarios in the AR6 database project increases in U.S. biomass consumption by the end of the century, with a mean production rate on the order of 16 EJ/year. The GCAM-DECARB scenarios developed for this study project 14.2–22.8 EJ of total annual biomass consumption in the United States by the end of the century, falling toward the middle of the AR6 range. The various IAMs included in the AR6 database typically include endogenous models of energy crop production and competition for land with the food and forestry sectors, and many include further sustainability constraints around water use, soil quality (removal of agricultural residues), or biodiversity (Butnar et al. 2020b). Decarbonization scenarios tend to be supply-limited, utilizing as much biomass resource as possible until competition for other land uses starts to become extreme (Figure 3.11).

7.1.2 Impacts of Harmonization on GCAM Bioenergy Supply

The top-down GCAM model and the bottom-up BT16 study adopt different paradigms for assessing how the biomass sector might respond to increasing yield in the future, which were harmonized in this study. GCAM projects intensification (i.e., crop yield increases) in response to higher prices and does not include an explicit technology improvement component. Our bottom-up assessment of the future biomass resource includes more current and granular estimates of energy crop yields and projections of future yield improvements. The GCAM scenarios with highest biomass use consume most of the biomass resource modeled in BT16. BT16, on the other hand, considers uniform management intensity but includes various projections of how agricultural technology improvement would lead to increasing future yields of both energy and conventional crops (thus freeing up more land for conventional crops). An initial harmonization was attempted by updating the basin-scale yields of energy grasses and energy trees in GCAM based on data. Because BT16 considers a wider range of energy crops, this harmonization involved selecting the highest-yielding individual energy grass species in each county as representative of the composite energy grass crop in BT16, and likewise for energy tree species selection. Although this crop selection could have been done on a cost-minimizing basis instead of a yield-maximizing basis, we felt that the latter approach was more appropriate given the very high carbon prices and biomass demand later in the century in our custom scenarios.

Updating GCAM to use BT16 bioenergy crop yields led to greater bioenergy crop supply. This is attributable to higher yields leading to lower bioenergy prices, especially in scenarios with higher bioenergy demand (e.g., SAF100% case). Figure 7.1 shows the impact of this harmonization (GCAMv6 is preharmonization; GCAM-DECARB is postharmonization).

The BT16 yields were higher than the default GCAMv6 assumptions for both herbaceous and woody bioenergy crops, although the difference was larger (i.e., improvement was greater) for herbaceous crops (Figure 7.1a). With these updated yields, the GCAM-DECARB scenarios produce more herbaceous bioenergy crops than the corresponding GCAMv6 scenarios (Figure 7.1b), although GCAM still produces more woody bioenergy crops overall. Conversely, BT16 favors herbaceous bioenergy crops, which generally have higher yields than woody bioenergy crops (Chapter 3).

Implications of the yield harmonization for land use were mixed. Less land was required per unit of biomass produced in the GCAM-DECARB scenarios (relative to GCAMv6) due to the higher yield assumptions from BT16 (Figure 7.1c). However, feedstock transportation and preprocessing assumptions from INL were also harmonized for the updated GCAM-DECARB scenarios, which resulted in the need for greater biomass feedstock supply to meet equivalent levels of demand (Figure 7.1d).

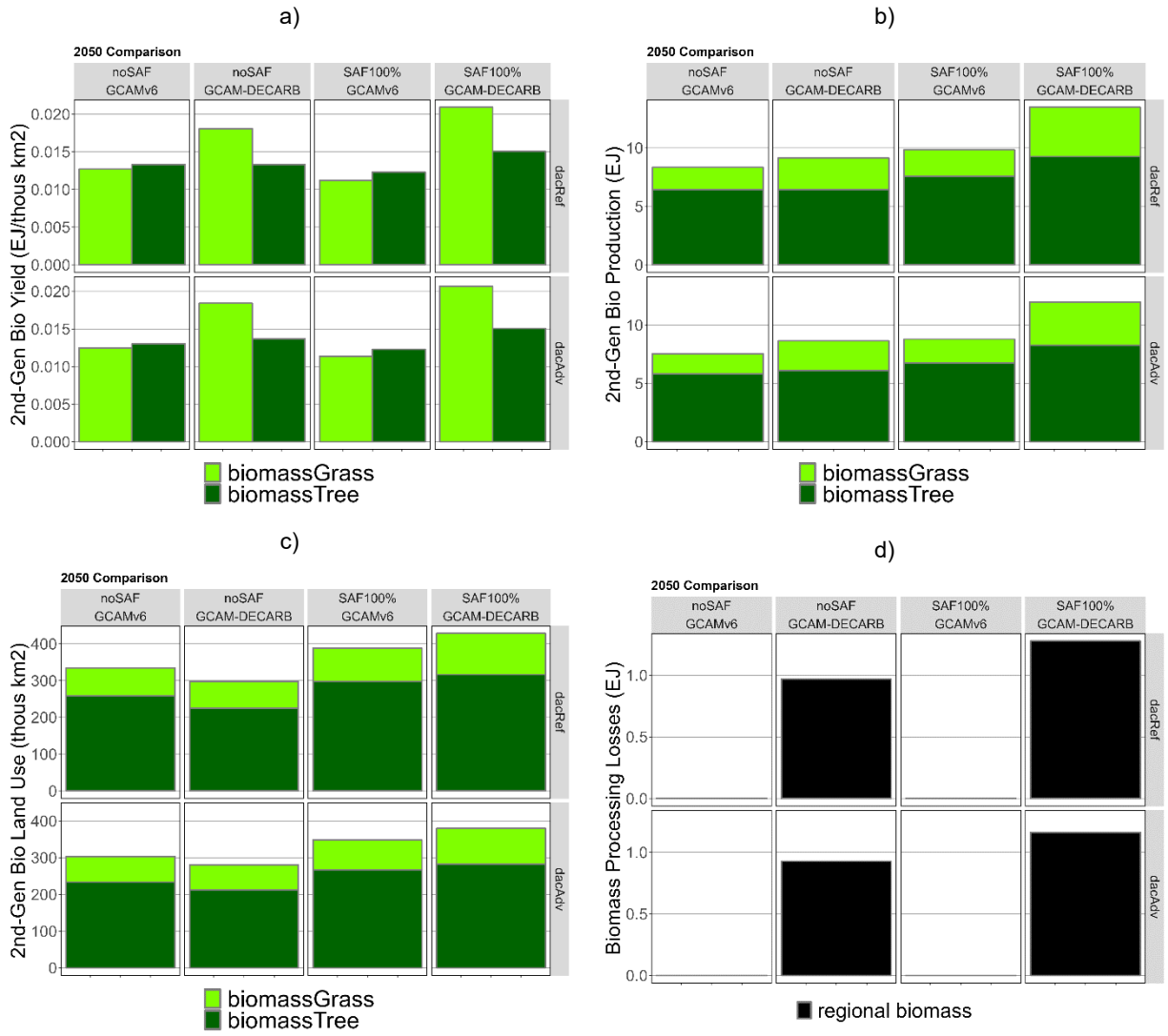

Figure 7.1. For the Ref.DAC case in 2050, a comparison of GCAM a) bioenergy crop yields, b) bioenergy crop production, c) bioenergy crop land allocation, and d) biomass transportation and preprocessing losses for GCAMv6 (preharmonization with bottom-up models) and GCAM-DECARB (postharmonization). "Regional biomass" in GCAM refers to aggregated cellulosic biomass from various sources.

7.2 Factors Affecting Pathway Choice and Decarbonization Potential

7.2.1 Sectoral Trends for Optimal Bioenergy Deployment

Biofuels are a cost-effective near-term option for decarbonizing aviation; efforts to meet the SAF target could prioritize feedstocks and pathways with the most potential to scale. When a binding 100% SAF demand by 2050 target is modeled, 80% of available biomass is used for SAF (and coproduced renewable diesel/gasoline) production. Notably, 1 MJ of ETJ coproduces 0.25 MJ of gasoline, whereas 1 MJ of FT-SPK coproduces 0.46 MJ of diesel and 1.06 MJ of naphtha. Biochemical conversion to alcohols combined with alcohol-to-jet technologies shows the most potential for conversion of agricultural residues and herbaceous feedstocks to SAF. Thermochemical conversion shows the most potential for conversion of woody biomass to SAF.

This is both because of the low cost of CCS in these pathways and the availability of SAF conversion technologies. These results could be sensitive to other parameters, such as lack of SAF blending possibilities and limitation in geologic sequestration sites, which are outside the scope of this study. Understanding the potential market for the coproducts from SAF production processes becomes increasingly relevant as the demand for liquid fuels declines in light- and medium-duty transport. Aggregation across fuel types in GCAM leads to underestimating the biomass needed to achieve the SAF target compared to more detailed pathway modeling, which explicitly tracks coproducts and their end uses.

In the absence of a binding SAF target, more biomass goes to electricity than with an SAF target, even if the leading pathways for SAF (previous paragraph) become financially competitive. The 2050 biomass use in our analysis ranges from 700 to 1,100 dry million metric tons, with electricity generation from bioelectricity plants reaching ~2 EJ (556 terawatt-hours) by 2050 without a binding SAF target—equivalent to 5% of projected electricity demand. In this scenario, bioelectricity constitutes about half of the total bioenergy production, with the rest being used in biofuel production. When the SAF target (35 billion gallons of biofuels, consistent with the SAF Grand Challenge volumetric target for meeting U.S. jet fuel demand, excluding coproducts) is met, bioelectricity production reduces to 0.2 EJ. The absence of leading conversion pathways (ETJ, SPK), however, limits the amount of biomass that may be used, with about 200 million metric tons of biomass remaining uneconomical for energy production compared to other sources. In the absence of an SAF target, GCAM indicates that emissions from the aviation sector would be offset by bioelectricity with CCS (or other carbon dioxide removal approaches). This finding is sensitive to the growth in low-carbon electricity and availability of CDR in such scenarios.

Coupling bioenergy with CCS can achieve net-negative GHG emissions capable of offsetting other hard-to-decarbonize sources. Biofuels with CCS can help decarbonize sectors such as aviation with coproducts being used in road transport. Bioelectricity with CCS accounts for a significant share of biomass use in economywide decarbonization scenarios because it offers carbon drawdown and could be operated flexibly[27] alongside variable renewable sources. The marginal cost of GHG abatement for CCS in connection with biomass-to-energy pathways is competitive among decarbonization strategies, particularly when CCS is paired with high-purity CO_2 process streams. This analysis did not account for colocation of bioenergy and CO_2 transport and storage infrastructure, which could be a focus of further analysis.

It is important to note that the scenarios presented in this report do not include a representation of the recently passed Inflation Reduction Act. Furthermore, the uniform, economywide carbon price employed by GCAM in the net-zero scenarios, which adds costs to emitting technologies and incentivizes CDR, represents a simple, stylized policy for achieving long-term emissions targets in a cost-effective manner. In the real world, decarbonization may be pursued via a variety of policies, including a collection of sectoral policies. Thus, the allocation of biomass across economic sectors may unfold differently in alternate policy regimes than it does with the uniform carbon price simplification employed in this analysis.

[27] With biomass gasification combined cycle plants

7.2.2 Comparison of Fuel Costs (MFSP)

The cost for biofuels production pathways in this study ranged from $2.4 to $5.0/GGE ($26 to $55/GJ), with CCS adding a small (<10%) cost margin. The fuel price results calculated by GCAM and the TEA are broadly comparable, though there are significant temporal differences. In contrast to GCAM, the TEA considers constant electricity and biomass prices with time and does not incorporate differences in prices across varying electricity sources. Consider the two SAF production pathways (ETJ and FT-SPK) that are represented explicitly within GCAM with different levels of CCS. The total current costs (2020) for the FT-SPK pathway in GCAM are $25/GJ without CCS, $26/GJ with partial CCS, and $30/GJ with full CCS. These costs are nearly equal to those computed within the TEA ($24/GJ, $26/GJ, and $31/GJ). However, the 2050 costs in GCAM are notably higher, $35–$53/GJ for FT-SPK without CCS and $40–$59/GJ with full CCS. This pattern is flipped for ETJ, where GCAM's current costs for the no CCS, partial CCS, and full CCS cases are $31/GJ, $31/GJ, and $33/GJ, respectively. In 2050, these costs are projected to rise to $42–$65/GJ, $43–$65/GJ, and $45–$67/GJ, respectively. The lower bounds for these 2050 costs are similar to those computed in the TEA ($42/GJ, $43/GJ, and $45/GJ). The ranges here correspond to the variability among scenarios with and without binding SAF targets, while the increased price with time reflects increasing biomass price since GCAM chooses more expensive biomass resources as demand increases.

One important caveat here is the low TRL for the pathways such as FT-SPK and gasification-to-methanol. While our analyses assume commercialized technologies, initial pilot/demonstration projects may be associated with higher project and process contingencies that add uncertainty to the costs of production noted above.

7.2.3 Comparison of GHG Emission Factors

The SAF and bioelectricity production pathways evaluated in this study may deliver near-zero emissions without CCS and net-negative emissions with CCS—with similar emission factors calculated in the GCAM analysis and the LCA. The slight differences may be attributed to the displacement method used in the static LCA calculated using GREET, which is overcome using the Bioeconomy AGE analysis (discussed later in this chapter). The life cycle GHG emissions for the ETJ pathway are 18 g CO_2e/MJ without CCS, -12 g CO_2e/MJ with partial CCS, and -118 g CO_2e/MJ with full CCS. This is similar to the estimates calculated by GCAM, where the corresponding values are 3 g CO_2e/MJ, -30 g CO_2e/MJ, and -139 g CO_2e/MJ. Similar trends are noted in the FT-SPK pathway as well, where the difference is less than 10 g CO_2e/MJ between the GCAM and LCA results. Notably, these differences are less dramatic than the differences between the GCAM and TEA cost results in the previous paragraph. The difference in the GCAM and LCA emission factor results is more pronounced for the bioelectricity generation pathway with CCS—the GCAM estimate is less negative (-250 g to -300 g CO_2e/MJ) than the -527 g CO_2e/MJ estimate from the GREET LCA. This is because the default net plant efficiency for combustion in GREET is lower, which leads to the requirement of a greater quantity of biomass per unit electricity generation, in turn resulting in higher biological carbon uptake.

7.2.4 Comparison of Marginal Cost of Greenhouse Gas Avoidance

Comparing the cost of GHG avoidance with the carbon price shows that at a mature modeled stage, a majority of bioenergy pathways may be economically viable by 2030, and all pathways become competitive shortly after 2040. These carbon prices, however, do not account for specific

incentives that may be offered in individual sectors or detailed supply-chain development. The bottom-up analysis discussed in Chapter 6 evaluates the cost of GHG avoidance. GCAM also estimates the carbon prices in each scenario. As such, it is useful in projecting the timeline on which various bioenergy pathways become financially competitive. The 2020 carbon price is \$0/t-CO_2. That said, the cost of GHG avoidance for several pathways (e.g., all the subcategories of the gasification to methanol pathway, and CFP without CCS) is negative because the costs of novel pathways with waste biomass are cheaper than incumbent products. This indicates that these pathways are competitive even without a carbon price. Several other pathways (cellulosic ethanol to jet fuel with full CCS, all subcategories of FT-SPK, and CFP with CCS) also become economically viable by 2030 as the cost of GHG avoidance reduces below the carbon price projected by GCAM. All the remaining pathways are anticipated to become economically viable by 2040 or shortly thereafter, with the mean carbon price reaching well above the costs of avoidance of all pathways post-2040. This escalation occurs in the last decade of the simulation (2040–2050) as residual emissions are reduced and removed to reach the target of net-zero emissions by 2050. While this approach is useful for getting an overall perspective on the readiness of these pathways, it is important to note that individual pathways may also be prioritized by giving incentives in hard-to-abate sectors such as aviation or methane mitigation (Singh et al. 2022), which is not directly accounted for in this analysis.

7.3 Quantitative Summary of Scenario Results Between GCAM and Bioeconomy AGE

In the net-zero GHG scenarios explored in this analysis via Bioeconomy AGE, economywide biomass feedstock demand in 2050 ranged from 13.5 EJ to 22.1 EJ (0.77–1.26 billion metric tons) across scenarios. BECCS is an important contributor to CDR, sequestering between 820 million metric tons CO_2 and 1,200 million metric tons of CO_2 per year by 2050 (this range is 700–1,100 million metric tons in GCAM). Both GCAM and Bioeconomy AGE indicate that in the absence of a binding SAF target, the main bioenergy use is in the form of electricity generation (2 EJ). These results would be influenced by uncertainties in other sectors such as the level of electrification in transport and industry.

A 100% SAF by 2050 (SAF100 scenario) target dramatically alters the way biomass is consumed, with almost 80% of the biomass being used in SAF (and renewable diesel/gasoline) production. The total biomass demand also increases by 20%–25% as compared to the decarbonization scenario with no SAF target. Here, bioelectricity production reduces to 0.2 EJ.

Accounting for the differences in the energy content of various feedstocks coupled with differences in the conversion efficiency of the pathways considered, the bottom-up analysis projects bioelectricity generation may require more biomass (about 22% higher) than projected in the top-down model. Bioelectricity generation in the DAC.Ref_noSAF scenario reaches ~2 EJ in 2050 in both GCAMv6 and Bioeconomy AGE, with more biomass required in Bioeconomy AGE (about 22% higher than the amount used in GCAM). This variation can likely be attributed to differences in conversion efficiency and energy content of different feedstocks. Because of all the aggregation steps in the GCAM model (GCAM combines second-generation crops, MSW, and crop residues into a single homogenous biomass commodity), it does not differentiate between different types of biomass use with different conversion technologies/end uses. As a result, GCAM uses an energy content of 17.5 GJ/metric ton of biomass across all biomass types

(except corn and soybean), whereas in Bioeconomy AGE, the energy content of each type of biomass varies (between 13 and 18 GJ/metric ton).

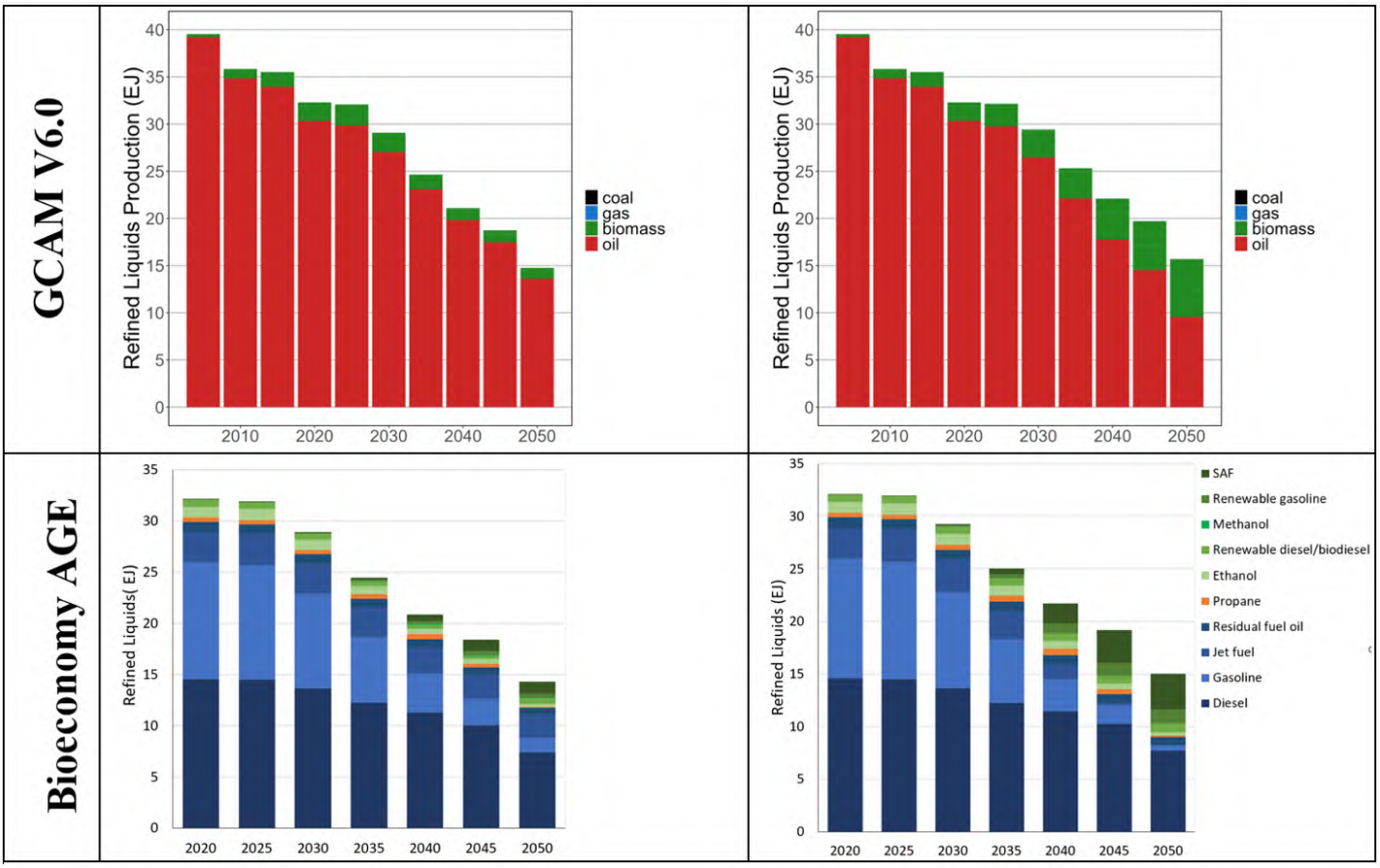

Figure 7.2. Aggregated refined liquids production in GCAMv6 vs. explicitly tracked liquid fuels in Bioeconomy AGE

7.4 Discussion of the Role and Strengths of Integrated Assessment Models and High-Resolution Process-Based Modeling

The approach adopted in this study provides insights and a road map for tackling complex energy system challenges such as decarbonization. Understanding divergence in modeling results and identifying avenues for data harmonization and cross-model linkages is valuable for determining future research priorities.

This work leverages the strengths of both IAMs and process models and is therefore able to deliver robust results via soft-linking. Soft-linking refers to a practical strategy used to assess a given decarbonization scenario with inputs from both top-down and bottom-up models (Shukla et al. 2015). As such, the mathematical architectures of the models are not hard-linked due to constraints around time and computational resources, but information exchange is used wherein outputs from one model constitute the inputs to another. For example, the Bioeconomy AGE analysis in Chapter 6 uses feedstock supply and demand from GCAM outputs. The estimated costs of avoidance obtained as a result in Chapter 6 are then compared to the carbon prices from GCAM.

Qualitatively, two important aspects overlooked by IAMs in the past have been material cycles and representation of coproducts. IAMs—particularly GCAM—do not focus on physical models of materials production even though they consider the economic value of bulk materials such as cement and steel (Pauliuk et al. 2017). While aggregated economic values are useful, they provide limited detail about sectoral mitigation opportunities. By using detailed process design linked with nationwide feedstock availability, our analysis can more effectively evaluate the costs and potential of bioenergy pathways to mitigate GHG emissions. The conversion pathways evaluated in Chapters 5–6 deliver energy (in the form of diesel or electricity) and chemicals (e.g., methyl ethyl ketone, acetone). Even when IAMs represent conversion pathways, they generally do not incorporate substantial detail around their coproducts. Traditional LCAs/TEAs, however, often have well-defined displacement or allocation strategies to account for these coproducts. Thus, the use of process models adds inherent value by providing detailed material flows that are not readily visible in IAMs.

The process-based analysis explicitly tracks fuel coproducts to avoid misallocation of biofuels across various sectors of the economy, which could occur in GCAM due to its lack of detail about fuel products. Liquid fuels in GCAM were previously represented as homogeneous blends with no explicit representation of gasoline, diesel, jet fuel, or residual fuel oil, treating outputs from biofuel technologies as a generic refined liquid that could go toward any end use (Figure 7.2). This could lead to misallocation of biofuel across different sectors of the economy.

Importantly, soft-linking in this project made it possible to configure GCAM to explicitly track SAF and its coproducts. For instance, process modeling indicates that the two key pathways for SAF production (ETJ and FT-SPK) coproduce 1.7 EJ of renewable gasoline and diesel in the DAC.Ref_BF35bil scenario. As gasoline/diesel demand is anticipated to reduce with electrification of road transport, these coproducts play a substantial role in this sector. Compared to the Bioeconomy AGE model, GCAM, by default, provides less detail regarding the output of different biofuel conversion technologies (in terms of primary fuel vs. coproducts), leading to uncertainty in the biofuel production share of different fuels. GCAM lumps together all cellulosic biomass types and passes them all through a very limited set of conversion process options (either cellulosic ethanol or FT-SPK pathways) that convert these feedstocks into generic energy carriers.

Beyond this study, the Bioeconomy AGE model has the capability to model different conversion pathways that are not presently incorporated into GCAM (Oke et al. 2022a, Kar et al. 2022, Oke et al. 2020b). Global, multi-sector, integrated modeling entails a tradeoff between limiting process detail in individual sectors to capture key inter-sectoral and inter-regional interactions. Further collaboration between bottom-up models and IAMs could help determine which additional pathways (e.g., other biomass-to-liquid-fuel pathways, anaerobic digestion of biogas to renewable natural gas, and conversion of biomass to chemicals and bioplastics) are most important and would most meaningfully increase GCAM's ability to shed light on the allocation of biomass throughout the energy system. This technology shift also impacts the amount of fuel coproduced with SAF and used in other sectors. Shifting from FT-SPK to ETJ favors the production of renewable gasoline (as a coproduct of SAF production) and reduces conventional gasoline consumption to near zero in the DAC.Ref_BF35bil.gal scenario.

On the other hand, allocation of coproducts often create substantial ambiguities in LCAs/TEAs, which are reduced in the Bioeconomy AGE analysis in this report. For example, if electricity is produced as a coproduct when producing liquid fuel, following a displacement allocation strategy would credit the liquid fuel with the emissions associated with production of the same amount of grid electricity. However, the emissions intensity of the electricity grid is itself anticipated to vary greatly in the long-term strategy of the United States, from ~0.4 kg CO_2e/kWh currently to near-zero in 2035. This introduces a large uncertainty around the displacement credits for electricity. Similarly, in the case of hydrogen, 95% of hydrogen is currently produced using steam methane reforming of natural gas, but accelerated efforts for green hydrogen are underway. Static LCAs/TEAs are not equipped to handle these changing temporal dimensions. However, using a coupled LCA and scenario analysis in Bioeconomy AGE to track the decarbonization evolution of the grid and other economic sectors (Chapter 6) addresses this issue. Here, instead of modeling a single process or product cycle, soft-linking enables us to use scenario data from GCAM to model economywide transformations over extended periods of time, reducing ambiguities associated with using process models alone to analyze highly dynamic sectors.

More generally, bottom-up models often lack broader economic and societal feedback. Shukla et al. (2015) find that bottom-up models' focus on energy systems, and not the economy, may make them overly optimistic in understanding technological progress, as they are unable to account for consumer preference. To some extent, the soft-linking approach in this report helps overcome this challenge.

7.5 Environmental Justice Considerations and Future Work[28]

This study points us to the broad directions future research could take for long-term policymaking and planning. Biomass feedstock could be utilized primarily for two objectives: energy production and CDR. The type of technological pathways chosen would determine the relative share of these two objectives being achieved. Of late, BECCS technologies have come to be considered within the larger umbrella of biomass carbon removal and storage technologies. In addition to energy pathways, this includes biochar production and long-lived wood products, among others. Future work could benefit from looking into understanding the interactions between these two objectives. Even within the context of energy production, bioelectricity, biofuels and biohydrogen are important planks. Bioelectricity pathways provide a greater volume of CO_2 per unit energy, while biofuel pathways provide high-purity CO_2 streams during their conversion and refining. Prioritizing either of these pathways would depend on policy goals on the role electrification or liquid fuels would play in the transport sector. The LCA of bioenergy and CDR pathways is also influenced by sensitivities around land use change parameters. Depending on the type of ecosystems being replaced for dedicated biomass cultivation and the allocation strategies for waste-versus-dedicated biomass could also be an important focus of future research. Finally, deployment of BECCS pathways particularly would be dependent on the availability, costs and risks of sinks. While these factors have been investigated in detail by other

[28] The scope for future work here is mentioned in the context of broader modeling and analytical studies. It may not necessarily correspond to recommendations for future DECARB efforts, for which a set of broader issues may take precedence.

researchers, incorporating them into economywide analyses could better inform regional planning.

Modeling analyses in this report focus broadly on representations of financially competitive resources and process modeling. However, actual decision-making on bioenergy-based decarbonization pathways may also prioritize community engagement and environmental justice considerations. Energy equity and environmental justice may be prioritized within future energy system analysis—for instance, by modeling the impacts of energy system decisions at the regional or community scale to assess geographic distributional impacts. In Chapter 4, we evaluated the extent of spatial overlap between identified biorefinery locations and disadvantaged communities, as identified by DOE's Disadvantaged Communities Reporter mapping tool. Although we find a substantial spatial overlap between potential biorefinery locations and tracts designated as disadvantaged, the analysis did not incorporate energy equity and environmental justice criteria ex ante. While the establishment of biorefineries can present economic opportunities within a community, it can also result in unintended consequences, including introduction or perpetuation of environmental burdens. Applying data from this study as input data to complete an energy equity and environmental justice analysis could produce lessons that would be valuable to other analysts embarking on high-resolution local analysis and offer insights into the practical implications of energy deployment for local regions.

Bioenergy also has an important role to play in the context of a just energy transition, which is the end goal of efforts to ensure that the transition away from fossil fuels happens equitably for communities by prioritizing the equitable distribution of the benefits and burdens of the energy system where fossil energy jobs are located. Bioenergy pathways involve a similar skill set to the current fossil fuel supply chain, and the bioenergy industry could facilitate transfer of skills for some fossil fuel professionals. Analysis by Patrizio et al. (2018) shows that concerted focus on BECCS could avert job losses of 40,000 coal workers and create an additional 22,000 jobs in the United States by mid-century. Employment attributed to the construction phase of solar and wind plants is much more significant than employment at baseload plants using bioenergy. This bodes well for a just transition because a scaled-up bioeconomy could offer stable jobs throughout the economic lifetime of such projects (Fragkos and Paroussos 2018). In addition to creating employment opportunities, alternative strategies could entail robust just transition plans in regions with high bioenergy potential. The literature suggests that the costs for such planning are relatively modest and would primarily entail retraining and outreach efforts *for communities where fossil energy jobs are located* (Pollin et al. 2019).

Future work in collaboration with social science methodologies and direct community engagement, along with geospatial software such as the U.S. Environmental Protection Agency's EJScreen, DOE's Disadvantaged Communities Reporter mapping tool, and/or the White House Council on Environmental Quality's Climate & Economic Justice Screening Tool may focus on answering questions about public perceptions of a bioeconomy. These research gaps, summarized by Buck (2019), would need to be addressed for individual life cycle stages of the technologies modeled in this report. Consider the case of bioenergy crop cultivation, where it is pertinent to investigate the decision-making ability of nonlandowning farmers to shift to bioenergy crops. Whether social desirability of these projects is influenced by the life cycle criteria air pollutant metrics estimated in Chapter 6 could also be an important determinant. The AR6 highlights that public perception of biomass conversion is less favorable than that of

solar/wind, but this may be due to a lack of knowledge about these conversion methodologies. As such, community engagement might also focus on enhancing public knowledge in this area. While pipeline transport and geologic sequestration of CO_2 have been very reliable in the United States, with few cases of substantial leaks (Romanak et al. 2014, Anderson et al. 2018, Alcalde et al. 2018), decisions around future infrastructure siting could potentially be made to avoid new burdens to historically impacted communities.

References

Alcalde, J., S. Flude, M. Wilkinson, G. Johnson, K. Edlmann, C. E. Bond, V. Scott et al. 2018. "Estimating geological CO_2 storage security to deliver on climate mitigation." *Nature Communications* 9(1): 2201. https://doi.org/10.1038/s41467-018-04423-1.

Anderson, J. S., K. D. Romanak, and T. A. Meckel. 2018. "Assessment of shallow subsea hydrocarbons as a proxy for leakage at offshore geologic CO_2 storage sites." *International Journal of Greenhouse Gas Control* 74: 19–27. https://doi.org/10.1016/j.ijggc.2018.04.010.

Bauer, N., D. Klein, F. Humpenöder, E. Kriegler, G. Luderer, A. Popp and J. Strefler. 2020. "Bio-energy and CO_2 emission reductions: an integrated land-use and energy sector perspective." *Climatic Change* 163: 1675–1693. https://doi.org/10.1007/s10584-020-02895-z.

Buck, H. J. 2019. "Challenges and opportunities of bioenergy with carbon capture and storage (BECCS) for communities." *Current Sustainable/Renewable Energy Reports*, 6(4): 124–130. https://doi.org/10.1007/s40518-019-00139-y.

Butnar, I., O. Broad, B. S. Rodriguez, and P. E. Dodds. 2020a. "The role of bioenergy for global deep decarbonization: CO_2 removal or low-carbon energy?" *GCB Bioenergy* 12(3): 198–212. https://doi.org/10.1111/gcbb.12666.

Butnar, I., P.-H. Li, N. Strachan, J. P. Pereira, A. Gambhir, and P. Smith. 2020b. "A deep dive into the modelling assumptions for biomass with carbon capture and storage (BECCS): A transparency exercise." *Environmental Research Letters* 15(8): 084008. https://doi.org/10.1088/1748-9326/ab5c3e.

Daioglou, V., S. K. Rose, N. Bauer, A. Kitous, M. Muratori, F. Sano, S. Fujimori et al. 2020. "Bioenergy technologies in long-run climate change mitigation: results from the EMF-33 study." *Climatic Change* 163: 1603–1620. https://doi.org/10.1007/s10584-020-02799-y.

Fragkos, P., and L. Paroussos. 2018. "Employment creation in EU related to renewables expansion." *Applied Energy* 230, 935–945. https://doi.org/10.1016/j.apenergy.2018.09.032.

Kar, S., T. R. Hawkins, G. G. Zaimes, D. Oke, H. Kwon, X. Wu, G. Zang et al. 2022. *Decarbonization Scenario Analysis Model: Evaluation of a Scenario for Decarbonization of the United States Economy.* Argonne, IL: Argonne National Laboratory. Technical Report, ANL-22/40.

Oke, D., J. B. Dunn, and T. R. Hawkins. 2022a. "The contribution of biomass and waste resources to decarbonizing transportation and related energy and environmental effects." *Sustainable Energy and Fuels* 6(3): 721–735. https://doi.org/10.1039/D1SE01742J.

Oke, D., J. B. Dunn, and T. R. Hawkins. 2022b. "Reducing economywide greenhouse gas emissions with electro-fuels and biofuels as the grid decarbonizes." *Energy and Environmental Science*, Submitted for Review.

Patrizio, P., S. Leduc, F. Kraxner, S. Fuss, G. Kindermann, S. Mesfun, K. Spokas et al. 2018. "Reducing US coal emissions can boost employment." *Joule* 2(12): 2633–2648. https://doi.org/10.1016/j.joule.2018.10.004.

Pauliuk, S., A. Arvesen, K. Stadler, and E. G. Hertwich. 2017. "Industrial ecology in integrated assessment models." *Nature Climate Change* 7(1): 13–20. https://doi.org/10.1038/nclimate3148.

Pollin, R., and B. Callaci. 2019. "The economics of just transition: a framework for supporting fossil fuel–dependent workers and communities in the United States." *Labor Studies Journal* 44(2): 93–138. https://doi.org/10.1177/0160449X18787051.

Romanak, K. D., B. Wolaver, C. Yang, G. W. Sherk, J. Dale, L. M. Dobeck, and L. H. Spangler. 2014. "Process-based soil gas leakage assessment at the Kerr Farm: Comparison of results to leakage proxies at ZERT and Mt. Etna." *International Journal of Greenhouse Gas Control* 30: 42–57. https://doi.org/10.1016/j.ijggc.2014.08.008.

Shukla, P. R., A. Garg, and H. H. Dholakia. 2015. *Energy-emissions trends and policy landscape for India* (Vol. 1). Allied Publishers. http://www.alliedpub.com/form/Search.aspx?Search=Energy-emissions%20trends%20and%20policy%20landscape%20for%20India.

Singh, U., M. Algren, C. Schoeneberger, C. Lavallais, M. O'Connell, D. Oke, C. Liang. 2022. "Technological avenues and market mechanisms to accelerate methane and nitrous oxide emissions reductions." *Iscience* 25(12): 105661. https://doi.org/10.1016/j.isci.2022.105661.